

# Human Perception and Control of Vehicle Roll Tilt in Hyper-Gravity

By

Torin Kristofer Clark

B.S. Aerospace Engineering  
University of Colorado at Boulder, 2008

S.M. Aeronautics and Astronautics  
Massachusetts Institute of Technology, 2010

SUBMITTED TO THE DEPARTMENT OF AERONAUTICS AND ASTRONAUTICS IN  
PARTIAL FULFILLMENT OF THE REQUIREMENTS FOR THE DEGREE OF

DOCTOR OF PHILOSOPHY IN AERONAUTICS AND ASTRONAUTICS

AT THE

MASSACHUSETTS INSTITUTE OF TECHNOLOGY

September 2013

© 2013 Torin Clark. All rights reserved.

The author hereby grants to MIT and The Charles Stark Draper Laboratory, Inc. permission to reproduce and to distribute publicly paper and electronic copies of this thesis document in whole or in any part medium now known or hereafter created.

Signature of Author: \_\_\_\_\_

Torin K. Clark  
Department of Aeronautics and Astronautics  
August 22, 2013

Accepted by: \_\_\_\_\_

Eytan H. Modiano  
Professor of Aeronautics and Astronautics  
Chair, Graduate Program Committee



# Human Perception and Control of Vehicle Roll Tilt in Hyper-Gravity

By

Torin Kristofer Clark

DOCTOR OF PHILOSOPHY IN AERONAUTICS AND ASTRONAUTICS  
AT THE  
MASSACHUSETTS INSTITUTE OF TECHNOLOGY

Certified by: \_\_\_\_\_  
Laurence R. Young  
Apollo Program Professor of Astronautics  
Professor of Health Sciences and Technology  
Massachusetts Institute of Technology  
Thesis Committee Chair

Certified by: \_\_\_\_\_  
Kevin R. Duda  
Senior Member of the Technical Staff  
Charles Stark Draper Laboratory, Inc.  
Thesis Committee Member

Certified by: \_\_\_\_\_  
Charles M. Oman  
Director of the Man Vehicle Laboratory, Senior Research Engineer, and Senior Lecturer  
Massachusetts Institute of Technology  
Thesis Committee Member

Certified by: \_\_\_\_\_  
Daniel M. Merfeld  
Professor of Otology and Laryngology  
Harvard Medical School  
Thesis Committee Member



# Human Perception and Control of Vehicle Roll Tilt in Hyper-Gravity

By  
Torin Kristofer Clark

Submitted to the Department of Aeronautics and Astronautics on  
August 21, 2013 in Partial Fulfillment of the Requirements for the Degree of  
Doctor of Philosophy in Aeronautics and Astronautics

## Abstract

Pilots and astronauts experience a range of altered gravity environments in which they must maintain accurate perception and control of vehicle orientation for tasks such as landing and docking. To study sensorimotor function in altered gravity, a hyper-gravity test-bed was produced using a centrifuge. Previous experiments have quantified static tilt perception in hyper-gravity; however, studies of dynamic tilt, such as those experienced by astronauts and pilots, have been entirely qualitative. Current dynamic models of orientation perception cannot reproduce the characteristic perceptions observed in hyper-gravity. The aims of this thesis are to: 1) quantify static and dynamic roll tilt perception in hyper-gravity, 2) study pilot manual control of vehicle roll tilt in hyper-gravity, and 3) modify a dynamic model to predict hyper-gravity orientation perception.

A long-radius centrifuge was utilized to create hyper-gravity environments of 1.5 and 2 Earth G's. In one experiment, over a range of roll tilt angles and frequencies, human subjects' (N=8) perceptions of orientation, in the dark, were assayed with a somatosensory task. Static roll tilts were overestimated in hyper-gravity with more overestimation at higher gravity levels and larger roll angles. Dynamic rotations were also overestimated in hyper-gravity, but generally less so than for static tilts. The amount of overestimation during dynamic rotations was dependent upon the angular velocity of the rotation with less overestimation at higher angular velocities.

In a second experiment, human subjects (N=12) were tasked with nulling a pseudo-random vehicle roll disturbance using a rotational hand controller. Initial nulling performance was significantly worse in hyper-gravity as compared to the 1 G performance baseline. However, hyper-gravity performance improved with practice, reaching near the 1 G baseline over the time course of several minutes. Finally, pre-exposure to one hyper-gravity level reduced the measured initial performance decrement in a subsequent, different hyper-gravity environment.

A modification to a previous dynamic spatial orientation perception model was proposed to allow for the prediction of roll tilt overestimation observed in hyper-gravity. It was hypothesized that the central nervous system treats otolith signals in the utricular plane differently from those out of plane. This was implemented in the model by setting a difference between the linear acceleration feedback gains in and out of the utricular plane. The modified model was simulated and found to accurately predict the static overestimation observed over a wide range of angles and hyper-gravity levels. Furthermore, it simulated the characteristic dependence of dynamic overestimation upon angular velocity with less overestimation at higher angular velocities. The modified model now allows for simulation across a range of altered gravity environments to predict human orientation perception.

We conclude that hyper-gravity results in misperception of static and dynamic roll tilt and decrements in pilot manual control performance. Perception and manual control errors due to altered gravity, such as those observed here in hyper-gravity, may impact the safety of future crewed space exploration missions, in terms of accidents or aborts.

Thesis supervisor:

Laurence R. Young

Apollo Program Professor Astronautics and Professor of Health Sciences and Technology



## Acknowledgements

To all of my advisers, mentors, professors, colleagues, labmates, friends, and family: thank you.

Thank you to all of my committee members for their time and support in helping me with this thesis: my MIT advisor, Larry Young, for supporting me without limit and providing opportunities that I could have only dreamed of; my Draper advisor, Kevin Duda, for practical advice on all matters when I often needed it and keeping me at Draper; Chuck Oman for thought provoking discussions and inspiring me on science; and Dan Merfeld for excellent feedback, promptness, and a remarkable understanding of what is important. Thank you to my thesis readers: Paul Dizio for incredible comments and his wealth of knowledge and Faisal Karmali for guiding me along the way and encouraging me in this field. Thank you to Jon How for serving as my Minor Advisor.

Thank you to Mike Newman and everyone at NASTAR Center for making these experiments happen. Mike championed these experiments as valuable and worthwhile, convinced everyone that they were safe, provided expertise from the science to operating the devices, and put in long hours to get all the little things done. Thank you to Caglar Unlu and Ebubekir Tipi for making the centrifuge do whatever crazy ideas we came up with and Amer Makahleh and Gregory Kennedy for tirelessly monitoring our subjects. I'll never forget all of the little things that made my (roughly) 22 trips to Southampton, PA special: Budget rental cars (hopefully with an E-ZPass), Monster Assault energy drinks, Days Inn and Ramada hotels, the air mattress, Parx Casino, the Jersey Turnpike (particularly the Vince Lombardi rest stop), and of course, Panera Bread.

The Man Vehicle Laboratory at MIT is without question the best lab in the world. I could not have possibly ended up in a more welcoming, fun, happy, inspirational, quirky, or funny laboratory if I had tried, instead of just getting really, really lucky. Thank you to all of my current and past officemates and labmates. Over my time here, there have become too many to list, but you are incredible, will go on to do remarkable things, and simultaneously kept me smiling and inspired for 5 very full years. Nothing was better than Warfish, sports analytics, or rallying the troops to head to the Muddy on Friday. Thank you.

Thank you to everyone else in the MVL that makes this a special place: Alan Natapoff for trivia-laden statistical help, Andy Liu for an open door, and Liz Zotos for solving each and every one of my problems and without question being the best administrative assistant at MIT and probably in the world. Thank you to the rest of the MVL faculty, Dava Newman, Jeff Hoffman, and Julie Shah for all that they bring to the lab. Thank you to Karen Wilcox for her support of all things important.

Thank you to my family and friends back in Colorado, most importantly Allie. You have been incredibly patient and understanding regarding why this has taken so long and tolerated the distance between Cambridge and Colorado. It has only been with your help and support that I gotten this far.

This work would not have been possible without the generous funding support from the National Space Biomedical Research Institute through NASA NCC9-58, Draper Laboratory, and the Boeing MIT Graduate Student Fellowship.

## Table of Contents

Abstract.....	5
Acknowledgements.....	7
Table of Contents.....	8
List of Acronyms .....	10
List of Figures.....	11
List of Tables .....	13
1.0 Introduction.....	14
2.0 Background.....	16
2.1 Orientation Perception Systems .....	16
2.2 G-Excess Illusion Introduction .....	17
2.3 Classic Static G-Excess Illusion Literature.....	18
2.4 Dynamic G-Excess Illusion Literature.....	20
2.5 Recent G-Excess Illusion Literature .....	21
2.6 Otolith Asymmetry Hypothesis .....	21
2.7 Manual Control in Hyper-Gravity.....	22
2.8 Summary and Comments on the Literature .....	22
2.9 G-Excess Illusion in Spatial Orientation Models.....	24
2.10 Coriolis Cross-Coupled Illusion Adaptation Literature .....	25
3.0 Aims and Hypotheses .....	27
4.0 Experiment 1: Orientation Perception in Hyper-Gravity .....	28
4.1 Methods for Experiment 1 .....	28
4.2 Results for Experiment 1.....	39
5.0 Experiment 2: Vehicle Control in Hyper-Gravity.....	55
5.1 Methods for Experiment 2 .....	55
5.2 Results for Experiment 2.....	61
6.0 Modeling Orientation Perception in Hyper-Gravity .....	72
6.1 Characteristics of Hyper-Gravity Perception to Model.....	72
6.2 Proposed Modification to Model .....	72
6.3 Evaluation of Modified Model in Hyper-Gravity .....	78
6.4 Novel Predictions of Modified Model .....	80
6.5 Summary of Model Modifications and Discussion.....	85
7.0 Discussion.....	87
7.1 Summary of Findings.....	87
7.2 Implications for General Altered Gravity Environments.....	88
7.3 Inter-Individual Differences.....	89
7.4 Adaptation to Hyper-Gravity .....	90
7.5 Development of a Pre-Exposure Countermeasure .....	90
7.6 Implications of the Model Modification .....	91
7.7 Limitations .....	91
7.8 Future Work .....	93
8.0 Conclusion .....	95
References.....	96
Appendices .....	106
A. Ormsby and Young Model for Static Perception.....	106
B. Observer Model.....	106
C. MATLAB Code for Experiment 1 Profiles.....	107
D. Differences between Cross-Coupled Adaptation and Centrifuge Paradigms .....	116
E. Forms for Experiment 1 .....	117



F.	Somatosensory Indicator and Verbal Training Data for Experiment 1 .....	127
G.	Cross-Coupled Adaptation Tables and Plots for Experiment 1 .....	133
H.	Upright Perception for Experiment 1 .....	136
I.	Static Tilt Steady-State Perception for Experiment 1 .....	136
J.	Dynamic Tilt and Dynamic Return Perception for Experiment 1 .....	141
K.	Transient Perceptions for Experiment 1 .....	144
L.	MATLAB Code for Experiment 2 Profiles.....	145
M.	Experiment 2 Methods .....	148
N.	Forms for Experiment 2 .....	151
O.	Experiment 2 Training .....	153
P.	Performance in 1 G for Experiment 2 .....	154
Q.	Outlier Trial from Experiment 2 .....	155
R.	Fits of Hyper-Gravity Performance by Trial for Experiment 2 .....	157
S.	Pre-Exposure Effects for Experiment 2 .....	158
T.	Alternate Modifications to Observer Model .....	159
U.	Effect of Frequency on Simulated Static Roll Tilt Perception.....	161
V.	Effect of Time Delay on Dynamic Tilt Perceptions.....	162
W.	Comparison of Dynamic Return Perception to Model Simulation .....	163
X.	Dynamic Tilt Simulation in 1.5 G across a Range of Frequencies .....	164
Y.	Model Prediction of Illusory Acceleration in Hyper-Gravity .....	164
Z.	Modified Observer Model Simulations of Validated 1 G Paradigms .....	165

## List of Acronyms

SD	spatial disorientation
CNS	central nervous system
GIF	gravito-inertial force
SVV	subjective visual vertical
TPAT	tactile perceived attitude transducer
SHP	subjective horizontal body position
SMS	space motion sickness
NASTAR	National AeroSpace Training and Research
ETC	Environmental Techtonics Corporation
IRB	Internal Review Board
COUHES	Committee on the Use of Humans as Experimental Subjects
MSSQ	Motion Sickness Susceptibility Questionnaire
SSQ	Simulator Sickness Questionnaire
RHC	rotational hand controller
RCAH	rate-control-attitude-hold
OVAR	off vertical axis rotation
PIO	pilot induced oscillation

## List of Figures

Figure 1: G-Excess Illusion in Aircraft Flight (Davis, Johnson et al. 2008).....	15
Figure 2: Simplified G-Excess Illusion Explanation .....	17
Figure 3: Comparison of Predictions from Utricular Shear (K=60 deg/G) and Tangent Models of G-Excess Illusion .....	19
Figure 4: Baseline Observer Model Cannot Predict Overestimation of Roll Tilt in Hyper-G.....	24
Figure 5: Experiment 1 Subject Supports .....	29
Figure 6: Centrifuge Motion Paradigm.....	29
Figure 7: Example Profile of Dynamic Roll Rotation .....	31
Figure 8: Example Roll Tilt Profile for a Single Complete Trial .....	31
Figure 9: Example Profile for a Complete Session.....	32
Figure 10: Somatosensory Indicator Operation .....	33
Figure 11: Cross-Coupled Adaptation Protocol Timeline .....	34
Figure 12: Example Somatosensory Indicator Training Profile.....	36
Figure 13: Example Verbal Training Profile .....	37
Figure 14: G-Exposure Profile.....	38
Figure 15: Mean Cross-Coupled Stimulus Intensities .....	39
Figure 16: Example Somatosensory Indicator Perception for 20 degrees and 0.125 Hz.....	40
Figure 17: Summary of Somatosensory Indicator Perception across All Angle and Frequency Combinations.....	42
Figure 18: Mean Upright Perception .....	43
Figure 19: Mean Static Tilt Steady-State Perception.....	44
Figure 20: Comparison of Current Static Tilt Steady State Perception to Utricular Shear and Tangent Models .....	45
Figure 21: Comparison of Current Static Tilt Steady State Perception to Ormsby and Young Models.....	46
Figure 22: Comparison of Current and Prior Static Tilt Steady State Perception to Modified Utricular Shear Model.....	47
Figure 23: Normalized Slope of Dynamic Rotations as a Function of G-Level by Angle and Frequency.....	49
Figure 24: Dynamic Tilt Model Predictions (Normalized).....	51
Figure 25: Static Tilt Transient Growth.....	51
Figure 26: Post-Return Transient Perception Delay .....	52
Figure 27: Example Roll Tilt Disturbance Profile .....	56
Figure 28: Rotational Hand Controller .....	57
Figure 29: Example Complete Testing Session for Experiment 2.....	58
Figure 30: Performance Decrements on First Trial in Hyper-Gravity.....	62
Figure 31: Hyper-Gravity Performance by Trial .....	63
Figure 32: Subjective Performance and Workload Reports in Hyper-Gravity by Trial .....	63
Figure 33: Hyper-Gravity Performance by Segment .....	64
Figure 34: Effect of Pre-Exposure on Hyper-Gravity Performance on First Trial .....	66
Figure 35: Cross-Coupled Illusion Intensity Reports.....	67
Figure 36: Static Observer Model (Only Otolith Pathways).....	73
Figure 37: Utricular Plane Coordinate Frame Rotation .....	75
Figure 38: Proposed Modification to Static Observer Model (Only Otolith Pathways).....	76
Figure 39: Static Perception in Modified Model with Varying Kau Values.....	77
Figure 40: Comparison of Static Tilt Steady-State Experimental Perception and Modified Observer Model Predictions .....	78
Figure 41: Comparison of Static Tilt Steady-State Previous Experimental Perception and Modified Observer Model Predictions .....	79

Figure 42: Comparison of Dynamic Roll Tilt Experimental Perception and Modified Observer Model Predictions ..... 80

Figure 43: Model Predicted Static Perception in Altered Gravity ..... 81

Figure 44: Model Predicted Static Roll Perception in Hypo-Gravity ..... 82

Figure 45: Model Predicted Dynamic Perception in 2.0 G across a Range of Frequencies ..... 83

Figure 46: Model Predicted Static Pitch Perception Compared to Previous Data (Correia, Hixson et al. 1965; Correia, Hixson et al. 1968)..... 84

## List of Tables

Table 1: Previous studies on G-Excess illusion .....	22
Table 2: Centrifuge Motion Paradigm Parameters Required for Testing G-Levels .....	29
Table 3: Summary of Independent and Dependent Variables for Experiment 1 .....	34
Table 4: Linear Static Tilt Steady-State Perception Model Results.....	44
Table 5: Modified Utricular Shear Model Results.....	47
Table 6: Dynamic Rotation Perception Model Results.....	50
Table 7: Roll Tilt Disturbance Parameters.....	55
Table 8: Four Orders of Sessions.....	59
Table 9: Summary of Independent and Dependent Variables for Experiment 2 .....	59
Table 10: Exponential Decay Fits for Hyper-Gravity Performance versus Segment .....	65
Table 11: Summary of Modified Model Parameters.....	77

## 1.0 Introduction

Pilots must maintain an accurate perception of vehicle orientation when manually flying aircraft or spacecraft. Significant misperceptions in vehicle orientation, or spatial disorientation (SD) (Gillingham and Previc 1996), may lead to incorrect pilot control inputs. Pilot spatial disorientation (Young 2003) remains a serious concern and a leading cause of both airplane (Bellenkes, Bason et al. 1992; Cheung, Money et al. 1995; Knapp and Johnson 1996; Neubauer 2000) and helicopter (Durnford, Crowley et al. 1995; Braithwaite, Groh et al. 1997; Braithwaite, Durnford et al. 1998; Curry and McGhee 2007) accidents. Disorientation and associated sensorimotor problems fortunately have not yet resulted in a fatal spacecraft accident (Thelen, Wood et al. 2010; Campbell and Garbino 2011), but evidence suggests that disorientation impacts performance and is a serious threat (McCluskey, Clark et al. 2001; Paloski, Oman et al. 2008; Moore, Dilda et al. 2011). A combination of unusual motions and novel environments are routinely experienced during piloted aircraft and spacecraft flight which contribute to misperceptions of vehicle orientation and may lead to accidents.

Novel motions and environments often result in misperceptions and disorientation. Several examples include rotating environments (Graybiel, Clark et al. 1960; Young, Hecht et al. 2001; Brown, Hecht et al. 2002; DiZio and Lackner 2002; Mast, Newby et al. 2002; Lackner and DiZio 2003), large tilts (Aubert 1861; Mueller 1916), off-vertical axis rotation (Merfeld, Young et al. 1993; Haslwanter, Jaeger et al. 2000; Vingerhoets, Medendorp et al. 2006; Vingerhoets, Van Gisbergen et al. 2007), and optokinetic stimulation (Zupan, Peterka et al. 2000). The orientation sensory system and central nervous system (CNS) misinterpret the novel sensory cues in these environments. In aerospace applications pilots are likely to experience a variety of novel motions which may lead to disorientation (Young 2003). In particular, altered gravity environments occur in both aircraft and spacecraft flight. These include microgravity (Benson, Guedry et al. 1997; Oman, Howard et al. 2003), hypo-gravity (Dyde, Jenkin et al. 2010; de Winkel, Clement et al. 2012; Harris, Jenkin et al. 2012), and hyper-gravity. In order to develop countermeasures to limit spatial disorientation in these altered gravity environments, we must understand how different gravity levels influence the pilot's perception and control of vehicle orientation. Total vehicle control is coupled with vehicle orientation in most aerospace vehicles. For example, in an aircraft a roll bank will initiate a turn while in a planetary landing vehicle with a fixed descent engine thruster, a roll tilt will create horizontal acceleration. While the full range of altered gravity levels are of interest, here we will study hyper-gravity, since it is most readily producible here on Earth.

One common hyper-gravity scenario is when an aircraft pilot is in a coordinated banked turn and is exposed to an increased gravito-inertial field. While in the turn, if the pilot makes a head movement, for example to view above or behind his/her aircraft, it can result in an illusory sensation of aircraft rotation. The head tilt, relative to the external world, is perceived as greater than that which is actually performed and the excess is attributed to aircraft rotation (Figure 1).

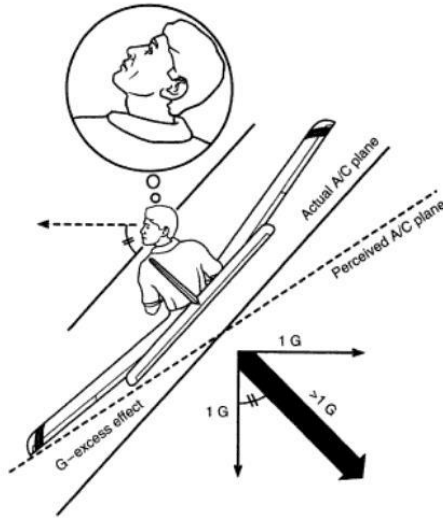


**Figure 1: G-Excess Illusion in Aircraft Flight (Davis, Johnson et al. 2008)**

The misperception can result in an incorrect control response of banking the aircraft in the opposite direction in an effort to counter the misperceived rotation. Incorrect control responses stemming from misperceptions can lead to dangerous maneuvers and increase the potential for an accident or an abort. This illusion is known as the “G-Excess Illusion” and is conceptually defined as follows: in a greater than Earth-G gravito-inertial field, tilts relative to the resultant gravito-inertial direction may be perceived as greater than they actually are.

The G-Excess illusion has traditionally been considered primarily for application to aircraft pilots. However, presumably it applies to spacecraft pilots and passengers as well when they encounter altered gravity environments. Shuttle astronauts when returning from extended microgravity exposure often report illusory rotation sensations when making pitch or roll head tilts during hyper-gravity reentry (Paloski, Oman et al. 2008). Furthermore, during planetary landings, in manual control modes (Bilimoria 2009; Duda, Johnson et al. 2009; Mueller, Bilimoria et al. 2009; Duda, Johnson et al. 2010) astronauts will need to accurately perceive vehicle orientation. The vehicle will roll and pitch during landing trajectories in order fly across the planetary surface. In the altered gravity of different planetary environments, the vehicle tilts may be disorienting in much the same way as the G-Excess illusion. In particular, there will likely be discrepancies between visual and vestibular responses as compared to what would be expected from the same motions on Earth. Spatial disorientation during a piloted lunar or Martian landing, if it results in an accident or abort, would be catastrophic. Hyper-gravity is also a unique environment for studying how the CNS integrates multiple, often conflicting, sensory cues.

To address these concerns, a better understanding of how hyper-gravity influences orientation perception in humans is necessary. Furthermore, we must evaluate how any misperceptions induced by hyper-gravity affect a pilot’s ability to control a vehicle, such as an aircraft or spacecraft. Pilot-in-the-loop tasks, such as landing, require continuous assessment of the vehicle state, in particular vehicle orientation, and the application of the appropriate control responses. Thus, we must focus on perception and control during and shortly after dynamic, active rotations. We aim to study how the perception and control of vehicle roll tilt is affected by hyper-gravity.

## 2.0 Background

### 2.1 Orientation Perception Systems

Spatial orientation refers to one's perception of body position relative to a reference frame, generally the surface of the Earth, or for space applications, possibly another planet. Spatial disorientation is traditionally defined as a "failure to correctly perceive attitude, position, or motion" of the vehicle (Gillingham and Previc 1996). There are many factors that influence spatial disorientation (see (Young 2003) for a review), but the cause is always an inability to properly integrate and interpret sensory signals. Sensory signals providing information to the CNS regarding orientation come from a variety of sources. In piloted flight, nominally the instrument panel is the dominant source of state information. However, inexperience, workload, and distractions may cause the pilot to disregard this information and rely more heavily on other sources. A key source of orientation signals is the vestibular system. Located in the inner ear, the vestibular system is comprised of the semicircular canals and the otolith organs. The semicircular canals, across the frequency range experienced in daily life, transduce angular velocity information to the brain (Fernandez and Goldberg 1971; Goldberg and Fernandez 1971; Goldberg and Fernandez 1971). The otolith organs function as linear accelerometers and signal gravito-inertial force (GIF) (Fernandez and Goldberg 1976; Fernandez and Goldberg 1976; Fernandez and Goldberg 1976). GIF ( $\vec{f}$ ) is the vector difference between gravity ( $\vec{g}$ ) and head acceleration ( $\vec{a}$ ), as given in Equation 1.

$$\vec{f} = \vec{g} - \vec{a} \quad (1)$$

Gravito-inertial force is actually a "specific" force (i.e. force per unit mass), but for simplicity it will be referred to simply as GIF. According to Einstein's equivalence principle (Einstein 1908), the otolith organs cannot disambiguate changes in head acceleration (i.e. translation) and changes in gravity (i.e. tilt). To make accurate perceptions from the ambiguous otolith information, the CNS uses information from additional sensory sources, or "sensory integration" (Zupan, Merfeld et al. 2002). In particular, the rotational information from the semicircular canals can be used to disambiguate gravity (i.e. tilts) from accelerations (i.e. translations). The visual system provides relative attitude and position information, as well as angular and linear velocity cues, however it will not be considered in detail here. For a complete review of visual perception, see (Cornsweet 1970). In addition, somatosensory sensors such as muscle spindles and pressure sensors in the skin (Lackner and Graybiel 1978; Lackner and Graybiel 1978) and even auditory cues can play a role in orientation perception. Some evidence supports the presence of a graviceptor located in the abdominal organs (Mittelstaedt 1995; Mittelstaedt 1996). Lastly, subjects tend to make errors toward their longitudinal body axis when they are tilted relative to gravity (Dyde, Jenkin et al. 2006), which suggests the presence of an "idiotropic vector" that attracts the subjective vertical (Mittelstaedt 1983). While the orientation perception system normally provides accurate estimates of orientation in everyday life, this is not always the case during the motions experienced in aircraft and spacecraft. These unique and often novel motions can result in illusions or spatial disorientation. Whether a specific set of motions, in a certain environment, results in spatial disorientation is often



modulated by an additional set of situational factors. These may include an individual’s experience, visual conditions, shifting reference frames, head movements, and workload.

## 2.2 G-Excess Illusion Introduction

The misperceptions associated with the G-Excess Illusion are generally attributed to a misinterpretation of otolith signals. A simplified explanation of the illusion is given in Figure 2. This explanation is effectively the “utricle shear hypothesis”, which is further elaborated upon in Section 2.3.

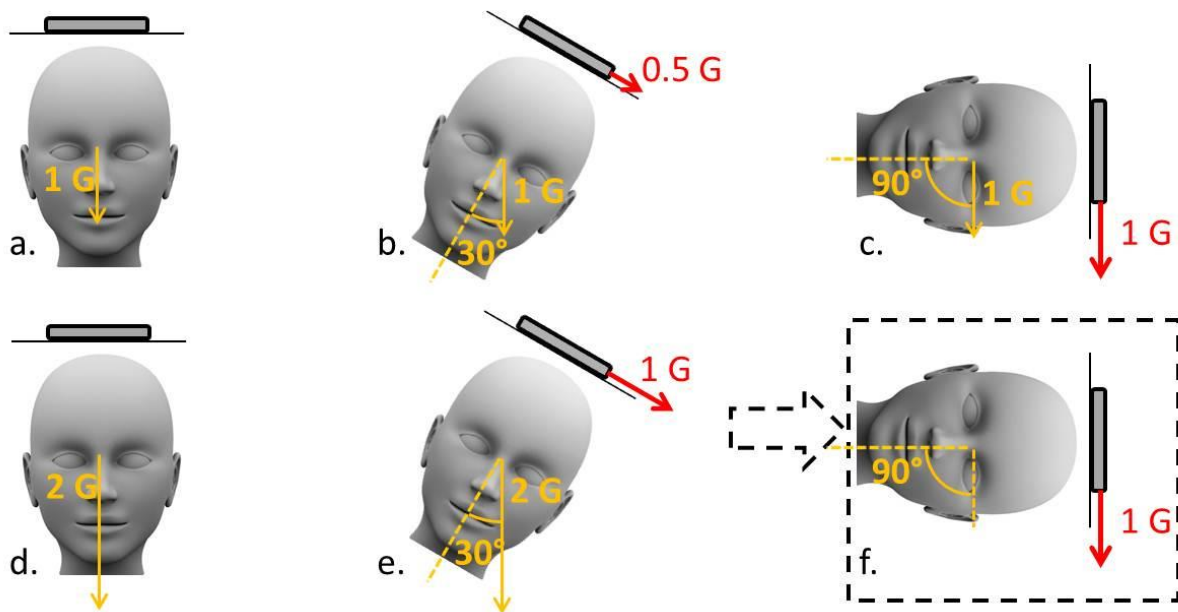


Figure 2: Simplified G-Excess Illusion Explanation

Above the human head figurines in Figure 2 are schematic representations of the GIF acting on the otoconial membrane of an otolith organ. In Figure 2a, when the head is upright on Earth (1 G’s) there is no shear force on the simplified otolith organ. In Figure 2b, a head tilt of 30 degrees creates a shear force of 0.5 G. A 90 degree head tilt corresponds to a shear force equal to 1 G (Figure 2c). Now consider the same head tilts in a hyper-gravity environment, such as 2 G’s. A head tilt of 30 degrees now results in a shear force of 1 G (Figure 2e). If the CNS interprets the otolith signal as if it were produced in a 1 G environment, this could cause the 30 degree tilt to be misperceived as a 90 degree tilt (Figure 2f). This is a simplified explanation of the illusion since there are otolith organs in both left and right inner ears and each is composed of utricular and saccular components (Guedry 1974). Each of the utricles and saccules has many neurons each of which are sensitive in different polarized directions (Lowenstein and Roberts 1949; Fernandez and Goldberg 1976; Fernandez and Goldberg 1976; Fernandez and Goldberg 1976). In addition, the CNS presumably integrates sensory information from a variety of sources in order to estimate the direction of gravity and the associated orientation of the head. Nonetheless, it is clear that the magnitude of gravity influences utricular otolith signals and this can result in misperceptions of tilt. Specifically, hyper-gravity may cause overestimation of roll tilt.

### 2.3 Classic Static G-Excess Illusion Literature

The G-Excess Illusion was first studied in detail during the 1960's using short-radius centrifuges (Noble 1949) to produce a hyper-gravity environment. It should be noted that here and throughout, "hyper-gravity", as we refer to it, does not actually have an increase in the magnitude of "gravity". Earth's gravitational force obviously remains constant, however, a sustained linear acceleration is provided such that the net GIF is greater than 1 Earth G. For simplicity, these paradigms will be referred to as "hyper-gravity" environments. In the centrifuge hyper-gravity paradigms, subjects were seated in the dark in a cab at the end of the centrifuge arm with their head tilted relative to the GIF. The centrifuge was then spun to the required speed to produce the desired GIF. Subjects reported their perception of roll tilt using a common technique called subjective visual vertical (SVV) (Aubert 1861; Tarnutzer, Fernando et al. 2012). In this task, a subject is presented with an illuminated line which they can rotate using a hand controller until it appears aligned with the vertical. Several studies at the time (Woellner and Graybiel 1959; Miller 1962; Colenbrander 1963) also measured subjects' ocular counter-rolling (rotation of the eye in response to roll tilt). Since vestibular signals drive ocular reflexes (see (Robinson 1981) for a review), recording eye movements can be a quantitative method to measure vestibular responses. Colenbrander found that in hyper-gravity environments subjects overestimated their roll angle using SVV and had larger ocular counter-rolling, consistent with the G-Excess Illusion. However, there is evidence that vestibular ocular reflexes qualitatively differ from perceptual responses (Merfeld, Park et al. 2005; Merfeld, Park et al. 2005), though they may influence the perceptual responses independent of the direct vestibular effects.

At nearly the same time, another experiment (Schone 1964) confirmed Colenbrander's perceptual findings. In addition, Schöne studied static pitch tilts using a variant of SVV. In hyper-G subjects perceived themselves more pitched back (nose-up). To explain these findings, Schöne proposed the "utricular shear hypothesis," which states that the perceived tilt is linearly proportional to the shear force in the plane of the utricles. For roll rotations, the utricular shear force is simply the product of the gravity-level (G) and sine of the actual roll angle ( $\theta_{act}$ ). Equation 2 states the utricular shear hypothesis for roll tilt perception ( $\theta_{per}$ ). The free parameter (K) was initially estimated as 64 degrees/G based upon pitch perception measures (Schone 1964), however later data for roll appear to support an estimate of 50-60 degrees/G (Schone and Parker 1967; Schone, Parker et al. 1967). Others (Miller and Graybiel 1966) further confirmed the previous finding of overestimation in static perception of roll angle in hyper-gravity, but also studied subjects with vestibular defects.

$$\theta_{per} = K * G * \sin(\theta_{act}) \quad (2)$$

The most complete G-Excess illusion study from the 1960's (Correia, Hixson et al. 1965; Correia, Hixson et al. 1968), studied pitch and roll angles ranging from +/- 30 degrees and G-levels up to 2 G's. In pitch, increasing G-levels resulted in increasingly large illusory pitched up estimations of tilt at all angles except for 30 degrees pitched nose down which was estimated fairly accurately at all G-levels tested. From morphological studies, it is known that when the head is pitched nose down by ~25-30

degrees relative to the GIF direction, the GIF is aligned perpendicular to the dominant plane of the utricles (Corvera, Hallpike et al. 1958; Curthoys, Betts et al. 1999). In this orientation, increasing the magnitude of the GIF does not create an increase in the shearing force in the utricular plane. Note that the concept of the utricular “plane” is an abstraction since the actual utricular surface is curved. In roll, increasing G-levels resulted in an overestimation of roll angle at all angles except for upright. Thus in both pitch and roll, a G-Excess illusion is prevalent. Correia et al.’s data, collected over a wider range of conditions, did not fit Schöne’s sine model (utricular shear hypothesis). Instead they found a tangent model to be a better empirical fit (Equation 3).

$$\theta_{per} = \text{atan}(G * \tan(\theta_{act})) \quad (3)$$

They hypothesized that the tangent model was the result of the “utricular compression component” influencing the otolith response. Alternatively Schöne et al. proposed the utricular shear hypothesis retains validity, but approaches a physiological limit at shear force magnitudes greater than 1 G (Schone and Parker 1967; Schone, Parker et al. 1967). Figure 3 provides a comparison of the predictions for the two models, relative to veridical perception of roll tilt.

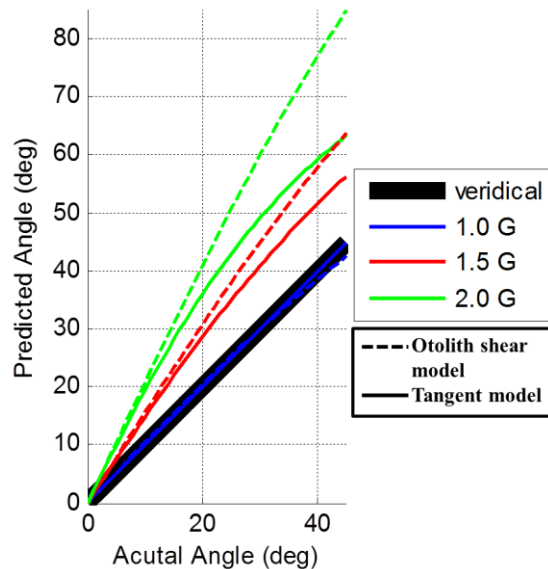


**Figure 3: Comparison of Predictions from Utricular Shear (K=60 deg/G) and Tangent Models of G-Excess Illusion**

Ormsby et al. (Ormsby and Young 1976) proposed yet another model for static orientation perception, which attempted to fit Schöne’s data. The model employed a nonlinear transformation of the GIF component perpendicular to the utricular plane. While the theoretical basis is different, the model predictions are qualitatively similar to the utricular shear and tangent models (see Appendix A for details).

The G-Excess illusion is closely related to the well-studied “elevator illusion” (Whiteside 1961) in which stationary visible objects appear to rise in hyper-gravity (Graybiel, Clark et al. 1947; Clark, Graybiel et al. 1948; Roman, Warren et al. 1963; Cohen 1970; Cohen 1970). This response corresponds

to an upright subject having a perception of being pitched nose up in hyper-gravity (Schone 1964; Correia, Hixson et al. 1968). In this paradigm, there is evidence that neck proprioception is critical to perceptual reports (Cohen 1973). The elevator illusion can be considered a subset of the G-Excess illusion, in which the subject is upright and only pitch perception is assayed using a variant of SVV (e.g. subject adjusts an illuminated point or line until it appears at the horizon).

The 1960's studies showed that for given gravity direction (i.e. tilt angle), the force magnitude influences subjective static perception of orientation. Specifically, hyper-gravity causes overestimation of roll tilt with higher gravity-levels generally causing greater overestimation. It should be mentioned that statistical tests were not applied in the majority of these studies and variability was generally not shown.

## **2.4 Dynamic G-Excess Illusion Literature**

All of the studies performed in the 1960's focused on the static or steady-steady G-Excess Illusion. Subjects waited at least 30 seconds in a given orientation to report their perception, ignoring the period during or shortly after changes in orientation. The focus on static perception was due to a methodological limitation. In these studies, the hyper-gravity environment was produced using short-radius centrifuges. To produce higher force levels the centrifuge must spin at faster rates. However, at high centrifuge rotation rates, out-of-plane head or whole-body rotations will cause a secondary illusion known as the Coriolis cross-coupled illusion (Graybiel, Clark et al. 1960; Guedry and Montague 1961; Melville Jones 1970). For a review of the Coriolis cross-coupled illusion, see (Guedry 1974) pp. 120-128. The secondary cross-coupled illusion prevented the study of hyper-gravity perception during or shortly after rotations, limiting researchers to measuring perceptions in static tilts carried out at constant centrifuge rotation speed.

In order to produce a hyper-gravity environment with limited rotational angular velocity a larger radius of rotation is required. In 1973, the first experiment (Gilson, Guedry et al. 1973) to study the G-Excess illusion using a high performance aircraft in a large coordinated turn was performed. This allowed for a 2 G environment to be achieved while limiting the cross-coupled illusion to near threshold. Within the aircraft, subjects then performed a series of active head tilts. There was a 100% occurrence of the illusion amongst subjects in the pitch plane. Subjects verbally reported qualitative illusory sensations after landing so it was not possible to quantify the magnitude or dynamics of the illusion. This study also found significant inter-subject variability. The authors attributed this to the important factor of the speed of the head pitch, which was not well controlled.

A later review of this work (Guedry and Rupert 1991) focused on the theoretical differences between the dynamic and static components of the G-Excess illusion. A given head tilt in a hyper-gravity field causes the otolith-membrane to not only displace farther than in a normal 1 G field, but also to move faster. They postulated that this will elicit signals from displacement-sensitive and rate-sensitive (Xerri, Barthelemy et al. 1987) otolith afferents that will differ from those that would be elicited from the same head tilt in 1 G. Both the displacement-sensitive and rate-sensitive signals must be integrated with cues from the semicircular canals and an expected response from the head tilt. Guedry and Rupert argue that the dynamic cues create conflicting inputs which introduce confusion for the subject and increase

variability in reporting. In conclusion, Guedry and Rupert state that head tilt rate is critical and further investigation is necessary into the dynamic component of the G-Excess illusion.

## 2.5 Recent G-Excess Illusion Literature

Chelette et al. studied the G-Excess Illusion as it commonly occurs for pilots of high performance aircraft (Chelette, Martin et al. 1995; Chelette 2001). In high performance aircraft, pilots often perform a head movement called “check six” in which they look over their shoulder to identify trailing aircraft. This head rotation can cause spatial disorientation and an illusory sensation of aircraft rotation. While previous experiments primarily used SVV, here perceptions were recorded by having subjects hold their right hand in an orientation they believed to be level and then a gimbal device which encased the hand would record the position (the tactile perceived attitude transducer or TPAT). Testing on a centrifuge and recording only static perceptions, subjects reported illusory tilt that increased for higher G levels and larger tilt angles. Another recent study used verbal reports and confirmed (Jia, Yu et al. 2002) subjects overestimate their tilt angle relative to the GIF direction in hyper-gravity.

There have been several recent studies of human perception during changes in the gravito-inertial environment associated with centrifuge spin-up. During spin-up, transient perceptions depend upon semicircular canal cues (Merfeld, Park et al. 2005). In particular, during spin-up for gondola centrifugation (i.e. GIF aligned with the subject’s body or “z-axis”), canal cues cause perceptions that transition from Earth-vertical to aligned near the net GIF (Tribukait and Eiken 2005; Tribukait and Eiken 2005). This transient effect of the canal cue has been demonstrated for roll tilt perception (Tribukait and Eiken 2006) as well as for pitch (Tribukait and Eiken 2006), and is also impacted by the subject’s flight experience (Tribukait and Eiken 2012). However, these studies focus on the transient effects during centrifuge *spin-up* and do not address orientation perception once in a *constant* hyper-gravity environment.

Lackner, DiZio, and colleagues performed the first and only studies on yaw tilt perception in altered gravity environments (e.g. 1.8 G and microgravity during parabolic flight). In these studies, recumbent subjects were tilted about their yaw axis (i.e. foot to head) and reported perceived direction of vertical by aligning a vertical bar with two hands. While in microgravity subjects made large perceptual errors, in hyper-gravity there was *no* significant difference compared to 1 G static perceptions (Bryan, Bortolami et al. 2007). Furthermore, estimates of angular displacement during short duration (e.g. ~2 second) yaw rotations were similar in hyper-gravity as in 1 G (Lackner and DiZio 2009). These results suggest that the G-Excess illusion does not occur for recumbent yaw tilts, as it does for pitch and roll.

## 2.6 Otolith Asymmetry Hypothesis

While the “otolith asymmetry hypothesis” has been proposed to explain space motion sickness (SMS) in microgravity (Diamond and Markham 1988; Diamond, Markham et al. 1990; Diamond and Markham 1991), it may also have applications to perceptions in hyper-gravity and is therefore briefly described here. The otolith asymmetry hypothesis proposes that there are likely differences in the masses of the otolithic membranes (Lychakov and Rebane 2005) or number of hair cells in the left and right ear. The differences will likely lead to asymmetries in discharge rates between the two sides in response to

identical GIF stimulation. In 1 G it is hypothesized that the CNS compensates for these asymmetries adequately, however in altered gravity environments the asymmetry is presumably not well compensated for (Diamond and Markham 1988; Diamond, Markham et al. 1990). In microgravity, it has been hypothesized that the uncompensated asymmetries are a form of sensory conflict and lead to SMS. In particular, they hypothesis postulates that individual astronauts with larger asymmetries should experience more extreme symptoms of SMS (Diamond and Markham 1992). In hyper-gravity it is unclear what the otolith asymmetry hypothesis would predict. Indeed any asymmetries presumably would be not well compensated for in hyper-gravity. This could manifest as subject-dependent left/right biases. However, data from prior hyper-gravity static perception experiments have not provided evidence to support this hypothesis (Schone 1964; Correia, Hixson et al. 1965; Correia, Hixson et al. 1968).

## 2.7 Manual Control in Hyper-Gravity

To our knowledge how the misperceptions in orientation in hyper-gravity might impact a dynamic pilot manual control task (such as flying a plane or planetary lander), have not be quantitatively studied. Glasauer and Mittelstaedt (Glasauer and Mittelstaedt 1992) studied the effect of gravitational level on perception of orientation using a reporting technique called subjective horizontal body position (SHP). In SHP, subjects lay on their side and adjusted their roll on a tilt board until they felt horizontal. From their data, they hypothesized that in addition to vestibular information, subjects use trunk localization information to estimate tilt (Mast and Jarchow 1996; Jarchow, Wirz et al. 2003). In contrast to SVV, TPAT, or static verbal measures, in SHP subjects do manually control body position using feedback. However, SHP is a pseudo-static task in that subjects adjust their position slowly, then check if they feel horizontal, then re-adjust. How hyper-gravity impacts a dynamic pilot control task remains an open question.

## 2.8 Summary and Comments on the Literature

A summary of the methods, conditions, and scope of previous research on the G-Excess Illusion is given in Table 1.

**Table 1: Previous studies on G-Excess illusion**

Study	G production mechanism		Rotation mechanism		Rotation Type		Axis of Rotation			Time frame		Response Type
	Centrifuge	Airplane	Head	Cab	Active	Passive	Pitch	Roll	Yaw	Dynamic	Static	
Colebrander 1963	X		X			X		X			X	SVV
Schöne 1964, 1967a,b	X		pitch	roll		X	X	X			X	SVV/Visual point
Miller and Graybiel 1966	X			X		X		X			X	SVV
Correia et al. 1965, 1968	X			X		X	X	X			X	SVV/Visual line
Gilson et al. 1973 Guedry et al. 1991		X	X		X		X	X		X	X	Qualitative verbal
Glasauer and Mittelstaedt 1992	X			X	X			X			X	SHP

Chelette et al. 1995, 2001	X		X	X	X	X	X				X	TPAT
Jia et al. 2002	X			X		X		X			X	Verbal
Bryan et al. 2007		X		X		X			X		X	Vertical indicator
Lackner and DiZio, 2009		X		X		X			X	X		Vertical indicator

The review of the G-Excess Illusion literature given in Table 1 reveals two areas that warrant further study. Only one set of studies (Gilson, Guedry et al. 1973; Guedry and Rupert 1991) considered perception of orientation *during* roll or pitch rotations in hyper-gravity. The authors hypothesized that how fast subjects tilted their heads, or the rate of tilt, had a substantial influence on the magnitude and intensity of the G-Excess Illusion and recommended further study. The dynamic portion of the G-Excess Illusion is critical to aerospace applications since either head or vehicle tilts are likely to occur at relatively high rates. To our knowledge no study has quantitatively measured subject perception during roll or pitch tilts in hyper-gravity, nor how tilt rate influences the G-Excess illusion.

Secondly, only a limited subset of studies has attempted to study the G-Excess Illusion when active tilts are made. It has been hypothesized (Oman 1982; Merfeld, Young et al. 1993) that the CNS uses neural “internal models” to predict expected sensory signals. When “active” movements (e.g. subject tilts their head or applies a control input to rotate the vehicle) are made the CNS sends a parallel “efference-copy” (Von Holst and Mittelstaedt 1950; Von Holst 1954) of the motor command which is incorporated into these models. Presumably pilots develop an internal model relating controller inputs to vehicle dynamics. However, during “passive” movements (e.g. where the motion device tilts the subject without their input) only sensory information is integrated to develop perceptions. The “internal model” hypothesis would predict potentially different perceptions to the same motions when they are actively or passively generated. Recent studies have shown evidence that the signals from “vestibular only” (VO) neurons depend on whether the motion is actively or passively generated (Boyle, Belton et al. 1996; McCrea, Gdowski et al. 1999; Roy and Cullen 2001; Roy and Cullen 2004). Thus far neurons demonstrating active vs. passive differences have been identified for SCC yaw responses and otolith translations, but presumably similar neurons exist for tilts responses as well. In aerospace applications, most of the tilt rotations will be actively generated, either through pilot head tilts or pilot controlled vehicle rotations. However, in autoflight the pilot will be passively tilted while monitoring and preparing for manual takeover.

The challenge in studying orientation perception during active tilt is that the subject must simultaneously control their tilt and report a perception. Gilson et al. (Gilson, Guedry et al. 1973) accomplished this by having subjects qualitatively report illusory sensations. Others (Glasauer and Mittelstaedt 1992; Chelette, Martin et al. 1995; Chelette 2001) have had subjects only report their perceptions well after the active tilt was completed (i.e. static component). An indirect way to quantitatively study perceptions during active tilt is in a manual control task (Dichgans, Held et al. 1972; Zacharias and Young 1981; Huang and Young 1988; Merfeld, Polutcho et al. 1996). In this task the subject attempts to remain upright in response to a tilt disturbance using a control inceptor. In order for the subject to generate effective control responses, accurate perception of tilt is required. A manual

control task is also highly applicable to aircraft and spacecraft systems since it tests how misperception of orientation can lead to incorrect control responses, potentially posing a safety risk.

## 2.9 G-Excess Illusion in Spatial Orientation Models

A variety of mathematical models have been proposed for the mechanisms of the vestibular system and spatial orientation perception (Mayne 1974; Borah, Young et al. 1978; Borah, Young et al. 1988; Green and Angelaki 2004; Laurens and Droulez 2007; Selva 2009). One of the better known models is based upon the engineering Observer system (Luenburger 1971). This family of models (Merfeld, Young et al. 1993; Merfeld and Zupan 2002; Zupan, Merfeld et al. 2002; Vingerhoets, Van Gisbergen et al. 2007; Newman 2009; Rader 2009; Rader, Oman et al. 2009; Vingerhoets, De Vrijer et al. 2009) can predict a variety of common illusions using only a small set of free parameters. However, the Observer model does not predict a static G-Excess illusion. In fact, at any hyper-gravity level the Observer model will predict a veridical perception of static tilt angle. We have simulated the model with a 20 degree roll rotation to the right over 8 seconds, a static tilt for 30 seconds, and a rotation back to upright over another 8 seconds at gravity levels of 1 G and 2 G. The different G-levels are produced by accelerating upwards at 0 and 1 G's, respectively. Obviously this would not be reproducible in a motion-base simulator because the range of motion would be exceedingly large; however it is convenient for simulation purposes because there are no secondary illusions that result from this “pure” acceleration. These simulations are done “in the dark” with all of the visual pathways deactivated and with the internal magnitude of gravity set to 1 G (see Appendix B and (Newman 2009) for details on Observer model parameters).

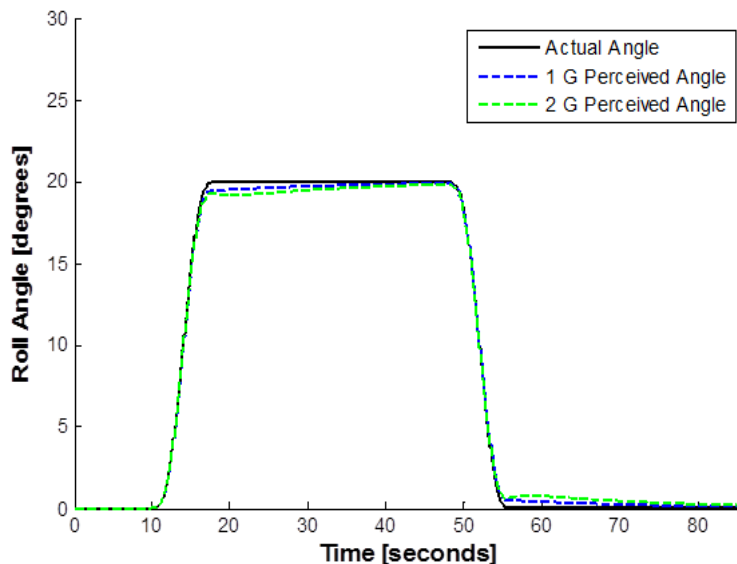


Figure 4: Baseline Observer Model Cannot Predict Overestimation of Roll Tilt in Hyper-G

As seen in Figure 4, while the perception is slightly altered by the hyper-G environment, it clearly does not result in either a dynamic or static overestimation of roll tilt. In addition, in hyper-gravity the Observer model will predict an illusory static acceleration upward (see Appendix Y). Large translational motions are not generally reported by subjects in prior hyper-gravity experiments. To our knowledge, no



dynamic model of spatial orientation predicts the G-Excess Illusion. However, Bortolami et al. (Bortolami, Rocca et al. 2006) have developed a model that predicts static orientation perceptions in altered gravity environments using vestibular and tactile cues as inputs to the model. In addition, Dai et al. (Dai, Curthoys et al. 1989) constructed a static model loosely based upon physiological mechanisms to predict perceptions over a range of altered gravity levels and orientations. Both models build upon the concept of a nonlinear otolith response (Ormsby and Young 1976), which has been applied to an Observer-like model to predict dynamic eye movements (Haslwanter, Jaeger et al. 2000). Parallel to the nonlinear otolith model is the concept of an “idiotropic vector” (Mittelstaedt 1983; Mittelstaedt 1986; Mittelstaedt 1989), which is an internal mechanism which drives perceptions in the direction of a person’s own longitudinal axis. Existing dynamic models of spatial orientation will require modification, either in parameters or structure, in order to predict perception in hyper-gravity. It is critical that any modifications maintain the model’s functionality in the well validated 1 G environment.

## **2.10 Coriolis Cross-Coupled Illusion Adaptation Literature**

Previous centrifuge studies have been limited to the static portion of the G-Excess Illusion, since out-of-plane rotations will result in the secondary Coriolis cross-coupled illusion (see (Guedry 1974) pp. 120-128 for a review). Two advances have made it possible to study the dynamic portion of the G-Excess Illusion using a centrifuge. First, long-radius (i.e. 6+ meters) centrifuges have become more readily available. With a larger radius of rotation, a given gravity-level can be produced using lower rotation speeds. This reduces the intensity of the cross-coupled illusion since it is dependent upon centrifuge rotation rate (Gray, Crosbie et al. 1961; Guedry and Montague 1961). Secondly, recent work has shown that humans can adapt to the cross-coupled illusion with repeated exposure (Young, Hecht et al. 2001; Brown, Hecht et al. 2002; DiZio and Lackner 2002; Hecht, Brown et al. 2002; Mast, Newby et al. 2002; Lackner and DiZio 2003; Young, Sienko et al. 2003; Adenot 2004; Bruni 2004; Lackner and DiZio 2005; Cheung, Hecht et al. 2007; Jarchow and Young 2007; Elias, Jarchow et al. 2008; Garrick-Bethell, Jarchow et al. 2008; Mateus 2008). Adaptation protocols have been developed (Bruni 2004; Cheung, Hecht et al. 2007; Jarchow and Young 2007), after which the intensity of the cross-coupled illusion is substantially decreased. For relatively low centrifuge rotation rates (< 15 rpm), some subjects report no sensation of the illusion. To prevent pre-exposure to the G-Excess Illusion during the cross-coupled adaptation protocol it can be applied with the subject located at the center of rotation. Many of the early adaptation protocols (Graybiel, Clark et al. 1960; Graybiel, Deane et al. 1968; Graybiel and Knepton 1972; Graybiel 1973; Brown, Hecht et al. 2002; Hecht, Brown et al. 2002; Young, Sienko et al. 2003) tended to induce substantial motion sickness. In one study, approximately 25% of subjects were unable to complete the protocol despite pre-screening individuals to exclude those who were highly susceptible to motion sickness (Brown, Hecht et al. 2002). However, an alternative is available using a “threshold-based adaptation protocol”. The intensity of the illusion is modulated, usually by adjusting the cab rotation rate, to keep it near the subject’s threshold level. Repeated exposure of a given stimulus level that is just slightly supra-threshold is presented until it becomes sub-threshold. At this point, the stimulus is incrementally increased by the experimenter. Threshold-based adaptation protocols have been shown

to dramatically reduce motion sickness symptoms and increase the percentage of subjects capable of completing the experiment (Cheung, Hecht et al. 2007). By pre-adapting subjects to the cross-coupled illusion, a long-radius centrifuge can be used to study the dynamics of the G-Excess Illusion. However it has not been established whether this pre-adaptation involves a change in otolith processing that may affect subsequent perception or control responses during testing in hyper-gravity. Furthermore, there is evidence that the intensity (in terms of illusory perception, oculomotor responses, and motion sickness) of the cross-coupled illusion is greater in hyper-gravity environments (Lackner and Graybiel 1984; Dizio, Lackner et al. 1987; Dizio and Lackner 1988) which may reduce the effectiveness of pre-adaptation.

### 3.0 Aims and Hypotheses

The objective of this thesis is to characterize how *hyper-gravity* affects human perception and control of vehicle roll orientation. This study has the following aims:

1. Empirically investigate human *perception* of orientation in hyper-gravity during *static* and *dynamic* vehicle roll tilt in the dark.
2. Empirically investigate human *manual control* and stabilization of vehicle roll tilt in hyper-gravity in the dark.
3. *Model* human *perception* of orientation in hyper-gravity using an Observer-type dynamic spatial orientation perception model.

Aims 1, 2, and 3 will be addressed in Sections 4.0, 5.0, and 6.0, respectively. Associated with these aims are the following high-level hypotheses. More specific hypotheses will be detailed in Sections 4.0 and 5.0.

1. Humans will *overestimate* static and dynamic roll tilt in hyper-gravity, as compared to 1 G, across a range of angles and frequencies. The amount of overestimation during dynamic roll tilts will be dependent upon the *angular velocity* of the roll tilt.
2. Hyper-gravity will causes pilot *performance to degrade* relative to 1G performance baselines, at least during initial hyper-gravity exposure.

Hypothesis 1 will be addressed in Section 4.0 and hypothesis 2 will be tested in Section 5.0.

## **4.0 Experiment 1: Orientation Perception in Hyper-Gravity**

Experiment 1 aims at addressing Aim 1 and testing Hypothesis 1. In Experiment 1, subjects reported their *perception* of roll tilts performed over a range of angles and frequencies, with static and dynamic components, performed at 1, 1.5 and 2 Earth G's. A long-radius centrifuge was used to create the hyper-gravity environment. To reduce the impact of the confounding Coriolis cross-coupled Illusion, a pre-experimental adaptation protocol was utilized (see Section 4.1.6). Subject's reported their roll tilt perception using a "somatosensory indicator", which they were trained to use prior to the experiment (see Section 4.1.7) as well as with verbal reports of static tilt (see Section 4.1.8). Finally, prior to experimentation each subject was briefly exposed to hyper-gravity without any roll tilt or task. This was intended to reduce the subject's anxiety and allowed them to become accustomed to the physiological responses associated with hyper-gravity (e.g. increased heart rate) prior to testing (see Section 4.1.9). Testing took place over two days. On the first day, in the following order, the subjects completed the first half of the cross-coupled illusion adaptation, somatosensory indicator training, verbal training, and the hyper-gravity exposure protocol. The second day began with the second half of the cross-coupled illusion adaptation, then refresher training on the somatosensory task and verbal reports, and finally all of the hyper-gravity testing sessions.

### **4.1 Methods for Experiment 1**

Subjects (N=8) were seated in the cab of the National AeroSpace Training and Research (NASTAR) Center's ATFS-400 long-radius centrifuge facing tangentially towards the direction of travel. Subjects were secured with a five-point harness seat-belt. A custom head and shoulder support was utilized to restrict roll or yaw head movements and provide support for the torso. Vacuum cushions provided uniform support across the shoulders and upper arms to reduce the influence of tactile cues and the interior of the cab was darkened to remove any visual cues. Subjects wore a custom-sized helmet with noise cancelling headphones to reduce auditory cues from the mechanical systems of the centrifuge. The headphones were also used for communication between the experimenter and the subject. An infrared camera allowed the experimenters to visually monitor the subject during testing. Figure 5 depicts the seated subject and the head and upper torso supports.

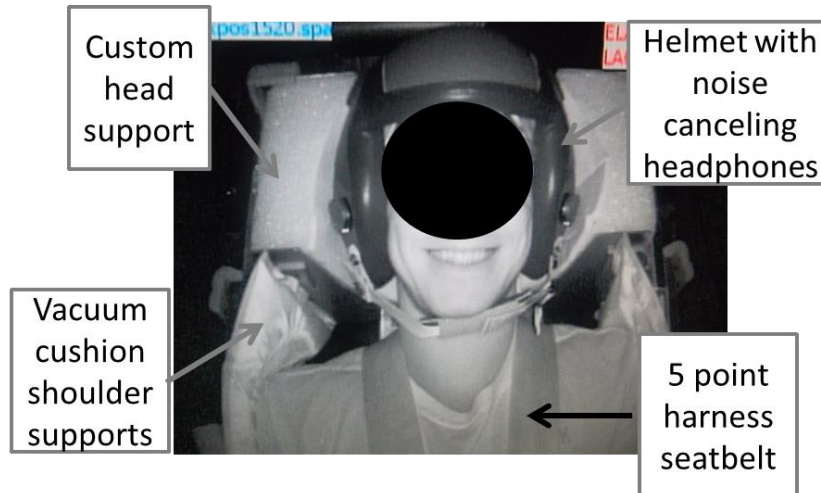


Figure 5: Experiment 1 Subject Supports

#### 4.1.1 Hyper-Gravity Motion Paradigm

The centrifuge cab was located on the end of the centrifuge arm (7.62 m) as seen in Figure 6. The centrifuge was slowly spun up to the desired GIF level over the time course of 60 seconds. The cab fully enclosed the subject such that the subject was not visible from outside the cab; however for pictorial purposes, Figure 6 shows a cutaway of the subject within the cab. During the spin-up the cab gradually rotated outwards such that the resultant GIF remained aligned with the body axis of the cab and z-axis of the subject (+G<sub>z</sub>). Thus from the subject's perspective, the direction of the GIF did not change; it only increased in magnitude to create the hyper-gravity environment.

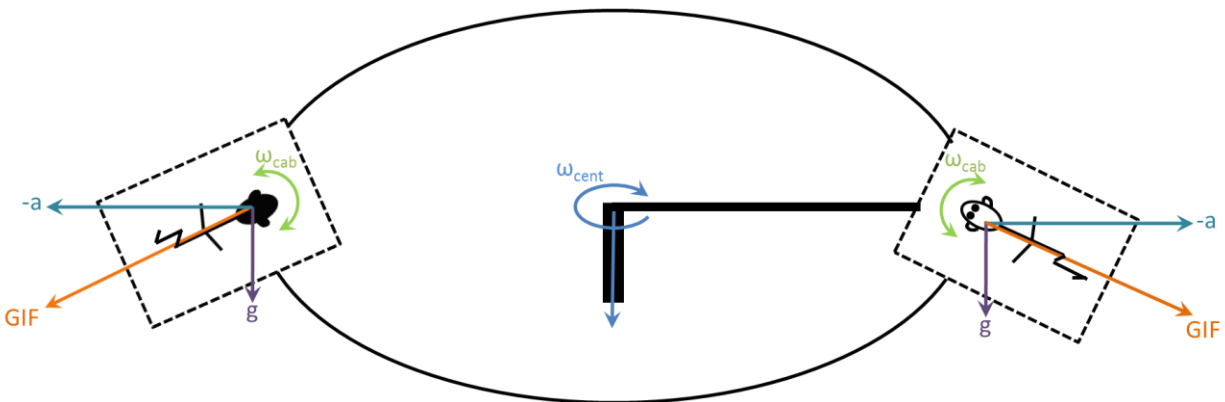


Figure 6: Centrifuge Motion Paradigm

The required planetary centrifuge rotation rates and baseline roll angle to remain aligned with the GIF for each gravity level tested are given in Table 2.

Table 2: Centrifuge Motion Paradigm Parameters Required for Testing G-Levels

Gravity level	Centrifuge rotation rate	Baseline roll angle
1 G	0 rpm, 0 deg/sec	0 deg
1.5 G	11.46 rpm, 68.76 deg/sec	48.19 deg
2 G	14.26 rpm, 85.56 deg/sec	60 deg

The desired G-level was produced at approximately the subject's head level (i.e. within 5-10 cm). This motion paradigm does provide a small gravity gradient along the length of the subject's body. However, this was limited by the large radius of the centrifuge and likely had a minor impact upon perceptions. For a 1.83 m (6 foot) tall seated subject, the maximum gradient was approximately 0.21 G's from head to feet and 0.13 G's from head to buttocks. Once the final G-level was reached, a 60 second wait time was provided for the transient effects of the spin-up to subside and to allow the subjects to become comfortable in the hyper-gravity environment. In the hyper-gravity environment, subjects then experienced a series of roll tilts during the testing period. Once complete, the centrifuge was spun-down, also over 60 seconds. Some subjects found the spin-down to provoke motion sickness symptoms, and thus for these subjects the spin-down was extended to 120 seconds to reduce the peak stimuli. Completion of the spin-up, transient wait, testing period, and spin-down took less than 19 minutes. After each testing session (see Section 4.1.3), the subject was removed from the centrifuge and provided a short break, of at least 20 minutes.

#### 4.1.2 Roll Tilt Profile

In the hyper-gravity environment, subjects experienced a series of passive cab rotations. The cab rotated about the subject's body-fixed roll axis (i.e. "x-axis"), with the center of rotation located at approximately the subject's head. Each rotation went from "upright", or aligned with the resultant GIF direction, to a specific final angle ( $\theta_f$ ) at a specific frequency ( $f$ ). The rotation profile is given in Equation 4 and was selected because it has no discontinuities in angular acceleration, angular velocity, or angle (Figure 7). Note that there is a step in the derivative of acceleration (i.e. jerk) and higher derivatives.

$$\theta(t) = \theta_f \left( ft - \frac{1}{2\pi} \sin(2\pi ft) \right) \quad (4)$$

The angles tested were 10, 20, and 40 degrees. All of the rotations were to the left (counterclockwise) except 20 degrees which was also tested to the right (clockwise). This allowed for the evaluation of the hypothesis that there are no directional asymmetries while keeping the number of trials and time the subjects were exposed to hyper-gravity manageable. Leftward tilts were selected as the primary direction because it tilted the cab back towards Earth vertical which in case of emergency stop during a tilt would leave the subjects closer to upright instead of at a large tilt angle. For simplicity, the more common leftward tilts are considered positive.

The frequencies of the rotations tested were 0.0625, 0.125, and 0.25 Hz (or rotation periods of 16, 8 or 4 seconds, respectively). The angles and frequencies were selected to span the region where sensory integration between semicircular canal and otolith cues is believed to occur for dynamic roll tilt (0.1-0.2 Hz) (Zupan, Merfeld et al. 2002; Grabherr, Nicoucar et al. 2008; Haburcakova, Lewis et al. 2012; Lim and Merfeld 2012). The maximum peak angular velocity (20 degrees/second for the combination of 40 degrees at 0.25 Hz) is not excessive to help limit the intensity of the Coriolis cross-coupled illusion, which roughly scales with angular velocity as well as net angular displacement. Finally these angles and frequencies are loosely representative of typical head movements made in daily life as well as rotations in

aircraft and spacecraft. The angular acceleration, velocity, and position are shown for an example roll rotation of 20 degrees and 0.125 Hz (8 second period) in Figure 7.

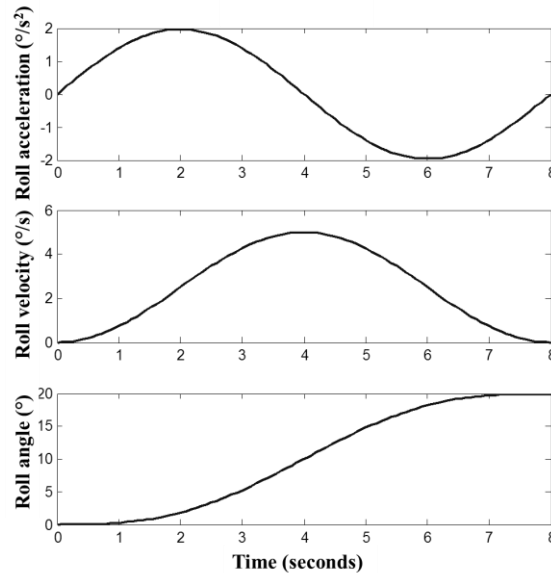


**Figure 7: Example Profile of Dynamic Roll Rotation**

After the cab tilt was completed, it remained in the resulting orientation for 30 seconds and then followed the reverse profile back to “upright” with respect to the GIF direction. After another 30 second stationary period at upright, the following roll tilt began. An example complete profile for a single tilt, with each phase of the trial labeled, is given in Figure 8.

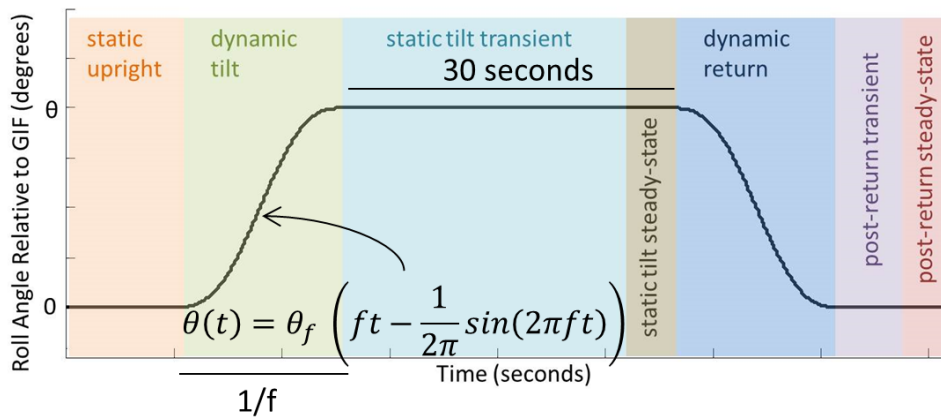


**Figure 8: Example Roll Tilt Profile for a Single Complete Trial**

### 4.1.3 Independent Variables

Each of the 12 roll tilt combinations (3 frequencies x 4 angles) was presented successively in a single session. To guard against the confound of adaptation within a session, randomized (“rand” function in MATLAB) orders of angles and frequencies were selected which also kept the presentations of angle and frequency within each session approximately evenly distributed. This prevented, for example, one particular angle from being presented three times at the beginning of a session. Different orders were

presented for each subject and for each session. Subjects remained naïve that either specific roll angles or frequencies were presented and this was confirmed in post-testing debriefs.

The 12 roll tilt combinations within a session were tested at a specific gravity level. The gravity levels tested were 1, 1.5, and 2 G's, each of which were presented twice, for a total of six testing sessions. Subjects had a break of at least 25 minutes between sessions. The gravity levels for each session were presented in counterbalanced orders with each gravity level presented in one of the first three sessions and one of the last three sessions. Figure 9 shows an example profile for a complete session at 1.5 G.

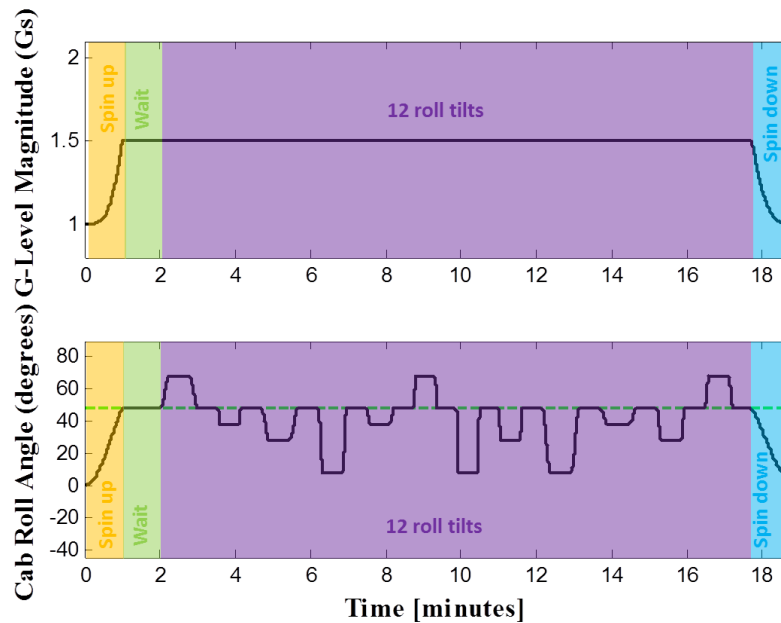


**Figure 9: Example Profile for a Complete Session**

Note the spin-up and wait periods, then the testing period of 12 roll tilts with a balanced presentation of each combination of angle and frequency, and finally the spin-down period. Cab roll angle in Figure 9 is shown relative to Earth vertical, so each roll tilt is performed about the 48.19 degree baseline roll angle at which the cab is aligned with the GIF direction. MATLAB code to produce these profiles for use in the NASTAR ATFS-400 centrifuge is provided in Appendix C.

#### 4.1.4 Dependent Variables

During the 12 roll tilts, subjects reported their perceived roll orientation using a “somatosensory indicator” (Wade and Curthoys 1997). As seen in Figure 10, the somatosensory indicator consisted of a 30.5 cm long metal bar, which pivoted at its center rotation axis and was connected to a potentiometer (Vishay Spectrol 601HE0000B01 Hall Effect Position Sensor) for recording the response. The bar was located approximately 35 cm from the midriff of the seated subject (Merfeld, Zupan et al. 2001). Subjects were instructed to hold the indicator at the ends with each hand using their finger tips and were not allowed to move their hands along the length of the bar (Merfeld, Zupan et al. 2001; Zupan and Merfeld 2003; Park, Gianna-Poulin et al. 2006). Subjects attempted to keep the bar aligned with their perceived gravitational-horizontal continuously. At the end of each trial, 10-15 seconds after returning to upright, subjects performed an “indicator reset”, in which they quickly deflected the indicator by at least 40



degrees in each direction several times and then attempted to reset it to horizontal. This action was aimed at making the initial perception for the ensuing trial independent from the final perception of the previous trial.

The somatosensory task has three primary advantages: 1) as compared to visual techniques, somatosensory responses are not potentially contaminated by torsional eye movements (Wade and Curthoys 1997), 2) as compared to single-handed tasks (Borah and Young 1982; Borah and Young 1983) fewer left/right asymmetries are likely to occur, and 3) as compared to verbal responses it is possible to obtain temporally continuous reports (Merfeld, Zupan et al. 2001).

The motor responses involved in the somatosensory task may be influenced by the altered GIF environment (Fisk, Lackner et al. 1993). In addition, the continuous task may be subject to a “hysteresis effect” in which subjects’ reports are influenced by their previous responses. We attempted to reduce this by explicitly instructing subjects to “report your current perceived orientation. If you realize your previous response was incorrect, please adjust accordingly such that your current response is as accurate as possible.” While we cannot be certain that hysteresis was entirely removed from all responses, we expect its effect was limited and similar across all gravity levels.

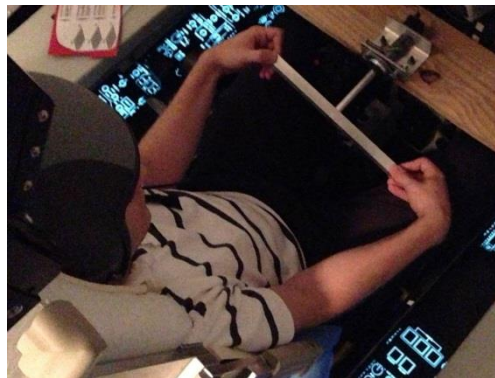


**Figure 10: Somatosensory Indicator Operation**

The subject’s perceptions were compared to the actual orientation of the cab with respect to the GIF direction as recorded from the simulator. The somatosensory indicator only rotated in roll so any perceived pitching or yawing rotation could not be reported.

As a secondary measure, during the static steady-state period of the trial (see Figure 8), subjects provided verbal reports of their perceived pitch and roll tilt to the nearest degree (e.g. “I am rolled 7 degrees to the right and pitched 1 degree forward”).

#### **4.1.5 Experimental Design**

The experimental design was fully within-subjects and complete, such that every subject experienced every combination of roll angle, roll frequency, and gravity level. The within-subjects design allowed for fewer total subjects, reducing the time spent completing pre-experimental protocols. The complete design was necessary to study interactions between independent variables. There were two replications of each treatment level combinations in order to test if adaptation was taking place.

**Table 3: Summary of Independent and Dependent Variables for Experiment 1**

Independent Variables	Treatment Levels			
G-Level	1.0 G	1.5 G	2.0 G	
Roll Angle	10 degrees	20 degrees	-20 degrees	40 degrees
Roll Frequency (Roll Time)	0.0625 Hz (16 sec)	0.125 Hz (8 sec)	0.25 Hz (4 sec)	
Dependent Variables				
Somatosensory Indicator Response				
Verbal Response				

#### 4.1.6 Cross-Coupled Stimulus Adaptation Protocol

As previously described (see Coriolis Cross-Coupled Illusion Adaptation Literature Section), when subjects make head rotations in a rotating environment, such as employed in Experiment 1, they will experience an illusory perception of rotation about an unexpected axis. The Cross-Coupled Stimulus Adaptation Protocol was designed to adapt subjects to this illusion through repeated exposure, such that subjects could effectively report perceptions of roll tilt in hyper-gravity.

The Cross-Coupled Stimulus Adaptation Protocol consisted of three phases (see Figure 11). In the main phase, the subject was incrementally adapted to the cross-coupled illusion by manipulation of the rotation rate. In the first and third phases, pre and post measures of the illusion’s intensity were taken to measure the adaptation that took place.

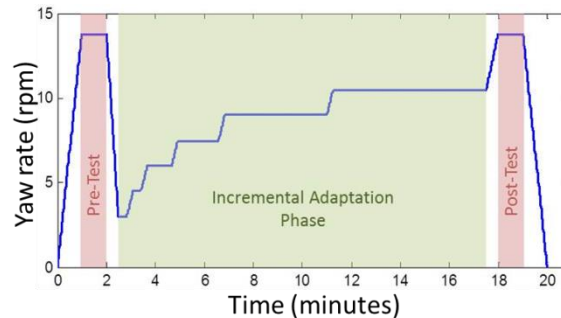


**Figure 11: Cross-Coupled Adaptation Protocol Timeline**

Subjects were seated in NASTAR Center’s Gyroflight simulator in the dark and secured with a waist seat-belt. Due to an equipment failure, subjects 7-8 completed this same protocol on MIT’s short-radius centrifuge. Subjects wore noise-cancelling headphones for communication between the experimenter and the subject. An infrared camera allowed the experimenters to visually monitor the subject during testing. Unlike the hyper-gravity protocol, here the simulator rotated in pure yaw about the subject’s body axis. This exposed the subject to the cross-coupled stimulus expected in the hyper-gravity protocol without exposing them to the G-Excess Illusion caused by hyper-gravity (see Appendix D). During each phase of the experiment, subjects repeated a series of four active head-on-body roll tilts, always in the same order: 1) from upright to right ear down, 2) right ear down back to upright, 3) upright to left ear down, and 4) left ear down back to upright. Each head tilt was approximately 40 degrees and completed in approximately 1 second. A headrest limited head tilts to 40 degrees and initially training helped ensure consistent timing. At least 10-15 seconds were provided between successive head tilts to let any illusory

motion sensations subside. The roll tilts during constant rotation about an Earth vertical axis mimicked the cross-coupled stimulus scenario in the hyper-gravity motion paradigm to encourage adaptation in the relevant plane of head rotation (Garrick-Bethell, Jarchow et al. 2008). In the adaptation protocol active head tilts were used despite the passive rotations experienced in the hyper-gravity tests. Previous successful adaptation protocols used active head rotations (Young, Hecht et al. 2001; Brown, Hecht et al. 2002; Hecht, Brown et al. 2002; Mast, Newby et al. 2002; Young, Sienko et al. 2003; Bruni 2004; Cheung, Hecht et al. 2007; Jarchow and Young 2007; Mateus 2008), and there is some evidence that adaptation is reduced when using passive rotations (Reason 1978; Reason and Benson 1978).

For initial pre-adaptation testing, the simulator was spun up, over 60 seconds, to the maximum yaw velocity that was experienced during the primary hyper-gravity protocol (14.26 rpm or 85.56 degrees per sec). In the pre and post testing, following each head tilt, subjects reported the *direction* of illusory rotation (generally either pitching forward or backward) and the relative *intensity* of the illusory tumbling sensation. The intensity was reported using the following scale: 0 corresponded to no unusual sensation such as would be experienced during a head tilt in everyday life and a 10 was arbitrarily assigned as the intensity of the first head tilt (Young, Hecht et al. 2001; Brown, Hecht et al. 2002; Hecht, Brown et al. 2002; Adenot 2004; Bruni 2004; Jarchow and Young 2007). The intensities of the remaining head tilts were then reported on this relative scale. For the pre-adaptation measure, subjects performed one series of the four head tilts.

Subjects then completed a threshold-based incremental adaptation procedure (Cheung, Hecht et al. 2007; Jarchow and Young 2007). The centrifuge was slowed to 3 rpm, a speed at which the cross-coupled illusion was near threshold. At this speed, subjects performed multiple series of the four head roll tilts. After each tilt, subjects reported if they felt *any* illusory pitching sensation. If the subject felt no illusory sensations for each of the four head tilts in a series, the yaw rate was increased by 1.5 rpm. Otherwise it remained the same and the procedure was repeated. The rotation rate increase was done over 15 seconds ( $0.6 \text{ deg/sec}^2$  acceleration) to remain sub-threshold (Cheung, Hecht et al. 2007). In this incremental fashion, as subjects adapted, the intensity of the cross-coupled illusion was increased by modulating the yaw rate. The incremental adaptation phase lasted 15 minutes. If, within the 15 minutes, a subject reached the 13.5 rpm level with no illusory perception, the rate would be increased one more time to 14.26 rpm (the maximum rate of the centrifuge in the hyper-gravity tests). It would then remain constant for the remainder of the 15 minutes, even if this speed became sub-threshold. The threshold-based adaptation technique was advantageous because subjects were only exposed to near threshold level illusions, making it less provocative of motion sickness than other adaptation protocols (Cheung, Hecht et al. 2007; Jarchow and Young 2007).

After the incremental adaptation phase was completed, the rotation rate was adjusted to 14.26 rpm for the post-adaptation testing phase. The post testing was identical to the pre testing and the intensity reports were always anchored to the first head tilt of the first pre-adaptation testing. The intensities in the post phase were compared to those from the pre phase as a measure of the adaptation that took place during the incremental adaptation phase. After the post-test the device was slowed down and the subject

was removed. The total time in the device was approximately 20 minutes. Subjects remained naïve that the purpose of this protocol was to adapt them to the cross-coupled stimulus.

The adaptation protocol was repeated twice, once the day before the hyper-gravity testing and again the morning of testing. Adaptation occurs not only within sessions on the same day, but also between sessions on consecutive days (Brown, Hecht et al. 2002; Hecht, Brown et al. 2002; Young, Sienko et al. 2003; Cheung, Hecht et al. 2007; Jarchow and Young 2007), particularly when subjects sleep between multiple exposures (Mateus 2008). The beneficial adaptive effect of multiple days of exposure tends to decrease after two days (Brown, Hecht et al. 2002; Hecht, Brown et al. 2002; Jarchow and Young 2007), so to limit the length of time required from subjects only two days of adaptation sessions were used.

#### 4.1.7 Indicator Training Protocol

While the somatosensory task was quite intuitive, subjects were provided training prior to the test sessions to ensure adequate performance. Subjects were trained by reporting during a 60 second, pseudorandom sum-of-sines roll tilt profile in 1 G (i.e. no planetary centrifuge rotation) in the dark. The motion consisted of three out-of-phase frequencies (0.061, 0.134, and 0.278 Hz), each with an amplitude of 15 degrees, for a maximum potential roll angle of 45 degrees. The first 10 and last 5 seconds of the profile were scaled such that it began and ended at an upright orientation. Figure 12 shows an example training profile and Appendix C provides MATLAB code for creating profiles.

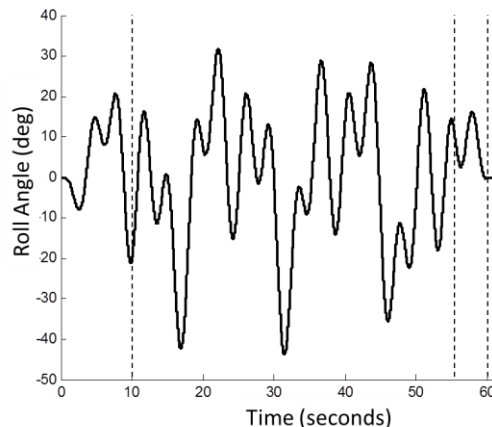


Figure 12: Example Somatosensory Indicator Training Profile

Following each trial, subjects received general feedback on performance (e.g. “You are reporting angles larger than you are experiencing. Try tilting the bar less aggressively.”). Quantitative performance scores (RMS error from upright) were provided intermittently every few trials. Subjects repeated trials until their performance, measured by RMS error, improved to a steady state. Usually 10-18 trials were presented in the primary training session on the first day. On the second day, 3-4 additional training trials were presented just prior to testing to ensure performance had not degraded. With training, subjects were generally able to report their perceptions quite well using the somatosensory indicator (see Appendix F for an example training trial and metrics for all subjects).

#### 4.1.8 Verbal Training Protocol

Subjects were trained on making verbal reports of static roll tilts prior to testing. Twenty static roll tilts to random angles of 40 degrees or less were presented in 1 G. Subjects reported their perceived pitch and roll angles to the nearest degree and then the experimenter provided the actual roll angle as feedback. Successive angles were always at least 15 degrees apart and rotations between angles were done over 8 seconds using the profile in Equation 4 (0.125 Hz). An example profile is given in Figure 13 and MATLAB code to create the profiles can be found in Appendix C. An additional five static roll tilts were presented just prior to testing to ensure performance had not degraded. See Appendix F for verbal training responses.

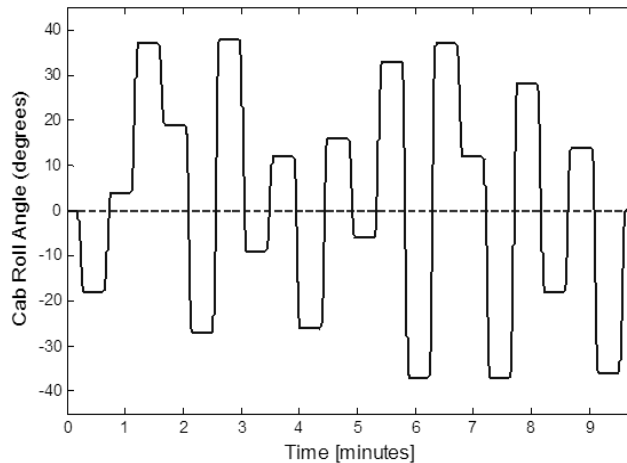
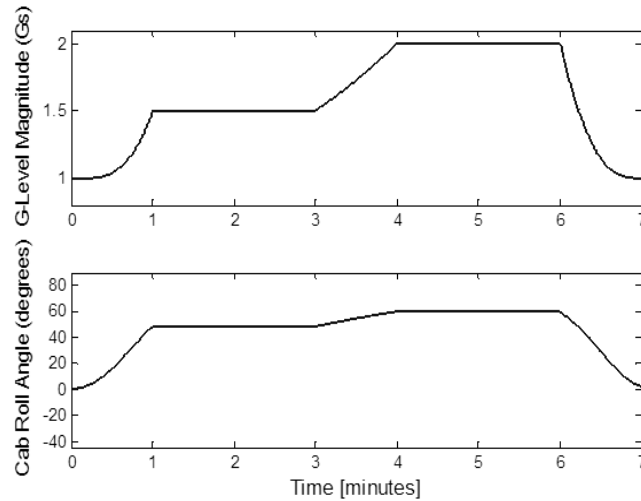


Figure 13: Example Verbal Training Profile

#### 4.1.9 G-Exposure Protocol

Prior to testing, subjects were exposed to hyper-gravity to help reduce anxiety and introduce the physiological effects of hyper-gravity. The centrifuge was spun up to 1.5 G's and then 2 G's for 2 minutes each. Transitions between gravity levels were 1 minute. The roll angle of the cab was adjusted to remain aligned with the net GIF. The profile used is given in Figure 13 and the MATLAB code is provided in Appendix C.



**Figure 14: G-Exposure Profile**

#### 4.1.10 Study Approval, Subjects, and Forms

All of the Experiment 1 protocols were approved by the Environmental Tectonics Corporation (ETC)/NASTAR Center’s Internal Review Board (IRB) and MIT’s Committee on the Use of Humans as Experimental Subjects (COUHES). Subject selection criteria included healthy females and males ages 18-65, with no known vestibular defects or conditions. Subjects who were highly susceptible to motion sickness were excluded from the study, as determined by scoring above the 90<sup>th</sup> percentile on the Motion Sickness Susceptibility Questionnaire (MSSQ) (Golding 1998; Golding 2006). Individuals with no history of any motion sickness (0<sup>th</sup> percentile on the MSSQ) may not have a normally functioning vestibular system and thus were also excluded from the study. In addition, subjects completed NASTAR Center’s medical screening questionnaire and if a subject responded “YES” to any of the questions, a FAA Class III Physical was required to participate in the experiment. Subjects also completed a waiver and liability form, a questionnaire on previous flight and centrifuge experiences, and a pre-exposure simulator sickness questionnaire (SSQ) (Keshavarz and Hecht 2011). After each cross-coupled stimulus protocol, the G-Exposure protocol, and each testing session, subjects completed a post-exposure SSQ form to monitor motion sickness. See Appendix D for proof of study approval and forms associated with Experiment 1. All subjects signed a written informed consent form.

Eight subjects were tested (5M/3F, ages 21-32, mean = 26, standard deviation = 3.2). Two subjects had minimal flight experience (< 50 hrs), two had minimal centrifuge experience (< 6 hrs), and the remainder had no prior flight or centrifuge experience. The subjects with prior experiences did not have results that appeared to differ from the remaining subjects. All subjects were able to complete the protocols and experienced no serious adverse effects. Motion sickness symptoms occurred for every subject, particularly resulting from the cross-coupled stimulus protocol and the spin down from hyper-gravity during testing sessions; however no subjects approached vomiting nor asked to stop the experiment. Due to technical issues Subject 1 only completed 4 sessions (omitting the second 1.5 and 2 G tests) and Subject 2 did not complete the last session at 2 Gs.

The level of significance was set to  $\alpha = 0.05$ .

## 4.2 Results for Experiment 1

The results from Experiment 1 address Hypothesis 1. First, the results from the cross-coupled stimulus protocol are presented; showing evidence that the adaptation was successful and secondary illusion intensity was reduced to very limited levels, allowing for less confounded perceptual testing in hyper-gravity. Next perception of roll tilt is shown across the different gravity levels tested, first for an example angle and frequency combination, and then across all combinations. Finally, statistical tests are applied to the perceptions during each phase of the roll tilt profile given in Figure 8: static upright, static tilt steady-state, dynamic tilt and return, static tilt transient, post-return transient, and post-return steady-state. Appendix F shows data from the subject's somatosensory indicator and verbal training.

### 4.2.1 Cross-coupled Stimulus Adaptation Training

Head tilt direction (e.g. left ear down, etc.) did not have a consistent effect on illusion intensity, so the four head tilts for each session were averaged by subject and are shown in Figure 15.

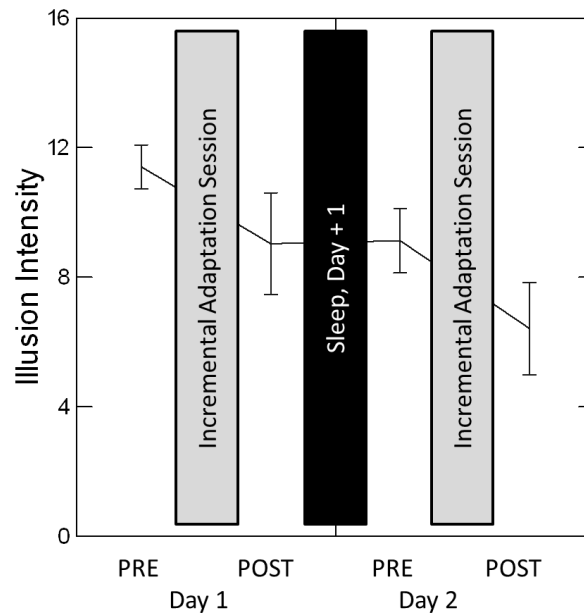


Figure 15: Mean Cross-Coupled Stimulus Intensities

Prior to any adaptation, the illusion intensity was relatively high (near the 10 value for the first head tilt). However, by a two-factor (pre vs. post session and day 1 vs. 2) repeated measures ANOVA, the incremental adaptation session significantly reduced the mean illusion intensity ( $F(1,7)=9.6$ ,  $p=0.018$ ) as did the effect of day ( $F(1,7)=37.2$ ,  $p<0.0005$ ). On average, the illusion intensity was reduced to approximately half of its initial value after the two 15 minute incremental adaptation sessions.

Further evidence that the secondary cross-coupled illusion had a limited effect during testing sessions can be found in the relatively infrequent and benign reports of the illusion during hyper-gravity testing. As expected, in 1G there were no reports of the illusion during any of the tilts (0/192) or returns (0/192). At 1.5 G, only 8.3% (15/180) of tilts and 13.3% (24/180) of returns caused *any* cross-coupled illusion. At 2 G, 15% (24/160) of tilts and 17.5% (28/160) of returns caused a supra-threshold cross-coupled illusion. The illusion was significantly more common at higher roll angular velocities and higher gravity levels,

where the centrifuge spin-rate was higher (see Appendix G for tables, plots, and statistics details). Only a small fraction of roll tilts and returns, even in hyper-gravity, caused *any* perceived cross-coupled illusion. In fact, four of eight subjects felt no cross-coupled illusion throughout testing and one subject felt it on only one trial. Furthermore, even when the cross-coupled illusion was supra-threshold, it was relatively weak. For example, the mean illusion intensity for the most provocative trial combination (i.e. the 2 G, 40 degree tilt, at 0.25 Hz case) was only 1.8 on the 10-based scale. Possibly most practically important, on post-session questionnaires all eight subjects on each of their six sessions always reported that any cross-coupled illusion they experienced did not “make it more challenging to operate the somatosensory indicator”.

Since we did not test any subjects in hyper-gravity without first undergoing the cross-coupled illusion protocol, we cannot be certain that the adaptation did not have any unexpected effects on perceptual responses in hyper-gravity. However, we have supporting, though not conclusive, evidence that through experiment design, the long-radius of the centrifuge, and the pre-adaptation protocol, the cross-coupled illusion had a limited effect on the hyper-gravity perceptual reports. See Appendix G for graphs of raw cross-coupled illusion protocol data by subject.

#### 4.2.2 Effect of Hyper-Gravity on Perception

Provided here are summary results of the somatosensory indicator perceptual reports during the roll tilt profile in each gravity level. Figure 16 shows the average subject perception during the time course of a single trial for one example: the 20 degree roll at 0.125 Hz in 1, 1.5, and 2 G’s.

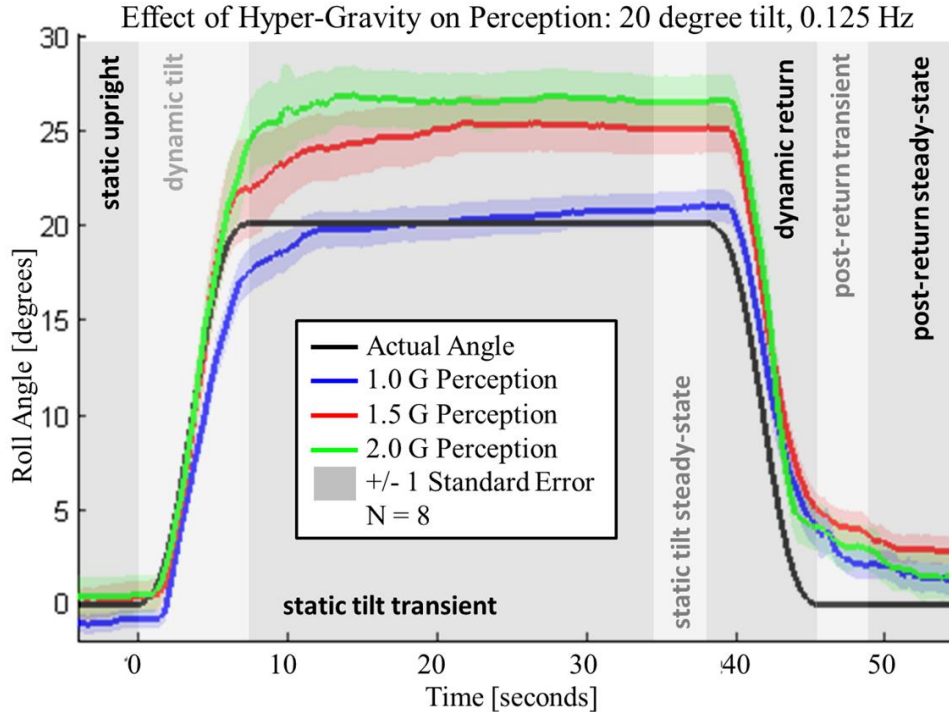


Figure 16: Example Somatosensory Indicator Perception for 20 degrees and 0.125 Hz



As seen in Figure 16, perception of roll tilt is altered by gravity level. In 1 G, subjects fairly accurately perceive their orientation with only slight delay errors during dynamic tilt, dynamic return, and post-return responses. However, in 1.5 G, subjects substantially overestimate their roll tilt, both in relation to the actual roll angle and the 1 G perception. The perceptual error is even larger in the 2 G case. These perceptual errors in hyper-gravity occurred across angle and frequency combinations tested as shown in Figure 17. For graphical purposes, a few trials were excluded from Figure 17 due to an indicator reset that occurred too early or late.

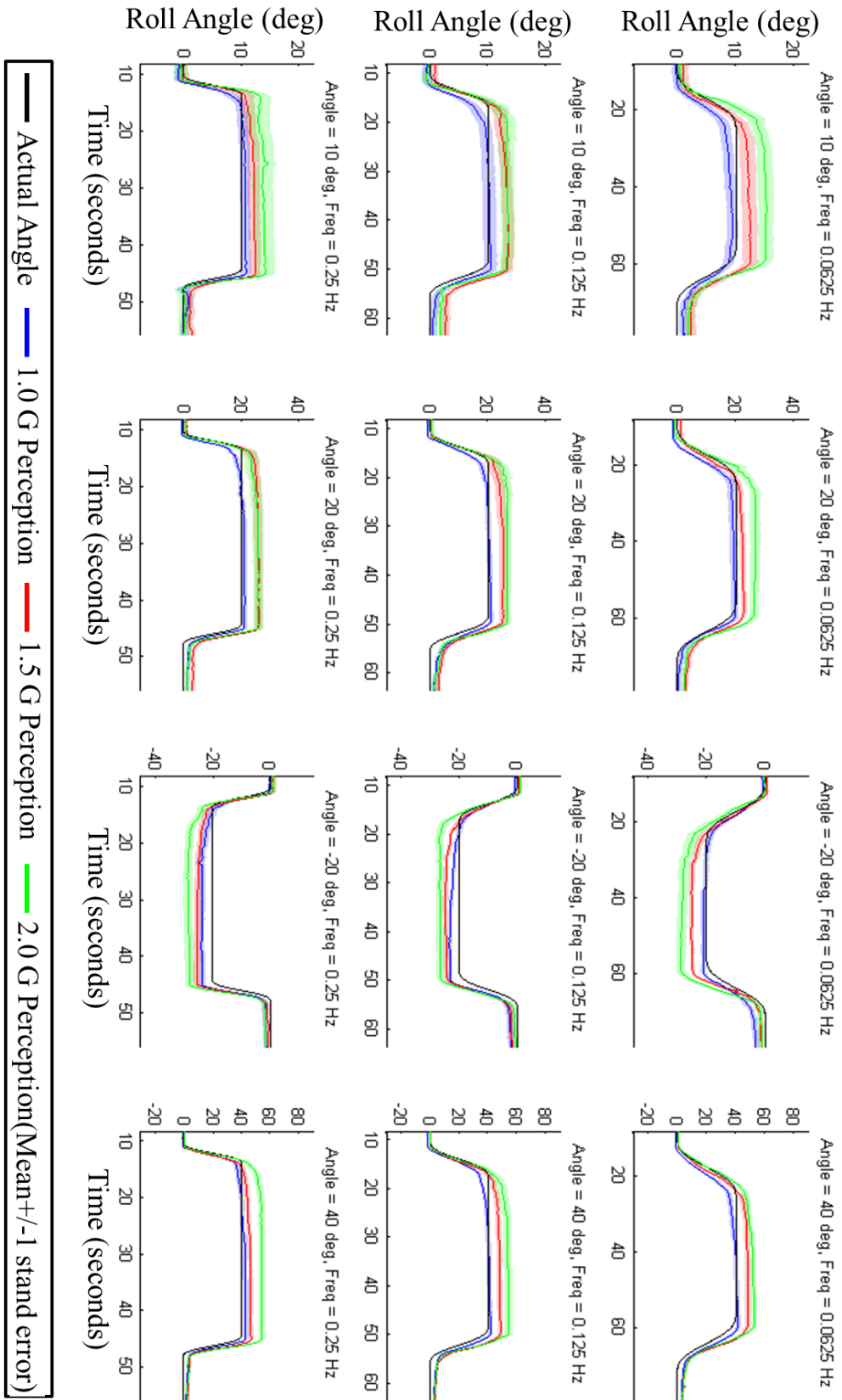


Figure 17: Summary of Somatosensory Indicator Perception across All Angle and Frequency Combinations

### 4.2.3 Upright Perception

The average somatosensory response over the last two seconds just prior to the beginning of the dynamic tilt was taken as a measure of upright perception (see Figure 8). An upright measure was taken at the beginning of each session (see Appendix H for details) and the subject means are shown in Figure 18. Positive angles correspond to a perception of being tilted to the left (counterclockwise).

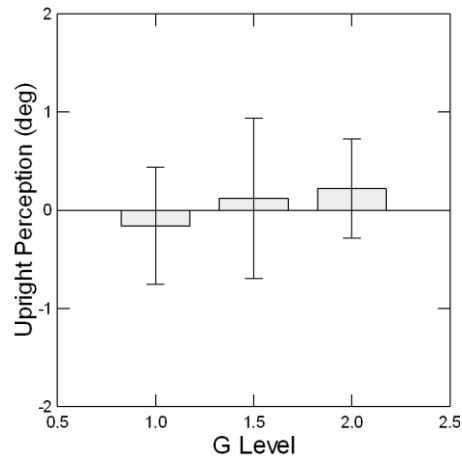
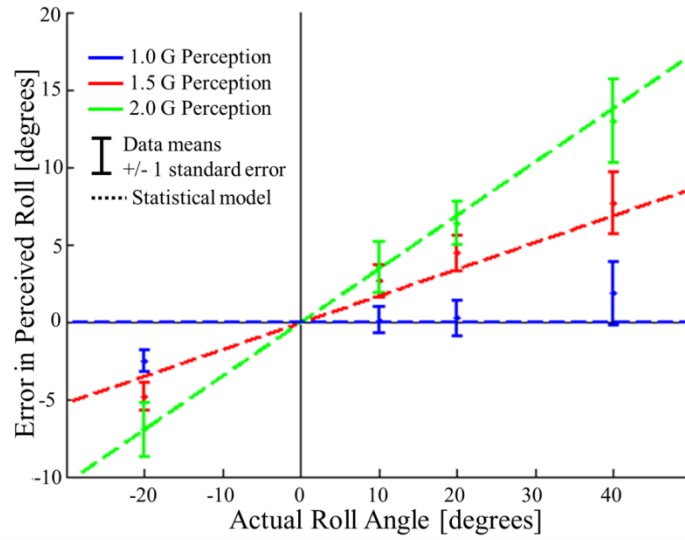


Figure 18: Mean Upright Perception

A hierarchical regression with  $(G - 1)$  as the independent variable and subject as the identifier found no evidence of hyper-gravity affecting upright perception ( $p > 0.05$ ). Even in hyper-gravity, subjects accurately perceived themselves as upright when they are upright. This is consistent with previous studies using SVV tasks, which did not apply statistical tests (Colenbrander 1963; Schone 1964; Correia, Hixson et al. 1965; Miller and Graybiel 1966; Schone and Parker 1967; Schone, Parker et al. 1967; Correia, Hixson et al. 1968).

### 4.2.4 Static Tilt Steady-State Perception

The metric for “steady-state” static tilt perception was the average somatosensory indicator response over the two seconds just prior to the beginning of the dynamic return. This was 28-30 seconds after the end of dynamic tilt (see Figure 8). The actual roll angle of the cab, relative to the GIF, was subtracted from the subjects’ perceptions to yield the perceptual error and is shown in Figure 19. Here, and throughout, positive errors indicate a perceived roll angle to the left (counterclockwise) of the actual angle and negative errors correspond to the perceived angle being to the right (clockwise) of the actual roll. No evidence was found that static tilt steady-state perception had any learning or adaptation effects (comparison of the same presentation in session 1-3 to that in session 4-6), so the two presentations were pooled. Furthermore, as expected, the static tilt steady-state perception showed no evidence of being dependent upon dynamic rotation parameters, particularly the roll frequency. Thus the presentations of specific angle at each of the three frequencies were pooled. Finally, no evidence was found that static tilt steady-state perception had any left/right asymmetries. See Appendix I for details.



**Figure 19: Mean Static Tilt Steady-State Perception**

In 1 G, on average subjects accurately perceived their roll tilt, though the -20 degree (to the right) roll angle was perceived as slightly (2-3 degrees) greater, or more to the right, than veridical. In 1.5 and 2 G, consistent perceptual errors were seen. Positive (to the left) angles had positive errors and negative angles had negative errors, corresponding to subjects overestimating their roll angle in hyper-gravity. To statistically test the effect of hyper-gravity the following hierarchical regression model was fit.

$$(\theta_{per} - \theta)_{ij} = \rho_i + \beta((G - 1)\theta) + \epsilon_{ij} \quad (5)$$

The error in perceived roll in degrees ( $\theta_{per} - \theta$ ) from the  $j^{\text{th}}$  measurement in the  $i^{\text{th}}$  subject were a function of the “G-Excess” term ( $(G-1)\theta$ ), where  $G$  is the gravity level (1, 1.5, or 2 G’s), and  $\theta$  is actual roll angle in degrees. In addition, the model has subject-dependent intercepts ( $\rho_i$ , where  $i = 1-8$  subjects). In the first stage of the regression, the subject’s random effects are accounted for ( $\rho_i$ ), accounting for the within-subjects design. In the second stage, the perceptual errors were regressed on the G-Excess term accounting for the subject-dependent intercepts. This analysis is appropriate for the within-subjects design and treats the effects of gravity and angle as linear over the values tested. The results from the model fit are given in Table 4. The subject intercepts were found to not be consistently different from zero (t-test), further supporting that when upright subjects accurately perceive themselves as upright, even in hyper-gravity.

**Table 4: Linear Static Tilt Steady-State Perception Model Results**

Coefficient	Units	Estimate	Standard Error	Z value	p-value
$\bar{\rho}_i$	Degrees	-0.065	0.82	-0.08	0.94
$\beta$	1 / G’s	0.35	0.026	13.39	<0.0005

The significantly positive  $\beta$  coefficient supports the hypotheses that 1) hyper-gravity causes overestimation of roll angle, 2) there is more overestimation at greater hyper-gravity levels, and 3) there is more overestimation in hyper-gravity at larger roll angles. In hyper-gravity, the perceptual errors in roll tilt were substantial; across the angles tested, the model indicates that the overestimation was approximately 17% of the actual roll angle in 1.5 G, and 35% in 2 G. The model predictions are overlaid on the data in Figure 19 and with only one significant free parameter (the “G-Excess” term) fit each of the 12 combinations of gravity level and roll angle well.

The model in Equation 5 and Table 4 is a population-level model that estimates the mean effect of hyper-gravity across subjects. Certain subjects exhibited a consistently much larger or smaller “G-Excess” effect than the population mean. See Appendix I for details.

#### 4.2.5 Comparison of Static Tilt Steady-State Perception to Previous Models

Section 2.3 presented two previously proposed models for static tilt steady-state perception in hyper-gravity: the utricular shear model (Equation 2) and the tangent model (Equation 3). Figure 20 shows the current dataset compared to these models, depicted as perceptual error (perceived angle minus actual angle).

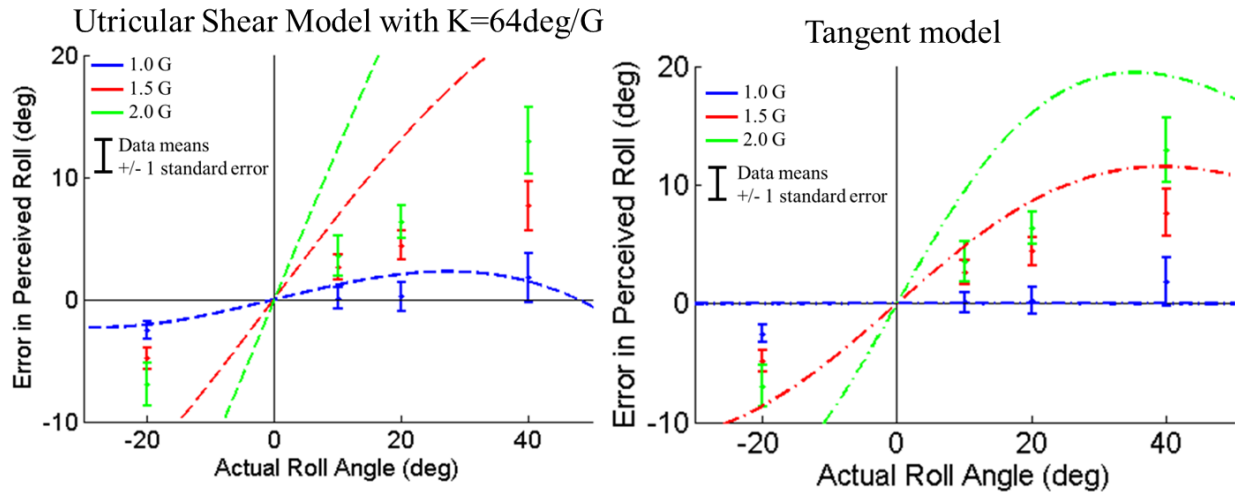


Figure 20: Comparison of Current Static Tilt Steady State Perception to Utricular Shear and Tangent Models

Both models effectively fit the current dataset in 1 G, however neither of the models appropriately explain the perceptual errors observed in hyper-gravity. In particular, both the utricular shear and tangent model predict much greater overestimation in hyper-gravity than was measured. In the utricular shear model, the free ‘K’ parameter can be reduced to better fit the hyper-gravity static perceptions, but at the expense of incorrectly predicting the 1 G responses. See Appendix I for a detailed comparison of current and previous data to the utricular shear and tangent models. The Ormsby and Young nonlinear transformation model (described in Section 2.3 and detailed in Appendix A) is also compared to the current data in Figure 21. The two variants of the model, in which the nonlinear alteration is modified, are shown.

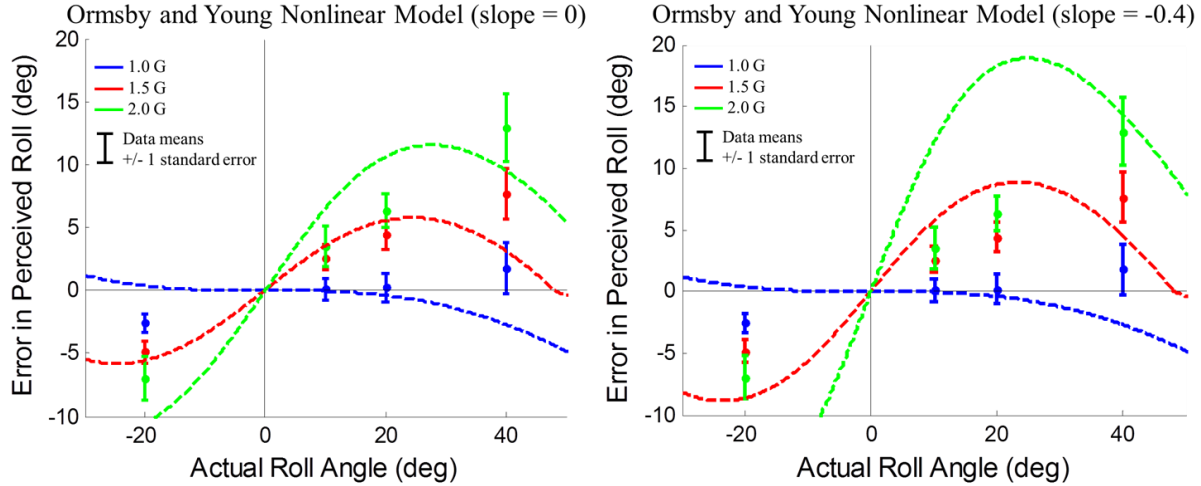


Figure 21: Comparison of Current Static Tilt Steady State Perception to Ormsby and Young Models

Both variants of the Ormsby and Young model do not fit the current data well. In particular, in order for the hyper-gravity overestimation to fit at larger angles (e.g. 40 degrees) it predicts too much overestimation at smaller angles (e.g. 10 and 20 degrees). Furthermore it does not predict the relatively accurate perceptions seen in all of the 1 G cases tested.

#### 4.2.6 Modified Utricular Shear Model for Static Tilt Steady-State Perception

Since the previously proposed models fail to sufficiently explain the overestimation measured in hyper-gravity, here we propose an alternative model. The model is empirical and ad hoc, but we provide some justification for the basis here. There is evidence now showing the change in the otolith afferent firing rates are approximately proportional to the force acting along the neuron's polarization direction in monkeys (Fernandez and Goldberg 1976; Fernandez and Goldberg 1976; Fernandez and Goldberg 1976). Hence it was logical for the proposed model to be of the form  $G \cdot \sin(\theta)$ , since that is the physical quantity causing changes in firing rates. On a micro-level,  $\theta$  may refer to the angle between the gravity force and an individual neuron's polarization direction. However, at a population-level,  $\theta$  may refer to the roll angle for example, where each neuron's gain is proportional to how closely its polarization direction is aligned with stimulation from roll tilt. Thus we began with the traditional utricular shear model (Equation 2), but rearranged it into 1 G and hyper-G terms and then added an additional free parameter to the hyper-gravity term ( $M$ ).

$$\theta_{per} = \rho_i + K * \sin(\theta_{act}) * [1 + M * (G - 1)] \quad (6)$$

This model allows for the 1 G and hyper-gravity perceptions to be fit separately, however both hyper-gravity levels across all angles still must be fit with a single free parameter. To account for the within-subjects design, a hierarchical regression was applied with subject as the identifier.

**Table 5: Modified Utricular Shear Model Results**

Coefficient	Units	Estimate	Standard Error	Z value	p-value
$\bar{\rho}_l$	Degrees	-0.29	0.83	-0.34	0.73
K	deg / G	64.6	1.53	42.1	<0.0005
M	unitless	0.26	0.035	7.48	<0.0005

For small angles, to achieve an accurate perception in 1 G, the K coefficient should be 57.3 deg/G ( $180/\pi$ ). Our fit has a slightly larger estimate which yields slight overestimation at small angles, but less underestimation at larger angles in 1 G. The K coefficient estimate is very similar to a previous traditional utricular shear fit of 64 deg/G (Schone 1964).

The estimated value of  $M = 0.26$ , implies that the overestimation seen in hyper-gravity is only about 26% of what would be expected from the traditional utricular shear model. As might be expected, the model fits the current data quite well across all of the gravity-levels and angles tested. It also, at least qualitatively, fits data from many of the previous SVV experiments well as seen in Figure 22 below.

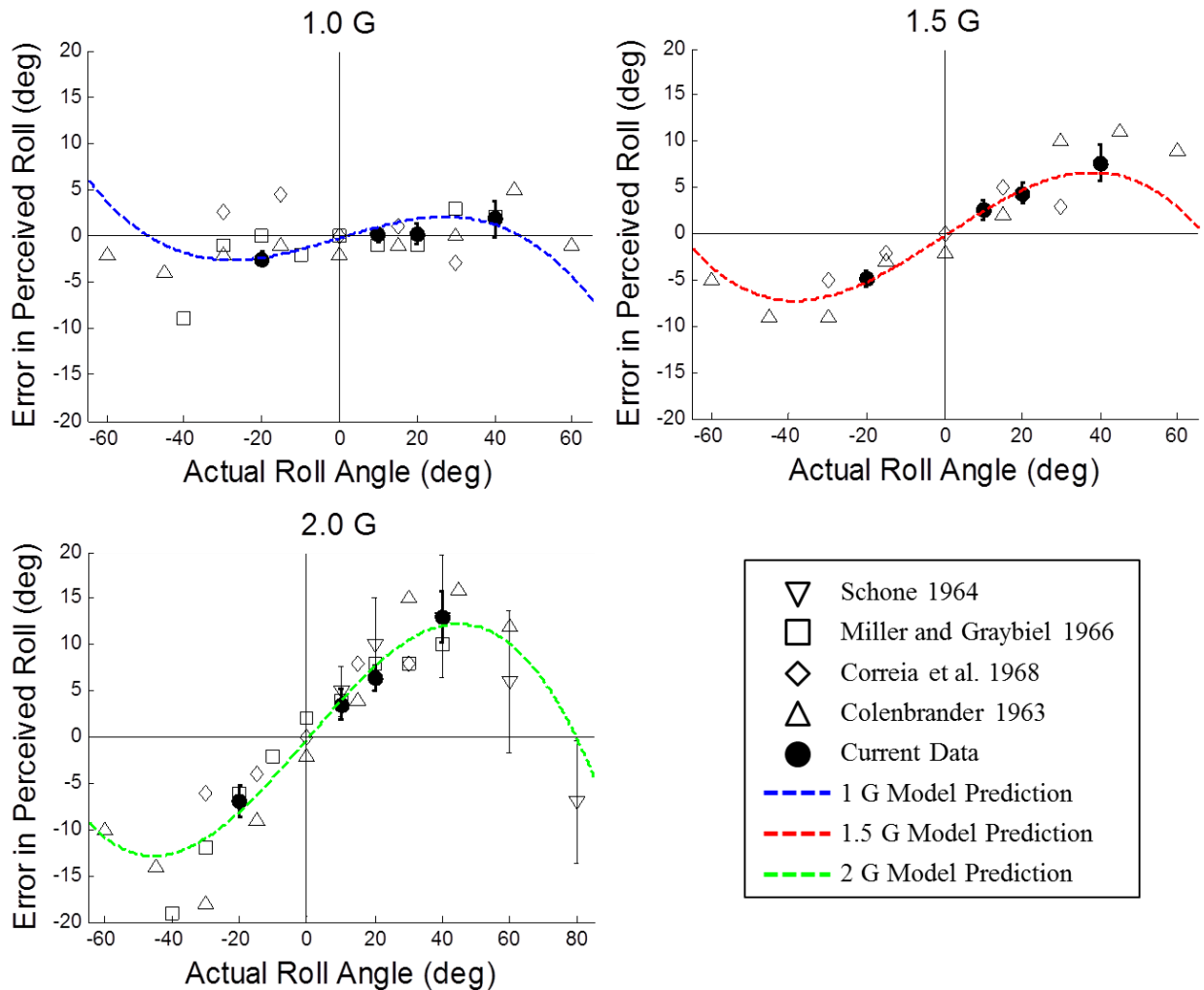


**Figure 22: Comparison of Current and Prior Static Tilt Steady State Perception to Modified Utricular Shear Model**

Prior experiments used a different methodology for measuring perceived roll (i.e. SVV), different motion devices, and tested at larger angles than the current dataset to which the proposed model was fit.

This provides support that the model predicts static roll perceptions over a large range of angles and hyper-gravity levels.

#### 4.2.7 Verbal Reports of Static Tilt Steady-State Perception

In addition to the somatosensory indicator, subjects also reported their static tilt steady-state perception verbally. Despite the pre-experimental training, these reports were far more variable. There was a significant left/right asymmetry at 1 G ( $t(7) = 5.21$ ,  $p = 0.001$ ) and at 1.5 G ( $t(7) = 3.25$ ,  $p = 0.014$ ), with rightward tilts (-20 degree) being perceived as larger than tilts to the left (20 degree). This may be due to the verbal report being a more cognitively mediated task which was affected by left tilts being presented three times more often than rightward tilts. Again, there was no evidence of learning or adaptation between sessions in the verbal reports.

Despite these limitations, from Equation 5, the “G-Excess” term was still significant for the verbal reports ( $\beta = 0.08$ ,  $Z(523) = 2.67$ ,  $p = 0.008$ ), indicating overestimation in hyper-gravity, with more overestimation at higher gravity levels and larger angles. The amount of overestimation in the verbal reports ( $\beta = 0.08$ ) was over 4 times smaller than that seen in the somatosensory task ( $\beta = 0.35$ ). This was especially true for the 40 degree tilts, where subjects may have been hesitant to verbally report such large angles based upon the distribution of previous roll tilts ( $\leq 40$  degrees). When considering only the 10 and 20 degree tilts, the magnitude of the “G-Excess” effect seen in the verbal reports was greater ( $\beta = 0.23$ ,  $Z(257) = 5.61$ ,  $p < 0.0005$ ), however it was still substantially smaller than the overestimation seen in the somatosensory task.

#### 4.2.8 Dynamic Tilt and Dynamic Return Perception

We hypothesized that that amount of overestimation in hyper-gravity during dynamic tilt and dynamic return would be dependent upon the roll rotation rate, specifically the peak angular velocity. To quantify the perception during dynamic rotations, the following metric was utilized. A linear fit was applied to the temporally central 50% of the dynamic rotation period (tilt or return), for both the actual roll rotation and the perceptual response. The slope of the perceptual response ( $m_{\text{per}}$ ) was normalized by the actual slope ( $m_{\text{act}}$ ) and used as the primary metric for the dynamic rotation perception (see Appendix J for details on the metric). The metric was selected because it was robust to subject sensorimotor reaction delays and differences in the perceptual response just proceeding the dynamic period. From training sensorimotor reaction delays were estimated to range from 0.05 to 0.35 seconds (see Appendix F for details) and pre-tilt errors were generally within +/- 5 degrees from upright on individual trials. While neither the actual dynamic rotation nor generally the perceptual responses were linear over the entire dynamic period, over the central 50% both were nearly linear. Perceptual responses that had  $R^2$  values  $< 0.75$  were rare and were excluded from the analysis (16 of 532 for tilts, and 18 of 532 for returns). A normalized slope metric of one indicates accurate dynamic perception, greater than one corresponds to overestimation, and less than one is underestimation. While the slope metric measures the rate of change of perceived roll tilt, we do not consider it a direct measure of perceived angular velocity. Subjects were instructed to instantaneously match the indicator position with perceived tilt, as opposed to match indicator rotation rate with perceived angular velocity. This is an important nuance since perceived angular velocity and



changes in perceived tilt are often dissociated (e.g. perceived tumbling from cross-coupled illusion without comparable changes in perceived orientation). Dynamic perception can be compared to static tilt steady-state perception by comparing the normalized slope metric to a ratio of the static tilt perceived angle to the actual angle.

There was no evidence for left/right asymmetries in the dynamic perception and thus the -20 and 20 degree cases were pooled. Figure 23 shows the dynamic perceptions (tilts and returns combined) as a function of gravity level for each of the angle and frequency combinations tested. Recall from Equation 5 and Table 4 that in 1 G static tilts were accurately perceived (normalized perception = 1), in 1.5 G there was ~17% overestimation (normalized perception = 1.17) and in 2 G there was ~35% overestimation (normalized perception = 1.35). For comparison, these benchmarks of static steady-state tilt perception are overlaid on the dynamic perception data.

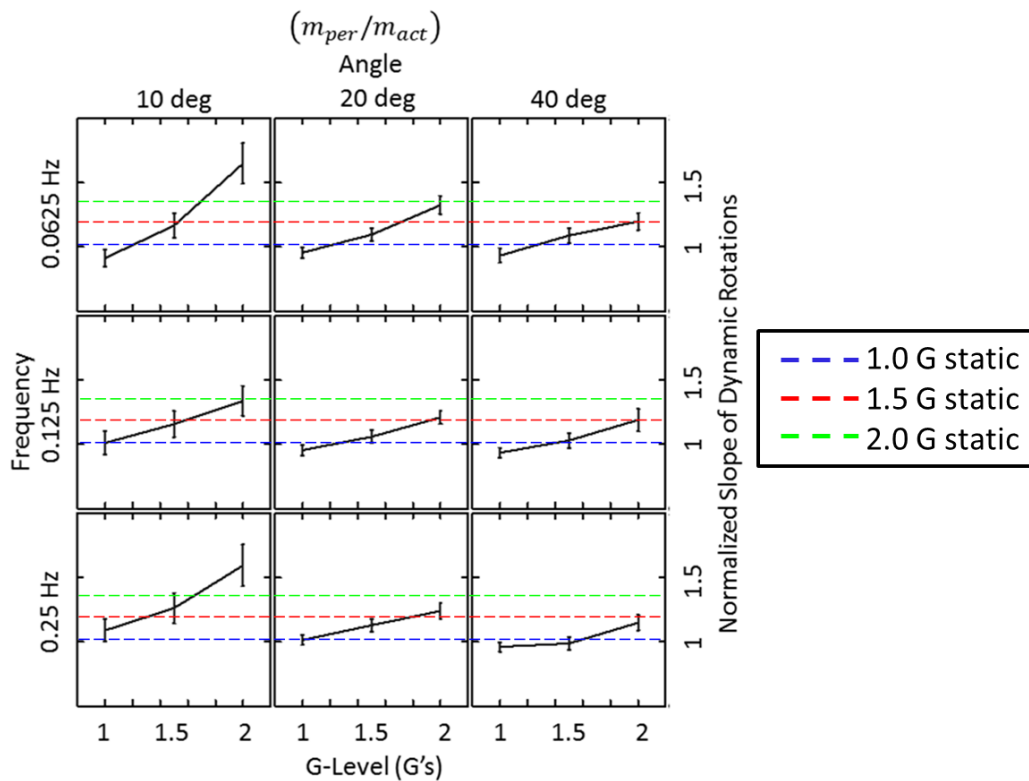


**Figure 23: Normalized Slope of Dynamic Rotations as a Function of G-Level by Angle and Frequency**

The positive trend in dynamic perception with increasing gravity level, shown in each tile of Figure 23, corresponds to overestimation in hyper-gravity that was greater at higher gravity levels. However, the proportional effect of gravity was not the same for every combination of angle and frequency. At small angles and lower frequencies, corresponding to low peak angular velocities (upper left of Figure 23), the trend with increasing gravity was very steep. Yet at larger angles and higher frequencies (bottom right of Figure 23) the effect of gravity was much smaller and was clearly less than the normalized static overestimation (dotted lines). To test the significance of this, the following hierarchical regression model was fit.

$$\left(\frac{m_{per}}{m_{act}}\right)_{ijk} = \rho_i + \lambda_j + \tau DIR + \beta(G - 1) + \kappa(G - 1)\omega_{peak} + \delta(G > 1)REP + \epsilon_{ijk} \quad (7)$$

In Equation 7,  $\rho_i$  is the intercept for subject  $i = 1-8$ ,  $\lambda_j$  is the 1 G response for the  $j$ th angle and frequency combination (3 angles x 3 frequencies:  $j = 1-9$ ), and DIR is the dynamic rotation direction and is either 0 for tilts or 1 for returns. The remaining terms all address the effect of hyper-gravity on the dynamic perceptual response, where  $G$  is the gravity level in G's,  $\omega_{peak}$  is the magnitude of the peak angular velocity for the rotation, REP is either 0 for the first session at a particular hyper-gravity level or 1 for the second session at that hyper-gravity level. The REP term is only active for hyper-gravity levels ( $G > 1$ ). In 1 G this term is omitted, even on the second session, since we expect there to be no adaptation in 1 G responses. In hyper-gravity, however, we hypothesize that sensory conflict may lead to adaptation or learning. The results from the model fit are given in Table 6.

**Table 6: Dynamic Rotation Perception Model Results**

Coefficient	Units	Estimate	Standard Error	Z value	p-value
$\bar{\rho}_i$	Unitless	0.90			
$\tau$	Unitless	0.157	0.024	-6.64	<0.0005
$\beta$	1/G's	0.45	0.050	8.91	<0.0005
$\kappa$	1/(G*deg/s)	-0.016	0.006	-2.76	0.006
$\delta$	1/G's	-0.065	0.029	-2.26	0.024

The significantly positive  $\beta$  and significantly negative  $\kappa$  terms indicate that 1) there was significant overestimation in hyper-gravity, 2) there was more overestimation at higher gravity levels, and 3) the amount of overestimation depended upon the angular velocity of the rotation. In particular, there was more overestimation at lower angular velocities and less at higher angular velocities. In addition, the significantly negative  $\delta$  term indicates that on the second repetition of a particular hyper-gravity level, subjects adapted and overestimated the dynamic rotation less than on the first repetition. Note that while there was evidence here for adaptation in dynamic rotations in hyper-gravity, there was none for static tilts. Finally, in all cases, the magnitude of the slope of dynamic returns was perceived as larger than dynamic tilts. However, the effects of hyper-gravity, angular velocity, and adaptation were similar for tilts and returns. To visualize the dynamic perceptual response in hyper-gravity, the dependence upon angular velocity and its relation to static overestimation, Figure 24 shows the model predictions from Equation 7 and Table 6 along with the raw data for just dynamic tilts in the first session of each gravity level (no adaptation effect).

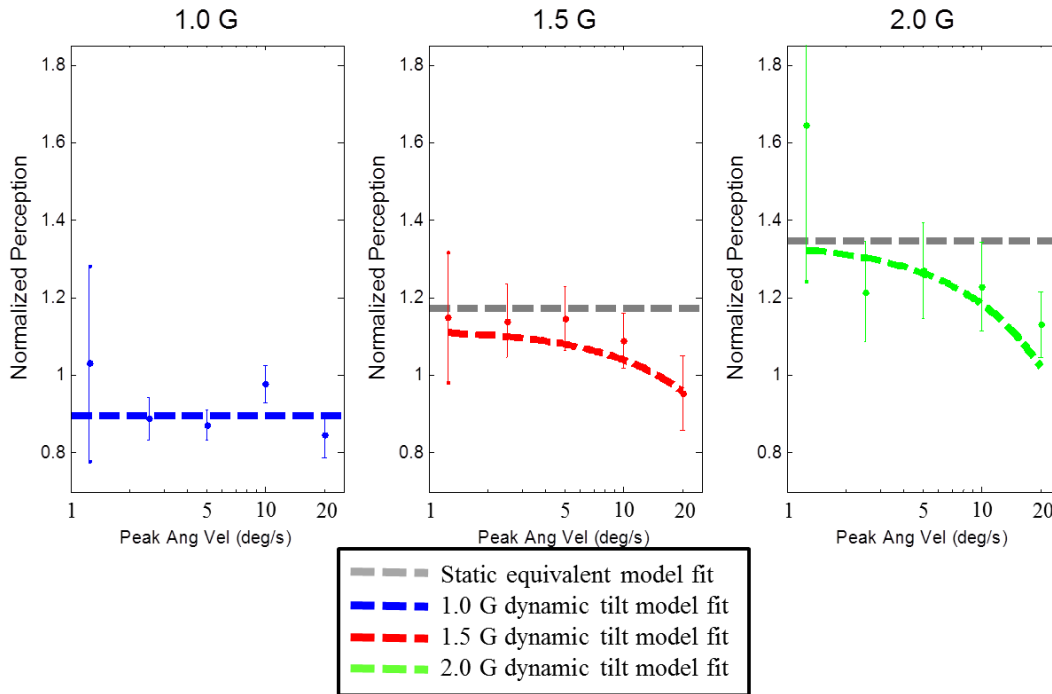


Figure 24: Dynamic Tilt Model Predictions (Normalized)

#### 4.2.9 Static Tilt Transient Perception

Related to the perceptual response during the dynamic tilt period is the perceptual response, just following the dynamic period (i.e. the static tilt transient perception). To quantify how the perceptual response changed during initial static tilt period, we calculated the difference in perception ( $\Delta_{\text{per}}$ ) after 26-28 seconds of static tilt (just prior to the static tilt steady-state period) and that after 0-2 seconds of static tilt (immediately following the dynamic tilt). The change in static tilt transient perception did not exhibit any left/right asymmetries, nor any dependence upon gravity level or frequency of the dynamic tilt (see Appendix K for details). As seen in Figure 25, there was a dependence upon the magnitude of the angle.

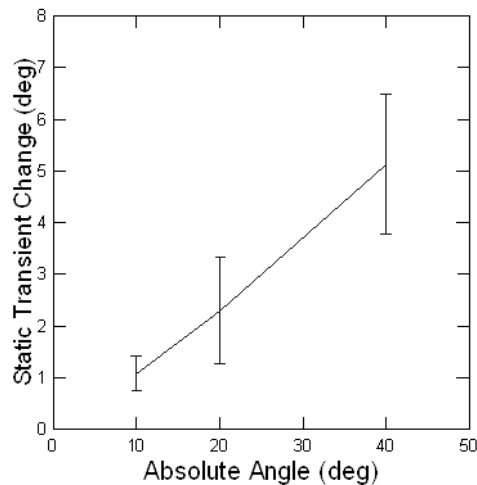
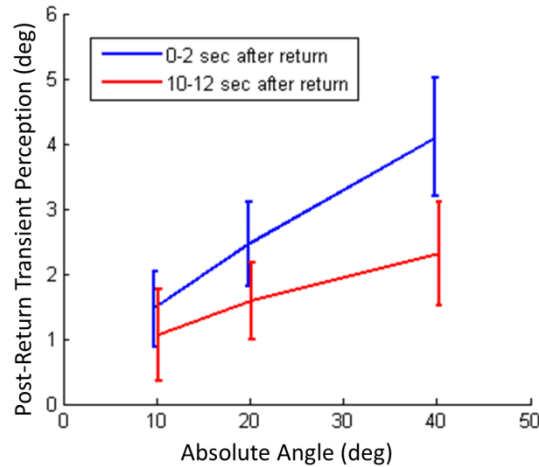


Figure 25: Static Tilt Transient Growth

The perceptual response grew to a larger angle during the static tilt transient period, with the growth proportional to the actual angle. A hierarchical regression model was fit with angle as the independent variable, subject as the identifier, and mean change in perceptual response as the dependent variable. The angle was statistically significant ( $\beta = 0.14$ ,  $Z(15) = 5.33$ ,  $p < 0.0005$ ) indicating 1) the static tilt angle was perceived as larger after 26-28 seconds of static tilt than immediately following dynamic rotation and 2) the amount of growth during the static tilt transient period was approximately 14% of the actual angle, resulting in more growth for larger angles.

#### 4.2.10 Post-Return Transient Perception

To quantify the post-return transient perception, the perceptual response just after (0-2 seconds) and a short time after (10-12 seconds) returning to upright were calculated. The post-return transient perception metrics did not exhibit any left/right asymmetries, nor any dependence upon gravity level or frequency of the dynamic tilt (see Appendix K for details).



**Figure 26: Post-Return Transient Perception Delay**

Figure 26 shows that immediately after returning to upright from a tilt angle (blue), the subject still perceived themselves as tilted in the direction of the previous tilt angle. Fitting a hierarchical regression with angle as the independent variable, subject as the indicator, and mean immediate post-return perception as the dependent variable found angle statistically significant ( $\beta = 0.087$ ,  $Z(15) = 3.71$ ,  $p < 0.0005$ ). Thus the magnitude in the immediate upright perception bias was proportional to the previous tilt angle (approximately 11%). After 10-12 seconds, the bias was reduced but was still significant ( $\beta = 0.066$ ,  $Z(15) = 5.3$ ,  $p < 0.0005$ ). The perceptual response did not appear to reach a steady-state after 12 seconds; however the indicator reset was performed part way through the 30 second upright period between trials, preventing a continuous perceptual response from being tracked beyond this duration.

#### 4.2.11 Summary of Results and Discussion

We characterized and quantified subject perceptions of static and dynamic whole-body roll tilt orientation in 1, 1.5, and 2 G environments across a wide range of tilt angles and frequencies. Confirming previous results, when initially upright, subject's perceived themselves as near upright in roll tilt, even in

hyper-gravity. Accurate roll tilt perception in hyper-gravity has been previously attributed by the utricular shear theory to the average plane of the utricles being aligned with the Earth horizontal in roll. Thus when the head is upright (no roll tilt), there is no additional interaural shear forces acting on the otolith membrane of the utricles when the gravity level is increased. While the current experiment was not designed to test this hypothesis, our perceptual data are consistent with it.

During static tilt, subjects misperceived their orientation in hyper-gravity. Specifically, subjects overestimated their roll tilt, with more overestimation at higher gravity levels and larger angles. At 1.5 G, the static roll angle was overestimated by approximately 17%, while at 2 G's it was 35%. The proportional effects of angle and gravity level should only be applied at the range of angles and gravity levels tested. Prior data, which match the current data well at up to the 40 degree angles tested, indicate that at angles much larger than 45 degrees the amount of overestimation begins to decrease with increasing angle, and may turn to underestimation near 90 degrees. Furthermore, while few studies have tested gravity levels much greater than 2 G, we would hypothesize that at more extreme gravity levels the amount of overestimation would be less than proportional to gravity level. In monkeys, at gravity levels greater than approximately 4 G's the otolith afferent firing rate reaches a limit and no longer behaves near linearly with changes in GIF stimulation (Fernandez and Goldberg 1976; Fernandez and Goldberg 1976; Fernandez and Goldberg 1976). While our primary interest was in hyper-gravity perception, as a control we also measured roll tilt perception in 1 G. These perceptions are traditionally characterized by slight overestimations for small angles and then underestimation for very large angles (i.e. at least >60 degrees), commonly referred to as E- and A-effects, respectively (Aubert 1861; Muller 1916). Our 1 G perceptions are near accurate and thus do not clearly show these phenomena. However, we tested at relatively small angles where these effects would be small and difficult to observe. Furthermore, A- and E-effects have been primarily studied using the SVV, whereas we used a somatosensory task which may not have these same characteristic errors in 1 G.

The current data could not be fit well with any of the previously proposed models (utricular shear, tangent, or Ormsby and Young nonlinear models). We proposed a modified version of the utricular shear model that, with two free parameters, not only fit the current data across three gravity levels and four angles, but also qualitatively fit previous data even at gravity and angle combinations to which the model was not specifically trained upon. The model is a simple empirical fit, but does indicate that the amount of overestimation in hyper-gravity is only about 26% of that expected from the traditional utricular shear model. We hypothesize that this large reduction in the expected static overestimation in hyper-gravity may be due to the CNS utilizing information from other static graviceptors (otolith cues out of the utricular plane, proprioceptive, tactile, somatosensory, or potentially trunk graviceptors). If the CNS appropriately utilizes graviceptor information beyond just the utricular plane it should be able to resolve accurate perception of orientation even in hyper-gravity. However, the fact that there is indeed some static overestimation in hyper-gravity indicates a dependence upon the utricular otolith sensory information.

Perceptual overestimation was also seen during dynamic tilts and returns in hyper-gravity. The amount of overestimation was less than during static rotations, however persisted across all angles and

frequencies tested. The magnitude depended upon the angular velocity of the rotation; at lower angular velocities more overestimation was observed and at higher angular velocities there was less overestimation. The angular velocity dependence of the hyper-gravity effect on perception is supportive of the CNS integrating otolith and semicircular canal sensory sources. The hyper-gravity paradigm affects the otolith signal, but presumably has almost no influence on the canal information. Furthermore the reliability of the canal signal is greater at higher rotation rates. Thus, less overestimation in hyper-gravity at higher rotation rates is consistent with CNS increasing the relative weighting on the canal signal as it becomes more reliable.

Perceptual transients existed during static tilt and following a return to static upright, which were proportional to the tilt angle, but did not depend upon gravity or rotation parameters (e.g. frequency). These transients may have been exaggerated by using the continuous version of the somatosensory indicator task. A discrete task (i.e. subjects align the bar, press a button to record the response, quickly rotate the bar back and forth, and then reset the bar) may have helped perceptual responses to be more independent from previous responses and thus reach a steady-state more quickly (Merfeld, Zupan et al. 2001).

Evidence of adaptation in the subject's perceptual response in hyper-gravity was identified for dynamic rotations, but not static tilts. During testing, there was no feedback provided by the experimenters to help drive this adaptation. Sustained sensory conflict between expected and actual afferent signals, as experienced in hyper-gravity, is well known to drive sensorimotor adaptation (Gonshor and Melvill Jones 1971; Kornheiser 1976; Reason 1978; Reason and Benson 1978; Oman, Bock et al. 1980; Oman, Lichtenberg et al. 1986; Welch, Bridgeman et al. 1998; Edgerton, McCall et al. 2001; Lackner and DiZio 2003; Bos and Bles 2004; Lackner and DiZio 2005; Seidler 2005; Nooij, Bos et al. 2008; Pettorossi, Panichi et al. 2013). While sensory conflict certainly existed for static tilts in hyper-gravity, there was not significant evidence for adaptation either in repetitions between sessions or within a session. The passive rotations and the lack of strong feedback from a secondary veridical sensory source may have limited adaptation. Studying adaptation was not the primary purpose of the current experiment so only two presentations of each stimulus were repeated. Additional or longer sessions in hyper-gravity may result in perceptual adaptation for static tilts in hyper-gravity. There was, however, evidence for adaptation in perceptual errors in hyper-gravity for dynamic rotations. During dynamic rotations there is feedback on the gravity-influenced otolith signal from the semicircular canals. While the rotations were still passive, the canal feedback may have helped drive adaptation more quickly than for static tilts. Only two sessions were presented for each gravity level so it remains uncertain how dynamic perceptual errors in hyper-gravity may continue to adapt. We hypothesize that with additional sessions, the dynamic perceptual errors in hyper-gravity would continue to decay towards veridical responses. The adaptation observed can be considered "context-specific adaptation" (Shelhamer, Clendaniel et al. 2002), in that the reduced overestimation in the second session of a particular hyper-gravity level was interrupted by sessions at other gravity levels and breaks between sessions.

## 5.0 Experiment 2: Vehicle Control in Hyper-Gravity

In Experiment 1, we characterized and quantified the misperceptions in roll orientation caused by hyper-gravity. Specifically, subjects overestimated their roll angle in hyper-gravity during both dynamic and static tilts. In Experiment 2, we aim to address Specific Aim 2 and test Hypothesis 2. We tested how the misperceptions made in hyper-gravity may impact performance on a pilot *manual control* task. Prior to the experiment, subjects were introduced to the cross-coupled illusion, trained at the manual control task, and exposed to the hyper-gravity environments to reduce anxiety prior to testing (Section 5.1.6).

### 5.1 Methods for Experiment 2

As in Experiment 1, NASTAR Center’s ATFS-400 long-radius centrifuge was used to create the hyper-gravity motion paradigm (Figure 6). The subjects’ (N=12) configuration was almost identical: seated in the dark with noise-cancelling head phones for two-way communication with the experimenter. The head and upper torso were supported by a custom head support and vacuum cushions to reduce localized haptic cues (Figure 5). The same motion paradigm to create the hyper-gravity environment was used as in Experiment 1 (Figure 6). However, instead of reporting perceptions of passive roll tilts using the somatosensory indicator, subjects used a rotational hand controller (RHC) to actively command roll control inputs and attempt to keep the cab of the centrifuge “upright” in response to a roll tilt disturbance. The entire protocol was completed in one day in the following order: cross-coupled illusion presentation protocol, training at the manual control task in 1 G, the G-Exposure protocol, and then the four sessions of testing.

#### 5.1.1 Roll Tilt Disturbance

The roll tilt motion disturbance was a computer-generated pseudo-random zero-mean sum-of-sines profile. Twelve harmonically-independent sinusoids were utilized ranging in frequency from 0.014 to 0.668 Hz (Table 7). The frequencies and phase shifts used were identical to a previous pre/post-flight manual control experiment (Merfeld 1996). The amplitudes of each sinusoid, however, were modified. Pilot experiments (see Appendix M) showed that for this task subjects were only able to effectively null frequencies less than 0.2 Hz. To ensure reasonable performance, the majority of the disturbance power was placed at lower frequencies and the amplitude was reduced by a decade at frequencies above 0.2 Hz.

**Table 7: Roll Tilt Disturbance Parameters**

Number	Frequency (Hz)	Phase (deg)	Tilt Amplitude (deg)
1	0.014	0	2.6472
2	0.024	37	2.6472
3	0.053	74	2.6472
4	0.083	111	2.6472
5	0.112	148	2.6472
6	0.151	185	2.6472
7	0.200	222	0.2647
8	0.258	259	0.2647

9	0.346	296	0.2647
10	0.434	333	0.2647
11	0.532	19	0.2647
12	0.668	47	0.2647

An example roll tilt disturbance profile is given in Figure 27 (see Appendix L for MATLAB code used to create profiles). The same disturbance profile was used for each trial except for a possible sign change (i.e. left versus right) to prevent subjects from realizing the disturbance was repeated. In post-experiment interviews, it was confirmed that subjects remained naïve to this repetition. The maximum roll tilt of the disturbance was 13.4 degrees and the maximum angular velocity was 7.13 degrees/second.

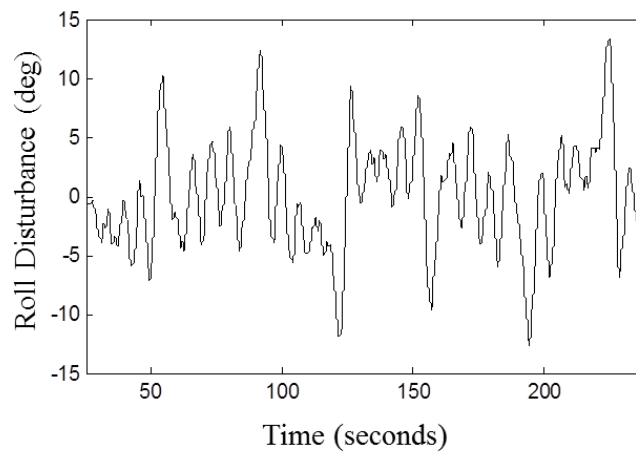


**Figure 27: Example Roll Tilt Disturbance Profile**

The profile for each trial lasted 214.8 seconds, however the first and last 5 seconds were scaled such that the profile begins and ends at upright. These beginning and ending portions were discarded prior to analysis, so the length of interest was 204.8 seconds. The duration was selected to match a previous experiment (Merfeld 1996) and was found to be reasonable to ensure subjects maintained focus.

### 5.1.2 Rotational Hand Controller

Subjects attempted to null out the roll disturbance using a RHC or joystick. Subjects were instructed to “keep the cab/vehicle as erect as possible.” The RHC consisted of a 30 cm long vertical rod that rotated about its center point and was located approximately 35 cm from the midriff of the seated subject (see Figure 28). Subjects held the RHC near its central rotation axis, such that no large hand or arm displacements were required to make control inputs. Subjects used whichever hand they preferred (i.e., their dominate hand) to operate the controller. The RHC was spring loaded such that the more the stick was deflected from upright the more resistance was felt. If released, the springs would cause the RHC to return to upright (nearly critically damped). The RHC could only rotate in roll and there were mechanical stops to prevent stick deflections of greater than +/- 45 degrees. The RHC orientation was recorded using a potentiometer (Vishay Spectrol 601HE0000B01 Hall Effect Position Sensor).





**Figure 28: Rotational Hand Controller**

The vehicle dynamics were rate-control-attitude-hold (RCAH), such that amount of stick deflection was proportional the commanded roll rate of the controlled vehicle (0.44 deg/sec of roll rate was commanded per degree of stick deflection with a maximum commanded roll rate of 20 deg/sec). The response dynamics of the vehicle were rapid, with software and actuation delays much less than the human sensorimotor delays. Without any disturbance, if the RHC was upright the vehicle would remain at its current roll orientation. These vehicle dynamics are similar to those of a helicopter or a lunar landing vehicle. The first order control system is relatively easy to control and can be mastered, even by non-pilots, fairly quickly. In the software there was a +/- 1 degree deadband about upright in the RHC such that small, unintended stick deflections did not gradually change vehicle orientation. To prevent a subject from commanding an unusual and uncomfortable orientation there were +/- 25 degree roll tilt safety limits in the software. During testing these limits were only reached on 1/144 trials (see Appendix Q). See Appendix M for a summary of the disturbance and control software architecture.

### **5.1.3 Independent Variables**

The primary independent variable in Experiment 2 was the gravity level. The same 1, 1.5, and 2 G levels were tested (see Table 2 for centrifuge rotation requirements). In addition, to study how performance changed over time, we presented multiple trials at each gravity level. Three consecutive trials in the same gravity level were presented in a session. As before, each session began with a 60 second spin-up period and a 60 period for the subject to acclimate prior to testing. Then three 214.8 second long trials were presented with 30 second breaks between trials. During the breaks, the vehicle cab remained upright (aligned with the GIF) and the subject remained at the testing gravity level. After the third trial, the centrifuge was spun-down over 60 seconds. During spin-up, acclimation, breaks, and spin-down the RHC was deactivated so any stick deflections would not influence cab orientation. The total time for a session was less than 15 minutes. Approximately 20 minute breaks were provided between sessions, in which the subject was removed from the centrifuge, and relaxed in the 1 G environment. Activities during the breaks were uncontrolled. An example profile for 1.5 G is given in

Figure 29. Note that in this experiment, the actual cab orientation during the trial period is also dependent upon subject RHC inputs.

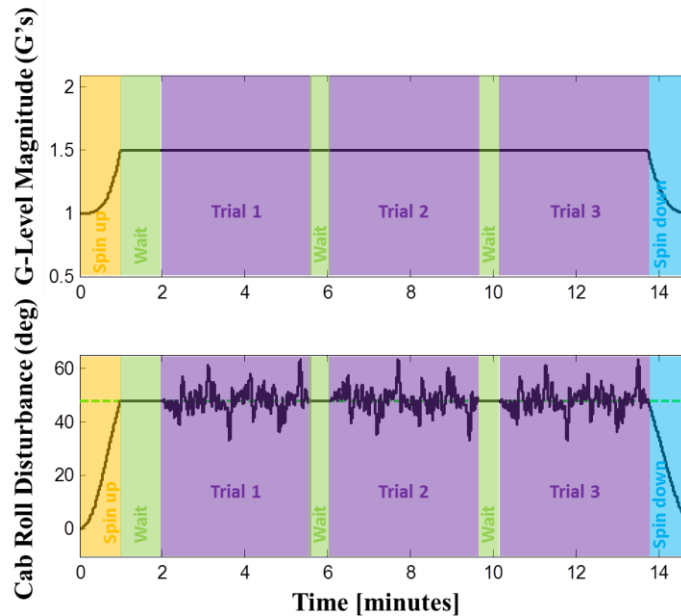


**Figure 29: Example Complete Testing Session for Experiment 2**

In addition to treating trial number as an independent variable, changes in performance were also studied within a trial. In analysis, each trial was split into 6 segments of 34 seconds each. Since each trial was identical except for a possible sign change (i.e. left vs. right), the disturbance was controlled within each short segment. Thus performance on any specific segment could be compared across trials (and gravity levels) since the disturbance was identical.

#### 5.1.4 Dependent Variables

Centrifuge spin rate, disturbance roll tilt, RHC position, and the resulting actual cab roll tilt were recorded at 100 Hz. The primary performance metric was the RMS error of the resulting cab roll tilt. Smaller RMS values indicated better manual control performance. In addition, the mean cab roll angle, standard deviation of the cab roll angle, and metrics for RHC inputs were considered as objective measures of performance and control strategy. Metrics in the frequency domain were used sparingly because the changes in performance observed during trials violated the stationary assumptions of the Fourier transformation. After each trial, during the 30 second break, subjects reported four items: 1) subjective estimate of performance on a 0-10 scale where 0 indicates perfect nulling performance and 10 indicates no nulling was accomplished, 2) subjective mental workload using the modified Bedford scale (Roscoe 1984; Roscoe and Ellis 1990), 3) the maximum Coriolis cross-coupled stimulus intensity experienced using the subjective scale developed in the pre-experimental protocol, and 4) motion sickness intensity rating. Subjects remained naïve to the hypotheses of the experiment to reduce the cognitive bias in their subjective reports.

### 5.1.5 Experimental Design

The design was fully within-subject and complete, such that every subject was tested in 1, 1.5 and 2 G conditions. As described above, sessions, consisting of three trials each, were presented at each of the gravity levels. Four distinct orders of gravity level presentation were utilized (Table 8), with each subject randomly being assigned to one of the orders such that the same number of subjects (N=3) was assigned to each order.

**Table 8: Four Orders of Sessions**

Order	Session 1	20min break	Session 2	20min break	Session 3	20min break	Session 4
A	1 G		1.5 G		2 G		1 G
B	1.5 G		1 G		2 G		1 G
C	1 G		2 G		1.5 G		1 G
D	2 G	1 G	1.5 G	1 G			

Orders A and B both had 1.5 G as the first hyper-gravity level presented, with the only difference between the two orders being the counter-balancing of whether 1 or 1.5 G was presented first. The same goes for orders C and D, except 2 G is the first hyper-gravity level presented. For all orders, the third session is the other hyper-gravity level that has yet to be presented. The fourth session is a repetition of 1 G to test for learning, fatigue or whether hyper-gravity testing influence 1 G performance. A summary of the independent and dependent variables for Experiment 2 is given in Table 9.

**Table 9: Summary of Independent and Dependent Variables for Experiment 2**

Independent Variables	Treatment Levels		
G-Level	1.0 G	1.5 G	2.0 G
Trial Number (within a session)	1 – 3		
Segment Number (within a trial)	1 – 6		
Dependent Variables			
RMS Error in Actual Cab Roll Angle			
Subjective Performance			
Subjective Workload			

### 5.1.6 Pre-Experimental Protocols

Prior to the primary experiment, three protocols were completed to prepare the subject. These included the Coriolis Cross-Coupled Presentation protocol, Manual Control Training, and the G-Exposure Protocol utilized in Experiment 1.

First, the subject completed the Coriolis Cross-Coupled Presentation Protocol. Based upon pilot experiments, the hyper-gravity testing for Experiment 2 provoked a much less intense cross-coupled illusion than in Experiment 1. While there was a continuous roll disturbance, subjects generally were able to keep the cab near upright (within +/- 10 degrees), avoiding the cross-coupled provoking large rotations experienced in Experiment 1. As a result, the full cross-coupled *adaptation* protocol performed for Experiment 1 was not used here. However, a *presentation* protocol was utilized which introduced subjects to the sensations of the cross-coupled illusion and fixed a scale to report illusion intensity. As in Experiment 1, subjects were seated in NASTAR Center’s Gyroflight simulator in the dark and secured

with a waist seat-belt. Subjects wore noise-cancelling headphones for communication and an infrared camera allowed the experimenters to monitor the subject during testing. The simulator was spun up in pure yaw rotation to 14.26 rpm (85.56 degrees per second), corresponding to the fastest planetary angular velocity experienced during the hyper-gravity testing. Once at this yaw rate, subjects performed a series of four active head-on-body roll tilts: 1) from upright to right ear down, 2) right ear down back to upright, 3) upright to left ear down, and 4) left ear down back to upright. Each head tilt was approximately 40 degrees in approximately 1 second. At least 10-15 seconds were provided between successive head tilts to let any illusory motion sensations subside. After each head tilt, subjects reported the *direction* (i.e. either primarily pitching forward or backward) and the relative *intensity* of the illusory tumbling sensation. The intensity was reported using the following scale: 0 corresponded to no unusual sensation such as would be experienced during a head tilt in everyday life and a 10 was arbitrarily assigned as the intensity of the first head tilt (Young, Hecht et al. 2001; Brown, Hecht et al. 2002; Hecht, Brown et al. 2002; Adenot 2004; Bruni 2004; Jarchow and Young 2007). After the series of four head tilts, the device was slowed down and the subject removed. Any cross-coupled illusion experienced during the experiment was reported using the intensity scale developed here.

Subjects were extensively trained in 1 G on the manual control task. Subjects were first briefed on the vehicle dynamics and how to use the RHC to control their orientation. Then in the ATFS-400, they were provided practice trials to learn the task, develop a suitable control strategy, and practice to steady-state performance levels. All practice trials were completed in the dark. On the first practice trial, no computer-controlled disturbance was provided to allow subjects to understand how their RHC inputs would affect cab roll tilt. Subjects were encouraged to rotate off to an angle and then try to make the appropriate control inputs to bring the cab back to upright. The following practice trials included a disturbance with the same parameters as that used in the experiment. On the first few trials, subjects were encouraged to try different control strategies and identify one which worked for them. Each trial was 214.8 seconds long. Following each trial subjects were provided qualitative feedback (e.g. you are controlling too aggressively), and intermittently were provided quantitative feedback (i.e. RMS error scores on previous trials). After each trial, subjects also reported subjective performance and workload scores for practice and to develop consistency. Training continued until subjects reached a competent and steady-state performance level in terms of RMS error scores. This took between six and 12 trials. Just prior to testing, 1-2 additional training refresher trials were presented to ensure performance levels were maintained. At the end of training when the subject had settled on a control strategy, they were instructed to maintain that control strategy throughout testing.

Subjects also completed the G-Exposure protocol described in Experiment 1, which introduced the physiological responses normal to hyper-gravity exposure and was intended to make them more comfortable. Hyper-gravity levels of 1.5 and 2 G's were experienced with no manual control or other task during the G-Exposure protocol.

### **5.1.7 Study Approval, Subjects, and Forms**

All of the Experiment 2 protocols were approved by the ETC/NASTAR Center's IRB and MIT's COUHES. As in Experiment 1, subject selection criteria included healthy females and males ages 18-65

with no known vestibular defects or conditions. MSSQ reports excluded individuals with high or no motion sickness susceptibility. Subjects also completed NASTAR Center's medical screening questionnaire, a waiver and liability form, a questionnaire on previous flight and centrifuge experiences, and a pre-exposure SSQ (Keshavarz and Hecht 2011). After the cross-coupled stimulus protocol, the G-Exposure protocol, and each testing session, subjects completed a post-exposure SSQ form to monitor motion sickness. See Appendix N for proof of study approval and forms associated with Experiment 2. Forms that were also used in Experiment 1 are in Appendix D. All subjects signed a written informed consent form.

Twelve subjects were tested (10M/2F, ages 22-38, mean = 27.5, standard deviation = 4.9). Subjects were randomly assigned to one of the four orders (Table 8), such that each order was completed by three subjects. Thus half of the subjects (N=6) experienced 1.5 G as the first hyper-gravity level and half (N=6) experienced 2 G as the first hyper-gravity level. One subject had flight experience (~390 hrs) and four had minimal centrifuge experience (< 2 hrs). One subject completed Experiment 1 approximately 11 months prior to completing Experiment 2. All other subjects had not completed Experiment 1. These subjects' results did not appear to differ from the remaining subjects. All subjects were able to complete the protocols and experienced no serious adverse effects. Minor motion sickness symptoms occurred for approximately half of the subjects, particularly resulting from the cross-coupled stimulus protocol and the spin down from hyper-gravity during testing sessions; however no subjects approached vomiting nor asked to stop the experiment. Five additional subjects completed portions of the training or the experiment, but were not able to continue due to technical issues. These subjects were omitted from the analysis.

The level of significance was set to  $\alpha = 0.05$ .

## **5.2 Results for Experiment 2**

### **5.2.1 Performance in 1 G**

The RMS error from upright was calculated as the primary performance metric for each trial. While there was often substantial improvement in performance during training (see Appendix O), during testing performance was fairly consistent in 1 G. Considering only the 1 G trials, a hierarchical regression model with session number (1 or 2), trial number (1, 2, or 3), and order (A, B, C, or D) as independent variables and RMS as the dependent variable found only trial number to be statistically significant ( $\beta = 0.13$ ,  $Z(55) = 2.28$ ,  $p = 0.023$ ). However, the decline in performance with repeated trials was primarily due to a decrement on the last trial of the last session (see Appendix P for figure). If the final trial was removed from the analysis, the RMS performance was consistent across session number, trial number, and order. The poor performance on the final trial may be attributed to a lack of focus in expectancy of completing the experiment or fatigue. The consistent performances across the first 5 trials (3 trials in the first session and first 2 trials in the second session) in 1 G were averaged for each subject to determine that individual's 1 G "baseline" performance. The 1 G baseline RMS errors varied between subjects (mean = 2.73 degrees, SD = 0.43 degrees, min = 2.05 degrees, max = 3.40 degrees), which represents individual differences in skill level at the manual control task. To account for this, all hyper-gravity

performances were calculated as differences from each subject’s individual 1 G baseline performance (mean of 5 trials). The consistency in 1 G performance between the first and second session indicates that the recent tests in hyper-gravity do not have a lasting effect that impairs performance on the second 1 G session.

### 5.2.2 Effect of Hyper-Gravity on Initial Performance

We hypothesized that there would be a performance decrement upon initial exposure to hyper-gravity. The difference between performance, in terms of RMS error, on the *first* trial in hyper-gravity and each subject’s 1 G performance baseline is shown in Figure 30. As mentioned earlier, half of the subjects (N=6) experienced 1.5 G as the first hyper-gravity level (orders A and B) and half (N=6) experienced 2 G as the first hyper-gravity level (orders C and D).

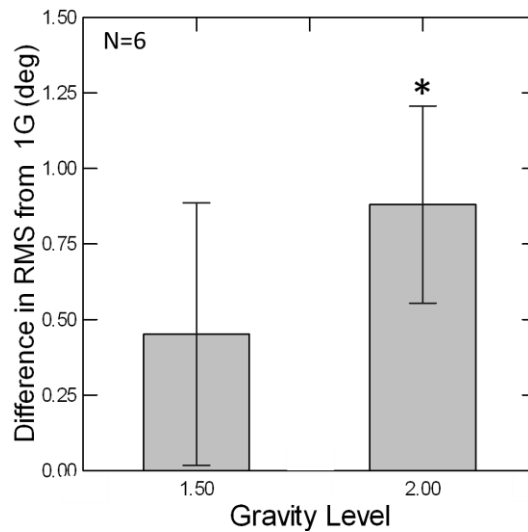
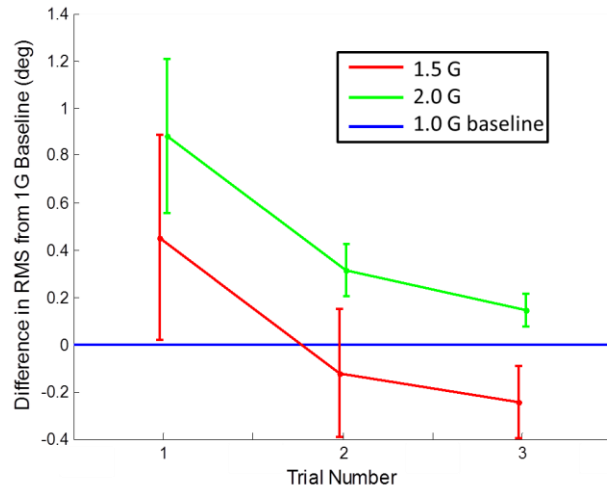


Figure 30: Performance Decrements on First Trial in Hyper-Gravity

The positive differences in RMS on the first trial in hyper-gravity indicate performance decrements relative to the 1 G performance baseline. Using a paired-samples t-test, the RMS in the 2 G condition was significantly greater than the 1 G performance baseline (mean = 0.88 degrees, SD = 0.80 degrees,  $t(5) = 2.70$ ,  $p = 0.043$ ). The effect in 1.5 G’s was trending towards a decrement, but was not statistically different from the 1 G performance baseline.

### 5.2.3 Change in Performance and Subjective Reports in Hyper-Gravity by Trial

We hypothesized that with practice, performance would improve in hyper-gravity. This was first investigated on a trial-by-trial basis. Figure 31 shows the difference in RMS between the first hyper-gravity session and the 1 G baseline across the three trials. One trial (subject 12, trial 3, gravity level = 2 Gs) was removed from Figure 31 as an outlier (difference in RMS from 1 G baseline = 2.89 degrees, Studentized residual = 5.16). On this particular trial, the subject made one uncharacteristic control reversal which resulted in the cab roll angle reaching the hard limits ( $\pm 25$  degrees) (see Appendix Q for details). The one very large error inflated the entire trial’s RMS error score.



**Figure 31: Hyper-Gravity Performance by Trial**

While there were initially large performance decrements in hyper-gravity on the first trial (trial 1 in Figure 31 is the same data as in Figure 30), performance improved on the second and third trials. In 1.5 G the performance may even improve to levels better than the 1 G baseline. These effects did not reach significance (see Appendix O for attempted statistical fits).

The individual differences from the 1 G baseline for the subjective reports of performance and the subjective reports of workload using the modified Bedford scale are shown in Figure 32.

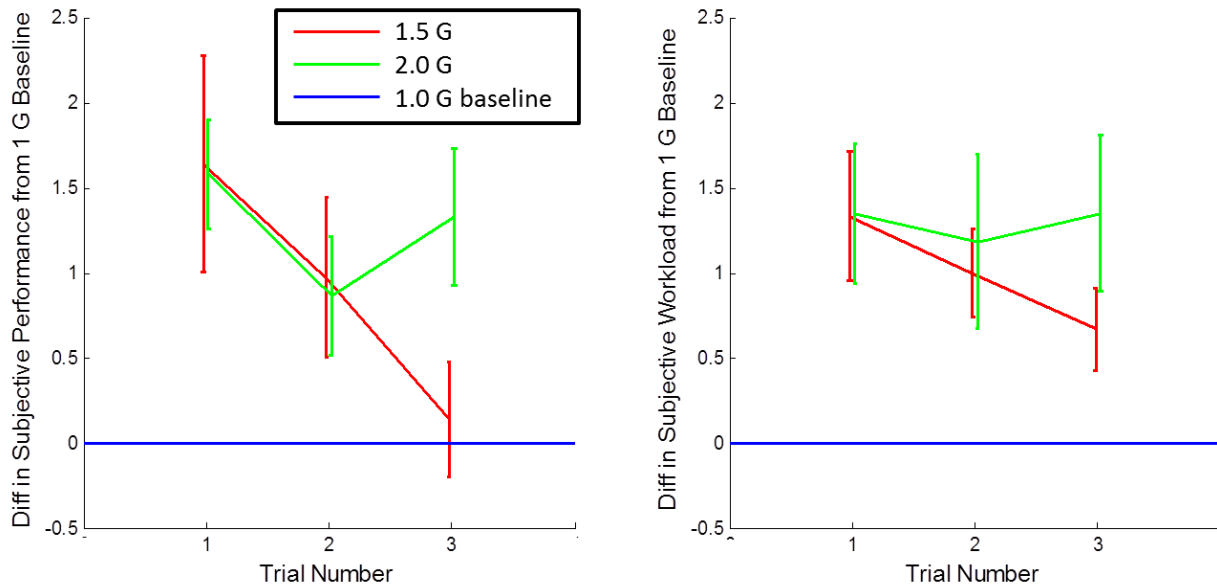


**Figure 32: Subjective Performance and Workload Reports in Hyper-Gravity by Trial**

On the first trial in hyper-gravity, subjective performance reports increased relative to the 1 G baseline, which corresponds to worse perceived performance (paired-samples t-tests; 1.5 G:  $t(5) = 2.58$ ,  $p = 0.049$ ; 2.0 G:  $t(5) = 4.93$ ,  $p = 0.004$ ). This corresponds well with the objective decrement in performance. Similarly, the subjective workload was higher on the first trial in hyper-gravity compared

to the 1 G performance (paired-samples t-tests; 1.5 G:  $t(5) = 3.49$ ,  $p = 0.018$ ; 2.0 G:  $t(5) = 3.29$ ,  $p = 0.022$ ). The subjective performance improved (lower scores) with successive trials at 1.5 G (hierarchical regression with subject as indicator, trial number as independent variable, and difference in subjective performance from 1 G baseline as dependent variable,  $\beta = -0.75$ ,  $Z(11) = -3.20$ ,  $p = 0.001$ ), however there was not significant evidence of improvement at 2 G's. Workload did not significantly improve over successive trials in 1.5 or 2 G's.

#### 5.2.4 Change in Performance in Hyper-Gravity by Segment

Adaptive changes in performance in hyper-gravity can be more precisely studied by considering changes *within* each trial. As detailed in Section 5.1.3, each trial was divided into 6 segments, each 34 seconds in length. Since the exact profile and magnitudes of the roll disturbance were not identical for each segment, the RMS for each segment was compared to the mean 1 G baseline from the respective segment. Recall that on every trial the same profile was used, except a possible left/right reversal, so the profile was identical for each specific segment. By concatenating the trials, the 6 segments per trial can be combined across the 3 trials to yield a total of 18 segments. The performance in the first hyper-gravity session, relative to the 1 G performance baseline is shown in Figure 33. The second segment of the third trial in 2 G's that was impacted by the one extreme error caused by a control reversal was omitted as an outlier both in Figure 33 and the statistical analysis (see Appendix Q for details).

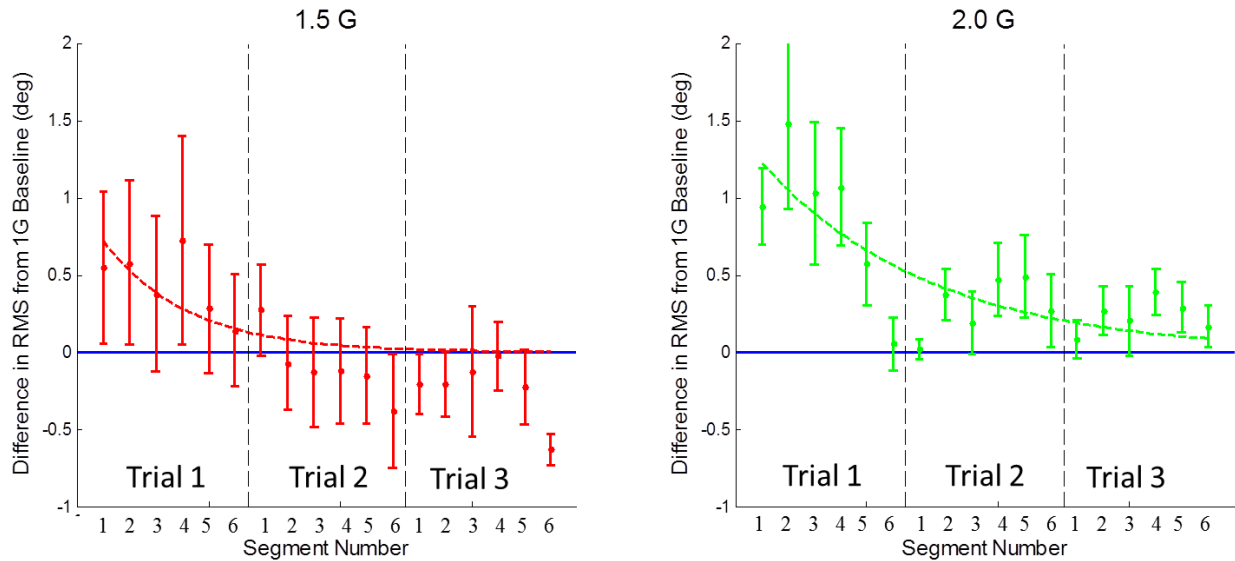


Figure 33: Hyper-Gravity Performance by Segment

In both 1.5 and 2 G's there was an initial performance decrement, with an increased RMS relative to the 1 G performance baseline. However, across segments the performance improved to near, or potentially even slightly better than, the 1 G performance level. To characterize the changes in hyper-gravity performance, the following exponential decay model was fit.

$$(RMS_{hyper-G} - RMS_{1G})_i = A_0 e^{(-\lambda(segment-1))} + \epsilon_i \quad (8)$$



The segment number ranged from 1-18 and separate models were fit for those individuals who experienced 1.5 G's first (orders A and B) versus those who had 2 G's as their first hyper-gravity session (orders C and D).

**Table 10: Exponential Decay Fits for Hyper-Gravity Performance versus Segment**

			95% Confidence Interval	
	Parameter	Estimate	Lower	Upper
1.5 G	$A_0$	0.72	0.11	1.33
	$\lambda$	0.31	-0.12	0.75
2.0 G	$A_0$	1.23	0.86	1.60
	$\lambda$	0.16	0.08	0.23

The model fits are shown graphically in Figure 33. In both 1.5 and 2 G's there was a significant initial performance decrement relative to the 1 G baseline ( $A_0$ ), with a slightly larger initial decrement in 2 G's. In the 2 G model, there was a significant exponential decay (improvement in performance) towards the 1 G baseline. In 1.5 G there was a trend of improvement, but it was not significant. The improvement in performance with segment, or adaptation to hyper-gravity can be characterized by the time constant ( $\tau = 1/\lambda$ ). The time constant for 1.5 G's was estimated to be 3.23 segments or 110 seconds and that for 2 G's was 6.25 segments (213 seconds).

### 5.2.5 Prior Hyper-Gravity Testing Effect on Future Hyper-Gravity Performance

While not an initial primary purpose of the experiments, manual control was tested 1.5 and 2 G's in all of the subjects; half of the subjects experienced 1.5 G first and half were tested in 2 G first. We hypothesized that prior exposure to one hyper-gravity level would reduce the initial performance decrement observed in another novel hyper-gravity level. To test this hypothesis, we compared performance in the subjects that experienced a particular hyper-gravity level first (without pre-exposure) to those that had it as the second hyper-gravity level (with pre-exposure). For example, performance in 1.5 G's was compared between orders A and B (without pre-exposure to 2 G's) and orders C and D (with pre-exposure to 2 G's). For 2 G performance, orders C and D had no pre-exposure to 1.5 G's and orders A and B did. There was not significant evidence it made a difference whether the pre-exposure session was the session just before or two sessions before the second hyper-gravity session (see Appendix S). Thus these orderings were pooled (for example orders C and D were pooled as 1.5 G performance with 2 G pre-exposure). Figure 34 compares performance in a particular hyper-gravity session with and without pre-exposure. Only the performance across the first trial is shown because the performance both with and without pre-exposure approached the 1 G performance baseline after the first trial (see Appendix S). For graphical purposes only one side of the standard error bars are shown.

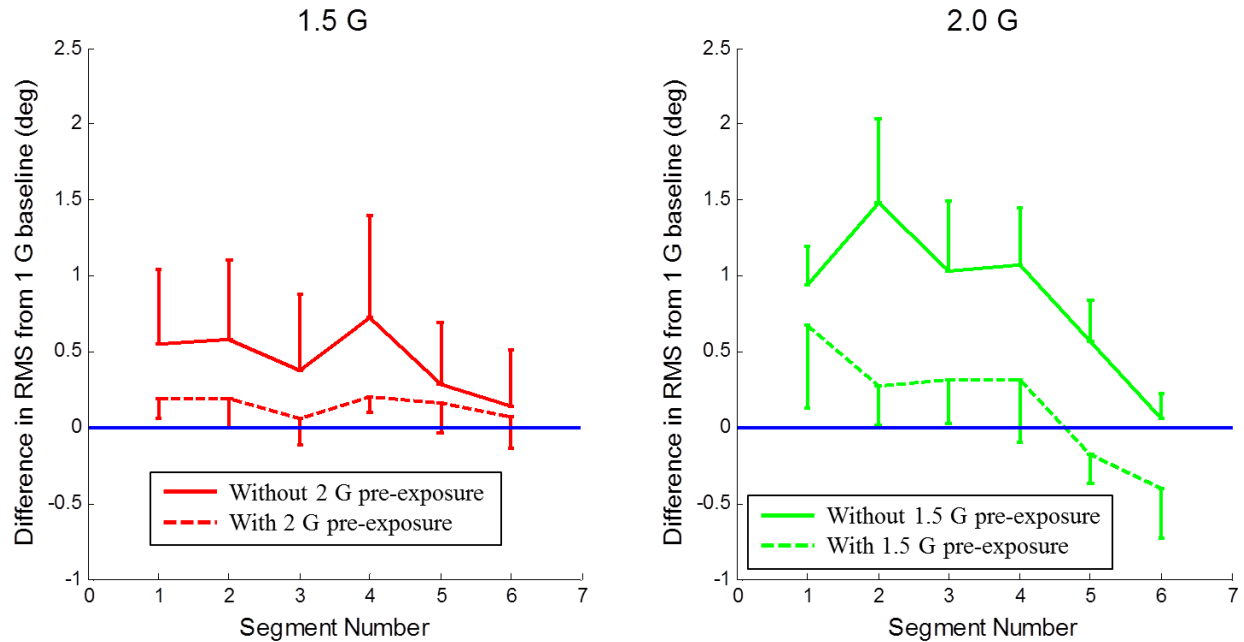


**Figure 34: Effect of Pre-Exposure on Hyper-Gravity Performance on First Trial**

As previously observed, without pre-exposure, there were large performance decrements initially in hyper-gravity (solid lines in Figure 34 are the same data from Trial 1 in Figure 33). However, with pre-exposure there were much smaller performance decrements. In 1.5 G (left side of Figure 34) with 2 G pre-exposure, the performance decrements were not significantly different from the 1 G performance baseline throughout the first trial. At 2 G (right side of Figure 34) with 1.5 G pre-exposure, on the first segment there was a substantial performance decrement. However the subjects adapted much more quickly than those without pre-exposure and after the second segment the performance was near the 1 G baseline. To test the effect of pre-exposure on performance, an ANCOVA model was constructed with hyper-gravity level (1.5 or 2 G) and pre-exposure ordering (with or without pre-exposure) as factors, segment as the covariate, and the difference in RMS from 1 G baseline as the dependent variable. There was a significant effect of pre-exposure on the difference in RMS from the 1 G baseline after controlling for the effect of segment,  $F(1,139) = 11.4, p = 0.001$ . The covariate, the segment number, was significantly related to the difference in RMS from the 1 G baseline  $F(1,139) = 8.11, p = 0.005$ . Neither the hyper-gravity level nor the cross-effect of hyper-gravity and pre-exposure were statistically significant ( $p > 0.05$ ). This indicates that while all groups adapted by having improved performance with increasing segment number, those with pre-exposure in another hyper-gravity level had smaller initial performance decrements.

### 5.2.6 Cross-Coupled Intensity Reports

During the 30 second breaks between trials, subjects reported the maximum Coriolis cross-coupled illusion intensity they experienced on the previous trial. The reported intensities, for the first session in 1 G and the first session in hyper-gravity (e.g. either 1.5 or 2 G's), are plotted by trial number in Figure 35.

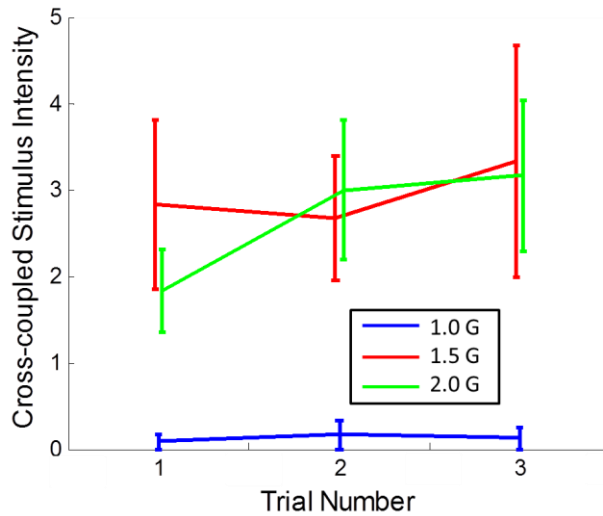


**Figure 35: Cross-Coupled Illusion Intensity Reports**

As expected there was nearly no reports of the cross-coupled illusion during 1 G testing. In hyper-gravity the illusion did occur much more regularly, though the intensity was generally quite low (e.g. on average an intensity of 2-3 on the 10-based scale). Somewhat surprisingly, there was no difference in the reported intensities in 1.5 and 2 G's despite the higher centrifuge spin-rate in 2 G. This comparison was across subjects, since half of the subjects tested in 1.5 G as the first hyper-gravity level and half tested in 2 G's; thus inter-individual differences may have confounded any differences between hyper-gravity levels. Grouping hyper-gravity levels together and using a hierarchical regression with subject as the identifier found no effect of trial number on illusion intensity ( $p > 0.05$ ). This finding suggests that the cross-coupled illusion was not a major contributor to the performance decrements observed in hyper-gravity (see Figure 31). While hyper-gravity performance showed clear evidence of improvement by trial, the cross-coupled stimulus intensity remained relatively constant across trials.

### 5.2.7 Summary of Results and Discussion

We conclude that hyper-gravity affects a pilot's ability to perform a manual control task, resulting in performance decrements. The initial performance decrements in hyper-gravity were substantial. In terms of RMS, average performance errors in 1.5 G were 0.72 degrees greater than the average 2.73 degrees 1 G baseline, corresponding to a 26% increase. In 2 G's initial performance was 45% worse (1.23 degrees) on average. Corresponding to these large initial decrements in objective performance measures, subjects reported their performance was worse and the workload was higher during the first trial in hyper-gravity. While it is clear that hyper-gravity is causing the manual control performance decrements, the exact mechanism is unclear. We hypothesize that the effect is primarily due to perceptual errors. Specifically, the overestimation of roll tilt observed in Experiment 1 caused subjects to make too large of inputs to the RHC resulting in over controlling and pilot induced oscillations (PIO).

However, hyper-gravity has additional effects that could contribute to the manual control performance decrements. First, initial exposure to hyper-gravity may cause physiological (e.g. increased heart rate) and mental (e.g. increased anxiety) effects that would not be present during 1 G testing. To try to reduce

the impact of these secondary issues, we exposed subjects to hyper-gravity prior to testing during the G-Exposure Protocol. Here, subjects experienced 1.5 and 2 G's for several minutes without any manual control task to become used to the environment and the associated physiological responses. In addition, during testing the spin-up or onset of hyper-gravity was done slowly, over one minute, and another minute was provided in hyper-gravity for subjects to acclimate prior to the initiation of the first trial.

Second, hyper-gravity impacts the accuracy of physical motor responses (Fisk, Lackner et al. 1993; DiZio and Lackner 2002; Kurtzer, DiZio et al. 2005; Lackner and DiZio 2005). We attempted to reduce the amount of physical motor response required in the task by having the rotational axis of the RHC centered in the subject's hand. Only small hand and lower arm rotations were required to make control inputs instead of larger full arm translational movements. Nonetheless, we cannot be certain that part of the performance decrement observed was not caused by hyper-gravity impacting motor responses, in addition to the perceptual pathways. A future experiment could attempt to reproduce only the motor effects of hyper-gravity, by using arm weights in 1 G testing, and compare the performance to the 1 G baseline.

Third, in our motion paradigm where hyper-gravity is produced on a centrifuge, the roll rotations may cause a supra-threshold Coriolis cross-coupled illusion. If supra-threshold, the secondary cross-coupled illusion would only occur in the hyper-gravity conditions, where there was planetary rotation. Since we are not able to produce a "pure" hyper-gravity environment without any cross-coupled stimulus, we cannot be certain the cross-coupled illusion did not have some role in the manual control performance decrements observed in hyper-gravity. However, there are several reasons to believe the impact was small. During testing, the intensity of the secondary illusion was very low; subjects generally reported maximum intensities of 1-4 for trials in hyper-gravity using the 0-10 scale developed during pre-experimental training. Furthermore, the cross-coupled illusory sensation would be primarily in pitch, which cannot be controlled by the subject and is perpendicular to the roll manual control task. However, the illusory sensation might be generally disorienting which may impact roll manual control performance. The fact that the hyper-gravity performance decrements decayed across trials, while the cross-coupled reports remained constant further indicates that any general disorientation from cross-coupling was not the primary cause of the hyper-gravity performance decrements. While hyper-gravity causes altered physiological responses, increased anxiety, altered motor control, and the cross-coupled illusion, each of which may have impacted the manual control performance, we hypothesize that the perceptual overestimation of roll tilt was the primary cause of the performance decrements observed.

We found that the large initial performance decrements in hyper-gravity improve with practice over time. The time frame was characterized for which the manual control adaptation or learning in hyper-gravity occurred. For an exponential decay of the performance decrements to the 1 G baseline, the time constant for 1.5 G's was estimated to be ~110 seconds and that for 2 G's was ~213 seconds. Thus, with practice, manual control performance in hyper-gravity will eventually return to baseline levels. However, for pilots and astronauts, performance during the first 100-200 seconds is often a critical time period for docking or landing tasks. Initial control errors prior to the completion of adaptation may be catastrophic in terms of leading to accidents or aborts.

The mechanism for what is causing the manual control learning or adaptation to the hyper-gravity environment is unclear. The time frame of the learning (hundreds of seconds) is likely too short for a neural sensory reinterpretation of canal and otolith cues as is hypothesized to occur over several hours to days during spaceflight (Young, Oman et al. 1984; Harm, Reschke et al. 1999; Merfeld 2003). Instead we hypothesize that the adaptation is primarily cognitive, and is made in an adjustment of the appropriate motor response for a given sensory perception of orientation. In hyper-gravity, static and dynamic roll tilt is overestimated. If the same motor response is made as would appropriate in 1 G for the perceived angle, the overestimation would result in over-controlling in hyper-gravity. However, when successive control errors are made, we hypothesize the CNS adjusts what the appropriate motor response is for a given perceived roll angle. In this fashion the subject's "gain" of motor response for perceived roll angle is reduced and performance improves. None of the subjects reported consciously making a cognitive change in their control strategy in hyper-gravity (i.e. reducing the response gain); however the adjustment may have been made subconsciously. A future experiment could measure roll tilt perception in hyper-gravity before and after manual control adaptation. If the perceptual errors persist than the adaptation can be attributed to a primarily cognitive adjustment in motor response for a given sensory perception as opposed to a sensory perception reinterpretation. In another future experiment, after training with the original vehicle dynamic, in testing all at 1 G the vehicle dynamics could be modified by increasing the gain of the RHC. This paradigm would require a similar cognitive adjustment of reducing the motor response for a perceived roll angle. However, the roll tilt perception would not be altered by hyper-gravity. If the adaptation to the altered vehicle dynamics is similar to that observed upon initial exposure to hyper-gravity, it would indicate that the primary adaptation mechanism in hyper-gravity is cognitive and not a sensory perception reinterpretation.

Subjects may have not been trained completely to a steady-state prior to the beginning of the experiment; however this is unlikely to have substantially contributed to the adaptation observed in hyper-gravity. If subjects were continuing to learn the manual control task during testing, we would have expected to see trial-by-trial improvements in 1 G as well, which were not observed. Instead the improvements were exclusively seen in hyper-gravity. We conclude that subjects were trained to steady-state prior to the beginning of the experiment and the adaptation in performance in hyper-gravity was a response to the novel environment.

In many adaptation paradigms, adapting to one altered environment will then require a re-adaptation back to the original environment. Interestingly, there was not significant evidence that adaptation to hyper-gravity impacted performance upon the second 1 G session. This would support "context-specific" adaptation (Shelhamer, Clendaniel et al. 2002) in which subjects were able to quickly revert to their 1 G-appropriate responses based upon the knowledge that they were no longer in hyper-gravity. The 20 minute breaks between sessions, in which subjects were outside of the centrifuge cab and in 1 G, also may have helped any required re-adaptation.

In 1.5 G there was a trend, though not significant, that with sufficient practice, performance could improve beyond the 1 G baseline. The 1.5 G mean RMS performances on the last 11 segments (nearly all of the last 2 trials) were all better than the 1 G baseline. One potential explanation for the enhanced

performance in 1.5 is that the utricular mass deflects more for a given roll tilt, hypothetically increasing sensitivity to roll tilt. If the otolith signal is properly interpreted, hyper-gravity should help reduce a subject's effective roll tilt threshold. If smaller roll tilts can be perceived in hyper-gravity then presumably they could be more effectively nulled out, resulting in super-1 G manual control nulling performance. However, in the three trials tested there was no evidence of this effect occurring in 2 G, where roll tilt sensitivity should be even more enhanced. Further investigations should study many more trials in hyper-gravity until the performance has clearly reached a steady-state. Note that the potential for a fully adapted subject to exceed 1 G baseline performance in altered gravity should only occur for hyper-gravity. *Hypo-gravity* environments, like on the moon or Mars, would have less utricular shear for a given roll tilt, reducing sensitivity, and hypothetically impairing even fully adapted manual control performance.

We found that pre-exposure in one hyper-gravity level reduced the initial performance decrements over the first trial in another hyper-gravity level. The second hyper-gravity level was completely novel; subjects had never done the task at that level nor had ever made the adaptive adjustment necessary for that level. However, having made a similar adjustment recently to another hyper-gravity level seems to have improved their adaptive capability. The adjustment was similar in that it required an adjustment of the subjects' "gain" of their motor response for a given perceived angle, but different in that the exact magnitude of the adjustment was novel. This finding supports the concept of "learning to learn" (Roller, Cohen et al. 2001; Seidler 2004; Seidler 2005; Mulavara, Cohen et al. 2009; Roller, Cohen et al. 2009; Mulavara, Feiveson et al. 2010; Batson, Brady et al. 2011; Turnham, Braun et al. 2012), in which recently adaptive experiences in relevant environments enhance the capability to adapt to other novel, but similar, environments. This is the first evidence that this effect exists for adaptation to altered gravity levels relevant for astronauts and pilots.

Interestingly, the cross-effect between hyper-gravity level and pre-exposure was not significant; indicating the positive effect of pre-exposure of 1.5 G for 2 G testing was similar to that with 2 G pre-exposure for 1.5 G testing. But this is not conclusive and warrants further study. Qualitatively, 2 G pre-exposure appeared to nearly immediately reduce performance decrements at 1.5 G to near, if not equal to, the 1 G performance baseline. However, pre-exposure to 1.5 G does not appear to immediately reduce 2 G performance to the 1 G baseline. Instead the initial decrement is only partially reduced, but adaptation occurs quickly and reaches the 1 G baseline in less than half of the time as without pre-exposure. While the nuances of adaptive generalization in altered gravity requires further study, it is clear that pre-exposure to either a more or less extreme hyper-gravity environment than that used for testing reduces the initial performance decrements.

We only tested scenarios in which the pre-exposure hyper-gravity level preceded the testing level by either a 20 minute break or two 20 minute breaks and a 12 minute 1 G testing session. With only 3 subjects in each of these sub-groups, we could not identify differences in the timing between pre-exposure and testing. However, the effect of timing on the pre-exposure enhancement warrants further research. In order to utilize altered gravity pre-exposure as a countermeasure for astronauts landing on the moon or

Mars, the timing separation between pre-exposure training and the critical manual control task would be weeks to months. Here, we have only shown the pre-exposure effect for less than one hour.

The operational impact of the observed piloting performance decrements warrants further study. Substantial increases in RMS errors were seen in hyper-gravity, however depending upon the task, errors of this magnitude may be acceptable. For planetary landing tasks, where precise nulling of vehicle orientation and horizontal drift is critical, even small performance decrements may be unacceptable. Future research simulations should consider specific, applied scenarios, such as planetary landing, to determine the impact of altered gravity on operational metrics such as touchdown velocities, touchdown precision and accuracy, and the percentage of attempts ending in abort or accident.

## 6.0 Modeling Orientation Perception in Hyper-Gravity

As described in Section 2.9 several attempts have been made to model human perception of *static* orientation in hyper-gravity, however to our knowledge there have been no attempts to model *dynamic* orientation perception in hyper-gravity. Many well-known dynamic orientation perception models, including Observer (Oman 1991; Merfeld, Young et al. 1993; Merfeld and Zupan 2002; Newman 2009; Vingerhoets, De Vrijer et al. 2009), can explain a wide-range of perceptual responses in 1 G, but are unable to predict the characteristic overestimation of roll tilt in hyper-gravity (see Figure 4). Here we propose a modification to the Observer model which can explain both static and dynamic perceptual responses in hyper-gravity, which were quantified in Experiment 1. The modified model is then simulated in several additional relevant altered gravity environments.

### 6.1 Characteristics of Hyper-Gravity Perception to Model

Through a simple modification we aim for the Observer model to mimic several of the characteristics of hyper-gravity roll tilt perception observed in Experiment 1. For static tilts, the perceptions associated with a wide range of roll tilts and gravity levels from 1-2 G's must be modeled. Specifically, we aim to model the overestimation in hyper-gravity that is greater for higher gravity levels and larger angles up to approximately 45 degrees before decreasing for very large angles (Schone 1964; Correia, Hixson et al. 1965; Miller and Graybiel 1966; Schone and Parker 1967; Schone, Parker et al. 1967; Correia, Hixson et al. 1968). For dynamic tilts, we hope to capture the relative amount of overestimation in hyper-gravity and its dependence upon rotation rate. The amount of dynamic overestimation predicted must be less than that for static tilts and less for rotations with higher angular velocities. In Experiment 1, there was evidence of adaptation in the perception of dynamic rotations in hyper-gravity, with less overestimation on the second repetition at a particular gravity level. Observer does not have adaptive mechanisms to model this effect, so we will only attempt to model the perceptions on the first repetition of dynamic rotations. If, through a single simple change, the model is able to reproduce this range of experimental perceptual responses in hyper-gravity, we can have increased confidence in the model predicting appropriate perceptions in simulation scenarios that are more complex and have yet to be experimentally validated.

### 6.2 Proposed Modification to Model

We propose that the CNS treats otolith stimulation *in* the utricular plane different than that *out* of the plane. In particular, the relative weighting on the otolith sensory conflict signal is not the same in all directions; signals resulting from the utricular plane are weighted differently than those out of the plane. The proposed modification is loosely inspired by the utricular shear theory. In the traditional utricular shear theory, it is assumed that the CNS estimates static orientation perception exclusively based upon the stimulation resulting for the shear forces acting in the plane of the utricular macula. Implementing this theory in the Observer framework would imply that signals in the utricular plane are weighted by some finite constant (related to 'K' in Equation 2), and those out of the plane are ignored (or weighted by zero).



While our proposed modification does not aim to completely ignore stimulation out of the utricular plane it does build upon the concept of weighting the signals differently as posited in the utricular shear theory. We acknowledge that the concept of a “utricular plane” is a significant simplification since the utricular macula is three-dimensional surface. However, we can simplify by considering the average plane of this surface, which can define the approximate orientation of this complex surface.

### 6.2.1 Review of the Otolith Pathways in the Model

The misperceptions (i.e. overestimation) in hyper-gravity environments are generally attributed to the processing of the otolith signals given their sensitivity to GIF stimulation. Figure 36 shows just the otolith related pathways in the Observer model structure. This reduced model can be considered the “static Observer” in that all pathways related to angular velocity processing and semicircular canals, which would only be active during dynamic stimulation, have been removed.

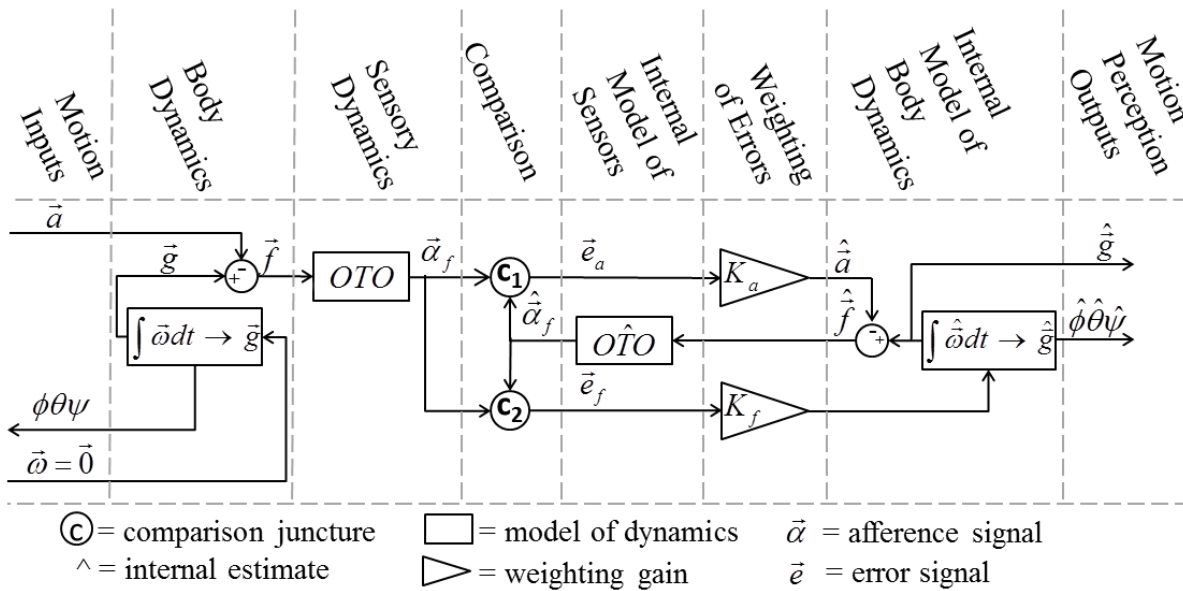


Figure 36: Static Observer Model (Only Otolith Pathways)

The model functions in a head-fixed right-handed coordinate system such that the x-axis aligns with naso-occipital axis, the y-axis aligns with the interaural axis, and the z-axis is perpendicular to the x- and y-axes. The positive direction of the x-axis is forward, of the y-axis is left and for the z-axis is cranial. All of the vectors in the model are then three dimensional with each component representing the signal along the corresponding [x y z] axis. The inputs to the model are three-dimensional linear acceleration ( $\vec{a}$ ) and typically angular velocity ( $\vec{\omega}$ ), however for the reduced static version of the model there is no angular velocity stimulation. More generally, given an initial gravity vector ( $\vec{g}_0$ ), angular rotations will yield a change in the orientation of gravity ( $\vec{g}$ ) which is accounted for by rotational kinematics ( $\int \vec{\omega} dt \rightarrow \vec{g}$ ), which is implemented using quaternion integration. By Equation 1, linear acceleration ( $\vec{a}$ ) and gravity ( $\vec{g}$ ) combine to yield the net GIF ( $\vec{f}$ ). The GIF is the input stimulation to the otolith organs (OTO), which are modeled with a diagonal transfer function matrix. Each diagonal element is a simple

low pass filter with a cutoff frequency of  $f_{oto} = 2$  Hz. This yields the otolith afferent response ( $\vec{\alpha}_f$ ). The model fundamentally hypothesizes there are neural implementations in the CNS of sensory ( $O\hat{T}O$ ) and body ( $\int \hat{\omega} dt \rightarrow \hat{g}$ ,  $\hat{f} = \hat{g} - \hat{a}$ ) dynamics. The model assumes that the internal models of both the body and sensory dynamics are accurate. Two error vectors ( $\vec{e}_a$  and  $\vec{e}_f$ ) represent specific aspects of the difference between the actual otolith afference ( $\vec{\alpha}_f$ ) and the expected otolith afference ( $\hat{\alpha}_f$ ). The linear acceleration error ( $\vec{e}_a$ ) is just the vector difference between the actual and expected afference, while the GIF rotation error ( $\vec{e}_f$ ) represents the rotation required to bring the otolith measurement of the GIF into alignment with the internally estimated otolith measurement of GIF. The mathematical formulations of these error calculations are given in Equations 9 and 10.

$$\vec{e}_a = \vec{\alpha}_f - \hat{\alpha}_f \quad (9)$$

$$\vec{e}_f = \frac{\vec{\alpha}_f \times \hat{\alpha}_f}{|\vec{\alpha}_f \times \hat{\alpha}_f|} \cos^{-1} \left( \frac{|\vec{\alpha}_f|}{|\vec{\alpha}_f|} \cdot \frac{|\hat{\alpha}_f|}{|\hat{\alpha}_f|} \right) \quad (10)$$

In the otolith pathways, two constant scalar feedback gains ( $K_a$  and  $K_f$ ) are used to “steer” the central estimates ( $\hat{a}$ ,  $\hat{g}$ , and more generally  $\hat{\omega}$ ) to values that minimize the sensory conflict errors ( $\vec{e}_a$  and  $\vec{e}_f$ ). Nominally these scalar gains weight each of the three components of the error vectors equivalently. The linear acceleration feedback gain ( $K_a$ ) scales the linear acceleration error ( $\vec{e}_a$ ) to feed it back to the central estimate of linear acceleration ( $\hat{a}$ ) and was fixed to -4.0 (Merfeld and Zupan 2002; Vingerhoets, Van Gisbergen et al. 2007; Newman 2009). The GIF feedback gain ( $K_f$ ) weights the GIF rotation error ( $\vec{e}_f$ ) to induce the internal estimate of gravity to align with the otolith measured GIF and was fixed to 4.0 [(degrees/second)/degrees] (Merfeld and Zupan 2002; Vingerhoets, Van Gisbergen et al. 2007; Newman 2009). From the actual ( $\vec{g}$ ) and estimated ( $\hat{g}$ ) gravity vectors, actual roll ( $\phi$ ), pitch ( $\theta$ ), and yaw ( $\psi$ ) orientation angles, as well as estimated angles ( $\hat{\phi}$ ,  $\hat{\theta}$ ,  $\hat{\psi}$ ) are computed by Euler angle transformations.

### 6.2.2 Modification in Model Structure

Previous versions of the model (Oman 1991; Merfeld, Young et al. 1993; Merfeld and Zupan 2002; Zupan, Merfeld et al. 2002; Vingerhoets, Van Gisbergen et al. 2007; Newman 2009; Rader 2009; Rader, Oman et al. 2009; Vingerhoets, De Vrijer et al. 2009) have all utilized *scalar* feedback gains. In doing so, there is an implicit assumption that rotations around and accelerations along x-, y-, and z-axes are equivalent. While the reduced number of free parameters and the simplicity of scalar feedback gains is attractive, it may not be physiological accurate. We propose using a vector feedback gain, specifically for the linear acceleration feedback ( $K_a$ ) to allow for different weightings of the linear acceleration sensory conflict error ( $\vec{e}_a$ ) in the utricular plane versus out of the plane. All of the vectors in the model, including the linear acceleration error vector ( $\vec{e}_a$ ), are in the head-fixed coordinate system defined above with the x-axis aligned with the naso-occipital axis and the y-axis with the interaural axis. The error vector must first be rotated into utricular plane-fixed coordinate system in order to differentially weight the

components in and out of this plane. We assumed a simplified planar utricular macula defined by two axes: the  $x'$ -axis which is pitched up by  $\theta_{utricle}$  from the head-fixed  $x$ -axis and the  $y'$ -axis which is aligned with the  $y$ -axis and the interaural axis. Figure 37 depicts the orientation of the coordinate frame which defines the utricular plane relative to the head-fixed frame.

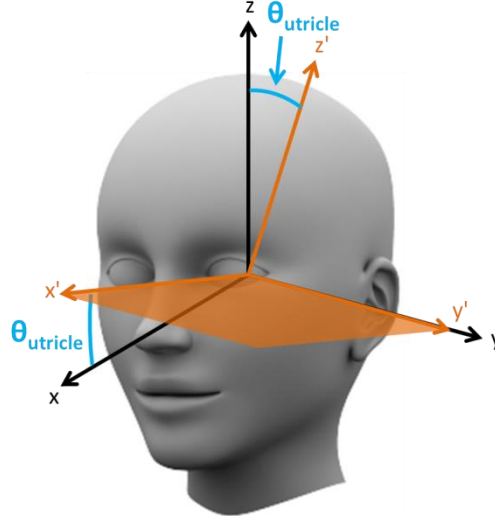


**Figure 37: Utricular Plane Coordinate Frame Rotation**

Otolith stimulation in the  $x'$ - and  $y'$ -axes is in the utricular plane, while that in the  $z'$ -axis is out of plane. The rotation matrix from the head-fixed coordinate system to the utricular plane system is given in Equation 11.

$$\begin{Bmatrix} e_{a_{x'}} \\ e_{a_{y'}} \\ e_{a_{z'}} \end{Bmatrix} = R(\theta_{utricle}) \begin{Bmatrix} e_{a_x} \\ e_{a_y} \\ e_{a_z} \end{Bmatrix} = \begin{bmatrix} \cos(\theta_{utricle}) & 0 & \sin(\theta_{utricle}) \\ 0 & 1 & 0 \\ -\sin(\theta_{utricle}) & 0 & \cos(\theta_{utricle}) \end{bmatrix} \begin{Bmatrix} e_{a_x} \\ e_{a_y} \\ e_{a_z} \end{Bmatrix} \quad (11)$$

Based upon morphology (Corvera, Hallpike et al. 1958; Curthoys, Betts et al. 1999), we fixed the value of  $\theta_{utricle}$  to 25 degrees, however this value has no impact upon roll tilt simulations and only effects pitch perceptions. Once in the utricular plane coordinate system, we propose the linear acceleration error vector ( $\vec{e}_a$ ) is now weighted by a vector of linear acceleration feedback gains ( $\vec{K}_a$ ), such that those errors in the  $x'$ - $y'$  plane can be weighted differently than those out of plane ( $z'$  direction).

$$\vec{K}_a = \begin{Bmatrix} K_{a_{x'}} \\ K_{a_{y'}} \\ K_{a_{z'}} \end{Bmatrix} = \begin{Bmatrix} K_{a_u} \\ K_{a_u} \\ K_{a_{u\perp}} \end{Bmatrix} \quad (12)$$

The central estimate of linear acceleration is then finally rotated from the utricular plane-fixed frame back to the normal head-fixed coordinate system.

$$\begin{Bmatrix} \hat{a}_x \\ \hat{a}_y \\ \hat{a}_z \end{Bmatrix} = R^{-1}(\theta_{utricle}) \begin{Bmatrix} \hat{a}_{x'} \\ \hat{a}_{y'} \\ \hat{a}_{z'} \end{Bmatrix} = R(-\theta_{utricle}) \begin{Bmatrix} \hat{a}_{x'} \\ \hat{a}_{y'} \\ \hat{a}_{z'} \end{Bmatrix} \quad (13)$$

A schematic of the proposed modification to the model is given in Figure 38.

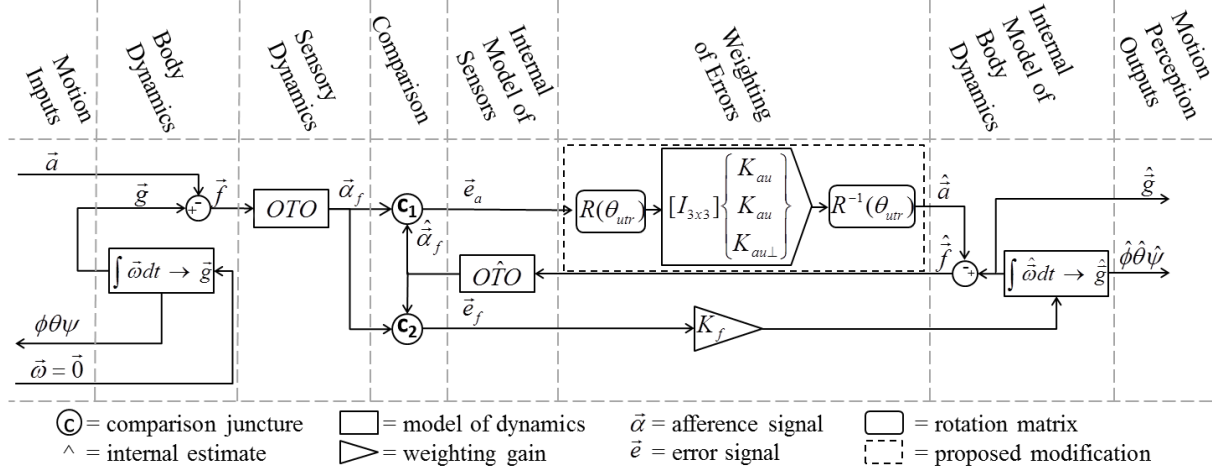


**Figure 38: Proposed Modification to Static Observer Model (Only Otolith Pathways)**

### 6.2.3 Fitting New Free Parameters in Model

The proposed modification to the model detailed in Section 6.2.2 introduces an additional free parameter. Previously all of the components of the linear acceleration error ( $\vec{e}_a$ ) were equally weighted by one feedback gain ( $K_a$ ). In the modified model, each of the components of the linear acceleration error ( $\vec{e}_a$ ) is now weighted by one of two independent feedback gains ( $K_{au}$  or  $K_{au\perp}$ ). In modeling, for simplicity we left the linear acceleration feedback gain on errors out of the utricular plane ( $K_{au\perp}$ ) at the nominal value of -4.0. The linear acceleration feedback gain on errors in the utricular plane ( $K_{au}$ ) was then set to mimic the average static perception observed in Experiment 1 for one specific hyper-gravity case. The model was implemented in MATLAB – Simulink 2012a (*The MathWorks*) software suite. The Simulink model was configured with a variable time-step fourth order Runge-Kutta differential equation solver (ode45 Dormand-Prince). The model was simulated with the scenario seen in Figure 4 (e.g. a 20 degree roll tilt at 0.125 Hz in 2 G's) at a 100 Hz sampling rate, using several different values for the utricular plane linear acceleration feedback gain ( $K_{au}$ ). The static perception (calculated as the mean perception from 28-30 seconds after reaching 20 degrees as in Experiment 1) from these simulations is shown as a function of feedback gain ( $K_{au}$ ) in Figure 39.

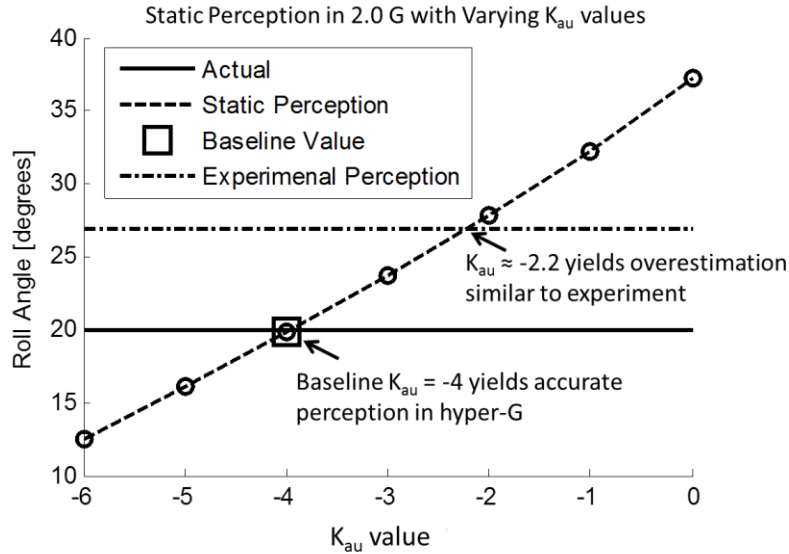


Figure 39: Static Perception in Modified Model with Varying  $K_{au}$  Values

Adjusting the utricular plane linear acceleration feedback gain ( $K_{au}$ ) relative to the out of plane gain ( $K_{au\perp}$ ) can produce over or underestimation in static perception in hyper-gravity. Of interest are the cases of when the utricular plane linear acceleration feedback gain is greater than the out of plane gain ( $K_{au} > K_{au\perp}$ ), which causes overestimation in the 2 G simulation. In Experiment 1, 2 G causes overestimation of approximately 35% of the actual roll angle, or for the example 20 degree case a perception of approximately 27 degrees. To produce this level of static overestimation in the model, the utricular plane linear acceleration feedback gain ( $K_{au}$ ) must be approximately -2.2. To keep with the prior practice of fitting the feedback parameters to the nearest integer value, we propose a value of -2.0. A summary of the modified parameters in the model is provided in Table 11.

Table 11: Summary of Modified Model Parameters

Parameter	Value	Units
$K_{au}$	-2.0	Unitless
$K_{au\perp}$	-4.0	Unitless
$\theta_{utricle}$	25	degrees

Only one additional free parameter has been added in the proposed modification by allowing for different feedback gains for the components of the linear acceleration error vector that are in the utricular plane versus those that are out of plane. It was fixed by matching the static perception in one particular hyper-gravity example (20 degree roll tilt in 2 G's) to that observed experimentally. It should be noted that it is the difference between the utricular plane and out of plane feedback gains that is essential to producing the desired static overestimation in hyper-gravity. Here the out of plane gain ( $K_{au\perp}$ ) was held at -4.0 and the in plane coefficient ( $K_{au}$ ) was modified. Alternatively the utricular plane value could be held at -4.0 and the out of plane gain adjusted (see Appendix O for details). In fact both gains could be modified to produce several combinations which would have the appropriate difference to produce the

static overestimation in hyper-gravity required. In addition, the orientation of the utricular plane was fixed to be pitched up by 25 degrees relative to the head-fixed coordinate system. This value has no influence upon roll tilt simulations, but does affect simulations with pitch rotations (see Section 6.4.3).

### 6.3 Evaluation of Modified Model in Hyper-Gravity

The modified model detailed in Section 6.2.2 and quantitatively fit in Section 6.2.3, was simulated and compared to static and dynamic roll tilt perceptions from Experiment 1.

#### 6.3.1 Evaluation of Static Tilt Perception Predictions

The modified model was first simulated across a range of different roll tilt angles and hyper-gravity levels and the static tilt perception (calculated as the mean perception from 28-30 seconds after reaching 20 degrees as in Experiment 1) and was compared to that observed in Experiment 1. In each simulation, the roll tilt profile shown in Figure 8 and defined in Equation 4 was utilized for a specific combination of angle (-30, -20, -10, 0, 10, 20, 30, 40, or 50 degrees) and gravity level (1, 1.5, or 2 G's).

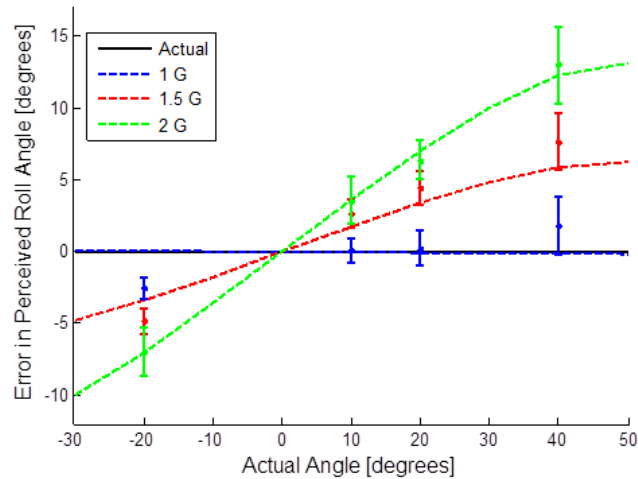


**Figure 40: Comparison of Static Tilt Steady-State Experimental Perception and Modified Observer Model Predictions**

Despite being fit for only a single combination of angle and hyper-gravity level (20 degrees and 2 G's), as seen in Figure 40 the modified model produced appropriate static perceptual responses across each of the combinations of angles and gravity levels tested in Experiment 1. The model is further compared to experimental static perceptions from previous experiments using SVV in Figure 41.

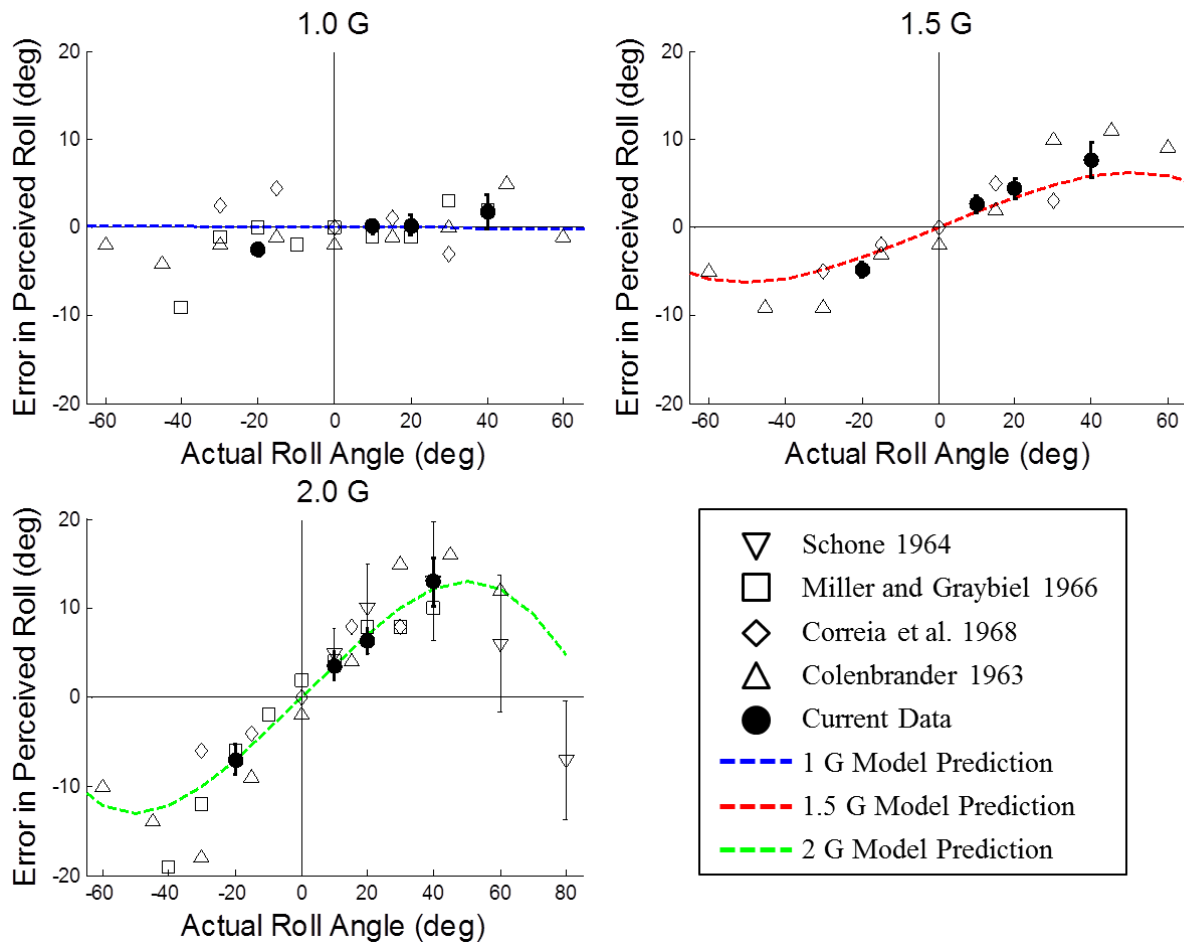


**Figure 41: Comparison of Static Tilt Steady-State Previous Experimental Perception and Modified Observer Model Predictions**

Even over the wider range of angles tested in previous experiments, the modified model, at least qualitatively, produces appropriate static tilt perceptions. In particular, the model produces less absolute overestimation in hyper-gravity at angles greater than approximately 45 degrees, mimicking previous experimental measures. All of the simulations in Figure 40 and Figure 41 were performed with a dynamic rotation frequency of 0.125 Hz. However, in agreement with experimental results (see Section 4.2.4), the simulated static tilt perception is unaffected by the dynamic rotation frequency (see Appendix U for details).

### 6.3.2 Evaluation of Dynamic Rotation Perception Predictions

For the model modifications to be relevant, the model must be able to simulate the experimental perceptions observed during dynamic rotation. To evaluate the model, it was simulated with the roll tilt profile shown in Figure 8 and defined in Equation 4 at 1, 1.5, and 2 G's. The roll tilt angle was held constant at 10 degrees and the dynamic rotation frequency was varied between 0.0625 and 1 Hz to match the peak angular velocities tested in Experiment 1 (1.25, 2.5, 5, 10, and 20 degrees/second). To allow for direct comparison, the same metric was utilized to quantify the dynamic rotation perception as in Experiment 1: the slope of a linear fit over the central 50% of the dynamic rotation period for the

simulated perceived roll angle normalized by that for the actual roll angle (see Section 4.2.8 and Appendix J for details). For each simulation, this metric was calculated specifically for dynamic tilts and compared to the mean experimental perception for the first repetition of dynamic tilts, as well as the normalized static tilt steady-state perception, in Figure 42. In Experiment 1, the second repetition of dynamic rotations showed evidence of adaptation and had less overestimation in hyper-gravity, which we will not model.

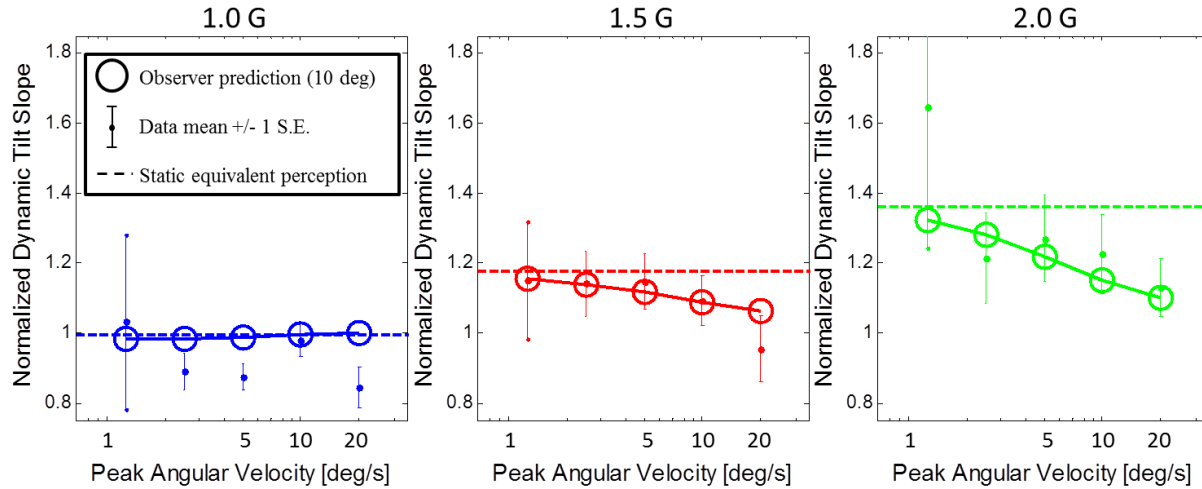


**Figure 42: Comparison of Dynamic Roll Tilt Experimental Perception and Modified Observer Model Predictions**

The modifications to the model allowed it to produce the characteristic responses of dynamic tilt perception in hyper-gravity. Specifically, the model predictions matched the experimental perceptions in terms of 1) near accurate perceptions in 1 G independent of angular velocity, 2) overestimation in hyper-gravity with more overestimation at higher gravity levels, 3) a characteristic dependence of overestimation in hyper-gravity on angular velocity, with less overestimation at higher angular velocities, and 4) across all dynamic conditions, less overestimation than static tilts. One point of difference between the model predictions and experimental perceptions was in 1 G perception. The dynamic tilt perception was approximately 90% of the actual roll tilt slope (see Table 6), and while the model predicts normalized dynamic tilt slopes less than one, the perception is nearly 98% of the actual roll tilt slope. This difference may be explained by the human sensorimotor response time delay which affects the experimental responses, but is absent in the simulation (see Appendix V for details). The dynamic returns were qualitatively similar and can be seen in Appendix W.

## 6.4 Novel Predictions of Modified Model

Once validated versus experimental perception in hyper-gravity, the modified model, as detailed in Figure 38 and Table 11, can be simulated in additional scenarios. These simulations generally have not been validated in Experiment 1 or elsewhere, but will provide potentially interesting hypotheses for future experiments.



### 6.4.1 Model Prediction of Static Perception in Hypo-Gravity

Just as in hyper-gravity, previous versions of the Observer model predicted accurate static roll tilt perceptions in hypo-gravity. To test the modified model's predictions it was simulated with the example 20 degree roll tilt and the static perception at various gravity levels is shown in Figure 43 as circles.

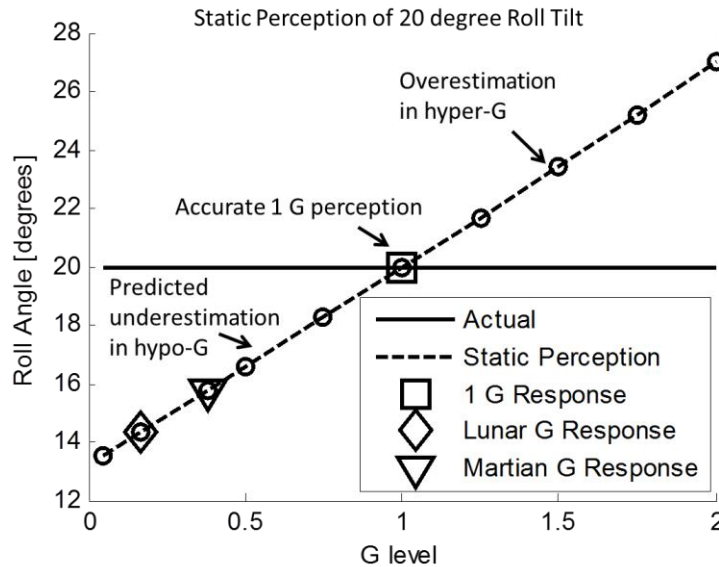
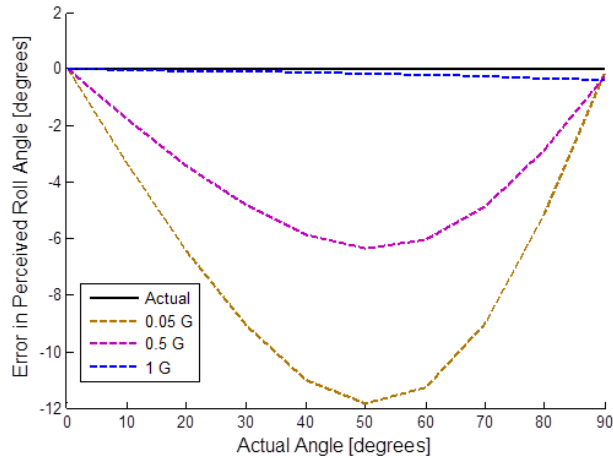


Figure 43: Model Predicted Static Perception in Altered Gravity

As intended, the model simulated the static overestimation in hyper-gravity and the accurate static perception in 1 G. However, the modified model also predicted *underestimation* of static roll tilt in hypo-gravity ( $0 < |\vec{g}| < 1$ ). The amount of predicted underestimation was more extreme for lower gravity levels. Of particular interest are the lunar ( $\sim 1/6$  G) and Martian ( $\sim 3/8$  G) hypo-gravity levels, which are specially marked in Figure 43 (diamond and triangle, respectively). At very small gravity levels (e.g. 0.05 G), the perception of the 20 degree roll tilt approaches  $\sim 13.2$  degrees or underestimation of  $\sim 34\%$  of the actual angle. Note that simulating the model at exactly 0 G results in a singularity when the gravity vector is normalized by its magnitude and was not simulated.

To our knowledge there have been two attempts at quantifying static roll perception in hypo-gravity (Dyde, Jenkin et al. 2009; de Winkel, Clement et al. 2012), but neither directly address the predictions in Figure 43. In the experiments, subjects only reported perception when upright (roll = 0 degrees) or on their side (roll = +90 or -90 degrees). At upright the model predicts accurate upright static perception independent of gravity level, in agreement with the hypo-gravity experiments. Similarly, at 90 degrees of roll tilt, the model prediction of static perception is accurate across the range of hypo-gravity levels. Only at acute angles does the model predict underestimation of static roll tilt in hypo-gravity. Future experiments should test a wide range of hypo-gravity levels and angles to test the validity of the model predictions in this relevant altered gravity regime. The model's predicted error in perceived static roll angle (error = perceived – actual) at 0.05, 0.5, and 1 G's across a range of angles is shown in Figure 44.



**Figure 44: Model Predicted Static Roll Perception in Hypo-Gravity**

There is some previous evidence (de Winkel, Clement et al. 2012) that at small hypo-gravity levels, the magnitude of gravity is too small to be used as a reference. Beyond this level, in the prior experiment the SVV generally aligned with the body longitudinal axis, as is common in microgravity. The threshold at which gravity is no longer used as a reference for perceptual orientation was seen to vary substantially amongst subjects, but on average was 0.3 G's (de Winkel, Clement et al. 2012). The gravity magnitude threshold effect is not present in model simulations. In the model, as long as the magnitude of gravity is greater than zero, near accurate perceptions are predicted at upright and 90 degrees of roll tilt, while acute angles result in underestimation. A previously proposed “idiotropic vector” (Mittelstaedt 1986; Mittelstaedt 1989; Vingerhoets, De Vrijer et al. 2009), which drives perceptions towards the body longitudinal axis, may be implemented to model the low hypo-gravity threshold effect when appropriate.

#### **6.4.2 Model Prediction of Dynamic Perception in Hyper-Gravity across Frequencies**

In Section 6.3.2 (Figure 42), the modified model's dynamic perceptions were validated against experimental measures at frequencies of 0.0625, 0.125, and 0.25 Hz in hyper-gravity. However the model can be simulated at a much wider range of conditions to more fully understand its predictions. In particular, it was simulated here for a 10 degree roll tilt in 2.0 G's at frequencies ranging over 500 fold, from 0.015625 to 8 Hz. The same ratio of perceived slope to actual slope for linear fits over the central 50% of the rotation period were utilized here as the metric and compared to the static overestimation from the model and the actual tilt.

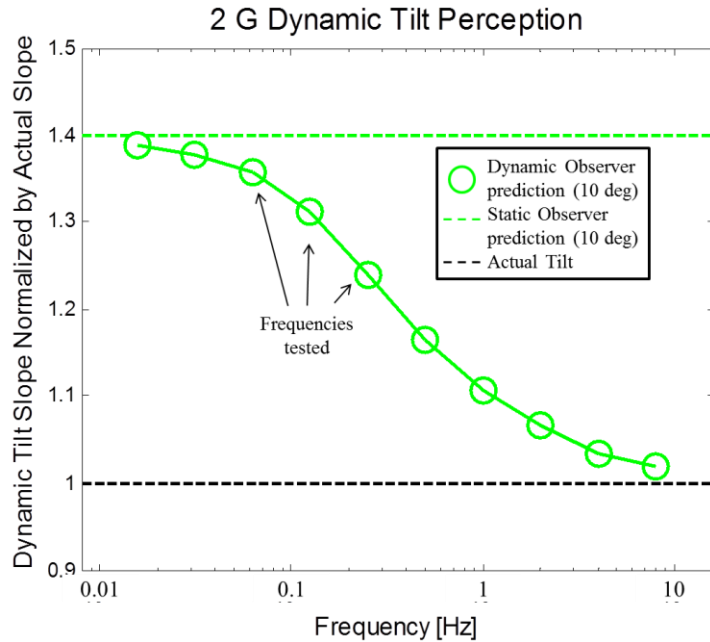


**Figure 45: Model Predicted Dynamic Perception in 2.0 G across a Range of Frequencies**

In Figure 45, the frequencies which were tested in Experiment 1 are identified; however the dynamic perception in 2 G's varies substantially across frequencies. As expected, at very low frequencies ( $< 0.05$  Hz) the predicted dynamic overestimation approaches the static level. At high frequencies ( $> 5$  Hz) the dynamic perception, even in 2 G's, approaches the actual rotation profile. At middle frequencies, there is a characteristic dependence of the amount of dynamic overestimation inversely depending on frequency. These predictions are consistent with the hypothesis of sensory integration: the CNS combines information from various sensory sources by weighting them roughly inversely proportional to their reliability. The semicircular canal cue is more reliable at higher frequencies and is presumably unaffected by altered gravity. The canal information should be weighted more heavily at higher frequencies relative to otolith signals, reducing the amount of overestimation in hyper-gravity. An identical dependence upon frequency can be seen in dynamic tilt perception in 1.5 G's (see Appendix X). While the very low frequencies could be experimentally validated, the higher frequencies would be difficult to validate using the same methodologies from Experiment 1. In fact, the top frequency of 0.25 Hz tested in Experiment was selected as near the maximum at which the continuous somatosensory indicator task remained feasible. In addition, for a centrifuge experiment increasing the roll rate of rotations at higher frequencies would increase the intensity of the Coriolis cross-coupled illusion and further confound the perceptual responses.

### 6.4.3 Model Prediction of Static Pitch Perception in Hyper-Gravity

To reduce the number of experimental conditions in Experiment 1, only roll tilt perception was tested. However, presumably hyper-gravity influences pitch tilt perception as well. The modified model was simulated with the same tilt profile (Figure 8), but in pitch and the static steady-state perceptual response was calculated. To directly compare to the most complete hyper-graviv static pitch perception dataset

(Correia, Hixson et al. 1965; Correia, Hixson et al. 1968), the model was simulated for angles of -30, -15, 0, 15, and 30 degrees and gravity levels of 1, 1.25, 1.5, 1.75, and 2 G's.

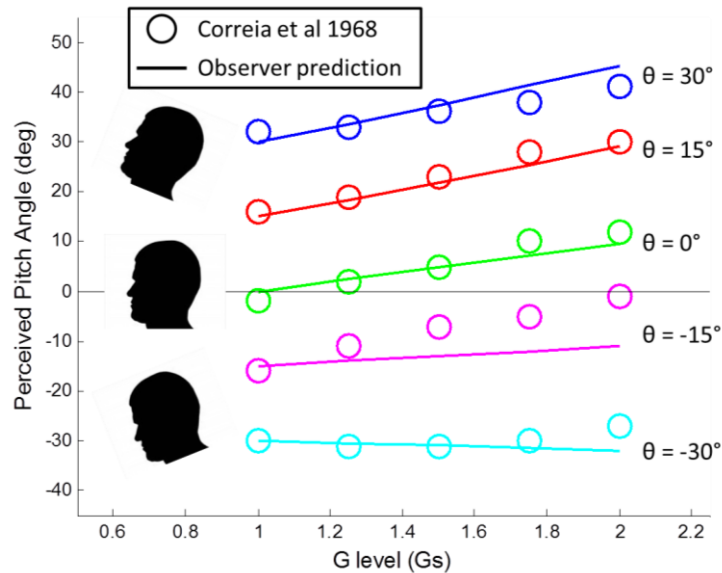


**Figure 46: Model Predicted Static Pitch Perception Compared to Previous Data (Correia, Hixson et al. 1965; Correia, Hixson et al. 1968)**

The model predicts qualitatively different static perceptions for pitch than for roll. Whereas roll tilt perception was symmetric about upright (0 degrees roll tilt), pitch perception is asymmetric. In particular, at upright (0 degrees of pitch tilt) there is a noticeable effect of gravity with hyper-gravity producing a perception of being pitched nose up. Increasing hyper-gravity levels cause a sensation of nose-up pitch relative to the 1 G level is a trend that exists for all of the angles simulated except for -30 degrees (pitched nose down). At this orientation, increasing gravity level has a nearly negligible effect of causing the perception to be more pitched nose-down. Each of these characteristics is well confirmed in the previous experimental dataset.

The asymmetry in the model's static pitch predictions can be attributed to the assumed utricular plane orientation. Only in orientations where increasing the gravity level modifies the stimulation of the otoliths in the utricular plane, will the perceptual response change with gravity level. For roll tilt, the null orientation where changes in gravity do not effect perception is upright. For pitch, a nose down pitch equal to  $\theta_{\text{utricle}} = 25$  degrees will yield accurate pitch perceptions even in hyper-gravity. Hence, the assumed orientation of the utricular plane is essential to the model's performance. It was assumed the plane was level in roll and pitched up 25 degrees relative to the head fixed coordinate frame based upon morphological studies. This assumption was suitable to fit the limited experimental data. A more precise "functional utricular plane" could be estimated by precisely measuring static pitch and roll tilt perception in 1 G and hyper-G and identifying the orientation at which there is no effect of hyper-gravity. The small effect of hyper-gravity at orientations near the functional utricular plane will be magnified at higher gravity levels, so at least 2 G should be used. Initial estimates to align the functional utricular plane with gravitational horizontal are zero degrees in roll and -25 of nose-down pitch.

## 6.5 Summary of Model Modifications and Discussion

We proposed a novel modification to a previous Observer-type dynamic spatial orientation model to allow it to predict the characteristic overestimation in roll tilt perception quantified in Experiment 1. The modification was based upon the hypothesis that the CNS treats otolith stimulation in the utricular plane different than that out of plane. This was implemented in the model by adjusting the feedback gain on the linear acceleration error to be different between errors in the utricular plane versus those out of plane. In doing so, the utricular plane was estimated to be pitched up by 25 degrees relative to head level based upon morphological studies. Furthermore an additional free parameter was added to the model (the linear acceleration feedback gain in the utricular plane) which was fixed to -2.0 to produce the appropriate amount of static overestimation for an example 20 degree roll tilt in 2 G's.

The modified model was simulated and found to qualitatively fit Experiment 1 results. In particular, static roll tilt perception was predicted over a range of angles and gravity levels, both from Experiment 1 and previous empirical studies. Dynamic roll perception showed the characteristic dependence of the amount of overestimation in hyper-gravity on the angular rotation rate. Furthermore the modifications to the model had no impact upon the veridical predictions of roll and pitch tilt in 1 G. Other well validated 1 G vestibular motion paradigms, including earth vertical yaw rotation, linear acceleration, off vertical axis rotation (OVAR), and post-rotation tilt, were only negligibly affected by the modifications (see Appendix Z for details).

Once validated for the conditions in Experiment 1, a series of relevant additional motion paradigms were then simulated in the modified model. First, the model was simulated with static roll tilt in hypo-gravity, which produced underestimation in roll tilt perceptions. The amount of underestimation was greater for more extreme (smaller) hypo-gravity levels, and peaked at approximately 45-50 degrees of roll tilt. To our knowledge, there is not a suitable hypo-gravity perceptual dataset, even for static tilts, which can be used to validate the model's predictions, and warranting a future experiment. Until then, the model predictions, extrapolated to hypo-gravity, can be used as a reasonable preliminary estimate of static roll tilt perception.

Second, dynamic roll tilt in hyper-gravity was simulated across a wide range of frequencies. The amount of overestimation had strong frequency dependence. Consistent with the concept of sensory integration, the amount of overestimation was reduced at higher frequencies. At very low frequencies ( $< 0.05$  Hz) the predicted overestimation approaches the static level, while at high frequencies ( $> 5$  Hz) it approaches the actual rotation profile. The dynamic prediction would indicate that astronauts and pilots in altered gravity environments may be less disoriented when making faster head or body tilts than low frequency or static tilts, due to the added veridical information provided by the semi-circular canals.

Finally the model was simulated with static pitch tilts and the asymmetric effect of hyper-gravity observed in a previous experiment was replicated. The pitch simulations, unlike roll tilt, are highly dependent upon the assumed pitch orientation of the utricular plane. The estimate of 25 degrees pitched up relative to head level based upon morphological studies was able to fit the experimental data well. However a future experiment could identify the pitch angle at which hyper-gravity has precisely no influence upon pitch perception and thus determine the "functional utricular plane" orientation.

Having validated the model to both static and dynamic roll tilt in hyper-gravity and qualitatively predicted static pitch perception, the model can now be simulated for more complex hyper-gravity scenarios. In addition, while it is an extrapolation of the validated model, it can also be simulated with complex hypo-gravity scenarios with a reasonable degree of confidence. For example the model could be practically utilized to gain a better understanding of astronaut perceptions during lunar or Martian landing profiles, which may have unique translational and rotational stimulation.

While the modifications within the model are able to explain a wide range of hyper-gravity perceptual responses, there are still limitations. Even the modified model predicts illusory linear acceleration in hyper-gravity that is not reported by subjects in terms of illusory sensations of displacement (see Appendix Y for details). The predicted illusory response in hyper-gravity is caused by the internal model of body dynamics representing the physical relationship between gravity, acceleration, and GIF

( $\hat{f} = \hat{g} - \hat{a}$ ). Since the internal estimate of gravity is assumed to have a magnitude of 1 G, the excess internal estimate of GIF is attributed to acceleration. Even when the subject is simply upright in a hyper-gravity environment the model predicts an illusory perception of vertical acceleration upward, both in the modified and unmodified versions.

There are a couple of potential explanations for why experimental subjects did not report illusory translation associated with the predicted acceleration. First, subjects were presumably aware of the motion capabilities of the centrifuge device. Knowledge or expectation that the centrifuge cab cannot enact translations may quench these sensations that may have existed for an unbiased observer (Wertheim, Mesland et al. 2001). Furthermore, other non-vestibular cues (proprioceptive, tactile, and somatosensory) may have helped quench illusory translation precepts. Neither an expectation of the device's feasible motions nor non-vestibular pathways are modeled in Observer. There is evidence (Merfeld, Zupan et al. 2001) that during centrifugation when the subject's precept of orientation is not aligned with the GIF (as is the case during roll tilt in Experiment 1), horizontal vestibular ocular reflex (VOR) eye movements occur. The horizontal VOR would correspond to the horizontal linear acceleration observed in the model simulations. An expectation in feasible motions or integration of non-vestibular cues could both explain the divergence between reported perceptions and the VOR response.

As discussed in Section 6.2.3, there are multiple combinations of in and out of the utricular plane linear acceleration feedback gains which have the appropriate difference to produce static overestimations in hyper-gravity. The particular pair in Table 11 was only selected for the simplicity of leaving the out of plane feedback gain at its prior value of -4.0. Future experiments, both in 1 G and in altered gravity could attempt to differentiate between the various combinations to identify a pair that most appropriately fits all conditions. Finally, the proposed modification is but one potential modification which could produce appropriate perceptual responses for the conditions tested in Experiment 1 in hyper-gravity. Other hypothesized modifications should be implemented and evaluated against the hyper-gravity experimental perceptions.

## 7.0 Discussion

### 7.1 Summary of Findings

We have found that proper sensorimotor performance is altered in hyper-gravity. First, we characterized roll tilt perception in hyper-gravity as assayed by a somatosensory indicator task. Static roll tilts were confirmed to be overestimated in hyper-gravity with the amount of overestimation greater for larger angles and higher gravity levels. While previous models were unable to appropriately fit the current data set, we proposed a modified version of the utricular shear model which empirically fit the current and previous data, even in conditions beyond which it was fit. For the first time, we characterized *dynamic* roll tilt perception in hyper-gravity across a range of angles and rotation frequencies. While overestimation again occurred in hyper-gravity, it was generally less than in the equivalent static case, and depended upon the angular velocity of the rotation. At higher angular velocities, when the semicircular canals are more reliable and presumably more heavily weighted by the CNS, there was less overestimation.

In a second experiment, we studied how misperceptions of roll tilt impacted a pilot's ability to perform a manual control task in hyper-gravity. In response to a computer-generated roll disturbance, subjects attempted to keep the cab aligned with the GIF using a rotational hand controller. Initially in hyper-gravity, there were large performance decrements relative to 1 G baseline performance. These were likely, at least partially, due to misperceptions of roll tilt causing subjects to make incorrect control inputs. However, with practice in hyper-gravity performance improved to near the 1 G performance baseline. For exponential decay fits of the performance decrements, the time constants were estimated to be approximately 110 seconds for 1.5 G and 213 seconds for 2 G. Finally, initial hyper-gravity performance was compared between two groups: those that experienced pre-exposure of doing the manual control task in another hyper-gravity level prior to testing and those that did not. The pre-exposure group showed less of an initial performance decrement. This supports the hypothesis that prior adaptations to altered gravity environments enhance adaptability on a future altered gravity adaptation.

Finally we proposed a simple modification to an existing model for dynamic orientation perception that was previously well validated in 1 G, but did not predict the characteristic overestimation in hyper-gravity. By differentially weighting linear acceleration sensory conflict errors in and out of the utricular plane, the model was able to predict perceptual errors in hyper-gravity. With one additional free parameter, the model predicted the static overestimation of roll tilt empirically observed in both the current as well as previous studies. In addition it predicted the characteristic dependence of dynamic overestimation in hyper-gravity on the angular velocity of the rotation, with less overestimation at higher angular velocities. The modified model was then simulated in various relevant scenarios. It predicted 1) underestimation of static roll tilt in hypo-gravity, 2) a transition in dynamic overestimation in hyper-gravity from near static tilt amounts at very low frequencies to accurate perceptions at very high frequencies, and 3) asymmetric perception of static pitch tilts in hyper-gravity which qualitatively fit data

from a previous study. Finally, the modifications to the model to produce appropriate altered gravity responses had negligible effects on simulations in 1 G that were previously well validated.

## 7.2 Implications for General Altered Gravity Environments

In the current set of experiments, we focused exclusively on altered gravity environments greater than Earth gravity (hyper-gravity). Aircraft pilots regularly experience hyper-gravity environments for short durations when performing coordinated turns and other aggressive maneuvers. Astronauts will experience hyper-gravity during launch. In both scenarios, the human pilots are presumably “adapted” to an Earth gravity environment and then experience motion in a hyper-gravity environment. The current findings regarding the hyper-gravity effects on roll tilt perception and control are directly applicable to these scenarios.

However there are several other aerospace applications in which altered gravity environments are encountered that are slightly different than the scenario studied here. First, we hypothesize that perception in microgravity, as experienced on orbit by astronauts, is qualitatively different from the effects seen in hyper-gravity. In microgravity the magnitude of gravity approaches zero such that it can no longer be used as an inertial reference cue for orientation perception. Several studies have investigated perception of orientation either during initial exposure or extended exposure to microgravity (Tafforin 1996; Young, Mendoza et al. 1996; Benson, Guedry et al. 1997; Clement 1998; Glasauer and Mittelstaedt 1998; Edgerton, McCall et al. 2001; Oman, Howard et al. 2003; Karmali and Shelhamer 2008; de Winkel, Clement et al. 2012). If the perceptual mechanisms in the CNS are qualitatively different than in the current hyper-gravity paradigm, the current findings cannot be directly applied to orientation perception or control in microgravity.

Hypo-gravity such as on the moon or Mars, however, we hypothesize is *qualitatively* similar to hyper-gravity. Specifically, hypo-gravity should cause less utricular shear for a given head tilt than in 1 G, causing static underestimation of roll tilt. In addition, dynamic perception in hypo-gravity should also depend upon the angular velocity of rotation with less underestimation at higher angular velocities. To our knowledge this has not been empirically verified in parabolic flight, however the modified Observer model quantitatively predicts these misperceptions. These perceptual predictions assume the human is adapted to an Earth 1 G environment. Obviously astronauts during transit to the moon, or in the future Mars, will experience extended microgravity exposure during which sensory orientation mechanisms are expected to adapt (Young, Oman et al. 1984; Parker, Reschke et al. 1985; Harm and Parker 1993; Merfeld, Christie et al. 1994; Merfeld 1996; Merfeld, Polutchko et al. 1996; Correia 1998; Harm, Reschke et al. 1999; Merfeld 2003). One might hypothesize that the increase in gravity level from the adapted state (microgravity) to the novel environment (hypo-gravity on the moon or Mars) might be similar to the increase from 1 G adapted to the novel hyper-gravity environment studied here. However, we would caution that the sensory adaptation to microgravity is unique and this comparison is wholly unvalidated. Altered gravity perceptual responses that involve a transition to or from microgravity are not addressed by the current study.



Nonetheless, the current study supports the hypothesis that *any* transition from one adapted gravity environment to an altered gravity level is likely to cause misperceptions of orientation. Specifically the otoliths organs functionality as graviceptors is dependent upon the magnitude of gravity and thus the central estimate of orientation will likely be initially impacted by altered gravity. If an astronaut or pilot is tasked with controlling a vehicle during initial exposure to altered gravity, the current study indicates manual control performance may be impaired. Incorrect control inputs due to misperceptions of vehicle orientation in altered gravity may lead to accidents or aborts. Future research needs to quantify these impacts for specific combinations of adapted and novel gravity states; however, the current experiment supports the hypothesis that sensorimotor performance will be impaired during any significant gravity transition until sensory adaptation can be completed.

### **7.3 Inter-Individual Differences**

The primary focus of the current set of experiments was to characterize the effect of hyper-gravity on the *mean* roll tilt perception and manual control performance. However, in taking these measures across many subjects, substantial individual differences were observed. For example, in the static roll tilt perceptions the “G-Excess” coefficient quantified the amount of overestimation for a given gravity level and angle. The overall coefficient was estimated to be 0.37 degrees of overestimation per degree of roll tilt per G above Earth gravity. When the model included a separate coefficient for each subject, the estimates for each individual subjects’ coefficient varied by almost a factor of four, from 0.13 to 0.48 (see Appendix I for details).

Furthermore, in the manual control task large variability was observed in both the initial performance decrement in hyper-gravity and how quickly each subject adapted. Particularly in 1.5 G, two subjects exhibited essentially no initial decrement compared to their 1 G performance baseline, one actually improved his/her performance, two showed some decrements, and one showed a very large decrement. In addition, while some subjects corrected their errors by the second segment (~34 seconds into the first trial) others took the entire first trial or longer (204+ seconds). Since only one of the same subjects was tested in both the perception and control experiments, we cannot address whether those individuals that showed small perceptual errors in hyper-gravity also had smaller initial performance decrements or faster manual control adaptations.

The cause(s) of the individual differences in subjects’ perceptual and control errors in hyper-gravity remain uncertain and warrant further study. Part of the variability can obviously be attributed to measurement errors. However, particularly in the static tilt measures, where numerous reports we made of the same condition without evidence of adaptation, the individual differences in the effect of hyper-gravity were statistically significant. These differences may be further attributed to differences in vestibular or extra-vestibular sensory function, sensory central processing strategies, previous experiences, or somatosensory reporting technique. In the manual control task, additional individual differences may exist in control strategy and cognitive ability to adapt quickly to incorrect control responses. Understanding these individual differences is not only scientifically important, but also operationally relevant. Identifying individuals who may have difficult functioning or adapting in altered

gravity environments could allow for personalized sensorimotor training pre-flight or modification of crew roles during critical mission phases.

## **7.4 Adaptation to Hyper-Gravity**

Adaptation in the perceptual and manual control errors in hyper-gravity was observed in only some of the measures. Static tilt steady-state perception, assayed by either the somatosensory task or verbal reports, did not show significant evidence of adaptation within or between hyper-gravity sessions. However, dynamic perception of roll tilts and returns did adapt between repeated sessions, but did not show adaptation within a session. Specifically, there was less dynamic overestimation on the second hyper-gravity session as compared to the first at a given hyper-gravity level. The fact there was adaptation for dynamic rotations, but not for static tilts might be expected; during dynamic rotations the CNS gets a strong veridical sensory feedback signal from the semicircular canals which were presumably unaffected by hyper-gravity. During static tilt the only feedback is from proprioceptive, tactile and somatosensory cues. Adaptation may occur eventually for static tilts, particularly when interspersed with dynamic rotations which provide extra feedback for a general reinterpretation of otolith cues, but it appears to require more time and trials than were presented in Experiment 1.

Adaptation to hyper-gravity occurred much more quickly in manual control performance. The time constants for adaptation were 100-200 seconds for manual control performance compared to between 15 minute sessions for dynamic perceptions. The difference might again be explained by the immediate feedback of each task. The manual control task is at least partially an active task in that subjects make control inputs for which they then get immediate sensory feedback. There is some uncertainty in that unexpected sensory feedback may be due to an incorrect control input or the continuous roll disturbance. However in the perceptual task, the rotations are entirely passive. Active motions are hypothesized to be processed differently than passive motions and to enhance adaptation (Von Holst and Mittelstaedt 1950; McCrea, Gdowski et al. 1999; Roy and Cullen 2001; Jamali, Sadeghi et al. 2009).

Furthermore, in the manual control task there are additional mechanisms for adaptation which may occur on shorter time scales. Repeated incorrect control inputs with sensory feedback may lead to a modification of one's control strategy. It is uncertain whether perceptual adaptation actually occurred within the 100-200 second time scale observed since no measures of perception were taken in Experiment 2. Future experiments should differentiate the mechanisms for adaptation across the different time scales observed.

## **7.5 Development of a Pre-Exposure Countermeasure**

In Experiment 2, large performance decrements were observed in a manual control task upon initial exposure to hyper-gravity. However, a separate set of subjects were "pre-exposed" to a different hyper-gravity level prior to the second, novel hyper-gravity did not experience nearly as large initial performance decrements. The effect of prior adaptation training improving subsequent adaptability has been identified for several sensorimotor tasks and altered environments (Roller, Cohen et al. 2001; Roller, Cohen et al. 2009; Batson, Brady et al. 2011; Turnham, Braun et al. 2012). Here we show this effect

exists for adaptation to altered *gravity* environments. This might be the first step in developing a pre-flight training/exposure countermeasure for astronauts experiencing altered gravity environments.

In Experiment 2, pre-exposure to one hyper-gravity level (e.g. 1.5 G's) prepared subjects for exposure to another, novel hyper-gravity level (2 G's) 20-40 minutes later. An effective pre-exposure countermeasure would need to build upon this in several ways. First, astronauts will experience a wide range of altered gravity environments. Those of particular interest are microgravity while on orbit and hypo-gravity on the moon or Mars. If hyper-gravity is proposed as the pre-exposure stimulus due to the simplicity in producing it on Earth using a centrifuge, it would need to be shown that hyper-gravity pre-exposure improves sensorimotor adaptation in novel micro- and hypo-gravity environments. Furthermore, to be an operational countermeasure the time duration between pre-exposure and the novel gravity environment would need to be weeks to months instead of less than an hour. Future experiments should aim to test the pre-exposure effect for hyper-gravity enhancing adaptation in micro- and hypo-gravity environments over extended durations. An effective pre-training countermeasure would be of significant benefit to astronauts, who need sufficient sensorimotor performance immediately upon entering novel gravitational environments for tasks such as vehicle landing and emergence vehicle egress.

## **7.6 Implications of the Model Modification**

In the Observer model, we proposed a modification that explained the static and dynamic perceptual responses in hyper-gravity. The modification assumes that the linear acceleration feedback error is weighted differently in and out of the utricular plane. If the CNS is behaving logically, a difference in weighting is presumably due to a difference in the quality and characteristics of the otolith signals in and out of the utricular plane. There is some evidence to support this implication. The resting discharge rate and sensitivity of otolith neurons from the superior nerve (mainly innervating the utricle) are greater than those from the inferior nerve (mainly innervating the sacculus which is nearly perpendicular to the utricle) (Fernandez and Goldberg 1976). Given the differences in the characteristics of the otolith neuron signals approximately in and out of the utricular plane, it is reasonable to hypothesize that the CNS would weight them differently.

## **7.7 Limitations**

In this set of experiments, the hyper-gravity environment was created using a centrifuge. While practical and cost effective for studying hyper-gravity, the methodology comes with a cost. The rotating environment of the centrifuge causes a secondary illusory perception, the Coriolis cross-coupled stimulus, when any out of planetary spin plane rotations are made. In our centrifuge motion paradigm, the roll tilts utilized will cause the cross-coupled illusion during planetary rotation necessary to create hyper-gravity. This secondary cross-coupled illusion is separate from the primary hyper-gravity induced misperceptions and would not occur in a “pure” hyper-gravity environment such as would be experienced on a more massive planet. We took several measures to reduce the intensity of the secondary cross-coupled illusion. The illusion's intensity is roughly proportional to the planetary spin rate, roll angular velocity, and net roll displacement of a tilt. To reduce the planetary spin rate for a desired hyper-gravity level a long-radius centrifuge was utilized. The roll angles and frequencies selected were kept within reasonable bounds to

avoid excessively large angles or angular velocities. Furthermore, in Experiment 1, where the roll angles experienced were much larger than in Experiment 2, a pre-experimental cross-coupled adaptation protocol was implemented which reduced the subjects' illusion intensities. Despite all of these efforts, the cross-coupled illusion still occurred during roll tilts in hyper-gravity on at least one trial for 5 of the 8 subjects in Experiment 1. The illusion occurred significant more often at higher gravity levels and faster angular velocities, so it may have acted as a confound. In Experiment 2, the cross-coupled illusion occurred at least once on most trials in hyper-gravity, but was almost never reported in 1 G. It could be hypothesized that the presence of the cross-coupled illusion was a significant contributor to the performance decrements observed in hyper-gravity. However, the fact that the performance decrements decayed across trials in hyper-gravity while the cross-coupled intensity reports were constant does not support this hypothesis.

The illusion intensities reported, even in hyper-gravity were generally very low in both experiments. Furthermore, it should be noted that the cross-coupled stimulus in our paradigm provoked an illusory pitching sensation, while the hyper-gravity induced overestimation of interest was in roll. Nonetheless, we cannot be certain that the cross-coupled illusion did not confound the roll tilt perceptual reports or control performance in hyper-gravity. For Experiment 1, we further cannot be certain that the cross-coupled adaptation protocol did not impact the sensory orientation mechanisms used to perceive roll tilt. The only way to verify the secondary cross-coupled stimulus issue did not impact hyper-gravity perception and control is to repeat the experiments in a non-rotating environment. For example, a high performance aircraft performing a coordinated turn could create hyper-gravity environments at such a low planetary angular velocity that the cross-coupled illusion would be sub-threshold.

In Experiments 1 and 2, subjects were in complete darkness during testing. Nominally, pilots and astronauts would have out-the-window visual cues as well as instrument displays to provide information about vehicle orientation. The current experiments demonstrated that when visual cues were not available, hyper-gravity will cause misperceptions and decrements in pilot manual control performance. However, presumably veridical visual information will improve these errors. This is a reasonable assumption though there are a few potential issues. First, in many aerospace applications veridical out-the-window visuals are not always available to pilots. In aircraft, clouds and low visibility may reduce or remove visual cues. In lunar landing and helicopter landings, dust blowback is a concern (1969; Brady and Paschall 2010; Clark, Young et al. 2011). Furthermore, out-the-window visual cues are not always veridical and may lead to additional perceptual illusions (see (Young 2003) for a review). Current aerospace instrument displays are generally quite reliable and pilots are trained to utilize them with confidence. However, in aircraft spatial disorientation accidents still occur with a relatively high frequency despite the presence of functioning instruments (Bellenkes, Bason et al. 1992; Cheung, Money et al. 1995; Durnford, Crowley et al. 1995; Knapp and Johnson 1996; Braithwaite, Groh et al. 1997; Braithwaite, Durnford et al. 1998; Neubauer 2000; Curry and McGhee 2007; Nooij and Groen 2011). Future experiments should aim to study the effect of hyper-gravity on perception and control when visual information is available. We hypothesize that misperceptions and control performance in most cases will

improve however there may be infrequent large errors which can be attributed to the effect of altered gravity on vestibular signals.

Finally we were limited, as nearly all flight simulation experiments are, in that we could not reproduce the same flight-related consequences that exist during real scenarios. Knowledge that one's life depends upon good performance may impact their responses. However, the degradations observed in hyper-gravity seem to be physiological in nature and are unlikely to be overcome with increased focus or effort.

## 7.8 Future Work

Specific topics and details on areas of future work are addressed throughout. Here, we highlight several specific research paths for future work.

- Sensorimotor function in other altered gravity levels. We hypothesize that hypo-gravity ( $\sim 1/6$  G for lunar and  $\sim 3/8$  G for Mars are of interest) will result in *underestimation* of roll tilt. Figure 44 provides static roll tilt perceptual predictions across multiple angles and hypo-gravity levels from simulation of the modified Observer model. Well controlled, acute angle roll tilts in hypo-gravity would require a tilt device mounted in a parabolic flight airplane.
- Pitch (dynamic and static) tilt perception in hyper-gravity. In the current study we have only addressed roll tilts. It is well known that pitch perception is also affected by hyper-gravity (Schone 1964; Correia, Hixson et al. 1968); however there is an asymmetry due to the orientation of the utricular plane within the head. A “functional utricular plane” could be estimated by identifying the pitch angle at which hyper-gravity has no impact upon pitch perception.
- Differences in utricular versus saccular otolith responses and processing. Overestimation of roll tilt in hyper-gravity suggests that signals originating from the utricle are processed differently (i.e. apparently weighted more heavily by the CNS) than those from the saccule. Neural recordings (Fernandez and Goldberg 1976; Fernandez and Goldberg 1976; Fernandez and Goldberg 1976) show differences in resting discharge rates and sensitivities, which may contribute to differences in processing. Future behavioral paradigms and electrophysiology techniques should examine these apparent differences.
- Adaptation of orientation perception in hyper-gravity. We found evidence for adaptation in dynamic roll tilt perception (i.e. less overestimation on the second session of a particularly hyper-gravity level than the first), but not for static tilts. Future experiments should characterize the time course and nature of this adaptation for both static and dynamic motions in hyper-gravity.
- Determine cause(s) of initial manual control performance decrements in hyper-gravity. We hypothesize the observed initial performance decrements were primarily caused by perceptual overestimation of roll tilt in hyper-gravity leading to over-controlling. However, we cannot rule out other causes. Hyper-gravity impacts physical motor responses necessary to operate the rotational hand controller and the cross-coupled stimulus which only occurs in hyper-gravity may cause general disorientation.
- Determine mechanism(s) of adaptation in manual control performance in hyper-gravity. We hypothesize that the primary cause of the observed improved performance over a few hundred

seconds is a cognitive adjustment in the necessary motor response for a particular perceived tilt. This could be tested by measuring roll tilt perception before and after manual control adaptation. If the adaptation is primarily cognitive, not perceptual, similar amounts of overestimation should be observed pre and post. In a second experiment, after training, the vehicle dynamics could be modified in the software. Specifically, the gain of the RHC could be increased to replicate the necessary cognitive adjustment without altering perception like in hyper-gravity. If the adaptation time course is similar for the vehicle dynamics modification as it was for hyper-gravity, it would suggest the adaptation mechanism is primarily cognitive.

- Extended manual control adaptation in hyper-gravity. In 1.5 G there was some evidence, though not significant, that performance may actually improve beyond 1 G baseline levels with sufficient time in hyper-gravity. This could be explained by hyper-gravity causing increased utricular shear displacement, leading to improved roll tilt sensitivity. Once a proper reinterpretation of the altered otolith signal is made, hypothetically the increased sensitivity could lead to enhanced manual control performance in hyper-gravity. To study this, hyper-gravity testing would need to be extended beyond the three 214 second trials in the current study.
- Characterize and develop an altered gravity pre-exposure countermeasure. We have shown that pre-exposure to one hyper-gravity level reduces the initial performance decrement in another, novel hyper-gravity level when the two are separated by 20-40 minutes, however several questions remain. How long does the pre-exposure effect last for (weeks to months would necessary for a lunar or Martian mission)? Does pre-exposure to hyper-gravity improve performance in hypo-gravity? How does repeated pre-exposure (multiple sessions, potentially at multiple hyper-gravity levels) affect performance? Is the pre-exposure effect task dependent (e.g. does pre-exposure for manual control improve posture in altered gravity)? How can pre-exposure training be optimized to ensuring initial performance while reducing training time (e.g. incremental exposure and/or refresher training)?
- Understand/predict inter-individual differences. We identified inter-individual differences in perception and control in hyper-gravity. What might be the cause(s) of these differences? Possible explanations include differences in vestibular or extra-vestibular sensory function, sensory central processing strategies, previous experiences, or somatosensory reporting technique. In the manual control task, additional individual differences may exist in control strategy and cognitive ability to adapt quickly to incorrect control responses.
- Extend to applied, operational domains. Our studies in hyper-gravity indicate that altered gravity will impact sensorimotor function, however how operationally relevant these effects are depend upon the task. Certain tasks may allow for small sensorimotor errors, while others are more critical. For example, in a planetary landing task, vehicle orientation must be tightly controlled and errors may lead to a catastrophic accident or abort. Future research should characterize these specific environments using operational metrics.

## 8.0 Conclusion

We conclude that humans make perceptual and manual control errors in hyper-gravity. Specifically, static roll tilt was overestimated in hyper-gravity, with more overestimation at higher gravity levels and larger angles. We provided a modified version of the utricular shear model that fit the static overestimation far superior than previously proposed models. Dynamic roll rotations were also overestimated, though generally less so than static tilts. The amount of overestimation was dependent upon the angular velocity of rotation with less overestimation at higher angular velocities. This finding is consistent with the hypothesis that the CNS integrates information from sensory sources based upon their reliability. At higher angular velocities the signals from the semicircular canals, which are presumably unaffected by hyper-gravity, are more reliable and thus more heavily weighted, resulting in less overestimation.

Manual control performance was initially much worse in hyper-gravity as compared to the 1 G performance baseline. Initial decrements were significant; in 1.5 G's the initial performance errors increased by an estimated 26% of the 1 G level, while in 2 G's it was 45%. These were likely, at least partially, due to misperceptions of roll tilt causing subjects to make incorrect control inputs. However, with practice in hyper-gravity, performance improved to near 1 G baseline levels over the time course of several minutes. Interestingly, pre-exposure to one hyper-gravity level reduced the initial performance decrements on another, novel hyper-gravity level. This supports the concept of enhanced adaptability through prior adaptation, now for the first time shown for adaptation to altered gravity environments.

We proposed a modification to a previous dynamic spatial orientation perception model in which the gain for linear acceleration feedback errors depended upon whether they were in or out of the utricular plane. This modification allowed for the model to predict the characteristic overestimation of roll tilt observed in hyper-gravity. The model simulated the amount of static overestimation observed empirically over a range of angles and gravity levels. In addition, it reproduced the characteristic dependence of overestimation during dynamic rotations on angular velocity. The simple modification may have some physiological justification in terms of differences in resting discharge rate and sensitivity between otolith neurons with polarization vectors near the utricular plane and those that are roughly perpendicular. It had negligible impact upon predictions for several well validated 1 G simulations.

Future work should aim to study additional altered gravity environments. For example, the modified model predicts underestimation of acute roll tilts in hypo-gravity, which has yet to be validated experimentally. Pilot manual control performance decrements in altered gravity, such as those observed here in hyper-gravity, are likely to impact the safety of future space exploration missions in terms of accidents or aborts. The reduction in initial manual control performance decrements through pre-exposure to another hyper-gravity environment may open the door for the development of an altered gravity pre-training countermeasure.

## References

1. (1969). Apollo 12 Technical Crew Debriefing. Houston, TX, NASA.
2. Adenot, S. (2004). Artificial Gravity: Changing the Intensity of Coriolis Cross-Coupled Stimulus with Head-Angle. Aeronautics and Astronautics. Cambridge, Massachusetts Institute of Technology. **S.M.:** 137.
3. Aubert, H. (1861). "Eine Scheinbare Bedeutende Drehung von Objekten bei Neigung des Kopfes nach rechts oder links." Arch Pathol Anat **20**: 381-393.
4. Batson, C. D., R. A. Brady, et al. (2011). "Gait training improves performance in healthy adults exposed to novel sensory discordant conditions." Experimental Brain Research **209**(4): 515-524.
5. Bellenkes, A., R. Bason, et al. (1992). "Spatial Disorientation in Naval Aviation Mishaps - a Review of Class a Incidents from 1980 through 1989." Aviation Space and Environmental Medicine **63**(2): 128-131.
6. Benson, A. J., F. E. Guedry, et al. (1997). "Microgravity vestibular investigations: Perception of self-orientation and self-motion." Journal of Vestibular Research-Equilibrium & Orientation **7**(6): 453-457.
7. Bilimoria, K. D. (2009). "Effects of Control Power and Guidance Cues on Lunar Lander Handling Qualities." Journal of Spacecraft and Rockets **46**(6): 1261-1271.
8. Borah, J. and L. R. Young (1982). Orientation Perception during Aircraft Coordinated Turns. AIAA 20th Aerospace Sciences Meeting. Orlando, FL.
9. Borah, J. and L. R. Young (1983). Spatial Orientation and Motion Cue Environment Study in the Total In-Flight Simulator. Brooks Air Force Base, TX, Air Force Human Resources Laboratory.
10. Borah, J., L. R. Young, et al. (1978). Sensory Mechanism Modeling. AFHRL-TR-78-83, Air Force Human Resources Laboratory, AFHRL-TR-78-83, Air Force Systems Command.
11. Borah, J., L. R. Young, et al. (1988). "Optimal Estimator Model for Human Spatial Orientation." Annals of the New York Academy of Sciences **545**: 51-73.
12. Bortolami, S. B., S. Rocca, et al. (2006). "Mechanisms of human static spatial orientation." Experimental Brain Research **173**(3): 374-388.
13. Bos, J. E. and W. Bles (2004). "Motion sickness induced by optokinetic drums." Aviation Space and Environmental Medicine **75**(2): 172-174.
14. Boyle, R., T. Belton, et al. (1996). "Responses of Identified Vestibulospinal Neurons to Voluntary Eye and Head Movements in the Squirrel Monkey." New Directions in Vestibular Research **781**: 244-263.
15. Brady, T. and S. Paschall (2010). The Challenge of Safe Lunar Landing. IEEE Aerospace Conference. Big Sky, MT.
16. Braithwaite, M., S. Groh, et al. (1997). Spatial Disorientation in U.S. Army Helicopter Accidents: an Update of the 1987-92 Survey to Include 1993-95. Report No. 97-13. Fort Rucker, AL, U.S. Army Aeromedical Research Laboratory.
17. Braithwaite, M. G., S. J. Durnford, et al. (1998). "Flight simulator evaluation of a novel flight instrument display to minimize the risks of spatial disorientation." Aviation Space and Environmental Medicine **69**(8): 733-742.
18. Brown, E. L., H. Hecht, et al. (2002). "Sensorimotor Aspects of High-Speed Artificial Gravity: I. Sensory Conflict in Vestibular Adaptation." Journal of Vestibular Research **12**(5-6): 271-282.
19. Bruni, S. (2004). Artificial Gravity: Neurovestibular Adaptation to Incremental Exposure to Centrifugation. Aeronautics and Astronautics. Cambridge, Massachusetts Institute of Technology. **S.M.:** 172.
20. Bryan, A. S., S. B. Bortolami, et al. (2007). "Influence of gravitoinertial force level on the subjective vertical during recumbent yaw axis body tilt." Experimental Brain Research **183**(3): 389-397.



21. Campbell, M. R. and A. Garbino (2011). "History of Suborbital Spaceflight: Medical and Performance Issues." Aviation Space and Environmental Medicine **82**(4): 469-474.
22. Chelette, T. L. (2001). "Measuring the Head Tilt Illusion During Sustained Acceleration." Human Systems IAC Gateway **12**(3): 4-6.
23. Chelette, T. L., E. J. Martin, et al. (1995). "The Effect of Head Tilt on Perception of Self-Orientation while in a Greater than One G Environment." Journal of Vestibular Research **5**(1): 1-17.
24. Cheung, B., K. Money, et al. (1995). "Spatial Disorientation-Implicated Accidents in Canadian Forces, 1982-92." Aviation Space and Environmental Medicine **66**(6): 579-585.
25. Cheung, C. C., H. Hecht, et al. (2007). "Threshold-based vestibular adaptation to cross-coupled canal stimulation." Journal of Vestibular Research-Equilibrium & Orientation **17**(4): 171-181.
26. Clark, B., A. Graybiel, et al. (1948). "The Illusory Perception of Movement Caused by Angular Acceleration and by Centrifugal Force during Flight .2. Visually Perceived Motion and Displacement of a Fixed Target during Turns." Journal of Experimental Psychology **38**(3): 298-309.
27. Clark, T. K., L. R. Young, et al. (2011). "Numerical Simulation of Human Orientation Perception during Lunar Landing." Acta Astronautica **69**(7-8): 420-428.
28. Clement, G. (1998). "Alteration of eye movements and motion perception in microgravity." Brain Research Reviews **28**(1-2): 161-172.
29. Clement, G., P. Denise, et al. (2007). "Human Ocular Counter-Rolling and Roll Tilt Perception during Off-Vertical Axis Rotation after Spaceflight." Journal of Vestibular Research-Equilibrium & Orientation **17**(5-6): 209-215.
30. Cohen, M. M. (1970). "Hand-Eye Coordination in Altered Gravitational Fields." Aerospace Medicine **41**(6): 647-&.
31. Cohen, M. M. (1970). "Sensory-Motor Adaptation and after-Effects of Exposure to Increased Gravitational Forces." Aerospace Medicine **41**(3): 318-&.
32. Cohen, M. M. (1973). "Elevator Illusion - Influences of Otolith Organ Activity and Neck Proprioception." Perception & Psychophysics **14**(3): 401-406.
33. Colenbrander, A. (1963). "Eye and Otoliths." Aeromedica acta **9**: 45-91.
34. Cornsweet, T. N. (1970). Visual Perception. New York, Academic Press.
35. Correia, M. J., W. C. Hixson, et al. (1965). Otolith Shear and Visual Perception of Force Direciton: Discrepancies and a Proposed Resolution. Pensacola, FL, Naval Aerospace Medical Institute.
36. Correia, M. J., W. C. Hixson, et al. (1968). "On Predictive Equations for Subjective Judgments of Vertical and Horizon in a Force Field." Acta Otolaryngologica (supplement) **230**: 1-20.
37. Correia, R. J. (1998). "Neuronal plasticity: adaptation and readaptation to the environment of space." Brain Research Reviews **28**(1-2): 61-65.
38. Corriea, M. J., W. C. Hixson, et al. (1968). "On Predictive Equations for Subjective Judgments of Vertical and Horizon in a Force Field." Acta Otolaryngologica (supplement) **230**: 1-20.
39. Corvera, J., C. S. Hallpike, et al. (1958). "A New Method for the Anatomical Reconstruction of the Human Macular Planes." Acta Otolayngologica **49**(1): 4-16.
40. Curry, I. P. and J. S. McGhee (2007). Spatial Disorientation as a Cause of Mishaps in Combat Helicopter Operations. Aviation, Space, and Environmental Medicine Meeting.
41. Curthoys, I. S., G. A. Betts, et al. (1999). "The Planes of the Utricular and Saccular Maculae of the Guinea Pig." Annals of the New York Academy of Sciences **871**: 27-34.
42. Dai, M. J., I. S. Curthoys, et al. (1989). "A Model of Otolith Stimulation." Biological Cybernetics **60**(3): 185-194.
43. Dai, M. J., T. Raphan, et al. (2011). "Prolonged reduction of motion sickness sensitivity by visual-vestibular interaction." Experimental Brain Research **210**(3-4): 503-513.
44. Davis, J. R., R. Johnson, et al. (2008). Fundamentals of Aerospace Medicine. Philadelphia, PA, Lippincott Williams & Wilkins.

45. de Winkel, K. N., G. Clement, et al. (2012). "The perception of verticality in lunar and Martian gravity conditions." Neuroscience Letters **529**(1): 7-11.
46. Diamond, S. G. and C. H. Markham (1988). "Ocular Torsion in Upright and Tilted Positions during Hypogravity and Hypergravity of Parabolic Flight." Aviation Space and Environmental Medicine **59**(12): 1158-1162.
47. Diamond, S. G. and C. H. Markham (1991). "Prediction of Space Motion Sickness Susceptibility by Disconjugate Eye Torsion in Parabolic Flight." Aviation Space and Environmental Medicine **62**(3): 201-205.
48. Diamond, S. G. and C. H. Markham (1992). "Validating the Hypothesis of Otolith Asymmetry as a Cause of Space Motion Sickness." Annals of the New York Academy of Sciences **656**: 725-731.
49. Diamond, S. G., C. H. Markham, et al. (1990). "Instability of Ocular Torsion in Zero Gravity - Possible Implications for Space Motion Sickness." Aviation Space and Environmental Medicine **61**(10): 899-905.
50. Dichgans, J., R. Held, et al. (1972). "Moving Visual Scenes Influence Apparent Direction of Gravity." Science **178**(4066): 1217-&.
51. Dizio, P. and J. R. Lackner (1988). "The Effects of Gravitoinertial Force Level and Head Movements on Post-Rotational Nystagmus and Illusory after-Rotation." Experimental Brain Research **70**(3): 485-495.
52. DiZio, P. and J. R. Lackner (2002). "Sensorimotor Aspects of High-Speed Artificial Gravity III: Sensorimotor Adaptation." Journal of Vestibular Research **12**(5-6): 291-299.
53. Dizio, P., J. R. Lackner, et al. (1987). "The Influence of Gravitoinertial Force Level on Oculomotor and Perceptual Responses to Coriolis, Cross-Coupling Stimulation." Aviation Space and Environmental Medicine **58**(9): A218-A223.
54. Duda, K. R., M. C. Johnson, et al. (2009). Design and Analysis of Lunar Lander Manual Control Modes. IEEE Aerospace Conference. Big Sky, MT: 1-16.
55. Duda, K. R., M. C. Johnson, et al. (2010). Design and Analysis of an Attitude Command Velocity Hold/Hover Hold plus Incremental Position Command Blended Control Mode for Piloted Lunar Landing. AIAA GNC Conference. Toronto, Ontario, Canada.
56. Durnford, S. J., J. S. Crowley, et al. (1995). Spatial Disorientation: a Survey of U.S. Army Helicopter Accidents 1987-1992 USARL Report No. 95-25. Fort Rucker, AL, U.S. Army Aeromedical Research Laboratory.
57. Dyde, R. T., M. R. Jenkin, et al. (2006). "The Subjective Visual Vertical and the Perceptual Upright." Experimental Brain Research **173**(4): 612-622.
58. Dyde, R. T., M. R. Jenkin, et al. (2009). "The Effect of Altered Gravity States on the Perception of Orientation." Experimental Brain Research **194**(4): 647-660.
59. Dyde, R. T., M. R. M. Jenkin, et al. (2010). "The Effect of Lunar Gravity on Perception: Ambient Visual Cues Have Less Effect on Orientation Judgements than They Do Under Normal Gravity." Journal of Vision **9**(8).
60. Edgerton, V. R., G. E. McCall, et al. (2001). "Sensorimotor Adaptations to Microgravity in Humans." Journal of Experimental Biology **204**(18): 3217-3224.
61. Einstein, A. (1908). "Uber das Relativitatsprinzip und die aus demselben gezogenen Folgerungen." Jahrb Radioakt **4**: 411-462.
62. Elias, P. Z., T. Jarchow, et al. (2008). "Incremental Adaptation to Yaw Head Turns during 30 RPM Centrifugation." Experimental Brain Research **189**(3): 269-277.
63. Fernandez, C. and J. M. Goldberg (1971). "Physiology of Peripheral Neurons Innervating Semicircular Canals of Squirrel Monkey. II. Response to Sinusoidal Stimulation and Dynamics of Peripheral Vestibular System." J Neurophysiol **34**(4): 661-675.
64. Fernandez, C. and J. M. Goldberg (1976). "Physiology of Peripheral Neurons Innervating Otolith Organs of Squirrel-Monkey. II. Directional Selectivity and Force-Response Relations." Journal of Neurophysiology **39**(5): 985-995.

65. Fernandez, C. and J. M. Goldberg (1976). "Physiology of Peripheral Neurons Innervating Otolith Organs of the Squirrel Monkey. I. Response to Static Tilts and to Long-Duration Centrifugation." Journal of Neurophysiology **39**(5): 970-984.
66. Fernandez, C. and J. M. Goldberg (1976). "Physiology of Peripheral Neurons Innervating Otolith Organs of the Squirrel Monkey. III. Response Dynamics." J Neurophysiol **39**: 996-1008.
67. Fisk, J., J. R. Lackner, et al. (1993). "Gravitoinertial Force Level Influences Arm Movement Control." Journal of Neurophysiology **69**(2): 504-511.
68. Garrick-Bethell, I., T. Jarchow, et al. (2008). "Vestibular Adaptation to Centrifugation Does Not Transfer Across Planes of Head Rotation." Journal of Vestibular Research **18**(1): 25-37.
69. Gillingham, K. K. and F. H. Previc (1996). Spatial Orientation in Flight. Fundamentals of Aerospace Medicine. R. DeHart. Baltimore, Williams & Wilkins. **2**: 309-397.
70. Gilson, R. D., F. E. Guedry, et al. (1973). "Observations on Perceived Changes in Aircraft Attitude Attending Head Movements Made in a 2-g Bank and Turn." Aerospace Medicine **44**(1): 90-92.
71. Glasauer, S. and H. Mittelstaedt (1992). "Determinants of Orientation in Microgravity." Acta Astronautica **27**: 1-9.
72. Glasauer, S. and H. Mittelstaedt (1998). "Perception of spatial orientation in microgravity." Brain Research Reviews **28**(1-2): 185-193.
73. Goldberg, J. M. and C. Fernandez (1971). "Physiology of Peripheral Neurons Innervating Semicircular Canals of Squirrel Monkey. I. Resting Discharge and Response to Constant Angular Accelerations." J Neurophysiol **34**(4): 635-660.
74. Goldberg, J. M. and C. Fernandez (1971). "Physiology of Peripheral Neurons Innervating Semicircular Canals of Squirrel Monkey. III. Variations among Units in Their Discharge Properties." J Neurophysiol **34**(4): 676-684.
75. Golding, J. F. (1998). "Motion Sickness Susceptibility Questionnaire Revised and its Relationship to Other Forms of Sickness." Brain Research Bulletin **47**(5): 507-516.
76. Golding, J. F. (2006). "Predicting Individual Differences in Motion Sickness Susceptibility by Questionnaire." Personality and Individual Differences **41**(2): 237-248.
77. Gonshor, A. and G. Melvill Jones (1971). "Plasticity in the Adult Human Vestibuloocular Reflex Arc." Proc Can Fed Biol Soc **14**(11).
78. Grabherr, L., K. Nicoucar, et al. (2008). "Vestibular thresholds for yaw rotation about an earth-vertical axis as a function of frequency." Experimental Brain Research **186**(4): 677-681.
79. Gray, R. F., R. J. Crosbie, et al. (1961). The Presence or Absence of Visual Coriolis Illusions at Various Combined Angular Velocities. Johnsville, Pennsylvania, U.S. Naval Air Development Center.
80. Graybiel, A. (1973). "Space Missions Involving the Generation of Artificial Gravity." Environ Biol Med **2**(2): 91-138.
81. Graybiel, A., B. Clark, et al. (1947). "The Illusory Perception of Movement Caused by Angular Acceleration and by Centrifugal Force during Flight .1. Methodology and Preliminary Results." Journal of Experimental Psychology **37**(2): 170-177.
82. Graybiel, A., B. Clark, et al. (1960). "Observations on Human Subjects Living in a "Slow Rotating Room" for Periods of Two Days " Archives of Neurology **3**(1): 55-73.
83. Graybiel, A., F. R. Deane, et al. (1968). Prevention of Overt Motion Sickness by Incremental Exposure to Otherwise Highly Stressful Coriolis Acceleration. NAMI Report.
84. Graybiel, A. and J. Knepton (1972). "Direction-Specific Adaptation Effects Acquired in a Slow Rotation Room." Aerospace Medicine **43**(11): 1179-&.
85. Green, A. M. and D. E. Angelaki (2004). "An Integrative Neural Network for Detecting Inertial Motion and Head Orientation." Journal of Neurophysiology **92**(2): 905-925.
86. Guedry, F. E. (1974). Psychophysics of Vestibular Sensation. Handbook of Sensory Physiology. Berlin, Springer-Verlag: 3-154.

87. Guedry, F. E. and E. K. Montague (1961). "Quantitative Evaluation of the Vestibular Coriolis Reaction." *Aerospace Medicine* **32**: 487-500.
88. Guedry, F. E. and A. H. Rupert (1991). "Steady-State and Transient G-Excess Effects." *Aviation Space and Environmental Medicine* **62**(3): 252-253.
89. Haburcakova, C., R. F. Lewis, et al. (2012). "Frequency Dependence of Vestibuloocular Reflex Thresholds." *Journal of Neurophysiology* **107**(3): 973-983.
90. Harm, D. L. and D. E. Parker (1993). "Perceived Self-Orientation and Self-Motion in Microgravity, After Landing and During Preflight Adaptation Training." *Journal of Vestibular Research* **3**(3): 297-305.
91. Harm, D. L., M. F. Reschke, et al. (1999). Visual-Vestibular Integration Motion Perception Reporting (DSO 604 OI-1). *Extended Duration Orbiter medical Project Final Report*. C. F. Sawin, G. R. Taylor and W. L. Smith: 5.2.1-5.2.12.
92. Harris, L. R., M. R. M. Jenkin, et al. (2012). "The Perception of Upright under Lunar Gravity." *Journal of Gravitational Physiology* **19**(2): 9-16.
93. Haslwanter, T., R. Jaeger, et al. (2000). "Three-dimensional eye-movement responses to off-vertical axis rotations in humans." *Experimental Brain Research* **134**(1): 96-106.
94. Hecht, H., E. L. Brown, et al. (2002). "Adapting to Artificial Gravity (AG) at High Rotational Speeds." *Proceedings of the European Symposium on Life in Space for Life on Earth* **501**: 151-155.
95. Huang, J. K. and L. R. Young (1988). "Visual-Field Influence on Manual Roll and Pitch Stabilization." *Aviation Space and Environmental Medicine* **59**(7): 611-619.
96. Jamali, M., S. G. Sadeghi, et al. (2009). "Response of Vestibular Nerve Afferents Innervating Utricle and Saccule During Passive and Active Translations." *Journal of Neurophysiology* **101**: 141-149.
97. Jarchow, T., M. Wirz, et al. (2003). "Perceived horizontal body position in healthy and paraplegic subjects: Effect of centrifugation." *Journal of Neurophysiology* **90**(5): 2973-2977.
98. Jarchow, T. and L. R. Young (2007). "Adaptation to head movements during short radius centrifugation." *Acta Astronautica* **61**(10): 881-888.
99. Jia, H., L. Yu, et al. (2002). "Perception of the Cabin Attitude Changes in Hypergravity." *Aviation Space and Environmental Medicine* **73**(3): 191-193.
100. Karmali, F. and M. Shelhamer (2008). "The Dynamics of Parabolic Flight: Flight Characteristics and Passenger Percepts." *Acta Astronautica* **63**(5-6): 594-602.
101. Keshavarz, B. and H. Hecht (2011). "Validating an Efficient Method to Quantify Motion Sickness." *Human Factors* **53**(4): 415-426.
102. Knapp, C. J. and R. Johnson (1996). "F-16 class mishaps in the US Air Force, 1975-93." *Aviation Space and Environmental Medicine* **67**(8): 777-783.
103. Kornheiser, A. S. (1976). "Adaptation to Laterally Displaced Vision - Review." *Psychological Bulletin* **83**(5): 783-816.
104. Kurtzer, I., P. A. DiZio, et al. (2005). "Adaptation to a Novel Multi-Force Environment." *Experimental Brain Research* **164**(1): 120-132.
105. Lackner, J. and P. DiZio (2009). "Angular displacement perception modulated by force background." *Experimental Brain Research* **195**(2): 335-343.
106. Lackner, J. R. and P. DiZio (2005). "Motor Control and Learning in Altered Dynamic Environments." *Current Opinion in Neurobiology* **15**(6): 653-659.
107. Lackner, J. R. and P. A. DiZio (2003). "Adaptation to Rotating Artificial Gravity Environments." *Journal of Vestibular Research-Equilibrium & Orientation* **13**(4-6): 321-330.
108. Lackner, J. R. and A. Graybiel (1978). "Postural Illusions Experienced during Z-Axis Recumbent Rotation and Their Dependence Upon Somatosensory Stimulation of Body-Surface." *Aviation Space and Environmental Medicine* **49**(3): 484-488.
109. Lackner, J. R. and A. Graybiel (1978). "Some Influences of Touch and Pressure Cues on Human Spatial Orientation." *Aviation Space and Environmental Medicine* **49**(6): 798-804.

110. Lackner, J. R. and A. Graybiel (1984). Influence of Gravito-inertial Force Level on Apparent Magnitude of Coriolis Cross-Coupled Angular Accelerations and Motion Sickness. The Aerospace Medical Panel Symposium on Motion Sickness: Mechanisms, Prediction, Prevention, and Treatment. Williamsburg, Virginia.
111. Laurens, J. and J. Droulez (2007). "Bayesian Processing of Vestibular Information." Biological Cybernetics **96**(4): 389-404.
112. Lim, K. and D. M. Merfeld (2012). "Signal detection theory and vestibular perception: II. Fitting perceptual thresholds as a function of frequency." Experimental Brain Research **222**(3): 303-320.
113. Lowenstein, O. and T. D. M. Roberts (1949). "The Equilibrium Function of the Otolith Organs of the Thornback Ray (Rafa-Clavata)." Journal of Physiology-London **110**(3-4): 392-415.
114. Luenburger, D. G. (1971). "An Introduction to Observers." IEEE Transactions on Automatic Control **16**: 596-602.
115. Lychakov, D. V. and Y. T. Rebane (2005). "Fish otolith mass asymmetry: Morphometry and influence on acoustic functionality (vol 201, pg 55, 2005)." Hearing Research **207**(1-2): 117-118.
116. Mast, F. and T. Jarchow (1996). "Perceived body position and the visual horizontal." Brain Research Bulletin **40**(5-6): 393-397.
117. Mast, F. W., N. J. Newby, et al. (2002). "Sensorimotor Aspects of High-Speed Artificial Gravity: II. The Effect of Head Position on Illusory Self Motion." Journal of Vestibular Research **12**(5-6): 283-289.
118. Mateus, J. (2008). The Effect of Sleep on the Adaptation to the Cross-Coupled Stimulus during Artificial Gravity. Aeronautics and Astronautics. Cambridge, Massachusetts Institute of Technology. **S.M.:** 75.
119. Mayne, R. (1974). A Systems Concept of the Vestibular Organs. Vestibular System. Part 2 - Psychophysics, applied aspects, and general interpretations. H. H. Komuber. Berlin, Springer-Verlag. **2**: 493-580.
120. McCluskey, R., J. B. Clark, et al. (2001). Correlation of Space Shuttle Landing Performance with Cardiovascular and Neurological Dysfunction Resulting from Spaceflight. NASA Bioastronautics Roadmap. Houston, TX, NASA.
121. McCrea, R. A., G. T. Gdowski, et al. (1999). "Firing Behavior of Vestibular Neurons during Active and Passive Head Movements: Vestibulo-spinal and Other Non-Eye-Movement Related Neurons." Journal of Neurophysiology **82**(1): 416-428.
122. Melville Jones, G. (1970). "Origin Significance and Amelioration of Coriolis Illusions from Semicircular Canals - a Non-Mathematical Appraisal." Aerospace Medicine **41**(5): 483-&.
123. Merfeld, D. M. (1996). "Effect of spaceflight on ability to sense and control roll tilt: Human neurovestibular studies on SLS-2." Journal of Applied Physiology **81**(1): 50-57.
124. Merfeld, D. M. (2003). "Rotation otolith tilt-translation reinterpretation (ROTTR) hypothesis: A new hypothesis to explain neurovestibular spaceflight adaptation." Journal of Vestibular Research-Equilibrium & Orientation **13**(4-6): 309-320.
125. Merfeld, D. M., J. R. I. Christie, et al. (1994). "Perceptual and Eye-Movement Responses Elicited by Linear Acceleration Following Spaceflight." Aviation Space and Environmental Medicine **65**(11): 1015-1024.
126. Merfeld, D. M., S. Park, et al. (2005). "Vestibular perception and action employ qualitatively different mechanisms. I. Frequency response of VOR and perceptual responses during Translation and Tilt." Journal of Neurophysiology **94**(1): 186-198.
127. Merfeld, D. M., S. Park, et al. (2005). "Vestibular perception and action employ qualitatively different mechanisms. II. VOR and perceptual responses during combined Tilt&Translation." Journal of Neurophysiology **94**(1): 199-205.
128. Merfeld, D. M., K. A. Polutchko, et al. (1996). "Perceptual responses to linear acceleration after spaceflight: Human neurovestibular studies on SLS-2." Journal of Applied Physiology **81**(1): 58-68.

129. Merfeld, D. M., L. R. Young, et al. (1993). "A Multidimensional Model of the Effect of Gravity on the Spatial Orientation of the Monkey." Journal of Vestibular Research **3**(2): 141-161.
130. Merfeld, D. M. and L. H. Zupan (2002). "Neural processing of gravito-inertial cues in humans. III. Modeling tilt and translation responses." Journal of Neurophysiology **87**(2): 819-833.
131. Merfeld, D. M., L. H. Zupan, et al. (2001). "Neural processing of gravito-inertial cues in humans. II. Influence of the semicircular canals during eccentric rotation." Journal of Neurophysiology **85**(4): 1648-1660.
132. Miller, E. F. (1962). "Counterrolling of the Human Eyes Produced by Head Tilt with Respect to Gravity." Acta Oto-Laryngologica **54**(1-6): 479-501.
133. Miller, E. F. and A. Graybiel (1966). "Magnitude of Gravito-inertial Force an Independent Variable in Egocentric Visual Localization of Horizontal." Journal of Experimental Psychology **71**(3): 452-460.
134. Mittelstaedt, H. (1983). "A New Solution to the Problem of the Subjective Vertical." Naturwissenschaften **70**(6): 272-281.
135. Mittelstaedt, H. (1986). "The Subjective Vertical as a Function of Visual and Extraretinal Cues." Acta Psychologica **63**(1-3): 63-85.
136. Mittelstaedt, H. (1989). "The Role of the Pitched-up Orientation of the Otoliths in Two Recent Models of the Subjective Vertical." Biological Cybernetics **61**(6): 405-416.
137. Mittelstaedt, H. (1995). "Evidence of Somatic Graviception from New and Classical Investigations." Acta Oto-Laryngologica: 186-187.
138. Mittelstaedt, H. (1996). "Somatic graviception." Biological Psychology **42**(1-2): 53-74.
139. Moore, S. T., V. Dilda, et al. (2011). "Galvanic Vestibular Stimulation as an Analogue of Spatial Disorientation After Spaceflight." Aviation Space and Environmental Medicine **82**(5): 535-542.
140. Mueller, E., K. D. Bilimoria, et al. (2009). Effects of Control Power and Inceptor Sensitivity on Lunar Lander Handling Qualities. AIAA SPACE 2009 Conference & Exposition. Pasadena, California.
141. Mueller, G. E. (1916). "Uber das Aubertsche Phanomen." Sinnesphysiol **19**(109).
142. Mulavara, A. P., H. S. Cohen, et al. (2009). "Critical features of training that facilitate adaptive generalization of over ground locomotion." Gait & Posture **29**(2): 242-248.
143. Mulavara, A. P., A. H. Feiveson, et al. (2010). "Locomotor Function after Long-Duration Space Flight: Effects and Motor Learning during Recovery." Experimental Brain Research **202**(3): 649-659.
144. Muller, G. E. (1916). "Uber das Aubertsche Phanomen." Z Sinnesphysiol **49**: 109-246.
145. Neubauer, J. C. (2000). "Classifying Spatial Disorientation Mishaps using Different Definitions - Analysis of Five Years of USAF Class A Mishaps." IEEE Engineering in Medicine and Biology Magazine **19**(2): 28-34.
146. Newman, M. C. (2009). A Multisensory Observer Model for Human Spatial Orientation Perception. Aeronautics and Astronautics. Cambridge, MA, Massachusetts Institute of Technology. **S.M.**
147. Noble, C. E. (1949). "The Perception of the Vertical .III. The Visual Vertical as a Function of Centrifugal and Gravitational Forces." Journal of Experimental Psychology **39**(6): 839-850.
148. Nooij, S. A. E., J. E. Bos, et al. (2008). "Velocity storage activity is affected after sustained centrifugation: a relationship with spatial disorientation." Experimental Brain Research **190**(2): 165-177.
149. Nooij, S. A. E. and E. L. Groen (2011). "Rolling into Spatial Disorientation: Simulator Demonstration of the Post-Roll (Gillingham) Illusion." Aviation Space and Environmental Medicine **82**(5): 505-512.
150. Oman, C. M. (1982). "A Heuristic Mathematical-Model for the Dynamics of Sensory Conflict and Motion Sickness." Acta Oto-Laryngologica: 3-44.

151. Oman, C. M. (1991). Sensory conflict in motion sickness: an observer theory approach. Pictorial Communication in Virtual and Real Environments. S. R. Ellis, M. K. Kaiser and A. Grunwald. London, Taylor & Francis: 362-367.
152. Oman, C. M., O. L. Bock, et al. (1980). "Visually Induced Self-Motion Sensation Adapts Rapidly to Left-Right Visual Reversal." Science **209**(4457): 706-708.
153. Oman, C. M., I. P. Howard, et al. (2003). The Roll of the Visual Cues in Microgravity Spatial Orientation. The Neurolab Spacelab Mission: Neuroscience Research in Space (NASA SP-2003-535). J. C. Buckey and J. L. Homick: 69-82.
154. Oman, C. M., B. K. Lichtenberg, et al. (1986). "Mit Canadian Vestibular Experiments on the Spacelab-1 Mission .4. Space Motion Sickness - Symptoms, Stimuli, and Predictability." Experimental Brain Research **64**(2): 316-334.
155. Ormsby, C. C. and L. R. Young (1976). "Perception of Static Orientation in a Constant Gravitoinertial Environment." Aviation Space and Environmental Medicine **47**(2): 159-164.
156. Paloski, W. H., C. M. Oman, et al. (2008). "Risk of sensory-motor performance failures affecting vehicle control during space missions: a review of the evidence." Journal of Gravitational Physiology **15**(2).
157. Park, S., C. Gianna-Poulin, et al. (2006). "Roll rotation cues influence roll tilt perception assayed using a somatosensory technique." Journal of Neurophysiology **96**(1): 486-491.
158. Parker, D. E., M. F. Reschke, et al. (1985). "Otolith Tilt-Translation Reinterpretation Following Prolonged Weightlessness - Implications for Preflight Training." Aviation Space and Environmental Medicine **56**(6): 601-606.
159. Pettorossi, V. E., R. Panichi, et al. (2013). "Prolonged asymmetric vestibular stimulation induces opposite, long-term effects on self-motion perception and ocular responses." Journal of Physiology **591**(7): 1907-1920.
160. Rader, A. A. (2009). Motion Perception with Conflicting or Congruent Visual and Vestibular Cues. Aeronautics and Astronautics. Cambridge, Massachusetts Institute of Technology. **PhD**.
161. Rader, A. A., C. M. Oman, et al. (2009). "Motion Perception During Variable-Radius Swing Motion in Darkness." Journal of Neurophysiology **102**(4): 2232-2244.
162. Reason, J. T. (1978). "Motion Sickness Adaptation - Neural Mismatch Model." Journal of the Royal Society of Medicine **71**(11): 819-829.
163. Reason, J. T. and A. J. Benson (1978). "Voluntary Movement Control and Adaptation to Cross-Coupled Stimulation." Aviation Space and Environmental Medicine **49**(11): 1275-1280.
164. Robinson, D. A. (1981). "The Use of Control-Systems Analysis in the Neurophysiology of Eye-Movements." Annual Review of Neuroscience **4**: 463-503.
165. Roller, C. A., H. S. Cohen, et al. (2009). "Improvement of Obstacle Avoidance on a Compliant Surface during Transfer to a Novel Visual Task after Variable Practice under Unusual Visual Conditions." Perceptual and Motor Skills **108**(1): 173-180.
166. Roller, C. A., H. S. Cohen, et al. (2001). "Variable practice with lenses improves visuo-motor plasticity." Cognitive Brain Research **12**(2): 341-352.
167. Roman, J. A., B. H. Warren, et al. (1963). "Some Observations on Behavior of a Visual Target and a Visual Afterimage during Parabolic Flight Maneuvers." Aerospace Medicine **34**(9): 841-&.
168. Roscoe, A. H. (1984). Assessing Pilot Workload in Flight. Bedford, Royal Aircraft Establishment.
169. Roscoe, A. H. and G. A. Ellis (1990). A Subjective Rating Scale for Assessing Pilot Workload in Flight: A Decade of Practical Use. Farnborough, Hampshire, Royal Aerospace Establishment.
170. Roy, J. E. and K. E. Cullen (2001). "Selective Processing of Vestibular Reafference during Self-Generated Head Motion." Journal of Neuroscience **21**(6): 2131-2142.
171. Roy, J. E. and K. E. Cullen (2004). "Dissociating self-generated from passively applied head motion: Neural mechanisms in the vestibular nuclei." Journal of Neuroscience **24**(9): 2102-2111.
172. Schone, H. (1964). "On the Role of Gravity in Human Spatial Orientation." Aerospace Medicine **35**: 764-772.

173. Schone, H. and D. E. Parker (1967). "Inversion of the Effect of Increased Gravity on the Subjective Vertical." Naturwissenschaften **54**(11): 288-289.
174. Schone, H., D. E. Parker, et al. (1967). "Subjective Vertical as a Function of Body Position and Gravity Magnitude." Naturwissenschaften **54**(11): 288.
175. Seidler, R. D. (2004). "Motor Learning Experiences Enhance Motor Adaptability." Journal of Cognitive Neuroscience **16**: 65-73.
176. Seidler, R. D. (2005). "Differential Transfer Processes in Incremental Visuomotor Adaptation." Motor Control **9**(1): 40-58.
177. Selva, P. (2009). Modeling of the vestibular system and nonlinear models for human spatial orientation perception. I'Institut superieur de l'Aeronautique et de l'Espace. Toulouse, L'Universite de Toulouse. **PhD**.
178. Shelhamer, M., R. A. Clendaniel, et al. (2002). "Context-specific adaptation of saccade gain in parabolic flight." Journal of Vestibular Research-Equilibrium & Orientation **12**(5-6): 211-221.
179. Tafforin, C. (1996). "Initial Moments of Adaptation to Microgravity of Human Orientation Behavior, in Parabolic Flight Conditions." Acta Astronautica **38**(12): 963-971.
180. Tarnutzer, A. A., D. P. Fernando, et al. (2012). "Temporal constancy of perceived direction of gravity assessed by visual line adjustments." Journal of Vestibular Research-Equilibrium & Orientation **22**(1): 41-54.
181. Thelen, D., B. Wood, et al. (2010). Significant Incidents and Close Calls in Human Spaceflight, NASA.
182. Tribukait, A. and O. Eiken (2005). "Perception of the head transversal plane and the subjective horizontal during gondola centrifugation." Perception & Psychophysics **67**(3): 369-382.
183. Tribukait, A. and O. Eiken (2005). "Semicircular canal contribution to the perception of roll tilt during gondola centrifugation." Aviation Space and Environmental Medicine **76**(10): 940-946.
184. Tribukait, A. and O. Eiken (2006). "Roll-tilt perception during gondola centrifugation: Influence of steady-state acceleration (G) level." Aviation Space and Environmental Medicine **77**(7): 695-703.
185. Tribukait, A. and O. Eiken (2006). "Semicircular canal influence on the visually perceived eye level during gondola centrifugation." Aviation Space and Environmental Medicine **77**(5): 500-508.
186. Tribukait, A. and O. Eiken (2012). "Flight Experience and the Perception of Pitch Angular Displacements in a Gondola Centrifuge." Aviation Space and Environmental Medicine **83**(5): 496-503.
187. Turnham, E. J. A., D. A. Braun, et al. (2012). "Facilitation of learning induced by both random and gradual visuomotor task variation." Journal of Neurophysiology **107**(4): 1111-1122.
188. Vingerhoets, R. A. A., M. De Vrijer, et al. (2009). "Fusion of Visual and Vestibular Tilt Cues in the Perception of Visual Vertical." Journal of Neurophysiology **101**(3): 1321-1333.
189. Vingerhoets, R. A. A., W. P. Medendorp, et al. (2006). "Time Course and Magnitude of Illusory Translation Perception during Off-Vertical Axis Rotation." Journal of Neurophysiology **95**(3): 1571-1587.
190. Vingerhoets, R. A. A., J. A. M. Van Gisbergen, et al. (2007). "Verticality Perception During Off-Vertical Axis Rotation." Journal of Neurophysiology **97**(5): 3256-3268.
191. Von Holst, E. (1954). "Relations between the Central Nervous System and the Peripheral Organs." British Journal of Animal Behavior **2**: 89-94.
192. Von Holst, E. and H. Mittelstaedt (1950). "Das Reafferenzprinzip." Naturwissenschaften **37**: 464-476.
193. Wade, S. W. and I. S. Curthoys (1997). "The effect of ocular torsional position on perception of the roll-tilt of visual stimuli." Vision Research **37**(8): 1071-1078.
194. Welch, R. B., B. Bridgeman, et al. (1998). "Dual adaptation and adaptive generalization of the human vestibulo-ocular reflex." Perception & Psychophysics **60**(8): 1415-1425.



195. Wertheim, A. H., B. S. Mesland, et al. (2001). "Cognitive suppression of tilt sensations during linear horizontal self-motion in the dark." Perception **30**(6): 733-741.
196. Whiteside, T. (1961). "Hand-Eye Coordination in Weightlessness." Aerospace Medicine **32**(8): 719-&.
197. Woellner, R. C. and A. Graybiel (1959). "Counterrolling of the Eyes and Its Dependence on the Magnitude of Gravitational or Inertial Force Acting Laterally on the Body." Journal of Applied Physiology **14**(4): 632-634.
198. Xerri, C., J. Barthelemy, et al. (1987). "Neuronal Coding of Linear Motion in the Vestibular Nuclei of the Alert Cat .1. Response Characteristics to Vertical Otolith Stimulation." Experimental Brain Research **65**(3): 569-581.
199. Young, L. R. (2003). Spatial Orientation. Principles and Practice of Aviation Psychology. Mahwah, New Jersey, Lawrence Erlbaum Associates, Inc., Publishers: 72-109.
200. Young, L. R., H. Hecht, et al. (2001). "Artificial Gravity: Head Movements during Short-Radius Centrifugation." Acta Astronautica **49**(3-10): 215-226.
201. Young, L. R., J. Mendoza, et al. (1996). "Tactile Influences on Astronaut Visual Spatial Orientation: Human Neurovestibular Studies on SLS-2." Journal of Applied Physiology **81**(1): 44-49.
202. Young, L. R., C. M. Oman, et al. (1984). "Spatial Orientation in Weightlessness and Readaptation to Earth's Gravity." Science **225**(4658): 205-208.
203. Young, L. R., K. H. Sienko, et al. (2003). "Adaptation of the vestibulo-ocular reflex, subjective tilt, and motion sickness to head movements during short-radius centrifugation." Journal of Vestibular Research-Equilibrium & Orientation **13**(2-3): 65-77.
204. Zacharias, G. L. and L. R. Young (1981). "Influence of Combined Visual and Vestibular Cues on Human Perception and Control of Horizontal Rotation." Experimental Brain Research **41**(2): 159-171.
205. Zupan, L. H. and D. M. Merfeld (2003). "Neural processing of gravito-inertial cues in humans. IV. Influence of visual rotational cues during roll optokinetic stimuli." Journal of Neurophysiology **89**(1): 390-400.
206. Zupan, L. H., D. M. Merfeld, et al. (2002). "Using Sensory Weighting to Model the Influence of Canal, Otolith and Visual Cues on Spatial Orientation and Eye Movements." Biological Cybernetics **86**(3): 209-230.
207. Zupan, L. H., R. J. Peterka, et al. (2000). "Neural processing of gravito-inertial cues in humans. I. Influence of the semicircular canals following post-rotatory tilt." Journal of Neurophysiology **84**(4): 2001-2015.

## Appendices

### A. Ormsby and Young Model for Static Perception

Based upon the otolith afferent recordings performed by Goldberg and Fernandez (Fernandez and Goldberg 1976; Fernandez and Goldberg 1976; Fernandez and Goldberg 1976), Ormsby and Young proposed a novel model (Ormsby and Young 1976) to explain static perception of roll and pitch orientation in altered gravity environments. In particular the model employs a nonlinear interpretation of GIF stimulation that is perpendicular to the utricular plane, which is assumed pitched up relative to head level by  $\alpha=25$ degrees. The nonlinear transformation of GIF stimulation to measured or perceived (denoted by  $\hat{\cdot}$ ) GIF is given below, where y is the interaural direction, z is perpendicular to the utricular plane, and x is determined by the right hand rule.

$$\hat{f}_x = f_x$$

$$\hat{f}_y = f_y$$

$$\hat{f}_z = \begin{cases} -\cos(\alpha) & \text{if } f_z < -\cos(\alpha) \\ f_z & \text{if } f_z = -\cos(\alpha) \\ 0.6f_z - 0.4\cos(\alpha) & \text{if } f_z > -\cos(\alpha) \end{cases}$$

An alternate nonlinear transformation was also proposed for the out of utricular plane GIF stimulation. Note that the previous one had no  $f_z$  dependence and is thus referred to as the slope = 0, while this version does, hence the slope = -0.4 reference.

$$\hat{f}_z = \begin{cases} -0.4f_z - 1.4\cos(\alpha) & \text{if } f_z < -\cos(\alpha) \\ f_z & \text{if } f_z = -\cos(\alpha) \\ 0.6f_z - 0.4\cos(\alpha) & \text{if } f_z > -\cos(\alpha) \end{cases}$$

### B. Observer Model

Details on the Observer model parameters and structure are provided elsewhere (Merfeld, Young et al. 1993; Zupan, Merfeld et al. 2002; Vingerhoets, Van Gisbergen et al. 2007; Newman 2009; Vingerhoets, De Vrijer et al. 2009). Specifics of the model relating to the pathways specific to otolith signal processing are details in Section 6.2.1. Here, some background is provided on the specifics for the simulations conducted in the current work. The latest structure and parameters of the Observer model proposed in (Newman 2009) were utilized for the simulations in Section 2.9 and were used as a starting point for the modifications proposed in Section 6.2. In all simulations, unless explicitly specified, the visual pathways of the model were deactivated. This corresponds to the subject closing their eyes or being in the dark (as opposed to open eyes in the light with a visual scene that moves with the subject). Obviously this mimics the scenario in Experiment 1. In all simulations the actual and internal estimation of gravity magnitude is set to 1 Earth G's. Since all simulations start with the subject upright, or initially aligned with gravity, the initial constant for the quaternion integration corresponds to upright ( $\vec{q}(t=0) = [1 \ 0 \ 0 \ 0]^T$ ). In addition, we assume an accurate perception of orientation at the beginning of the simulation, so the internal constant of quaternion integration also corresponds to upright ( $\hat{\vec{q}}(t=0) = [1 \ 0 \ 0 \ 0]^T$ ). Unless stated otherwise, all of the simulations used 100 Hz sampling rates.

## C. MATLAB Code for Experiment 1 Profiles

Code to create a complete testing session for Experiment 1 (see Figure 9 for an example) is provided below. The user selects the desired “Glevel” for the session (1, 1.5, or 2 G’s) and then runs the script. The “output” variable contains the required information for a “Space mode” profile on the NASTAR ATFS-400. The first column of output is the commanded planetary spin rate of the centrifuge in rotations per minute. The second column is the commanded roll angle, relative to Earth vertical, of the centrifuge cab in degrees. The third column is the commanded pitch angle and for this experiment is always set to zero. Each row is the set of the commanded values at an instant in time which the time step between successive rows fixed at 0.01 seconds. The “output” variable should be copied into a .txt file and saved. Then on the ATFS-400 computer system the file type should be converted to a .space file by renaming the file from “Example.txt” to “Example.space”. These .space files are then loaded for experimentation. The naming convention, if trying to use previously saved files, is “MIT\_GExcess\_‘Glevel’\_‘Number’”, so for example the seventh 1.5 G profile would be “MIT\_GExcess\_15\_7.space” and the third 1.0 G profile would be “MIT\_GExcess\_10\_3.space”.

```
clc; clear all; close all

%% This program calculates a roll angle profile comprised of a series of 12
%% roll tilts for use on the NASTAR ATFS-400 centrifuge

%% User Inputs
% filename = 'MIT_GExcess_20_5.txt';
Glevel = 1.5; % # of G's we want to test at, 1, 1.5, or 2

dt = 0.01; % sec, time step
angle = [-10 -20 -40 20]; % roll angle magnitudes we want to test, deg
freq = [0.0625 0.125 0.25]; % acceleration frequencies we want to test, Hz

% angle = [-40]; % roll angle magnitudes we want to test, deg
% freq = [0.25]; % acceleration frequencies we want to test, Hz

cent_rad = 7.62; % centrifuge radius in m

if Glevel == 1
    t_spinup = 20; % time allowed for spin up, sec
    t_spindown = 20; % time allowed for spin down, sec
    t_rest = 5; % time allowed to adjust to G, sec
else
    t_spinup = 60; % time allowed for spin up, sec
    t_spindown = 60; % time allowed for spin down, sec
    t_rest = 60; % time allowed to adjust to G, sec
end

t_between = 30; % time allowed between tilts

%% Set up inputs for file
% Concatenate list of angles and freq's together
freq_vect = [];
angle_vect = [];
for i = 1:length(angle)
    for j = 1:length(freq)
        freq_vect((i-1)*length(freq)+j) = freq(j);
        angle_vect((i-1)*length(freq)+j) = angle(i);
    end
end

counterbalanced = 0;
iter = 1;
while counterbalanced == 0
    % Randomize order of angles and frequencies
```

```

freq_order = randperm(length(freq_vect));
freq_rand = freq_vect(freq_order);
angle_rand = angle_vect(freq_order);

% For test matrices
samples = zeros(3,4);
order = zeros(3,4);
for i = 1:length(freq_rand)
    if (angle_rand(i) < -9) && (angle_rand(i) > -11)
        pos1 = 1;
    elseif (angle_rand(i) < -19) && (angle_rand(i) > -21)
        pos1 = 2;
    elseif (angle_rand(i) < 21) && (angle_rand(i) > 19)
        pos1 = 3;
    elseif (angle_rand(i) < -39) && (angle_rand(i) > -41)
        pos1 = 4;
    else
        display(['Angle is: ', -num2str(angle_rand(i))])
    end

    if freq_rand(i) == 0.25
        pos2 = 1;
    elseif freq_rand(i) == 0.125
        pos2 = 2;
    elseif freq_rand(i) == 0.0625
        pos2 = 3;
    end

    samples(pos2, pos1) = samples(pos2, pos1) + 1;
    order(pos2, pos1) = i;
end
appear_angle = mean(order,1);
appear_freq = mean(order,2);

% Check to see how balanced the proposed order is
bal_tol = 1; % How far from perfectly balanced can we tolerate?
rep_tol = 0; % How many exact repetitions are allowed?
bal_min = (length(freq_rand)-1)/2 + 1 - bal_tol;
bal_max = (length(freq_rand)-1)/2 + 1 + bal_tol;
if (min(appear_angle) > bal_min) && (max(appear_angle) < bal_max) && (min(appear_freq) > bal_min) &&
(max(appear_freq) < bal_max)
    % then things are counterbalanced
    if sum(diff(angle_rand)==0) <= rep_tol
        % then only a few angles are immediately repeated
        display(['The number of iterations was: ', num2str(iter)]);
        counterbalanced = 1;
    end
end
iter = iter + 1;
% presentation = [freq_rand' angle_rand']
end

%% Display final trajectory
display(['The Glevel is: ', num2str(Glevel), 'Gs'])
disp(' ')
display('The samples tested are:')
disp(' Angles (deg)')
disp(' 10 20 -20 40')
disp(['0.25 Hz ', num2str(samples(1,:))])
disp(['0.125 Hz ', num2str(samples(2,:))])
disp(['0.0625 Hz ', num2str(samples(3,:))])
disp(' ')
display('The order tested is:')
disp(' Angles (deg)')
disp(' 10 20 -20 40')
disp(['0.25 Hz ', num2str(order(1,:))])
disp(['0.125 Hz ', num2str(order(2,:))])
disp(['0.0625 Hz ', num2str(order(3,:))])

%% Trajectory formation
%% Spin up
time = [0:dt:t_spinup]';

G_cent_start = sqrt(Glevel^2-1);
cent_vel_start = sqrt(9.81*G_cent_start/cent_rad)/t_spinup * time;
G = 1/9.81 * sqrt((cent_vel_start.^2 * cent_rad).^2 + 9.81^2);

a_cent = sqrt(G.^2 - 1); % centripetal acceleration, G's

```

```

theta = 180/pi*atan(a_cent/1);           % roll angle of centrifuge with respect to vertical

%% Wait for subject to adjust
time_new = [time(end)+dt:dt:time(end)+t_rest]';
G_new = G(end)*ones(length(time_new),1);
theta_new = theta(end)*ones(length(time_new),1);

time = [time; time_new];
G = [G; G_new];

theta = [theta; theta_new];

%% Perform the 12 roll tilts
theta_baseline = theta(end);

for i = 1:length(freq_order)
    % Perform a roll over
    T = 1/freq_rand(i);
    theta_f = angle_rand(i);
    t = [dt:dt:T]';
    A = 2*pi*theta_f/(T^2);
    for j = 1:length(t)
        theta_new = A*T/(2*pi) * (t-T/(2*pi)*sin(2*pi*t/T));
    end
    time = [time; t+time(end)];
    theta = [theta; theta_new+theta_baseline];

    % Wait for the time in between
    t_wait = [(time(end)+dt:dt:time(end)+t_between)]';
    time = [time; t_wait];
    theta = [theta; theta(end)*ones(length(t_wait),1)];

    % Roll back
    for j = 1:length(t)
        theta_new = theta(end) - A*T/(2*pi) * (t-T/(2*pi)*sin(2*pi*t/T));
    end
    time = [time; t+time(end)];
    theta = [theta; theta_new];

    % Wait for time upright
    t_wait = [(time(end)+dt:dt:time(end)+t_between)]';
    time = [time; t_wait];
    theta = [theta; theta(end)*ones(length(t_wait),1)];

    % Update the G vector
    G_new = G(end)*ones(2*length(t)+2*length(t_wait),1);
    G = [G; G_new];
end

%% Spin down
time_new = [dt:dt:t_spindown]';

cent_vel_slow = 2;           % rpm
cent_vel_slow_rad = cent_vel_slow * (2*pi/60);   % rad/s
cent_vel_stop = cent_vel_start(end) - (sqrt(9.81*G_cent_start/cent_rad)-cent_vel_slow_rad)/t_spindown *
time_new; % rad/s
G_new = 1/9.81 * sqrt((cent_vel_stop.^2 * cent_rad).^2 + 9.81^2); % G-level, G's

a_cent_new = sqrt(G_new.^2 - 1);           % centripetal acceleration, G's
theta_new = 180/pi*atan(a_cent_new/1);     % roll angle of centrifuge with respect to vertical

time = [time; time(end)+time_new];
G = [G; G_new];
theta = [theta; theta_new];

%% Calculate at the end
a_cent = sqrt(G.^2 - 1);           % centripetal acceleration, G's
cent_vel_rad = sqrt(a_cent*9.81/cent_rad); % centrifuge spin rate, rad/s
cent_vel = (60/(2*pi)) * cent_vel_rad; % centrifuge spin rate, rpm

pitch = zeros(length(theta),1);
roll = theta;
output = [cent_vel roll pitch];

% dlmwrite(filename, output, 'delimiter', '\t');

```

```

%% Plot
figure
subplot(5,1,1); plot(time, G); ylabel('G-level magnitude (Gs)')
% subplot(4,1,2); plot(time, a_cent); ylabel('Centripetal acceleration (Gs)')
subplot(5,1,2); plot(time, cent_vel); ylabel('Centrifuge Angular Velocity (rpm)')
subplot(5,1,3); plot(time, roll); ylabel('Cab Roll Angle (degrees)')
subplot(5,1,4); plot(time(2:end), diff(roll)/dt); ylabel('Cab Roll Vel (deg/s)')
subplot(5,1,5); plot(time(3:end), diff(roll,2)/(dt^2)); ylabel('Cab Roll Acc (deg/s^2)')

figure
subplot(2,1,1); plot(time/60, G, 'LineWidth', 2);
ylabel('G-Level Magnitude (Gs)'); axis([time(1) time(end)/60 0.8 2.1])

subplot(2,1,2); plot(time/60, theta_baseline+0*time, 'r--', time/60, theta, 'LineWidth', 2);
ylabel('Cab Roll Angle (degrees)'); axis([time(1) time(end)/60 -45 90]);
xlabel('Time [minutes]');

```

Code to create a somatosensory indicator training profile for Experiment 1 (see Figure 12 for an example) is provided below. The “output” variable contains the required information for a “Space mode” profile on the NASTAR ATFS-400. The first column of output is the commanded planetary spin rate of the centrifuge in rotations per minute (in this case 0 rpm). The second column is the commanded roll angle, relative to Earth vertical, of the centrifuge cab in degrees. The third column is the commanded pitch angle and for this experiment is always set to zero. Each row is the set of the commanded values at an instant in time which the time step between successive rows fixed at 0.01 seconds. The “output” variable should be copied into a .txt file and saved. Then on the ATFS-400 computer system the file type should be converted to a .space file by renaming the file from “Example.txt” to “Example.space”. These .space files are then loaded for experimentation. The naming convention, if trying to use previously saved files, is “MIT\_SomatTrain\_‘Number’.space”, so for example the second profile would be “MIT\_SomatTrain\_1.space”.

```

clc; clear all; close all

%% This program calculates a psuedorandom sum-of-sines roll angle profile
%% to be used as inputs for the NASTAR ATFS-400 centrifuge

%% User Inputs
dt = 0.01; % sec, time step
freq = [0.061, 0.134, 0.278]; % frequencies of sin waves in Hz
phase = [0 111 259]; % phase angles of sin waves in degrees
amp = [15 15 15]; % amplitudes of sin waves in degrees
t_tot = 60; % total time of profile in seconds
t_acc = 10; % start up time in seconds
t_dec = 5; % slow down time

% offset = 360*rand(1);
offset = 2*pi*rand(1);

%% Calculations
time = [0:dt:t_tot]'; % time vector, seconds
% Magnitude scalar so that we get a smooth start up and slow down
mag = zeros(length(time), 1); % magnitude gain vector, ranges from 0 to 1
for i = 1:length(time)
    if time(i) <= t_acc
        % start up time
        mag(i) = 1/t_acc*time(i);
    elseif (time(i) > t_acc) && (time(i) <= t_tot-t_dec)
        % steady time
        mag(i) = 1;
    else
        % slow down time
        mag(i) = -1/t_dec*time(i) + 1/t_dec*t_tot;
    end
end
end

```

```

figure
plot(time, mag); xlabel('Time [sec]'); ylabel('Magnitude Gain')

% Sum-of-sines calculation
theta = zeros(length(time), 1);
for i = 1:length(time)
    summation = 0;
    for j = 1:length(freq)
        % sum up all of the sines at each frequency
        summation = summation + amp(j)*sin(2*pi*freq(j)*time(i) + (phase(j)+offset));
    end
    theta(i) = mag(i) * summation;
end

cent_rad = 7.62; % centrifuge radius in m
G = ones(length(time), 1);
a_cent = sqrt(G.^2 - 1); % centripetal acceleration, G's
cent_vel_rad = sqrt(a_cent*9.81/cent_rad); % centrifuge spin rate, rad/s
cent_vel = (60/(2*pi)) * cent_vel_rad; % centrifuge spin rate, rpm

%% Bonus time
extra_time = 10;
end_ang_vel = 2;
time = [time; (time(end)+dt:dt:time(end)+extra_time)'];
cent_vel_end = (dt:dt:extra_time)' * end_ang_vel/extra_time;
cent_vel_end_rad = cent_vel_end * (2*pi/60);

G_new = sqrt(((cent_vel_end_rad.^2 * cent_rad)/9.81).^2 + 1);
a_cent_new = sqrt(G_new.^2 - 1); % centripetal acceleration, G's
theta_new = 180/pi*atan(a_cent_new/1); % roll angle of centrifuge with respect to vertical

cent_vel = [cent_vel; cent_vel_end];
pitch = zeros(length(theta)+extra_time*100,1);
roll = [theta; theta_new];

output = [cent_vel roll pitch];

%% Plot
figure; hold on
plot(time, roll, 'k', 'LineWidth', 2); xlabel('Time [sec]'); ylabel('Roll Angle [degrees]'); title('Example
Roll Motion Profile')
figure
plot(time, cent_vel);
% line([t_acc t_acc], [-sum(amp) sum(amp)], 'LineWidth', 2); line([t_tot-t_dec t_tot-t_dec], [-sum(amp)
sum(amp)], 'LineWidth', 2)
% axis([0 t_tot+t_extra -sum(amp) sum(amp)]); box on;

```

Code to create a verbal training profile for Experiment 1 (see Figure 13 for an example) is provided below. The “output” variable contains the required information for a “Space mode” profile on the NASTAR ATFS-400. The first column of output is the commanded planetary spin rate of the centrifuge in rotations per minute (in this case 0 rpm). The second column is the commanded roll angle, relative to Earth vertical, of the centrifuge cab in degrees. The third column is the commanded pitch angle and for this experiment is always set to zero. Each row is the set of the commanded values at an instant in time which the time step between successive rows fixed at 0.01 seconds. The “output” variable should be copied into a .txt file and saved. Then on the ATFS-400 computer system the file type should be converted to a .space file by renaming the file from “Example.txt” to “Example.space”. These .space files are then loaded for experimentation. The naming convention, if trying to use previously saved files, is

“MIT\_VerbalTrain\_long,space” for the profile with 20 roll angles in it and “MIT\_VerbalTrain\_short.space” for the refresher profile with only 5 roll angles.

```

clc; clear all; close all

%% This program calculates a roll angle profile comprised of a series of 20
%% roll tilts for use on the NASTAR ATFS-400 centrifuge

%% User Inputs
dt = 0.01; % sec, time step
Glevel = 1; % # of G's we want to test at, 1, 1.5, or 2
max_angle = 40;
min_change = 15;

% num_tilts = 5;
num_tilts = 20;

angle = round(2*max_angle*rand(1,num_tilts)-max_angle); % roll angle magnitudes we want to test, deg
for i = 1:num_tilts
    if i >= 2
        % make sure two consecutive angle are at least 15 degrees apart
        while (abs(angle(i)-angle(i-1))<min_change)
            angle(i) = round(2*max_angle*rand(1,1)-max_angle);
        end
    end
end

freq = [0.125]; % acceleration frequencies we want to test, Hz

% angle = [-40]; % roll angle magnitudes we want to test, deg
% freq = [0.25]; % acceleration frequencies we want to test, Hz

cent_rad = 7.62; % centrifuge radius in m

t_spinup = 10; % time allowed for spin up, sec
t_spindown = 0; % time allowed for spin down, sec
t_rest = 0; % time allowed to adjust to G, sec
t_between = 20; % time allowed between tilts

%% Calculations
%% Spin up

% if Glevel == 1.5
% data = xlsread('file.xls');
% elseif Glevel == 2
% data = xlsread('file20.xls');
% end

time = [0:dt:t_spinup]';

G_cent_start = sqrt(Glevel^2-1);
cent_vel_start = sqrt(9.81*G_cent_start/cent_rad)/t_spinup * time;
G = 1/9.81 * sqrt((cent_vel_start.^2 * cent_rad).^2 + 9.81^2);

a_cent = sqrt(G.^2 - 1); % centripetal acceleration, G's
theta = 180/pi*atan(a_cent/1); % roll angle of centrifuge with respect to vertical

%% Wait for subject to adjust
time_new = [time(end)+dt:dt:time(end)+t_rest]';
G_new = G(end)*ones(length(time_new),1);
theta_new = theta(end)*ones(length(time_new),1);

time = [time; time_new];
G = [G; G_new];

theta = [theta; theta_new];

%% Perform the 12 roll tilts
theta_baseline = theta(end);

% Concatenate list of angles and freq's together
freq_vect = [];
for i = 1:length(angle)
    freq_vect = [freq_vect freq];

```



```

end
angle_vect = [];
for i = 1:length(freq)
    angle_vect = [angle_vect angle];
end

freq_rand = freq_vect;
angle_rand = angle_vect;

for i = 1:length(freq_rand)
    % Perform a roll over
    T = 1/freq_rand(i);
    if i == 1
        theta_i = 0;
    else
        theta_i = angle_rand(i-1);
    end
    theta_f = angle_rand(i);
    t = [dt:dt:T]';
    A = 2*pi*(theta_f-theta_i)/(T^2);
    for j = 1:length(t)
        theta_new = A*T/(2*pi) * (t-T/(2*pi))*sin(2*pi*t/T) + theta_i;
    end
    time = [time; t+time(end)];
    theta = [theta; theta_new+theta_baseline];

    % Wait for the time in between
    t_wait = [(time(end)+dt:dt:time(end)+t_between)]';
    time = [time; t_wait];
    theta = [theta; theta(end)*ones(length(t_wait),1)];

    % Update the G vector
    G_new = G(end)*ones(length(t)+length(t_wait),1);
    G = [G; G_new];
end

% Roll back
A = 2*pi*(theta(end))/(T^2);
for j = 1:length(t)
    theta_new = theta(end) - A*T/(2*pi) * (t-T/(2*pi))*sin(2*pi*t/T);
end
time_new = time(end)+t;
time = [time; time_new];
theta = [theta; theta_new];
% Update the G vector
G_new = G(end)*ones(length(t),1);
G = [G; G_new];

%% Spin down
time_new = [dt:dt:t_spinup]';

cent_vel_slow = 2; % rpm
cent_vel_slow_rad = cent_vel_slow * (2*pi/60); % rad/s
cent_vel_stop = cent_vel_start(end) - (sqrt(9.81*G_cent_start/cent_rad)-cent_vel_slow_rad)/t_spinup * time_new;
% rad/s
G_new = 1/9.81 * sqrt((cent_vel_stop.^2 * cent_rad).^2 + 9.81^2); % G-level, G's

a_cent_new = sqrt(G_new.^2 - 1); % centripetal acceleration, G's
theta_new = 180/pi*atan(a_cent_new/1); % roll angle of centrifuge with respect to vertical

time = [time; time(end)+time_new];
G = [G; G_new];
theta = [theta; theta_new];

%% Calculate at the end
a_cent = sqrt(G.^2 - 1); % centripetal acceleration, G's
cent_vel_rad = sqrt(a_cent*9.81/cent_rad); % centrifuge spin rate, rad/s
cent_vel = (60/(2*pi)) * cent_vel_rad; % centrifuge spin rate, rpm

pitch = zeros(length(theta),1);
roll = theta;
output = [cent_vel roll pitch];

%% Plot
figure
subplot(4,1,1); plot(time, G); ylabel('G-level magnitude (Gs)')
subplot(4,1,2); plot(time, a_cent); ylabel('Centripetal acceleration (Gs)')
subplot(4,1,3); plot(time, cent_vel); ylabel('Centrifuge Angular Velocity (rpm)')
subplot(4,1,4); plot(time, roll); ylabel('Cab Roll Angle (degrees)')

figure

```

```

subplot(2,1,1); plot(time/60, G, 'LineWidth', 2);
ylabel('G-Level Magnitude (Gs)'); axis([time(1) time(end)/60 0.8 2.1])

subplot(2,1,2); plot(time/60, theta_baseline+0*time, 'r--', time/60, theta, 'LineWidth', 2);
ylabel('Cab Roll Angle (degrees)'); axis([time(1) time(end)/60 -45 90]);
xlabel('Time [minutes]');

```

Code to create a G-Exposure profile for Experiment 1 (see Figure 13 for an example) is provided below. The “output” variable contains the required information for a “Space mode” profile on the NASTAR ATFS-400. The first column of output is the commanded planetary spin rate of the centrifuge in rotations per minute. The second column is the commanded roll angle, relative to Earth vertical, of the centrifuge cab in degrees. The third column is the commanded pitch angle and for this experiment is always set to zero. Each row is the set of the commanded values at an instant in time which the time step between successive rows fixed at 0.01 seconds. The “output” variable should be copied into a .txt file and saved. Then on the ATFS-400 computer system the file type should be converted to a .space file by renaming the file from “Example.txt” to “Example.space”. These .space files are then loaded for experimentation. The naming convention, if trying to use previously saved files, is “MIT\_GExposure\_1520.space” for the profile that first exposes 1.5 G’s and then 2.0 G’s.

```

clc; clear all; close all

%% This program calculates a profile for G-Exposure for use on the NASTAR
%% ATFS-400 centrifuge

%% User Inputs
dt = 0.01; % sec, time step
% Glevel = 1.5; % # of G's we want to test at, 1, 1.5, or 2
% Glevel2 = 2;
Glevel = [1.5 2];

cent_rad = 7.62; % centrifuge radius in m

t_spinup = 60; % time allowed for spin up, sec
t_spindown = 60; % time allowed for spin down, sec
t_rest = 120; % time allowed to adjust to G, sec

%% Calculations
%% Spin up
time = [0:dt:t_spinup]';

G_cent_start = sqrt(Glevel(1)^2-1);
cent_vel_start = sqrt(9.81*G_cent_start/cent_rad)/t_spinup * time;
G = 1/9.81 * sqrt((cent_vel_start.^2 * cent_rad).^2 + 9.81^2);

a_cent = sqrt(G.^2 - 1); % centripetal acceleration, G's
theta = 180/pi*atan(a_cent/1); % roll angle of centrifuge with respect to vertical

%% Wait for subject to adjust
time_new = [time(end)+dt:dt:time(end)+t_rest]';
G_new = G(end)*ones(length(time_new),1);
theta_new = theta(end)*ones(length(time_new),1);

time = [time; time_new];
G = [G; G_new];

theta = [theta; theta_new];
theta_baseline = theta(end);

if length(Glevel) > 1
    %% Spin up more
    time_new = [dt:dt:t_spinup]';

    G_cent_start2 = sqrt(Glevel(2)^2-1);
    cent_vel_start = (sqrt(9.81*G_cent_start2/cent_rad)-sqrt(9.81*G_cent_start/cent_rad))/t_spinup * time_new +
cent_vel_start(end);
    G_new = 1/9.81 * sqrt((cent_vel_start.^2 * cent_rad).^2 + 9.81^2);

```

```

a_cent_new = sqrt(G_new.^2 - 1); % centripetal acceleration, G's
theta_new = 180/pi*atan(a_cent_new/1); % roll angle of centrifuge with respect to vertical

time = [time; time(end)+time_new];
G = [G; G_new];
theta = [theta; theta_new];

%% Wait for subject to adjust
time_new = [time(end)+dt:dt:time(end)+t_rest]';
G_new = G(end)*ones(length(time_new),1);
theta_new = theta(end)*ones(length(time_new),1);

time = [time; time_new];
G = [G; G_new];

theta = [theta; theta_new];
theta_baseline = theta(end);
end

%% Spin down
time_new = [dt:dt:t_spinup]';

cent_vel_slow = 2; % rpm
cent_vel_slow_rad = cent_vel_slow * (2*pi/60); % rad/s
if length(Glevel) > 1
    cent_vel_stop = cent_vel_start(end) - (sqrt(9.81*G_cent_start2/cent_rad)-cent_vel_slow_rad)/t_spinup *
time_new; % rad/s
else
    cent_vel_stop = cent_vel_start(end) - (sqrt(9.81*G_cent_start/cent_rad)-cent_vel_slow_rad)/t_spinup *
time_new; % rad/s
end
G_new = 1/9.81 * sqrt((cent_vel_stop.^2 * cent_rad).^2 + 9.81^2); % G-level, G's

a_cent_new = sqrt(G_new.^2 - 1); % centripetal acceleration, G's
theta_new = 180/pi*atan(a_cent_new/1); % roll angle of centrifuge with respect to vertical

time = [time; time(end)+time_new];
G = [G; G_new];
theta = [theta; theta_new];

%% Calculate at the end
a_cent = sqrt(G.^2 - 1); % centripetal acceleration, G's
cent_vel_rad = sqrt(a_cent*9.81/cent_rad); % centrifuge spin rate, rad/s
cent_vel = (60/(2*pi)) * cent_vel_rad; % centrifuge spin rate, rpm

pitch = zeros(length(theta),1);
roll = theta;
output = [cent_vel roll pitch];

%% Plot
figure
subplot(4,1,1); plot(time, G); ylabel('G-level magnitude (Gs)')
subplot(4,1,2); plot(time, a_cent); ylabel('Centripetal acceleration (Gs)')
subplot(4,1,3); plot(time, cent_vel); ylabel('Centrifuge Angular Velocity (rpm)')
subplot(4,1,4); plot(time, roll); ylabel('Cab Roll Angle (degrees)')

figure
subplot(2,1,1); plot(time/60, G, 'LineWidth', 2);
ylabel('G-Level Magnitude (Gs)'); axis([time(1) time(end)/60 0.8 2.1])

subplot(2,1,2); plot(time/60, theta_baseline+0*time, 'r--', time/60, theta, 'LineWidth', 2);
ylabel('Cab Roll Angle (degrees)'); axis([time(1) time(end)/60 -45 90]);
xlabel('Time [minutes]');

```

#### **D. Differences between Cross-Coupled Adaptation and Centrifuge Paradigms**

The Coriolis cross-coupled adaptation protocol was designed to stimulate the cross-coupled illusion in a similar manner as the most extreme stimulus experienced during hyper-gravity testing sessions on the centrifuge. In particular, the pre- and post- tests during the adaptation protocol were performed at the same planetary rotation rate as the maximum centrifuge spin rate experienced during testing (e.g. 14.26 rpm or 85.56 deg/sec for the 2 G sessions). All of the tilts in both scenarios were roll tilts and the head tilts performed during training were 40 degrees to match the maximum tilt tested on the centrifuge. As on the centrifuge, all adaptation rotations were either from upright to a specific angle or from an angle back to upright; there were no rotations between different non-upright angles. The intention of these similarities was to expose and adapt subjects to the cross-coupled stimulus as they might experience during testing, without pre-exposing them to the hyper-gravity environment.

However, there were several differences between the testing and adaptation sessions that could not be, or were not, replicated. First, all of the roll tilts during adaptation were active head-on-body tilts, while those during the experiment were passive whole-body rotations. We aimed to drive adaptation quickly and active tilts are known to enhance adaptation compared to passive rotations. Also, the roll tilts were performed in roughly one second whereas the fastest rotation during testing occurred over four seconds (0.25 Hz). We found subjects struggled to make smooth, active head tilts at a slow enough rate to match four seconds. Note that a faster rotation will elicit a stronger cross-coupled stimulus, so the adaptation training was more provocative than even the most extreme case during testing. Finally, it was not possible to match the paradigms in terms of orientation relative to the planetary rotation and the direction of the net gravito-inertial force. During testing, the centrifuge rotation axis was Earth-vertical, but the direction of the net gravito-inertial force was rotated away from vertical (48.19 degrees for 1.5 G, and 60 degrees for 2 G). The roll tilts were perpendicular to both the centrifuge rotation axis and the gravito-inertial direction, but started from an orientation aligned with the net gravito-inertial. In the adaptation training, without any centrifugation, the planetary rotation axis and the gravito-inertial direction were aligned and thus all roll tilts started from an orientation aligned with *both*. While we do not believe this to be a significant difference, it is worth noting that the two paradigms will cause the cross-coupled illusion to stimulate different canals. During adaptation training, we could have started subjects tilted off of upright such that we matched the exact canal stimulation of one of the hyper-gravity testing paradigms (1.5 or 2 G, since the two level has different baseline tilts), but then subjects' orientation relative to the net gravito-inertial direction would have been different than in centrifuge testing. We believe otolith feedback, dependent upon orientation relative to gravito-inertial direction, is critical to the adaptation process so we selected to match the orientation relative to gravity instead of relative to the planetary rotation axis.


## E. Forms for Experiment 1

**MIT** Committee On the Use of Humans as  
Experimental Subjects

MASSACHUSETTS INSTITUTE OF TECHNOLOGY  
77 Massachusetts Avenue  
Cambridge, Massachusetts 02139  
Building E 25-143B  
(617) 253-6787

---

**To:** Laurence Young  
37-219

**From:** Leigh Finn, Chair  
COUHES 

**Date:** 12/21/2011

**Committee Action:** Approval

**COUHES Protocol #:** 1111004764

**Study Title:** Human Orientation Perception during Vehicle Role Tilt in Hyper-Gravity

**Expiration Date:** 12/14/2012

The above-referenced protocol has been APPROVED following Full Board Review by the Committee on the Use of Humans as Experimental Subjects (COUHES).

If the research involves collaboration with another institution then the research cannot commence until COUHES receives written notification of approval from the collaborating institution's IRB.

It is the Principal Investigator's responsibility to obtain review and continued approval before the expiration date. Please allow sufficient time for continued approval. You may not continue any research activity beyond the expiration date without COUHES approval. Failure to receive approval for continuation before the expiration date will result in the automatic suspension of the approval of this protocol. Information collected following suspension is unapproved research and cannot be reported or published as research data. If you do not wish continued approval, please notify the Committee of the study termination.

**Adverse Events:** Any serious or unexpected adverse event must be reported to COUHES within 48 hours. All other adverse events should be reported in writing within 10 working days.

**Amendments:** Any changes to the protocol that impact human subjects, including changes in experimental design, equipment, personnel or funding, must be approved by COUHES before they can be initiated.

Prospective new study personnel must, where applicable, complete training in human subjects research and in the HIPAA Privacy Rule before participating in the study.

COUHES should be notified when your study is completed. You must maintain a research file for at least 3 years after completion of the study. This file should include all correspondence with COUHES, original signed consent forms, and study data.

---

**To:** Laurence Young  
37-219

**From:** Leigh Fim, Chair  
COUHES

**Date:** 10/24/2012

**Committee Action:** Amendment to Approved Protocol

**COUHES Protocol #:** 1111004764

**Study Title:** Human Orientation Perception during Vehicle Role Tilt in Hyper-Gravity

**Expiration Date:** 12/14/2012

The amendment to the above-referenced protocol has been APPROVED following expedited review by the Committee on the Use of Humans as Experimental Subjects (COUHES).

This approval covers the following change(s)/modification(s):

-The Man-Vehicle Laboratory (MVL) Short-Radius Centrifuge (SRC) will be used to complete the protocol due to the GyroFlight simulator undergoing repairs for an extended period of time. The actual protocol will not be changed, only the device used to complete the protocol.

If the research involves collaboration with another institution then the research cannot commence until COUHES receives written notification of approval from the collaborating institution's IRB.

It is the Principal Investigator's responsibility to obtain review and continued approval before the expiration date. Please allow sufficient time for continued approval. You may not continue any research activity beyond the expiration date without COUHES approval. Failure to receive approval for continuation before the expiration date will result in the automatic suspension of the approval of this protocol. Information collected following suspension is unapproved research and cannot be reported or published as research data. If you do not wish continued approval, please notify the Committee of the study termination.

**Adverse Events:** Any serious or unexpected adverse event must be reported to COUHES within 48 hours. All other adverse events should be reported in writing within 10 working days.

**Amendments:** Any changes to the protocol that impact human subjects, including changes in experimental design, equipment, personnel or funding, must be approved by COUHES before they can be initiated.

Prospective new study personnel must, where applicable, complete training in human subjects research and in the HIPAA Privacy Rule before participating in the study.

COUHES should be notified when your study is completed. You must maintain a research file for at least 3 years after completion of the study. This file should include all correspondence with COUHES, original signed consent forms, and study data.

**APPENDIX C**  
**ETC / NASTAR CENTER INSTITUTIONAL REVIEW BOARD CHECKLIST**

ETC / NASTAR Center Institutional Review Board Checklist

Experiment Title: Human Orientation Perception during Vehicle Roll Tilt in Hyper-Gravity  
Date: June 28, 2012

Requirements for approval:

- X\_\_\_ Risks to subjects have been minimized.
- X\_\_\_ Risks to subjects are reasonable in relation to anticipated benefits.
- X\_\_\_ Selection of subjects is equitable. Vulnerable populations are not unduly at risk.
- X\_\_\_ Appropriate safeguards have been included to protect the rights, welfare, and safety of any test subjects that are likely to be vulnerable to coercion or undue influence.
- X\_\_\_ Voluntary informed consent will be sought.
- X\_\_\_ Informed consent is properly documented. The description of the experiment and risks is clear, accurate, and complete.
- X\_\_\_ The IRB's legal advisor has reviewed the informed consent statement and concurred with its contents.
- X\_\_\_ Experimental procedures include adequate provisions for monitoring and assuring the health and safety of test subjects.
- X\_\_\_ Adequate provisions exist for protecting the privacy of information about test subjects and the confidentiality of data.
- X\_\_\_ Any ethical issues and financial conflicts of interest involving the Investigators have been addressed.
- X\_\_\_ The Investigators have completed the required training.

Considerations:

- Yes\_\_ Will a member of the IRB participate in: (a) a dry-run or demonstration of the test protocol; or (b) witness testing of the first test subject?
- Yes\_\_ Will the IRB monitor/observe testing or conduct future reviews of this experiment? If yes, define: Paul Comtois will periodically monitor testing and report to the IRB.
- Yes\_\_ Has the IRB visited the test facility and viewed the test equipment?
- Yes\_\_ Have representatives of the IRB inspected the test facility and test equipment?
- Yes\_\_ Have the facility and/or test equipment been previously approved by the IRB or used in experiments previously approved by the IRB? The facility has. The ATFS-400 ahs not been previously approved.

IRB Action

- Proposal approved as presented
- Proposal approved (specific IRB recommended changes were incorporated).  
Note: All IRB recommended changes incorporated and reviewed by the IRB. Final approval was issued on June 28, 2012.
- Proposal tabled pending response to IRB concerns or request for more information
- Proposal disapproved

Vote: For 9 \_\_\_ Against 0 \_\_\_ Abstained \_\_\_

Environmental Tectonics Corporation  
IRB Guidelines  
November 24, 2010

C-1





## Scoring the MSSQ- Short

### Section A (Child) (Question 3)

Score the number of types of transportation not experienced (i.e., total the number of ticks in the 't' column, maximum is 9).

Total the sickness scores for each mode of transportation, i.e. the nine types from 'cars' to 'big dippers' (use the 0-3 number score key at bottom, those scores in the 't' column count as zeroes).

$$MSA = (\text{total sickness score child}) \times (9) / (9 - \text{number of types not experienced as a child})$$

*Note 1.* Where a subject has not experienced any forms of transport a division by zero error occurs. It is not possible to estimate this subject's motion sickness susceptibility in the absence of any relevant motion exposure.

*Note 2.* The Section A (Child) score can be used as a pre-morbid indicator of motion sickness susceptibility in patients with vestibular disease.

### Section B (Adult) (Question 4)

Repeat as for section A but using the data from section B.

$$MSB = (\text{total sickness score adult}) \times (9) / (9 - \text{number of types not experienced as an adult})$$

### Raw Score MSSQ-Short

Total the section A (Child) MSA score and the section B (Adult) MSB score to give the MSSQ-Short raw score (possible range from minimum 0 to maximum 54, the maximum being unlikely)

$$\text{MSSQ raw score} = \text{MSA} + \text{MSB}$$

### Percentile Score MSSQ-Short

The raw to percentile conversions are given below in the Table of Statistics & Figure, use interpolation where necessary.

Alternatively a close approximation is given by the fitted polynomial where y is percentile; x is raw score  
 $y = a.x + b.x^2 + c.x^3 + d.x^4$

$$\begin{aligned} a &= 5.1160923 & b &= -0.055169904 \\ c &= -0.00067784495 & d &= 1.0714752e-005 \end{aligned}$$

Table of Means and Percentile Conversion Statistics for the MSSQ-Short (n=257)

Percentiles Conversion	Raw Scores MSSQ-Short		
	Child Section A	Adult Section B	Total A+B
0	0	0	0
10	.0	.0	.8
20	2.0	1.0	3.0
30	4.0	1.3	7.0
40	5.6	2.6	9.0
50	7.0	3.7	11.3
60	9.0	6.0	14.1
70	11.0	7.0	17.9
80	13.0	9.0	21.6
90	16.0	12.0	25.9
95	20.0	15.0	30.4
100	23.6	21.0	44.6
Mean	7.75	5.11	12.90
Std. Deviation	5.94	4.84	9.90

Table note: numbers are rounded

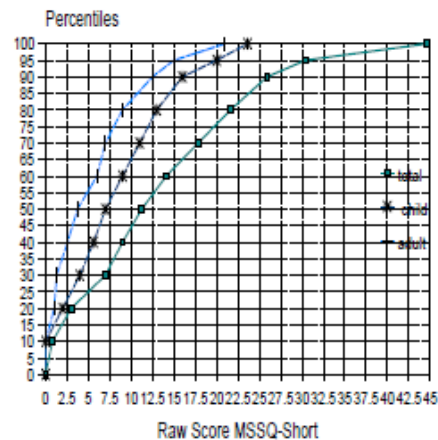


Figure: Cumulative distribution Percentiles of the Raw Scores of the MSSQ-Short (n=257 subjects).

### Reference Note

For more background information and references to the original Reason & Brand MSSQ and to its revised version the 'MSSQ-Long', see:

Golding JF. Motion sickness susceptibility questionnaire revised and its relationship to other forms of sickness. *Brain Research Bulletin*, 1998; 47: 507-516.

Golding JF. (2006) Predicting Individual Differences in Motion Sickness Susceptibility by Questionnaire.

*Personality and Individual Differences*, 41: 237-248.



**IMPORTANT NOTICE AND DISCLAIMER**

Certain simulators and training devices used in the NASTAR Center may expose participants to gravitational forces (G-forces), motions, and simulated altitudes similar to those experienced during actual flight by astronauts and jet fighter pilots. G-forces, motions, and simulated altitudes can cause some individuals to experience symptoms of motion sickness, altitude sickness, claustrophobia and/or other disorientating effects.

Accordingly, you should NOT PARTICIPATE in any NASTAR Center training, experiences, or activities if you have any of the following conditions. Please check all that apply.

- | YES                                 | NO                                  |  |
|-------------------------------------|-------------------------------------|--|
| <input checked="" type="checkbox"/> | <input checked="" type="checkbox"/> | <del>Otitis, sinusitis, bronchitis, asthma, or other respiratory disorders.</del>  |
| <input checked="" type="checkbox"/> | <input checked="" type="checkbox"/> | <del>Dizziness or vertigo.</del>   |
| <input checked="" type="checkbox"/> | <input checked="" type="checkbox"/> | <del>Fainting spells, or any other loss of consciousness.</del>  |
| <input checked="" type="checkbox"/> | <input checked="" type="checkbox"/> | <del>Seizures.</del>   |
| <input checked="" type="checkbox"/> | <input checked="" type="checkbox"/> | <del>Tuberculosis.</del>   |
| <input checked="" type="checkbox"/> | <input checked="" type="checkbox"/> | <del>Recent significant trauma (broken bones, concussions, poisonings, etc.)</del>   |
| <input checked="" type="checkbox"/> | <input checked="" type="checkbox"/> | <del>History of decompression syndrome (DCS).</del>  |
| <input checked="" type="checkbox"/> | <input checked="" type="checkbox"/> | <del>SCUBA Diving within the past 24 hours.</del>  |
| <input checked="" type="checkbox"/> | <input checked="" type="checkbox"/> | <del>Anemia or other blood disorders.</del>  |
| <input checked="" type="checkbox"/> | <input checked="" type="checkbox"/> | <del>Heart or circulatory disorders, implanted devices, stents.</del>  |
| <input checked="" type="checkbox"/> | <input checked="" type="checkbox"/> | <del>Mental disorder, treatment or medications for depression.</del>   |
| <input checked="" type="checkbox"/> | <input checked="" type="checkbox"/> | <del>Claustrophobia.</del>   |
| <input checked="" type="checkbox"/> | <input checked="" type="checkbox"/> | <del>Alcohol or drug dependence or abuse.</del>  |
| <input checked="" type="checkbox"/> | <input checked="" type="checkbox"/> | <del>Currently pregnant, or recently post-partum (less than 6 weeks), or if you have recently spontaneously or voluntarily terminated a pregnancy.</del> |
| <input checked="" type="checkbox"/> | <input checked="" type="checkbox"/> | <del>Diabetes.</del>   |
| <input checked="" type="checkbox"/> | <input checked="" type="checkbox"/> | <del>Cancer.</del>   |
| <input checked="" type="checkbox"/> | <input checked="" type="checkbox"/> | <del>Acid Reflux disorder, treated or untreated.</del>   |

Additionally, the NASTAR Center may require details and a recommendation from your personal physician, or an Aero Medical Examiner (AME) regarding any of the following conditions before a determination can be made if you can participate in any of the NASTAR Center training programs or experiences.

- | YES                                 | NO                                  |  |
|-------------------------------------|-------------------------------------|--|
| <input checked="" type="checkbox"/> | <input checked="" type="checkbox"/> | <del>Acid reflux disorder, treated or untreated.</del>   |
| <input checked="" type="checkbox"/> | <input checked="" type="checkbox"/> | <del>Borderline Hypertension, treated or untreated.</del>  |
| <input checked="" type="checkbox"/> | <input checked="" type="checkbox"/> | <del>Surgery and other hospital admissions within the past 5 years.</del><br>(Please state reason for admission). _____                                    |
| <input checked="" type="checkbox"/> | <input checked="" type="checkbox"/> | <del>Visits to physicians (other than regular checkups &amp; physicals) in the last 3 years.</del><br>(Please state nature and reason for visit(s)). _____ |
| <input checked="" type="checkbox"/> | <input checked="" type="checkbox"/> | <del>Previously attempted suicide.</del>   |
| <input checked="" type="checkbox"/> | <input checked="" type="checkbox"/> | <del>Use of prescription medications.</del><br>(Please state medication(s)). _____   |
| <input checked="" type="checkbox"/> | <input checked="" type="checkbox"/> | <del>Previously rejected for life or health insurance.</del><br>(Please state reason for rejection). _____   |

Persons having any health concerns regarding their suitability to participate in NASTAR Center training and activities should obtain their personal physician's approval, since the NASTAR Center does not assume any responsibility in this regard.

I HAVE READ THIS RELEASE AND WAIVER OF LIABILITY, ASSUMPTION OF RISK AND INDEMNITY AGREEMENT, FULLY UNDERSTAND ITS TERMS, UNDERSTAND THAT I HAVE GIVEN UP SUBSTANTIAL RIGHTS BY SIGNING IT, AND HAVE SIGNED IT FREELY AND VOLUNTARILY WITHOUT ANY INDUCEMENT, ASSURANCE OR GUARANTEE BEING MADE TO ME AND INTEND MY SIGNATURE TO BE A COMPLETE AND UNCONDITIONAL RELEASE OF ALL LIABILITY TO THE GREATEST EXTENT ALLOWED BY LAW.

Signature: \_\_\_\_\_ Date: \_\_\_\_\_  
Print Name: \_\_\_\_\_



**RELEASE AND WAIVER OF LIABILITY,  
ASSUMPTION OF RISK AND IDEMNITY AGREEMENT**

IN CONSIDERATION of being permitted to participate in any NASTAR Center activities or being permitted to enter for any purpose any RESTRICTED AREA (defined as any area requiring special authorization, credentials, or permission to enter or any area to which admission by the general public is restricted or prohibited, including but not limited to NASTAR Center Training areas, classrooms and equipment), I, the undersigned, for myself, my personal representatives, assigns, heirs, and next of kin:

1. ACKNOWLEDGE, agree and represent that I am qualified, in good health, and in proper physical condition to participate in NASTAR Center activities. \_\_\_\_\_(initials)
2. FULLY UNDERSTAND that: (a) NASTAR CENTER ACTIVITIES (Centrifuge rides at elevated, sustained G; altitude chamber experiences at lower than normal atmospheric pressure; motion simulator experiences that involve sustained motions in the axes of pitch, roll, and yaw) INVOLVE AND PRESENT RISKS AND DANGERS OF SERIOUS BODILY INJURY, INCLUDING PERMANENT DISABILITY, PARALYSIS AND DEATH ("RISKS"); (b) these RISKS may be caused by my own actions, or inactions, the actions or inactions of others participating in the ACTIVITIES, or the condition in which the ACTIVITIES takes place; (c) there may be OTHER RISKS AND SOCIAL AND ECONOMIC LOSSES either not known to me or not readily foreseeable at this time; and I FULLY ACCEPT AND ASSUME ALL SUCH RISKS AND ALL RESPONSIBILITY FOR LOSSES, COSTS, AND DAMAGES I incur as a result of my participation in the ACTIVITIES. \_\_\_\_\_(initials)
3. HEREBY RELEASE, WAIVE, DISCHARGE AND COVENANT NOT TO SUE the NASTAR Center or its administrators, directors, agents, officers, members, volunteers, and employees, and any other participants, sponsors, advertisers, and owners and lessors of premises on which the ACTIVITIES take place, (each considered one of the "RELEASEES" herein) all for the purpose herein referred to as "RELEASEES," FROM ALL LIABILITY TO THE UNDERSIGNED, his/her personal representatives, assigns, heirs, and next of kin FOR ANY AND ALL LOSS OR DAMAGES, AND ANY CLAIM OR DEMANDS THEREFOR, ON ACCOUNT OF INJURY TO THE PERSON OR PROPERTY OR RESULTING IN DEATH OF THE UNDERSIGNED, WHETHER CAUSED BY THE NEGLIGENCE OR GROSS NEGLIGENCE OF THE RELEASEES OR OTHERWISE WHILE THE UNDERSIGNED IS UPON THE RESTRICTED AREA. \_\_\_\_\_(initials)
4. HEREBY AGREE TO INDEMNIFY AND SAVE AND HOLD HARMLESS the RELEASEES and each of them FROM ANY LOSS, LIABILITY, DAMAGE, OR COST they may incur arising out of or related to the ACTIVITIES WHETHER CAUSED BY THE NEGLIGENCE OR GROSS NEGLIGENCE OF THE RELEASEES OR OTHERWISE, including, but not limited to, indemnification from the cost of any litigation expenses, attorney fees, loss, liability, damage, or cost which may be incurred as the result of such claim. \_\_\_\_\_(initials)
5. HEREBY enter into NASTAR Center premises and ACTIVITIES voluntarily and ASSUME FULL RESPONSIBILITY FOR ANY RISK OF BODILY INJURY, DEATH OR PROPERTY DAMAGE arising out of or related to the EVENT(S) whether caused by the NEGLIGENCE OR GROSS NEGLIGENCE OF RELEASEES or otherwise. \_\_\_\_\_(initials)
6. HEREBY acknowledge that THE ACTIVITIES MAY BE VERY DANGEROUS and involve the risk of serious injury and/or death and/or property damage. I also expressly acknowledge that INJURIES RECEIVED MAY BE COMPOUNDED OR INCREASED BY NEGLIGENT RESCUE OPERATIONS OR PROCEDURES OF THE RELEASEES. \_\_\_\_\_(initials)
7. HEREBY agree that this Release and Waiver of Liability, Assumption of Risk and Indemnity Agreement extends to all acts by the RELEASEES, INCLUDING NEGLIGENT RESCUE OPERATIONS and is intended to be as broad and inclusive as is permitted by the laws of the Commonwealth of Pennsylvania and that if any portion thereof is held invalid, it is agreed that the remaining portion shall, notwithstanding, continue in full legal force and effect. \_\_\_\_\_(initials)

I HAVE READ THIS RELEASE AND WAIVER OF LIABILITY, ASSUMPTION OF RISK AND INDEMNITY AGREEMENT, FULLY UNDERSTAND ITS TERMS, UNDERSTAND THAT I HAVE GIVEN UP SUBSTANTIAL RIGHTS BY SIGNING IT, AND HAVE SIGNED IT FREELY AND VOLUNTARILY WITHOUT ANY INDUCEMENT, ASSURANCE OR GUARANTEE BEING MADE TO ME AND INTEND MY SIGNATURE TO BE A COMPLETE AND UNCONDITIONAL RELEASE OF ALL LIABILITY TO THE GREATEST EXTENT ALLOWED BY LAW.

Signature: \_\_\_\_\_ Date: \_\_\_\_\_

Print Name: \_\_\_\_\_

## Flight and Centrifuge Hours and Experience

---

### Flight Background:

Initial Training: \_\_\_\_\_

Years Flying: \_\_\_\_\_

Years Flying Acrobatics: \_\_\_\_\_

Fight Time: \_\_\_\_\_

Total Acrobatic Time: \_\_\_\_\_

### Flight Experience in the last:

12 months \_\_\_\_\_ hrs \_\_\_\_\_ flights

90 days \_\_\_\_\_ hrs \_\_\_\_\_ flights

30 days \_\_\_\_\_ hrs \_\_\_\_\_ flights

### Centrifuge Background:

Have you ever been on a centrifuge?; \_\_\_\_\_

If so how many times?; \_\_\_\_\_

How many total hours?; \_\_\_\_\_

Did you ever make head movements?; \_\_\_\_\_

How fast were you spinning?; \_\_\_\_\_

Did you become motion sick?; \_\_\_\_\_

Did you vomit?; \_\_\_\_\_

### Experience in the last:

12 months \_\_\_\_\_ hrs

90 days \_\_\_\_\_ hrs

30 days \_\_\_\_\_ hrs

Name: Subject's Name \_\_\_\_\_

Date: \_\_\_\_\_

# Simulator Sickness Questionnaire (SSQ)

Adapted from Robert S. Kennedy and colleagues under various projects. For additional information contact Robert S. Kennedy, RSK Assessment, Inc., 1040 Woodcock Road, Suite 227, Orlando, FL 32803, (407) 894-5090.

## Pre-Exposure Medical Information

1. Are you in your usual state of fitness? YES NO

If not, please indicate the reason:

\_\_\_\_\_

2. Have you been ill in the past week? YES NO

If your answer is yes, please indicate:

a. the nature of your illness (flu, cold, etc.)

b. severity of your illness VERY MILD MILD MODERATE SEVERE VERY SEVERE

c. length of illness: \_\_\_\_\_ days

d. major symptoms:

e. Are you fully recovered? YES NO

3. How much alcohol have you consumed during the past 24 hours?

\_\_\_\_\_ 12 oz cans/bottles of beer \_\_\_\_\_ ounces of wine \_\_\_\_\_ ounces of hard liquor

4. Do you use tobacco products (nicotine) in any form? YES NO

If yes, how much a day? \_\_\_\_\_

4. Please check off all medication you have used in the past 24 hours.

a. NONE

b. sedatives or tranquilizers \_\_\_\_\_

c. aspirin, Tylenol, other analgesics \_\_\_\_\_

d. anti-histamines \_\_\_\_\_

e. decongestants \_\_\_\_\_

f. other (please specify) \_\_\_\_\_

5. How many hours of sleep did you get last night? \_\_\_\_\_ hours

9. Are you colorblind? YES NO

10. Do you need corrective lenses? YES NO

11. What are you wearing today? CONTACTS GLASSES NONE

12. Do you have any known vestibular defect or condition? YES NO

13. Please list any other comments regarding your present physical state which might affect your performance.

\_\_\_\_\_

## POST Exposure SSQ Symptom Checklist

Instructions: Circle how much each symptom below is affecting you right now.

#	Symptom	Severity			
1.	General discomfort	None	Slight	Moderate	Severe
2.	Fatigue	None	Slight	Moderate	Severe
3.	Headache	None	Slight	Moderate	Severe
4.	Eye strain	None	Slight	Moderate	Severe
5.	Difficulty focusing	None	Slight	Moderate	Severe
6.	Salivation increased	None	Slight	Moderate	Severe
7.	Sweating	None	Slight	Moderate	Severe
8.	Nausea	None	Slight	Moderate	Severe
9.	Difficulty concentrating	None	Slight	Moderate	Severe
10.	"Fullness of the head"	None	Slight	Moderate	Severe
11.	Blurred vision	None	Slight	Moderate	Severe
12.	Dizziness with eyes open	None	Slight	Moderate	Severe
13.	Dizziness with eyes closed	None	Slight	Moderate	Severe
14.	*Vertigo	None	Slight	Moderate	Severe
15.	**Stomach awareness	None	Slight	Moderate	Severe
16.	Burping	None	Slight	Moderate	Severe

- \* Vertigo is experienced as a loss of orientation with respect to vertical upright.  
 \*\* Stomach awareness is usually used to indicate a feeling of discomfort which is just short of nausea.

On a scale of 0-10, rate your overall feeling of motion sickness. \_\_\_\_\_  
 0 - no symptoms      1 - any symptom no matter how slight      3 - minimal warmth, fatigue  
 5 - stomach awareness      7 - moderate nausea      9 - incipient vomiting  
 10 - vomiting

On a scale of 0-10, rate your feeling ofvection; that is how much you feel like you are moving. \_\_\_\_\_  
 0 - None      3 - Slight      6 - Moderate      10 - Severe

On a scale of 0-10, rate your average feeling of the cross-coupling illusion that you experience during the last session. \_\_\_\_\_  
 0 - None      10 - as much as during my first head turn

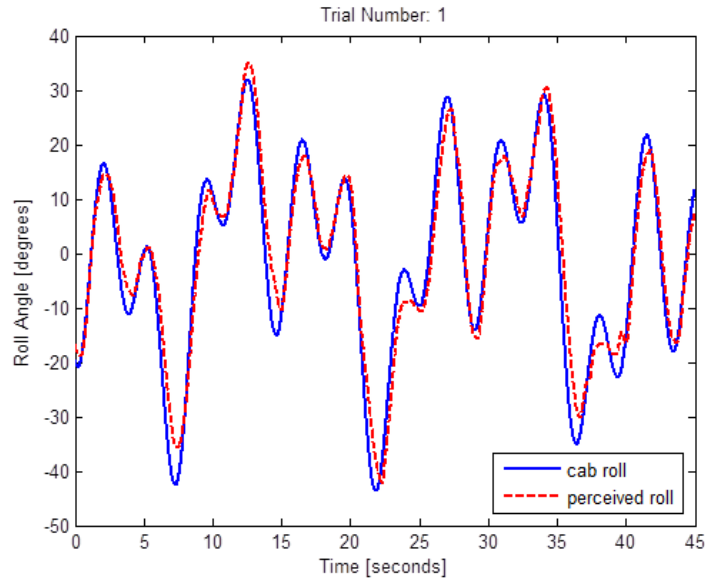
Did the cross-coupled illusion make it more challenging to operate the indicator (YES or NO)? \_\_\_\_\_

Name: Subject's Name Here

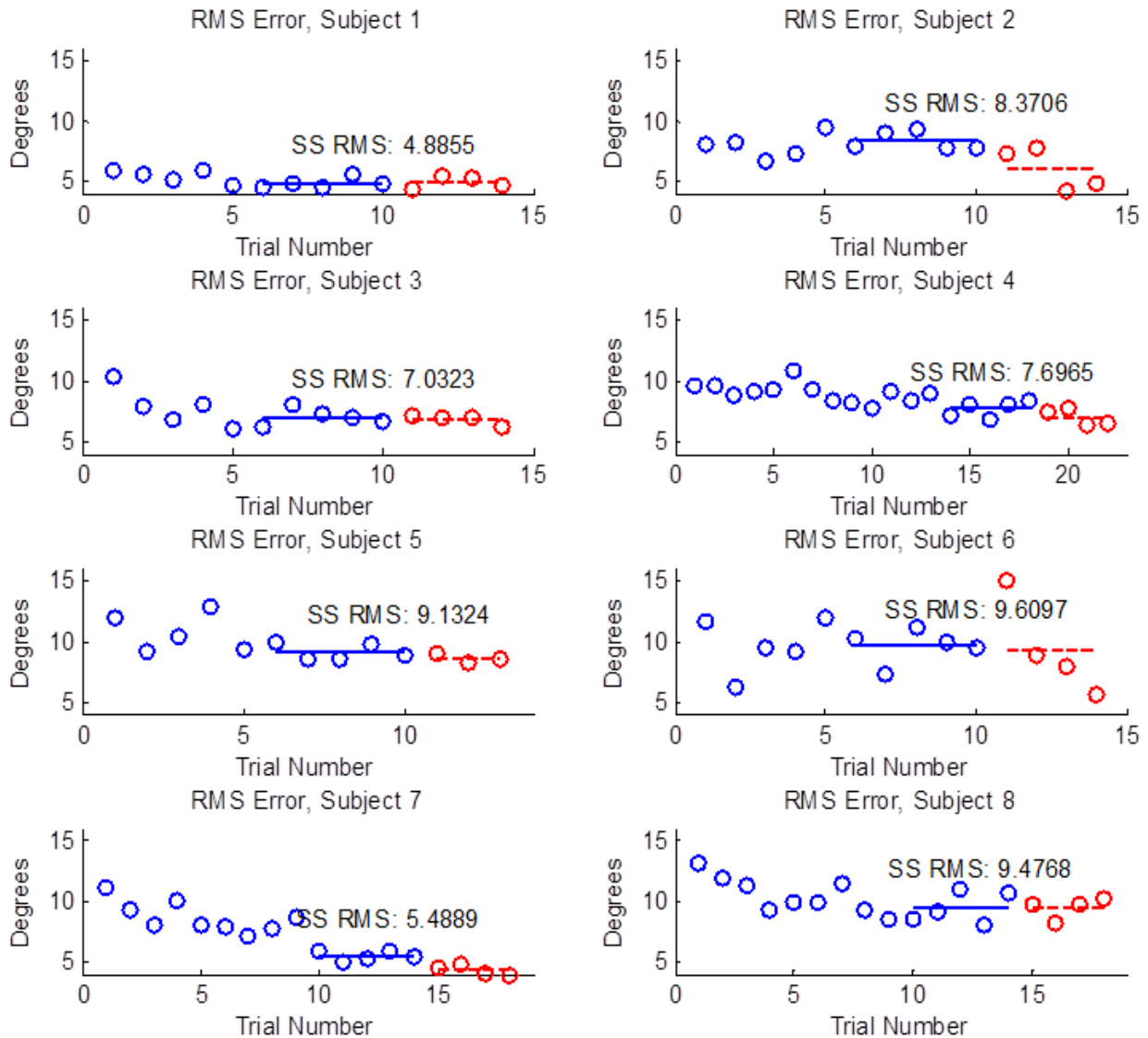
Date: 02 - 14 - 11

## F. Somatosensory Indicator and Verbal Training Data for Experiment 1

As described in Sections 4.1.7, subjects underwent training to use the somatosensory indicator effectively. An example training profile near the end of training is given below. The 10 second start up and 5 second ending times have been removed for graphical purposes. The perceived roll angle accurately tracks the actual vehicle roll angle.



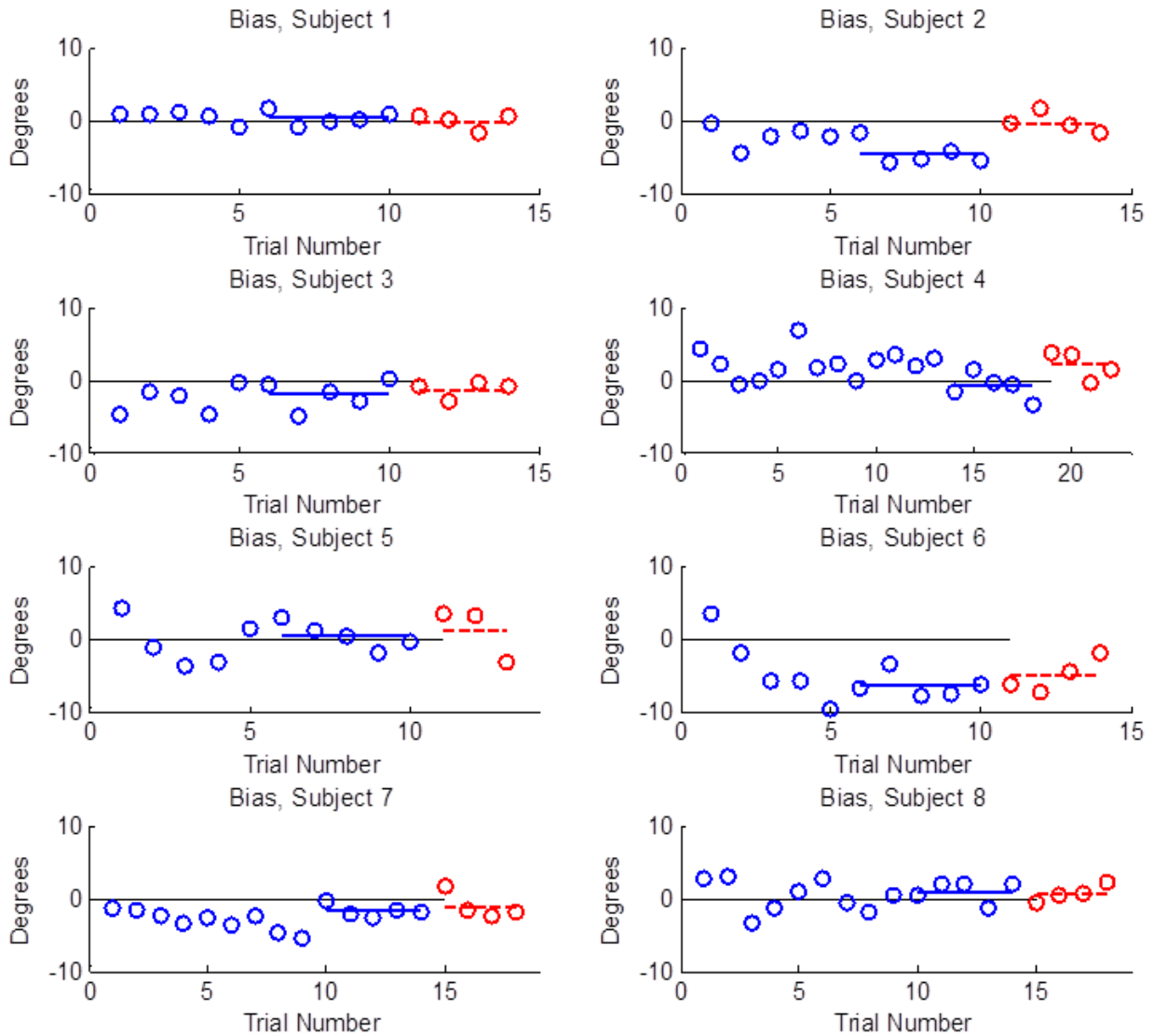
To quantify the subject's effectiveness on each training trial, the RMS error between the actual cab roll tilt and the subject's indicated roll tilt was calculated (lower RMS scores indicate better performance). These scores are shown for each successive training trial in the figure below. The mean of the last 4 trials from the first training session was taken as a steady-state (SS) measure of RMS and is noted for each subject below. In addition to the primary training session on day 1 (blue circles), 3-4 refresher training sessions were completed on day 2 (red circles) prior to testing to ensure the mean performance was similar to that at the end of day 1.



As seen in the figure above, subject's performance using the indicator generally improved with training. There was some variability in performance between subjects, but all subjects were able to train to a competent level of performance. The performance on the refresher training on day 2 was generally as good as or better than the performance at the end of the first day of training.

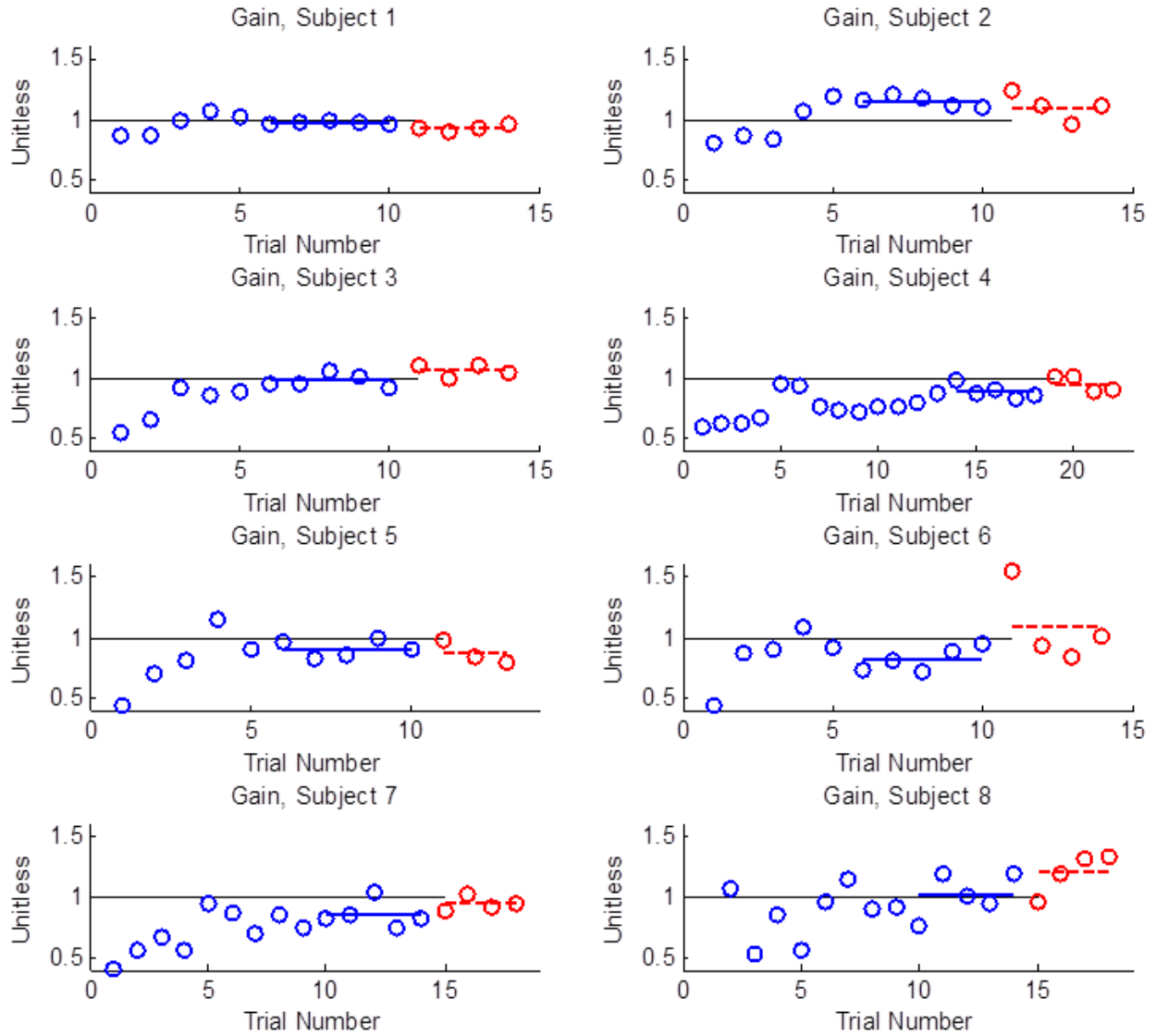
To quantify the types of errors being made a simple input/output model was fit to the relationship between the actual roll tilt and indicated roll tilt for each trial. The model included a bias, gain, and time delay and was fit in the frequency domain. This simple model was able to explain the response dynamics of the indicator fairly well on most trials. The bias parameter on each trial is shown in the figure below.





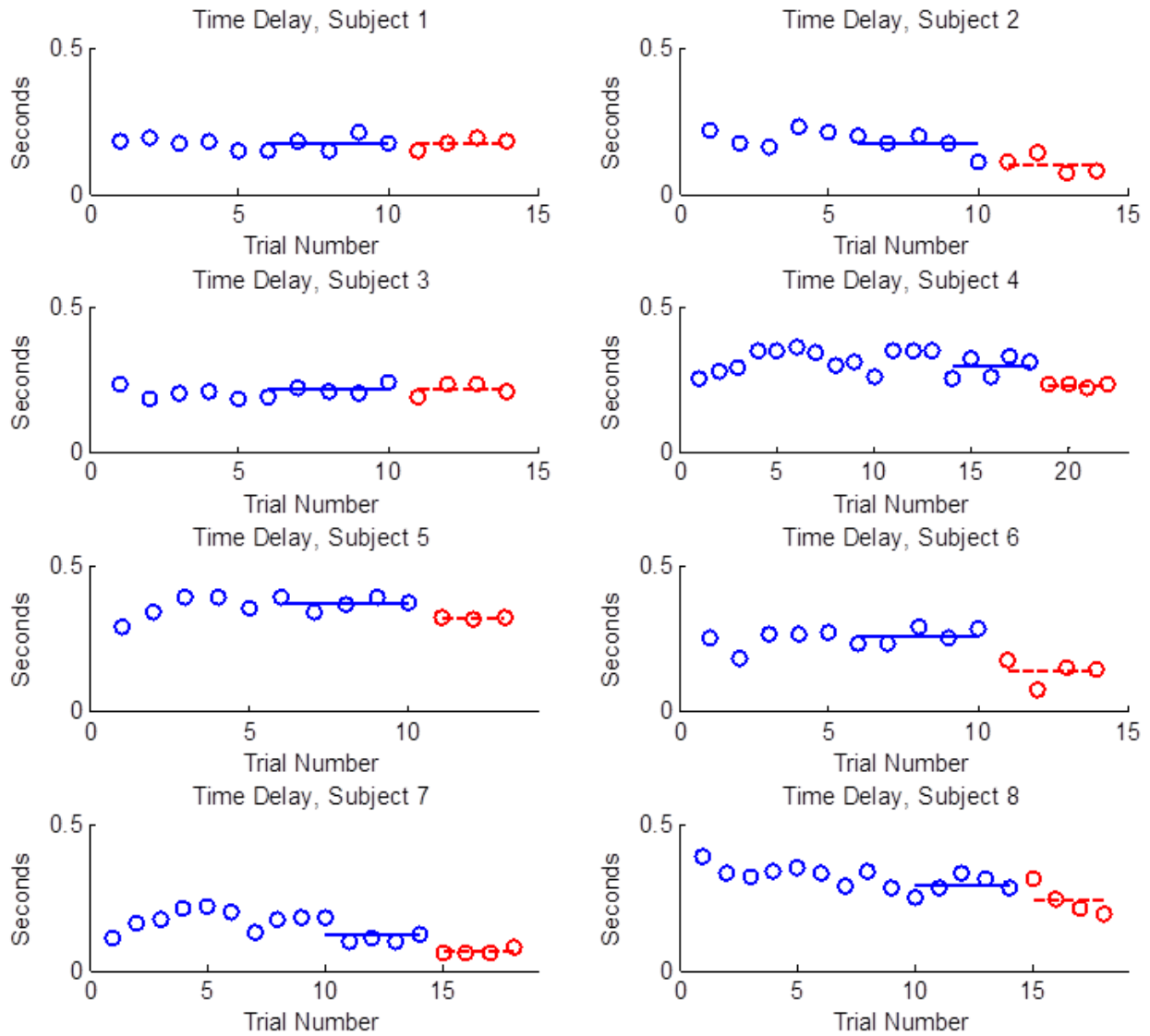
Each subject's bias on each trial was generally within 1-2 degrees of zero, corresponding to no left/right bias. Subjects 2 and 6 had a consistent bias to the right (negative) during training on day 1, though only subject 6's persisted on the day 2 refresher.

The gain of the indicated response to the actual response is shown in the figure below. A value of 1 indicates the indicated response is proportional to actual roll tilt, while less than 1 corresponds to a smaller response than actually experienced.



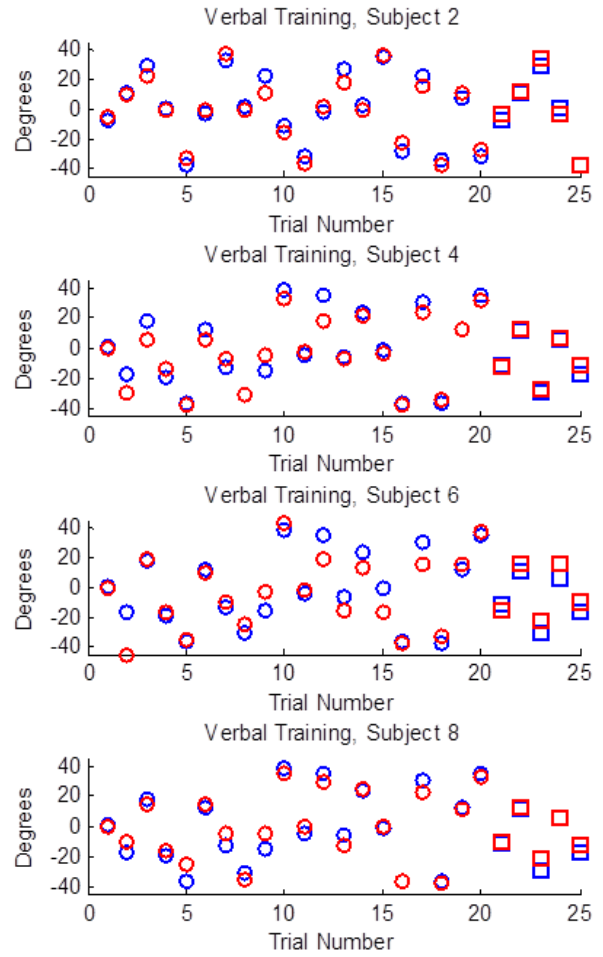
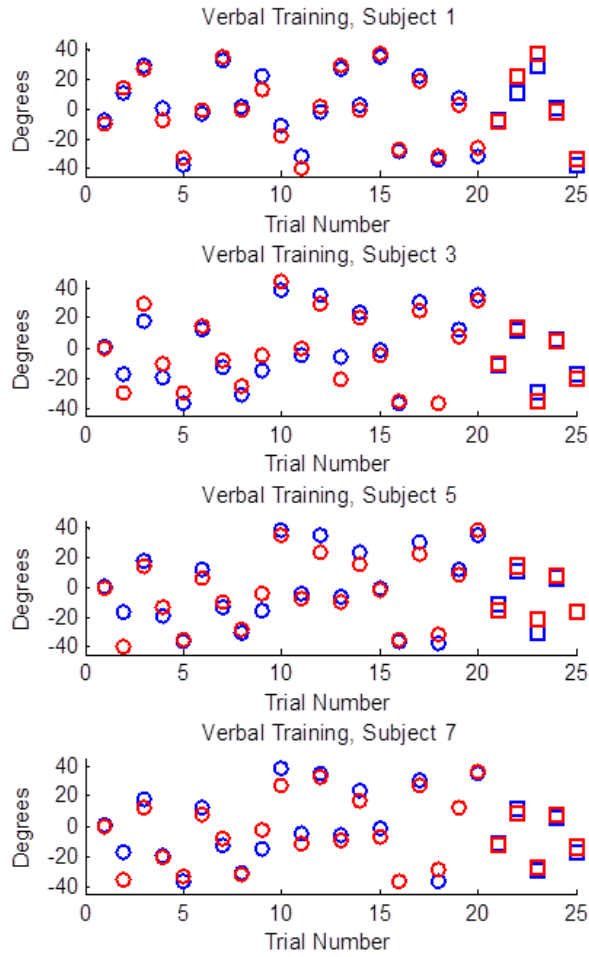
Nearly all subjects initially had a gain of less than 1 and reported smaller tilts than were actually experienced. However, with training most subjects were able to increase the indicated responses to reach a gain of near one.

Finally, the time delay associated with the indicated response is given in the figure below.



The time delays generally did not change much during training. In fact, feedback was not provided regarding time delay since we did not believe subjects could be easily coached to improve their response times. There was substantial variability between individual subjects, with time delays ranging from 0.1 seconds to 0.35 seconds.

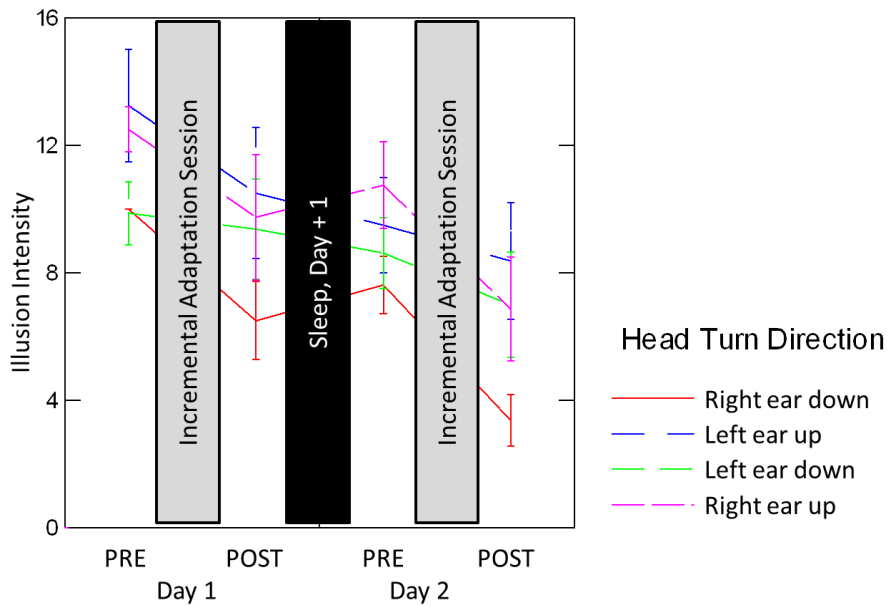
In addition to the training of the somatosensory indicator task, subjects were also provided an opportunity to train at the verbal reporting task as detailed in Section 4.1.8. The actual verbal angles are shown in blue and the reported are shown in red. The training on the first day is shown as circles and those from the second day are indicated by squares.



There was not clear evidence that the training improved the accuracy of verbal reports, however subjects did generally respond fairly accurately.

## G. Cross-Coupled Adaptation Tables and Plots for Experiment 1

Cross-coupled illusion intensities during adaptation by head turn direction.

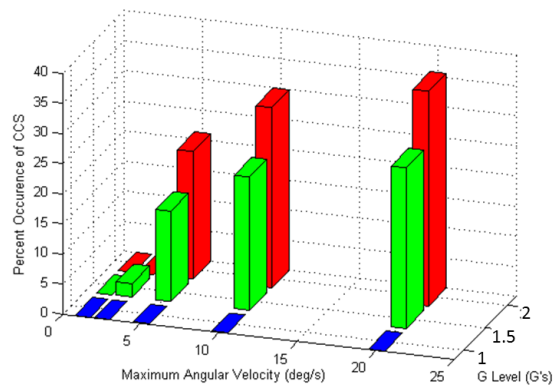
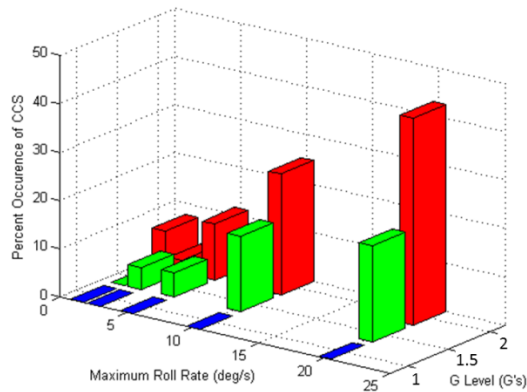


A three factor (pre vs. post, day 1 vs. 2, and head turn direction) repeated measures ANOVA model with Bonferroni corrections for multiple comparisons found none of the head turn directions to significantly differ from each other. This is somewhat surprising based upon previous studies that find differences between head turn directions (Brown, Hecht et al. 2002; Young, Sienko et al. 2003; Jarchow and Young 2007; Mateus 2008). Illusion intensities for every head turn direction are reduced through the adaptation protocol.

During hyper-gravity testing the illusion occurrence percentages (and fractions) are given in the tables and figures below for roll tilts (left) and returns (right).

Fraction of tilt trials with ANY cross-coupled stimulus illusion						
	Overall	1.25 deg/s	2.5 deg/s	5 deg/s	10 deg/s	20 deg/s
1.0 G	0% (0/192)	0% (0/16)	0% (0/48)	0% (0/64)	0% (0/48)	0% (0/16)
1.5 G	8.3% (15/180)	0% (0/15)	4.4% (2/45)	5% (3/60)	15.6% (7/45)	20% (3/15)
2.0 G	15% (24/160)	7.7% (1/13)	2.4% (1/41)	11.5% (6/52)	25% (10/40)	42.9% (6/14)

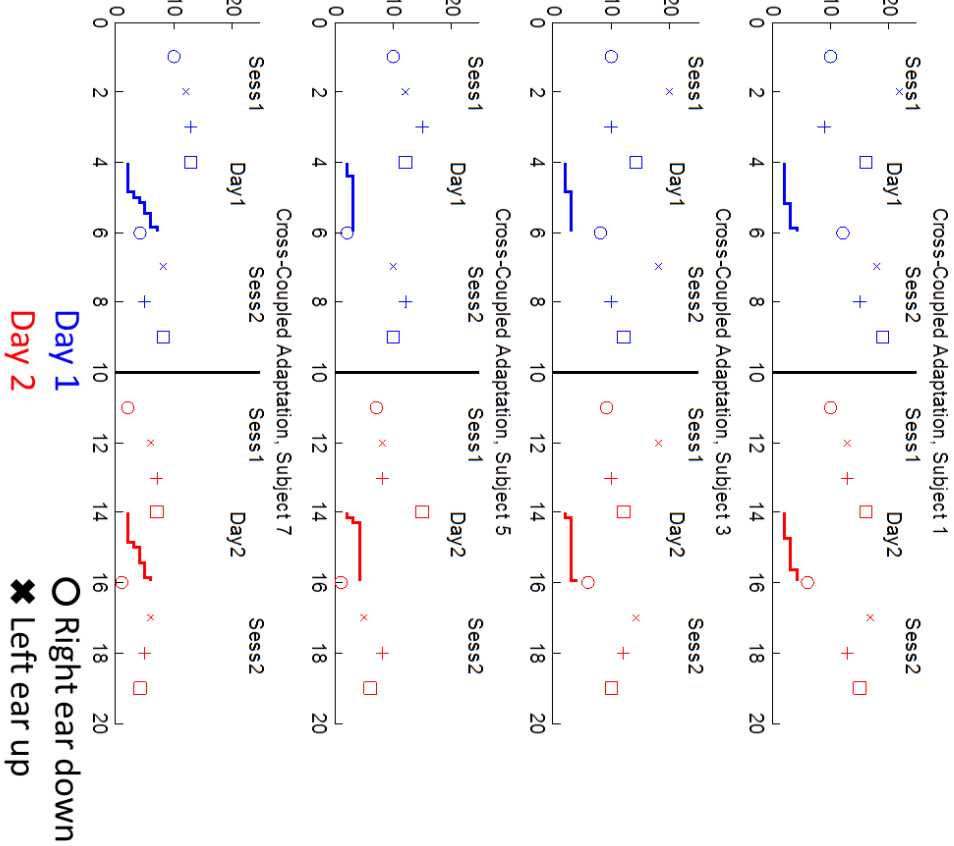
Fraction of return trials with ANY cross-coupled stimulus illusion						
	Overall	1.25 deg/s	2.5 deg/s	5 deg/s	10 deg/s	20 deg/s
1.0 G	0% (0/192)	0% (0/16)	0% (0/48)	0% (0/64)	0% (0/48)	0% (0/16)
1.5 G	13.3% (24/180)	0% (0/15)	2.2% (1/45)	15% (9/60)	22.2% (10/45)	26.7% (4/15)
2.0 G	17.5% (28/160)	0% (0/13)	0% (0/41)	21.2% (11/52)	30.0% (12/40)	35.7% (5/14)



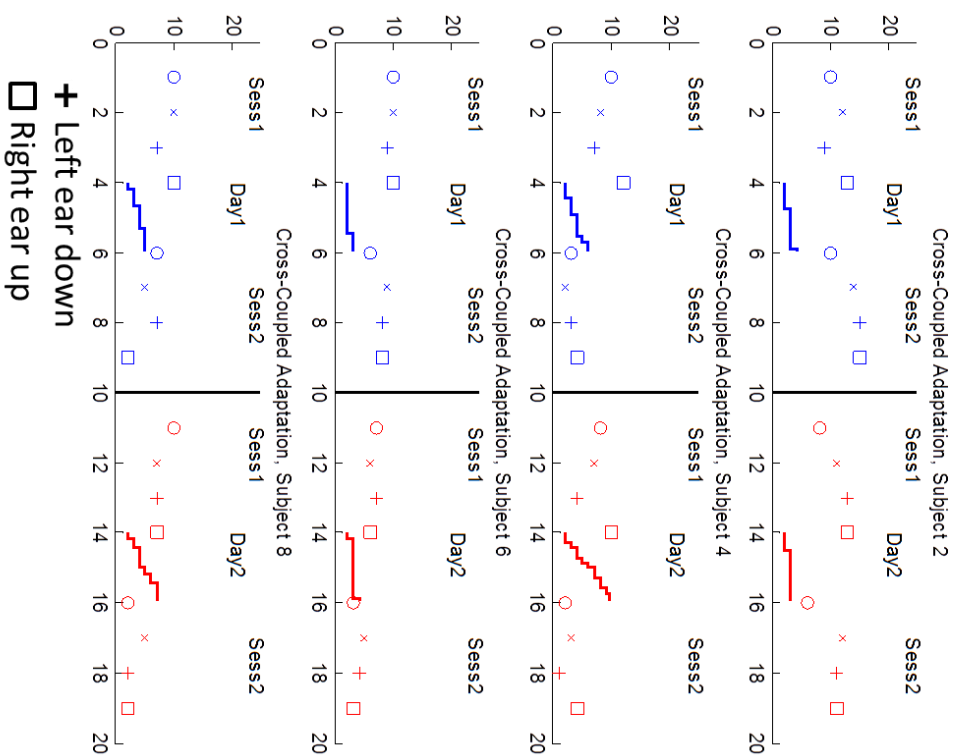
First for tilts, using a 3-way contingency table with G-level and angular velocity found there to be a significant interaction of G-level and angular velocity on the fraction of trials in which the cross-coupled illusion occurred ( $G^2 = 67.08$ ,  $df = 22$ ,  $p < 0.0005$ ). The effect of gravity level when the interaction of angular velocity was removed was significant ( $G^2 = 44.18$ ,  $df = 10$ ,  $p < 0.0005$ ), as was the effect of angular velocity when the interaction of gravity level was removed ( $G^2 = 26.66$ ,  $df = 12$ ,  $p = 0.0086$ ). Similar results were found of the prevalence of the cross-coupled illusion during returns. There was a significant interaction ( $G^2 = 94.46$ ,  $df = 22$ ,  $p < 0.0005$ ), and both G-level ( $G^2 = 54.58$ ,  $df = 10$ ,  $p < 0.0005$ ) and angular velocity ( $G^2 = 43.58$ ,  $df = 12$ ,  $p < 0.0005$ ) were significant when the interaction of the other variable was removed. This contingency table analysis was performed using <http://www.vassarstats.net/abc.html> since the functionality was not available in SYSTAT.

The complete data set is plotted by subject for the cross-coupled stimulus protocol below. The individual data points represent reports of illusion intensity in pre and post tests for each individual head tilt. In general, the intensities were reported as lower in the post tests and on the second day. The staircase lines show the yaw rate over the time course of the 15 minute incremental adaptation phases. The yaw rate always starts out at 1.5 rpm. As the subject adapts and the illusion becomes sub-threshold at a given yaw rate, the rate is increased. For all subjects, the rate increased at least once per incremental adaptation phase. Generally the rate increased more and more quickly during the incremental adaptation phase on day 2. Subject 4 on day 2 even reached the maximum yaw rate of 14.26 rpm.

### Subjective Intensity or Adaptation Threshold (RPMs)

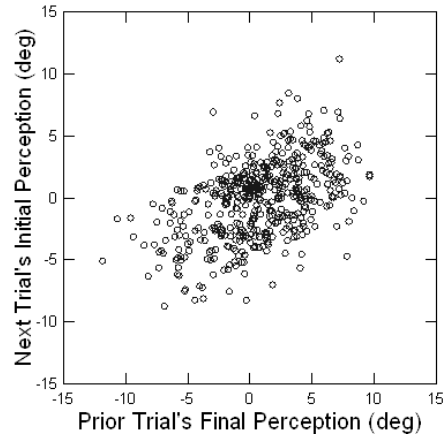


### Subjective Intensity or Adaptation Threshold (RPMs)



## H. Upright Perception for Experiment 1

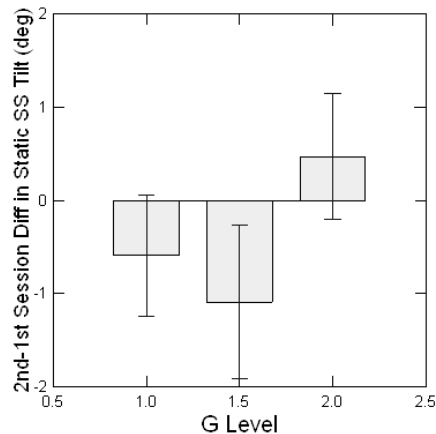
Upright perception measurements were only considered at the beginning of each session. While the subject is upright between each trial, the perception after returning to upright was dependent upon the previous roll angle direction and magnitude (see Section 4.2.10). Even after the indicator reset, the upright perception is still significantly, though weakly, correlated with the perception just prior to the reset ( $r(530)=0.49$ ,  $p<0.0005$ ).



To be conservative and avoid a measure of upright perception that is contaminated by the previous roll tilts, upright perception measurements were only considered at the beginning of each session.

## I. Static Tilt Steady-State Perception for Experiment 1

One might hypothesize that with repeated exposure to hyper-gravity, subjects could learn or adapt to the environment and the perceptual errors might decay or even be eliminated. To test for this each combination of roll angle, frequency, and gravity level was presented twice: once in the first three sessions and once in the second three sessions. The subject's perception of a same combination of conditions was compared between the first presentation and the second. These differences, averaged by subject, are given for each gravity level in the figure below.



It is not expected that any changes should be seen in the 1 G condition, unless some adaptation to hyper-gravity is maladaptive to the 1 G case. However if the amount of overestimation seen in

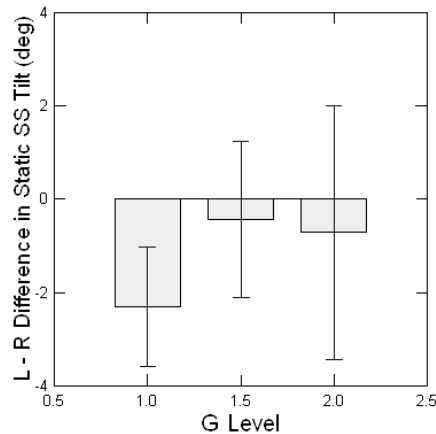


hyper-gravity (1.5 and 2 G) is reduced on the second presentation, we would expect to see a negative difference in the figure above. The results of three pairwise t-tests for each of the three gravity levels are given in the table below.

	Mean difference	t-value	d.f.	p-value
1 G	-0.593	-0.908	7	0.394
1.5 G	-1.092	-1.328	7	0.226
2 G	0.468	0.695	7	0.509

There is no evidence to support the hypothesis that learning of adaptation in perceptual responses is occurring between sessions. This was not a primary purpose of this experiment, however this lack of evidence allows for the pooling of data across sessions. The lack of adaptation in these static perceptual responses may be due to the passive rotations, where the sensory conflicts between expected and actual sensory measurements are not as emphasized as would be in active rotations.

Previous studies of static tilt steady-state perception in hyper-gravity have qualitatively concluded that there is no asymmetry in perceptual effects between left or right roll tilts (Colenbrander 1963; Schone 1964; Correia, Hixson et al. 1965; Correia, Hixson et al. 1968). There were clear asymmetries in pitch perception for pitching forward vs. backwards, which were attributed to morphological orientation of the dominant plane of the utricles (Corvera, Hallpike et al. 1958; Curthoys, Betts et al. 1999). However, only roll was considered in the current study, so it was hypothesized that there would be no left/right asymmetries. To test this, the 20 degree roll tilts at all three frequencies, were tested both to the right (-20 degrees) and left (+20 degrees). The differences between left and right 20 degree tilts in subject mean static tilt steady-state perception are shown in the figure below for each gravity level.

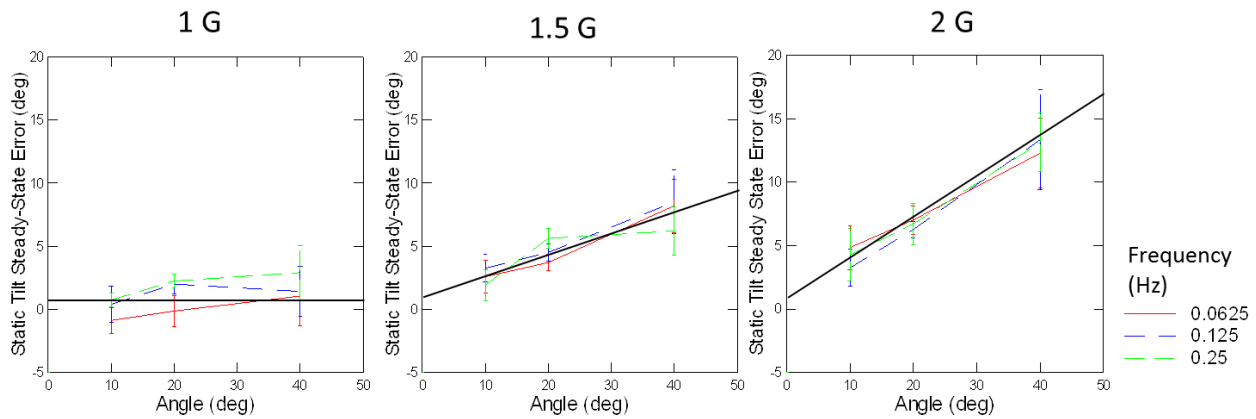


At the 1 G level, there is a small trend towards rightward (-20 degree) tilts being perceived as larger than leftwards (+20 degree) tilts. However, three paired t-tests (table below) showed there to be no significant asymmetries in left vs. rightward tilts at any of the gravity levels tested.

	Mean difference	t-value	d.f.	p-value
1 G	2.312	1.798	7	0.115
1.5 G	0.437	0.262	7	0.801

2 G	0.714	0.262	6	0.802
-----	-------	-------	---	-------

Presumably, after a certain period of time of static tilt, the perception of that tilt becomes independent of the particular dynamic rotation parameters (i.e. frequency) to get to that tilt angle. We hypothesized that the 28-30 seconds after the completion of the dynamic rotation, during the static tilt “steady-state” period, is sufficient time for the perceptual response to become independent of the dynamic rotation parameters. The figure below shows the static tilt steady-state perceptual errors (perceived angle – actual angle) pooled by session repetition and left vs. right, across actual roll angle for each gravity level.



The different colors represent the responses by the frequency of the preceding dynamic rotation. Overlaid, in the black line, is the model fit from Equation 5 and Table 4, which has no frequency dependence. Clearly there is no consistent difference between any of the frequency levels and the mean across frequencies at any of the angles of gravity levels tested. Adding frequency as a continuous variables to the model in Equation 5 and Table 4 is insignificant ( $p > 0.05$ ). Thus it is reasonable to pool the static tilt steady-state perceptions across frequencies.

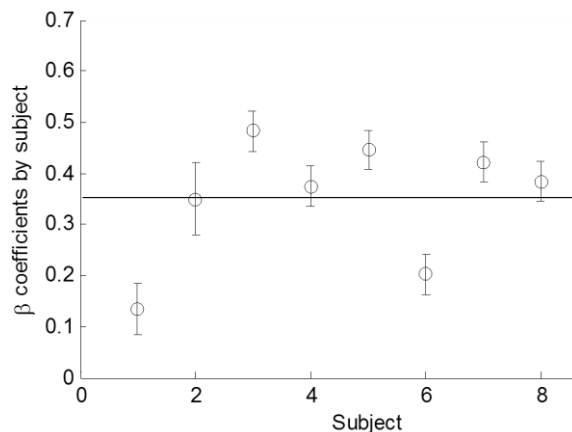
Some subjects exhibited a “G-Excess” effect that was consistently greater than or less than the population-level model described in Equation 5 and Table 4. To address this, a model was built that had subject dependent “G-Excess” term coefficients, as seen in the equation below.

$$(\theta_{per} - \theta)_{ij} = \rho_i + \beta_i((G - 1)\theta) + \epsilon_{ij}$$

The results for this model are given in the table below.

	$i$	Coefficient	Standard Error		$i$	Coefficient	Standard Error	Z-value	p-value
$\rho$	1	0.71	0.86	$\beta$	1	0.13	0.050	2.64	0.009
	2	-1.68	0.96		2	0.35	0.070	5.02	<0.0005
	3	3.67	0.81		3	0.48	0.039	12.30	<0.0005
	4	-1.46	0.81		4	0.38	0.039	9.55	<0.0005
	5	-0.82	0.81		5	0.45	0.039	11.35	<0.0005
	6	-0.92	0.81		6	0.20	0.039	5.15	<0.0005
	7	-2.85	0.81		7	0.42	0.039	10.74	<0.0005
	8	2.42	0.81		8	0.38	0.039	9.77	<0.0005
	Mean	-0.12			Mean	0.35			

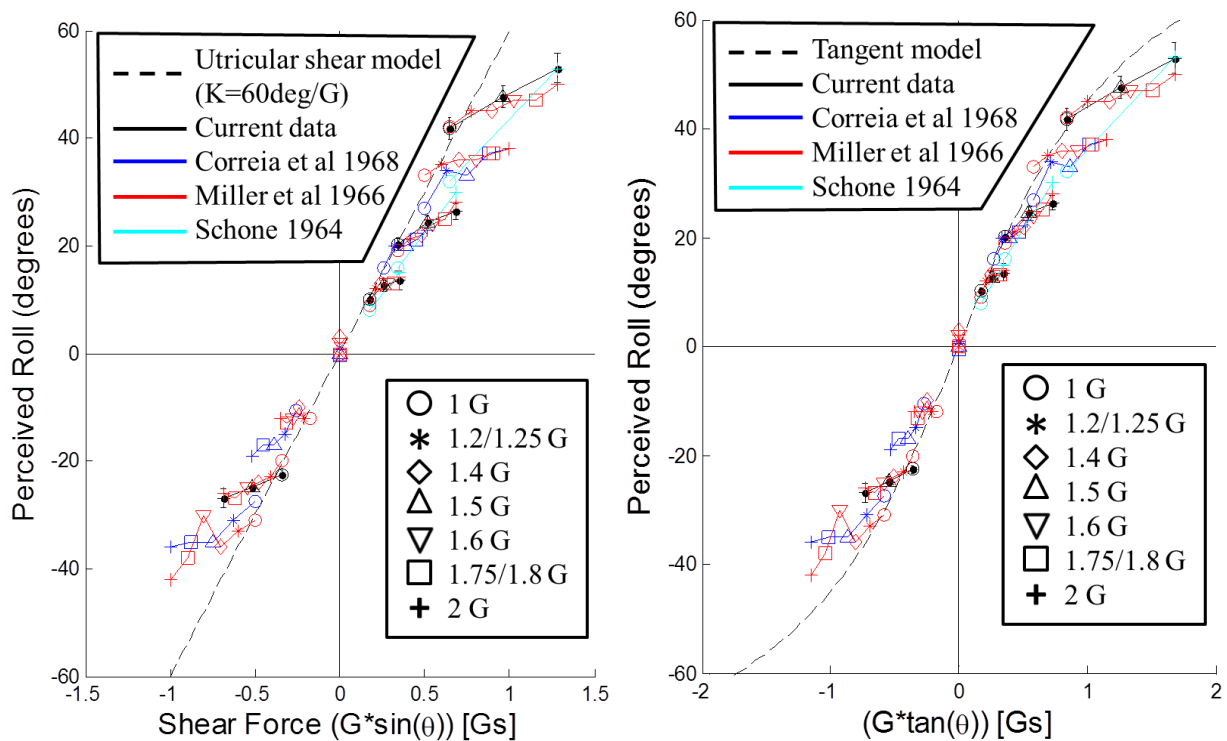
All eight subjects exhibited significant overestimation in hyper-gravity (with more overestimation at higher gravity-levels and larger angles), as seen in the significantly positive  $\beta_i$  coefficients. However, the amount of overestimation, or the magnitude of the “G-Excess” effect, varied substantially between subjects. The plot below shows the estimated  $\beta_i$  coefficients for each subject with the standard errors associated with the estimates.



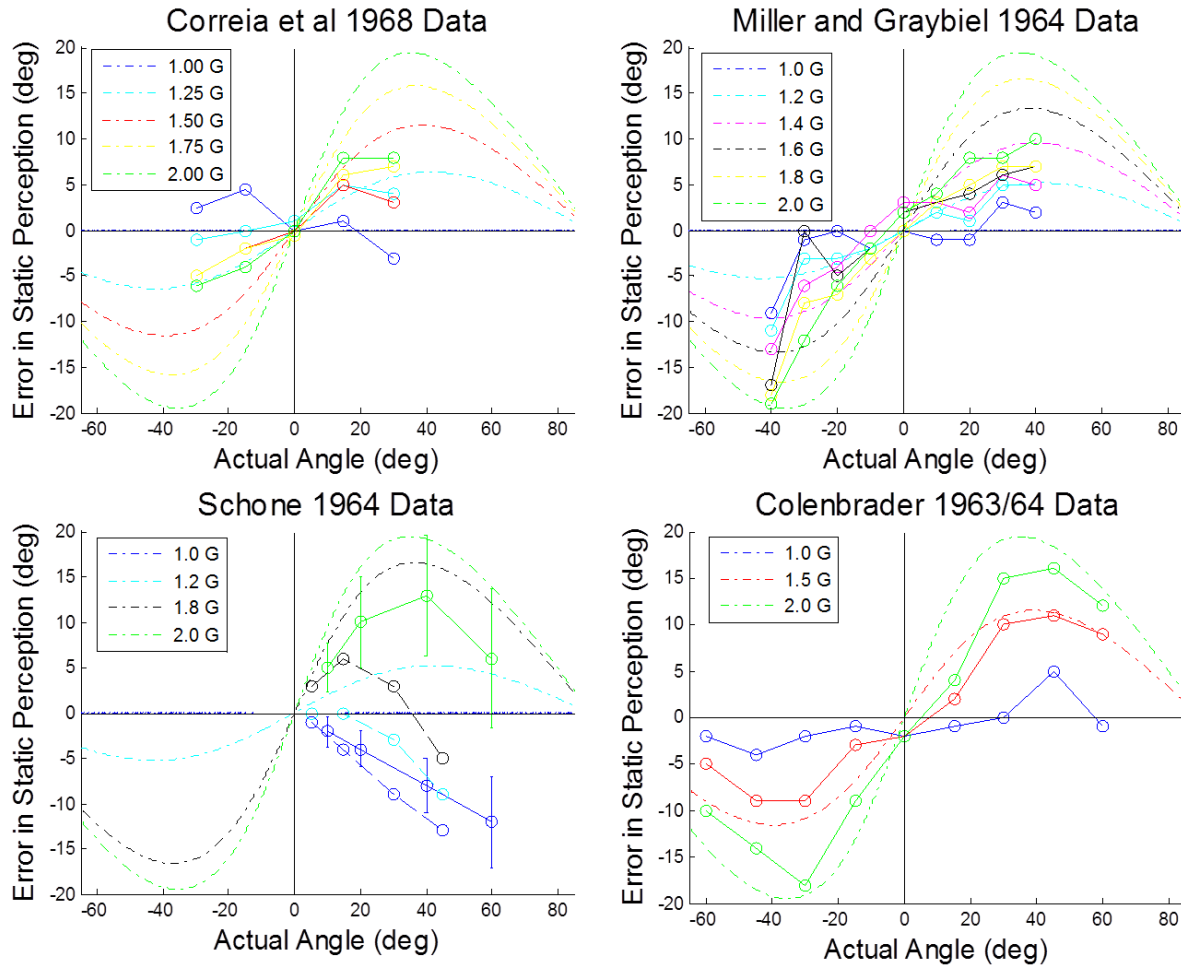
The solid line indicates the average  $\beta$  coefficient from the population-level model in Equation 5 and Table 4. Subjects 1 and 6 showed much less overestimation than the sample mean and subjects 3 and 5 exhibited slightly more overestimation. Thus, while all subjects with functioning vestibular systems are likely to overestimate their roll angle in hyper-gravity, the amount of overestimation may vary by as much as a factor of four between individuals.

The previously proposed utricular shear and tangent models were unable to effectively fit the static steady-state perceptions measured in the current study (see Section 4.2.5). At first, this might suggest a discrepancy between the current data and the previous SVV studies upon which the previous models were developed (Colenbrander 1963; Schone 1964; Correia, Hixson et al. 1965; Miller and Graybiel 1966; Schone and Parker 1967; Schone, Parker et al. 1967; Correia, Hixson et al. 1968). This would not necessarily be unexpected given the differences in methodology (e.g. SVV vs. somatosensory task reports). However, across the conditions which were evaluated in both the current and previous studies, the current dataset at least qualitatively matches previous results quite well (see Section 4.2.6 and Figure

22). Thus it appears the major discrepancy is between the data (both the current and previous studies) and the previously proposed models (e.g. utricular shear and tangent models). At least part of this confusion may be due to plotting techniques which made the lack of fit difficult to observe in prior publications. The plots upon which both the utricular shear (Schone 1964; Schone and Parker 1967; Schone, Parker et al. 1967) and tangent (Correia, Hixson et al. 1965; Correia, Hixson et al. 1968) model were qualitatively validated upon, showed the raw perceived angle ( $\theta_{per}$ ) on the y-axis as opposed to the error in perceived angle ( $\theta_{per} - \theta_{act}$ ). Since the majority of the variation in the perceived angle is simply due to the actual angle, this plotting technique makes it difficult to observe hyper-gravity effects. For example, the plots below show static perceived angles from the current study (solid black) and previous studies as a function of either the utricular shear force [ $G \cdot \sin(\theta_{act})$ ] or the tangent model equivalent [ $G \cdot \tan(\theta_{act})$ ], as depicted in Figures 7 and 12 of (Correia, Hixson et al. 1968).



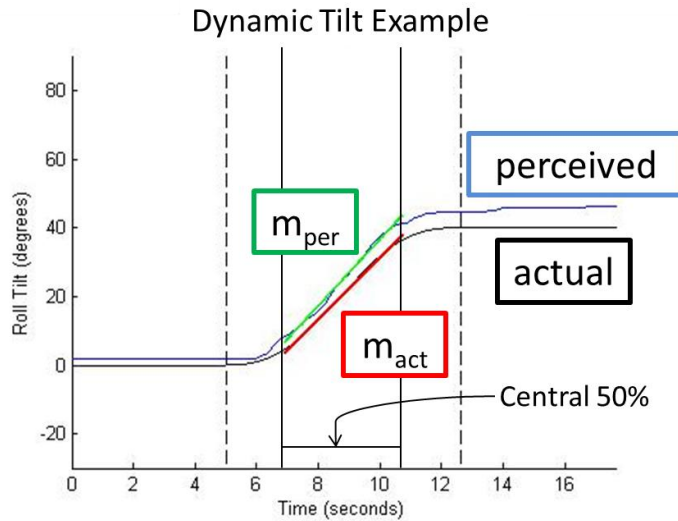
In the plots above, it may appear that the current and previous data roughly match the utricular shear (left plot) and tangent model (right plot). However under greater scrutiny, particularly for larger angles, the higher gravity levels do not show as large of a perceived roll angle as either the utricular shear or tangent model would hypothesize. This can be seen far more clearly when plotting the error in perceived roll angle on the y-axis, such that the inherent variability simply due to the actual angle is removed. This is done in the plot below with comparison to the tangent model (which predicts less overestimation in hyper-gravity than the utricular shear model and is thus a more conservative comparison).



When plotting the static perceptions from the previous studies in terms of error in perceived angle, it becomes readily apparent that even the tangent model predicts far too much overestimation in hyper-gravity. In Miller and Graybiel, -40 degree tilts yield similar amounts of overestimation as the tangent model in several hyper-gravity conditions, but there is also large overestimation errors in 1 G which may indicate a systematic error at this testing condition. Also, the static perceptual errors were much smaller for +40 degrees, further suggesting an abnormality in the -40 degree condition. In Schöne, there is a large E-effect (e.g. underestimation) in 1 G and also 1.2 G, however there is still not as much overestimation as would be expected from the tangent model in larger hyper-gravity conditions. Colenbrander's data most closely matches the tangent model predictions, but still systematically has less overestimation in hyper-gravity than expected. This apparent lack of fit between previous studies and either the utricular shear or tangent models was previously noted on pg. 100 (footnote 26) of (Guedry 1974). The modified utricular shear model proposed herein (see Section 4.2.6), not only fits the current static perception data well, but also qualitatively matches previous data sets.

## J. Dynamic Tilt and Dynamic Return Perception for Experiment 1

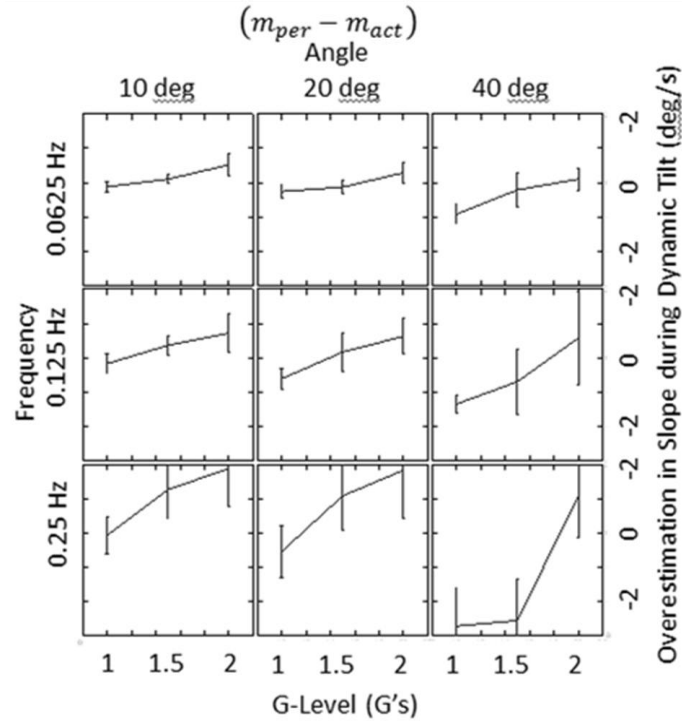
For an example dynamic roll tilt the linear slope metric is shown in the figure below.



For the 8 second (0.125 Hz), 40 degree roll tilt, the central 50% of the dynamic tilt period (~7-11 seconds) is taken and a linear fit is done for both the perceptual fit (green line) and the actual (red line). The ratio of the slopes of these linear fits ( $m_{per}/m_{act}$ ) is then taken as the primary metric for dynamic tilt perception. When there is dynamic overestimation  $m_{per} > m_{act}$  and the ratio will be greater than 1. When there is accurate perception the ratio will be near 1.

As seen, over the central 50% of the dynamic tilt period (shown by vertical solid black lines), the profile is nearly linear. The slope metric provided a fairly robust metric to characterize the perceptual response during dynamic rotation periods.

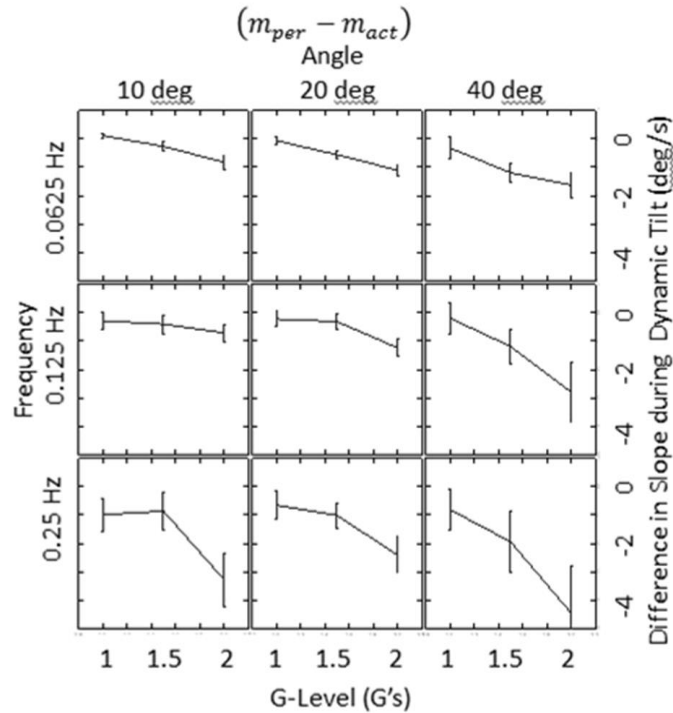
In addition to the analysis done in Section 4.2.8, to verify that there is overestimation in hyper-gravity across all angles and frequencies tested the perceptual slope was compared directly to the actual slope and the effect of gravity was tested at each angle and frequency combination. The plot below shows the differences between perceived and actual slope for dynamic tilt.



A significant positive effective of gravity would indicate overestimation in hyper-gravity. To test this, a hierarchical regression was performed with (G-1) as the independent variable and subject as the indicator for each angle and frequency. The results are provided in the table below.

Angle (degrees)	Frequency (Hz)	$\gamma$ estimate	p-value
10	0.0625	0.68	0.001
10	0.125	1.02	0.009
10	0.25	2.26	0.034
20	0.0625	0.60	0.001
20	0.125	1.20	<0.0005
20	0.25	2.23	0.008
40	0.0625	1.18	<0.0005
40	0.125	1.95	0.021
40	0.25	3.23	0.015

At all angles and frequencies tested, there is a positive effect of gravity level, confirming that hyper-gravity causes overestimation during dynamic tilts. The same analysis is done below for dynamic returns. Note that the slopes are negative for returns so a negative trend of gravity indicates overestimation.



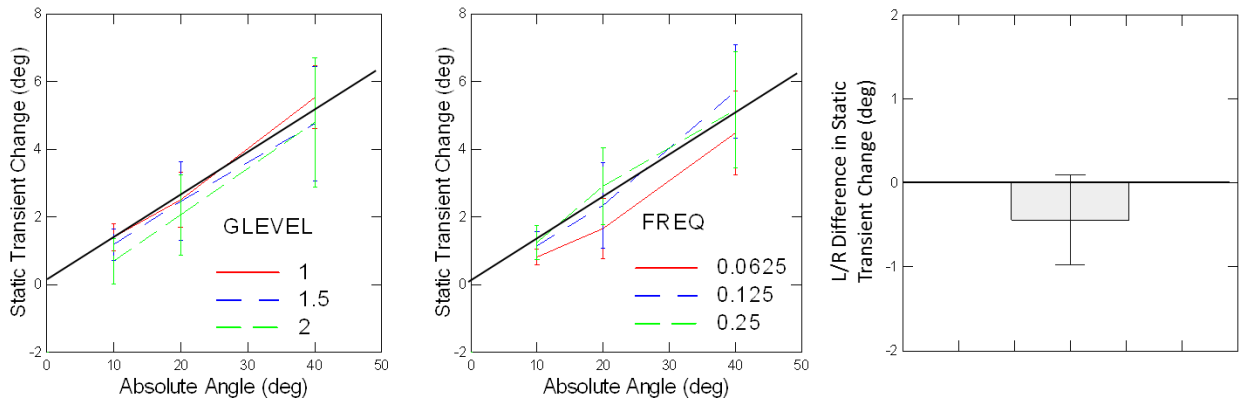
Angle (degrees)	Frequency (Hz)	$\gamma$ estimate (sign reversed)	p-value
10	0.0625	0.69	<0.0005
10	0.125	0.45	0.211
10	0.25	1.78	0.038
20	0.0625	1.11	<0.0005
20	0.125	1.03	0.011
20	0.25	1.50	0.034
40	0.0625	1.30	0.001
40	0.125	2.48	0.001
40	0.25	3.52	0.018

For dynamic returns, all combinations of angle and frequency had a significant effect of gravity except a 10 degree rotation at 0.125 Hz. However, the effect was trending in the correct direction and was bounded by neighboring angles and frequency by a significant result, so it may be reasonable to expect with additional subjects this result would become significant. For both tilts and returns, there is evidence at all angles and frequencies tested that gravity level has an effect on dynamic perceptions in the direction of overestimation in hyper-gravity.

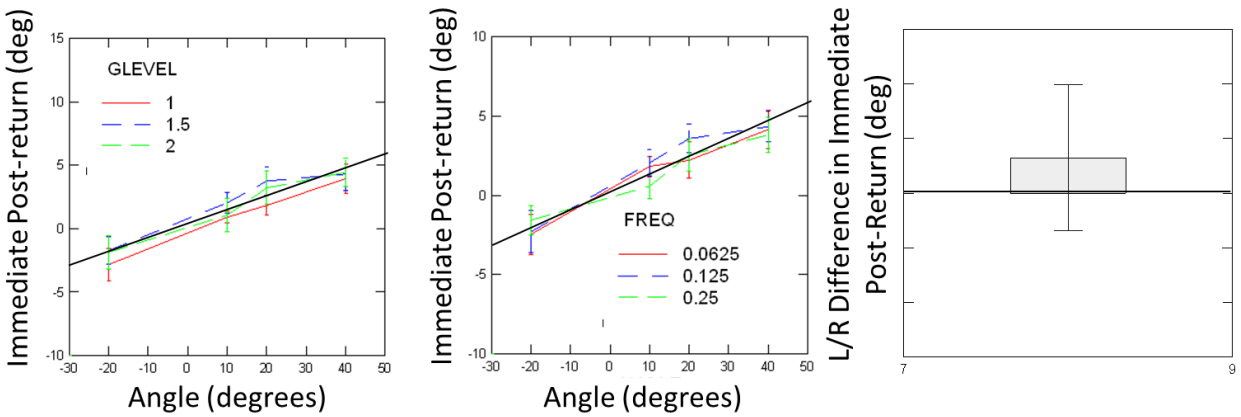
### K. Transient Perceptions for Experiment 1

The plots below show static tilt transient perceptual growth was not significantly affected by the gravity level, frequency of the rotation, or whether the tilt was to the left vs. the right. Thus, the results were pooled for the analysis in Section 4.2.9.

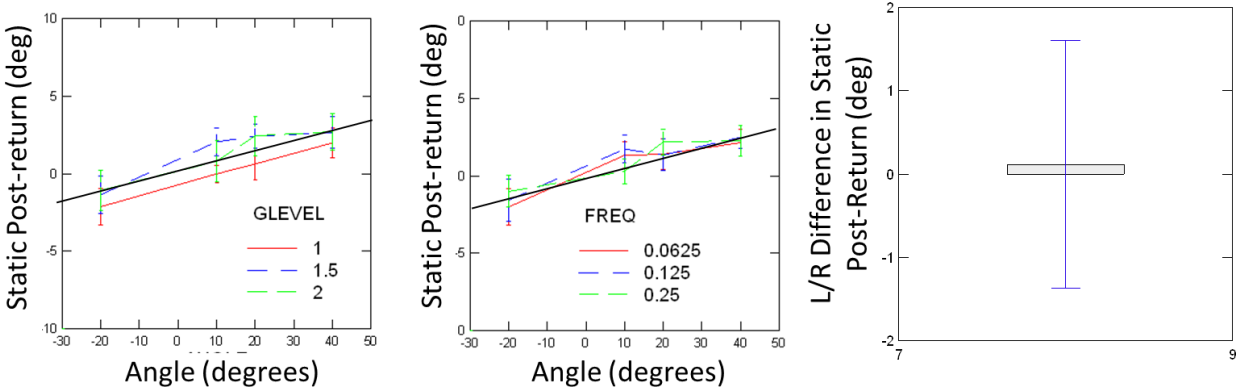




The plots below show the perception immediately post-return was not significantly affected by the gravity level, frequency of the rotation, or whether the tilt was to the left vs. the right. Thus, the results were pooled for the analysis in Section 4.2.10.



Similarly, after 10-12 seconds post-return the perceptual response was not significantly affected by gravity level, frequency, or tilt direction, so the results were pooled.



## L. MATLAB Code for Experiment 2 Profiles

Code to create a complete testing session for Experiment 2 (see Figure 29 for an example) is provided below. The user selects the desired “Glevel” for the session (1, 1.5, or 2 G’s) and then runs the script.

The “output” variable contains the required information for a “Space mode” profile on the NASTAR ATFS-400. The first column of output is the commanded planetary spin rate of the centrifuge in rotations per minute. The second column is the commanded roll angle, relative to Earth vertical, of the centrifuge cab in degrees. The third column is the commanded pitch angle and for this experiment is always set to zero. The fourth column determines whether the RHC is active (1) or deactivated (0). Each row is the set of the commanded values at an instant in time which the time step between successive rows fixed at 0.01 seconds. The “output” variable should be copied into a .txt file and saved. Then on the ATFS-400 computer system the file type should be converted to a .space file by renaming the file from “Example.txt” to “Example.space”. These .space files are then loaded for experimentation. The naming convention, if trying to use previously saved files, is “MIT\_GControl\_‘Glevel’\_‘NumberofTrials’\_‘Number’.space”, so for example the first 1.5 G profile with 3 trials for testing would be “MIT\_GControl\_15G\_3trial\_1.space”. This code was also used to create the training profiles, but setting the “Glevel” to 1 and the “num\_trials” to 1.

```

clc; clear all;
close all;

%% This program calculates a sum-of-sines roll disturbance profile
%% to be used as inputs for the NASTAR ATFS-400 centrifuge

%% Inputs
Glevel = 1;
Glevel = 1.5;
% Glevel = 2;

% num_trials = 1;
num_trials = 3;      % number of trials in the session

ang_limit = 25;      % degrees from "upright"
vel_limit = 20;      % degrees/second

cent_rad = 7.62;     % centrifuge radius in m
t_between = 30;      % time allowed between tilts
t_upright = 5;       % time to get back to upright after a trial, sec
t_start = 5;         % time to start a disturbance
t_stop = 5;          % time to stop a disturbance
dt = 0.01;           % sec

% Input spectrum (from Merfeld 1996, Table 2)
freq = [0.014; 0.024; 0.053; 0.083; 0.112; 0.151; 0.200; 0.258; 0.346; 0.434; 0.532; 0.668]; % Hz
mag = [2.3995; 2.3988; 2.3808; 2.2982; 2.1044; 1.7106; 1.2360; 0.8709; 0.6185; 0.5216; 0.4786; 0.4536]; % deg
mag = 2.6472*[1; 1; 1; 1; 1; 1; 0.1; 0.1; 0.1; 0.1; 0.1; 0.1]; % deg
phase = pi/180 * [0; 37; 74; 111; 148; 185; 222; 259; 296; 333; 19; 47]; % rad
% zeropts = [19.74 70.04 116.78]; % the points where the response is 0, dependent upon profile inputs
% t_final = 204.8; % sec
t_final = 204.8 + t_start + t_stop; % sec
% t_final = 80 + t_start + t_stop;

%% Spin up time
if Glevel == 1
    t_spinup = 20;      % time allowed for spin up, sec
    t_spindown = 20;    % time allowed for spin down, sec
    t_rest = 5;         % time allowed to adjust to G, sec
else
    t_spinup = 60;      % time allowed for spin up, sec
    t_spindown = 60;    % time allowed for spin down, sec
    t_rest = 60;        % time allowed to adjust to G, sec
end

time = [0:dt:t_spinup]';
mancont_on = zeros(length(time), 1);

G_cent_start = sqrt(Glevel^2-1);
cent_vel_start = sqrt(9.81*G_cent_start/cent_rad)/t_spinup * time;
G = 1/9.81 * sqrt((cent_vel_start.^2 * cent_rad).^2 + 9.81^2);

```

```

a_cent = sqrt(G.^2 - 1);           % centripetal acceleration, G's
theta = 180/pi*atan(a_cent/1);    % roll angle of centrifuge with respect to vertical

%% Wait for subject to adjust
time_new = [time(end)+dt:dt:time(end)+t_rest]';
G_new = G(end)*ones(length(time_new),1);
theta_new = theta(end)*ones(length(time_new),1);
mancont_on_new = zeros(length(time_new),1);

time = [time; time_new];
G = [G; G_new];
theta = [theta; theta_new];
mancont_on = [mancont_on; mancont_on_new];

theta_baseline = theta(end);

for j = 1:num_trials
    %% Calculate pseudorandom sum-of-sines profile
    time_new = [dt:dt:t_final]';
    G_new = G(end)*ones(length(time_new),1);
    mancont_on_new = ones(length(time_new),1);

    %   rand_phase = 2*pi*rand(1);   % randomize the starting point in the profile
    if num_trials == 1
        rand_phase = 0;           % starting point for training
    else
        rand_phase = 2*pi*0.4;    % starting point for testing
    end

    theta_new = zeros(length(time_new), 1);
    for i = 1:length(freq)
        %   theta_new = theta_new + mag(i)*sin(2*pi*freq(i)*(time_new+zeroPT(j)) + phase(i));
        theta_new = theta_new + mag(i)*sin(2*pi*freq(i)*time_new + phase(i) + rand_phase);
    end

    % every other trial switch the sign of the profile
    if rand(1) > 0.5
        theta_new = - theta_new;
    end

    % grow the disturbance at the beginning and decay it the end (smoothly)
    for i = 1:length(time_new)
        if time_new(i) <= t_start
            theta_new(i) = time_new(i)/t_start * theta_new(i);
        elseif time_new(i) >= (t_final-t_stop)
            theta_new(i) = (t_final-time_new(i))/t_stop * theta_new(i);
        end
    end

    theta_new = theta_new + theta_baseline;

    time = [time; time(end)+time_new];
    G = [G; G_new];
    theta = [theta; theta_new];
    mancont_on = [mancont_on; mancont_on_new];

    %% Back to zero
    %   time_new = [dt:dt:t_upright]';
    %   G_new = G(end)*ones(length(time_new),1);
    %   mancont_on_new = zeros(length(time_new),1);
    %
    %   theta_new = -(theta(end)-theta_baseline)/t_upright*time_new + theta(end);
    %
    %   time = [time; time(end)+time_new];
    %   G = [G; G_new];
    %   theta = [theta; theta_new];
    %   mancont_on = [mancont_on; mancont_on_new];

    %% Time between the trials
    if j < num_trials
        time_new = [time(end)+dt:dt:time(end)+t_between]';
        G_new = G(end)*ones(length(time_new),1);
        theta_new = theta(end)*ones(length(time_new),1);
        mancont_on_new = zeros(length(time_new),1);

        time = [time; time_new];
        G = [G; G_new];
        theta = [theta; theta_new];
        mancont_on = [mancont_on; mancont_on_new];
    end
end

```

```

    end
end

%% Spin Down
time_new = [dt:dt:t_spindown]';
mancont_on_new = zeros(length(time_new),1);

cent_vel_slow = 2;           % rpm
cent_vel_slow_rad = cent_vel_slow * (2*pi/60); % rad/s
cent_vel_stop = cent_vel_start(end) - (sqrt(9.81*G_cent_start/cent_rad)-cent_vel_slow_rad)/t_spindown *
time_new; % rad/s
G_new = 1/9.81 * sqrt((cent_vel_stop.^2 * cent_rad).^2 + 9.81^2); % G-level, G's

a_cent_new = sqrt(G_new.^2 - 1); % centripetal acceleration, G's
theta_new = 180/pi*atan(a_cent_new/1); % roll angle of centrifuge with respect to vertical

time = [time; time(end)+time_new];
G = [G; G_new];
theta = [theta; theta_new];
mancont_on = [mancont_on; mancont_on_new];

%% Calculate at the end
omega = diff(theta)/dt; % roll angular rate, deg/s

a_cent = sqrt(G.^2 - 1); % centripetal acceleration, G's
cent_vel_rad = sqrt(a_cent*9.81/cent_rad); % centrifuge spin rate, rad/s
cent_vel = (60/(2*pi)) * cent_vel_rad; % centrifuge spin rate, rpm

pitch = zeros(length(theta),1);
roll = theta;

ang_min = (theta_baseline - ang_limit)*ones(length(time),1);
ang_max = (theta_baseline + ang_limit)*ones(length(time),1);
vel_min = - vel_limit + zeros(length(time),1);
vel_max = vel_limit + zeros(length(time),1);

%output = [cent_vel roll pitch mancont_on ang_min ang_max vel_min vel_max];
output = [cent_vel roll pitch mancont_on];

%% Plot the outputs
figure;
subplot(5,1,1); plot(time, G); ylabel('G Level')
subplot(5,1,2); plot(time, cent_vel); ylabel('Centrifuge speed (rpm)')
subplot(5,1,3); plot(time, mancont_on); ylabel('Control Activated');
subplot(5,1,4); hold on; plot(time, theta, time, 0*time+theta_baseline);
plot(time, ang_min, '--r', time, ang_max, '--r'); ylabel('Disturbance Angle (deg)');
subplot(5,1,5); hold on; plot(time(1:end-1), omega); ylabel('Disturbance Angular Velocity (deg/s)');
xlabel('Time (sec)');
plot(time, vel_min, '--r', time, vel_max, '--r');

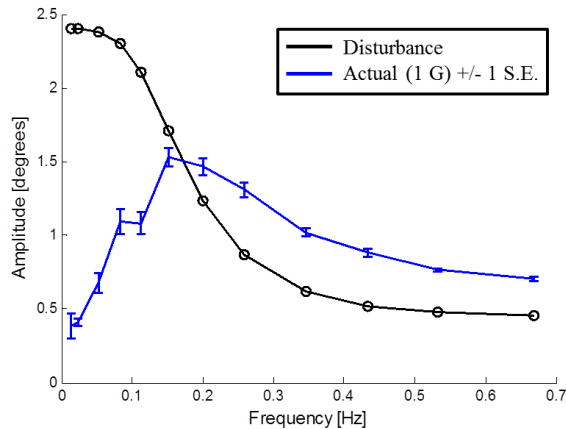
figure;
subplot(3,1,1); plot(time, theta, time, 0*time+theta_baseline); hold on;
plot(time, ang_min, '--r', time, ang_max, '--r'); ylabel('Roll Angle (deg)');
subplot(3,1,2); hold on; plot(time(2:end), omega); ylabel('Roll Velocity (deg/s)');
plot(time, vel_min, '--r', time, vel_max, '--r');
subplot(3,1,3); plot(time(3:end), diff(omega)/dt); ylabel('Roll Accel (deg/s^2)'); xlabel('Time (sec)');

figure;
subplot(2,1,1); plot(time/60, G, 'k', 'LineWidth', 2); axis([0 max(time/60) 0.5 2.1]);
subplot(2,1,2); plot(time/60, 0*time+theta_baseline, 'g--', time/60, theta, 'k', 'LineWidth', 2);
axis([0 max(time/60) -10 65]); xlabel('Time [minutes]');

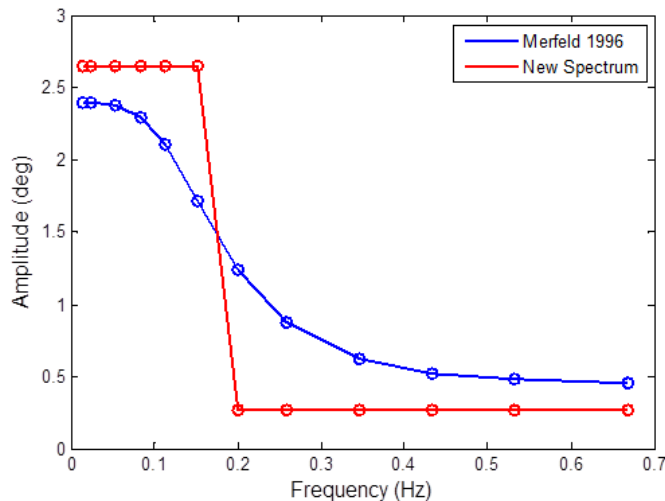
```

## M. Experiment 2 Methods

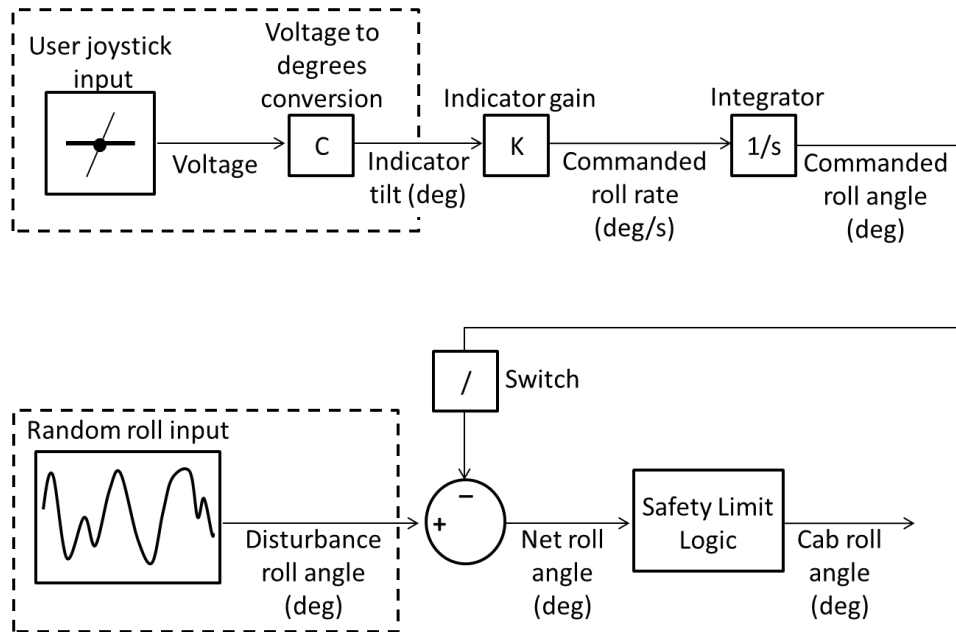
Originally we aimed to use the same disturbance profile parameters, including the amplitudes at each frequency, as a previous pre/post-flight manual control experiment (Merfeld 1996). However a pilot study showed that even in 1 G, subjects were only able to null the disturbance at frequencies less than 0.2 Hz. The plot below shows a single subject's average performance. The disturbance and the net actual cab roll angle were transformed to the frequency domain at the input frequencies. When the actual cab amplitude was less than the disturbance amplitude, nulling was accomplished at that frequency.



The majority of the nulling was accomplished at lower frequencies. Up to 0.151 Hz, there was still some nulling of the disturbance. However at 0.2 Hz and higher, no nulling was accomplished; in fact energy was added to the disturbance signal. This is likely due to the human delay in sensory-control response which makes the control inputs inappropriate by the time they are actually made. In effect, the bandwidth of the system was exceeded. To avoid much of the performance issues being due to this, the disturbance amplitudes at each frequency were modified such that the majority of the spectrum was at frequencies below 0.2 Hz. The current disturbance is compared to the Merfeld 1996 disturbance in the plot below. The same frequencies are used, but the amplitudes are modified to be more suitable for this task. In the current task the vehicle dynamics are rate-control-attitude-hold (first order system), while in the Merfeld 1996 study the vehicle was attitude-control (0-th order system). This likely explains the poor performance seen at higher frequencies in this study that were not observed in the Merfeld 1996 study.



A schematic of the software architecture used to implement the vehicle dynamics, RHC inputs, roll disturbance, and safety limits is shown in the figure below.



As described above the indicator gain (K) was set to 0.44 degrees per second of roll rate commanded per degree of RHC tilt. The switch allowed the RHC to be deactivated between trials and during spin-up and spin-down. The safety limit logic prevented the AFTS-400 from actuating any commanded rotations that exceeded +/- 25 degrees from “upright” (aligned with the GIF). These limits were not reached by any subjects during testing.

## N. Forms for Experiment 2

**MIT** Committee On the Use of Humans as  
Experimental Subjects

MASSACHUSETTS INSTITUTE OF TECHNOLOGY  
77 Massachusetts Avenue  
Cambridge, Massachusetts 02139  
Building E 25-143B  
(617) 253-6787

---

**To:** Laurence Young  
37-219

**From:** Leigh Finn, Chair  
COUHES 

**Date:** 12/20/2012

**Committee Action:** **Approval**

**Committee Action Date** 12/20/2012

**COUHES Protocol #** 1211005320

**Study Title** Pilot Control of Vehicle Roll Tilt in Hyper-Gravity

**Expiration Date** 12/19/2013

The above-referenced protocol has been APPROVED following Full Board Review by the Committee on the Use of Humans as Experimental Subjects (COUHES).

If the research involves collaboration with another institution then the research cannot commence until COUHES receives written notification of approval from the collaborating institution's IRB.

It is the Principal Investigator's responsibility to obtain review and continued approval before the expiration date. Please allow sufficient time for continued approval. You may not continue any research activity beyond the expiration date without COUHES approval. Failure to receive approval for continuation before the expiration date will result in the automatic suspension of the approval of this protocol.

Information collected following suspension is unapproved research and cannot be reported or published as research data. If you do not wish continued approval, please notify the Committee of the study termination.

**Adverse Events:** Any serious or unexpected adverse event must be reported to COUHES within 48 hours. All other adverse events should be reported in writing within 10 working days.

**Amendments:** Any changes to the protocol that impact human subjects, including changes in experimental design, equipment, personnel or funding, must be approved by COUHES before they can be initiated.

Prospective new study personnel must, where applicable, complete training in human subjects research and in the HIPAA Privacy Rule before participating in the study.

You must maintain a research file for at least 3 years after completion of the study. This file should include all correspondence with COUHES, original signed consent forms, and study data.



125 James Way, Southampton, PA USA 18966  
 Phone 215-355-9100 Fax 215-357-4000 Web etcusa.com

March 4, 2013

To: Larry Young, Principle Investigator; Michael Newman, Co-Investigator; Torin Clark, Co-Investigator

Subject: Addendum to the Human Orientation Perception during Vehicle Roll Tilt in Hyper-Gravity Experiment

The ETC IRB has reviewed the Addendum to the Human Orientation Perception during Vehicle Roll Tilt in Hyper-Gravity experiment dated 6/28/2012, rev 2. The following members reviewed the Addendum:

<u>Member</u>	<u>Gender</u>	<u>Affiliated</u>	<u>Scientist</u>	<u>Degree</u>	<u>Specialty</u>
Dick Leland (Chair)	M	Y	Y	BA, MA	Pilot, HF
Rich Hamilton (CoChair)	M	N	Y	MD	Aerospace Med
Scott Dyer	M	Y	Y	AS	Elec Tech
Jack Sigda	M	Y	Y	Ph. D.	Elec Eng
Leon Hrebien	M	N	Y	Ph. D.	Aerosp Eng, Phys
Glenn King	M	Y	Y	BA	Pilot, Test Sub
Jim Cashel	M	Y	N	JD	Law
Jocelyn Dyer (Advocate)	F	Y	N	N/A	Admin
Paul Comtois	M	Y	N	BS, MS	Pilot, Aero SME

All IRB members have approved the Addendum content and concur that it can be handled as an Addendum to the original experiment.

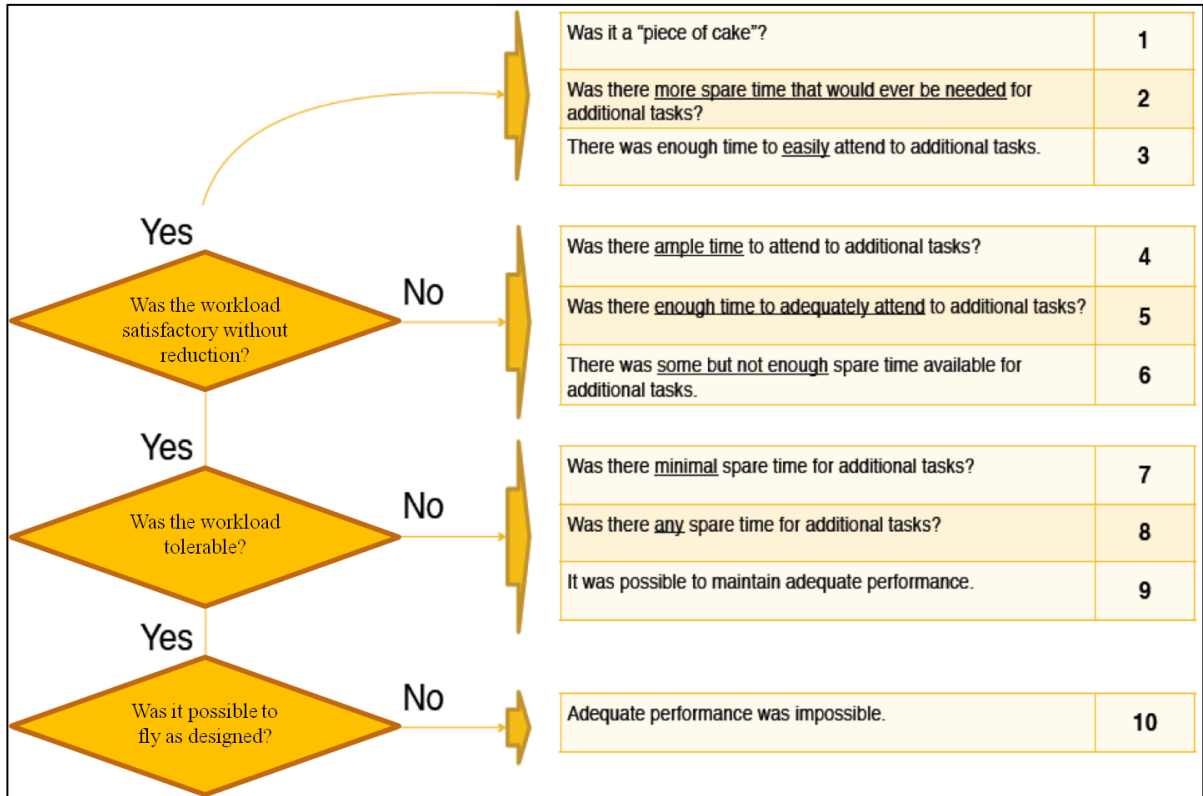
*Richard A. Leland*

Richard A. Leland

ETC IRB Chair

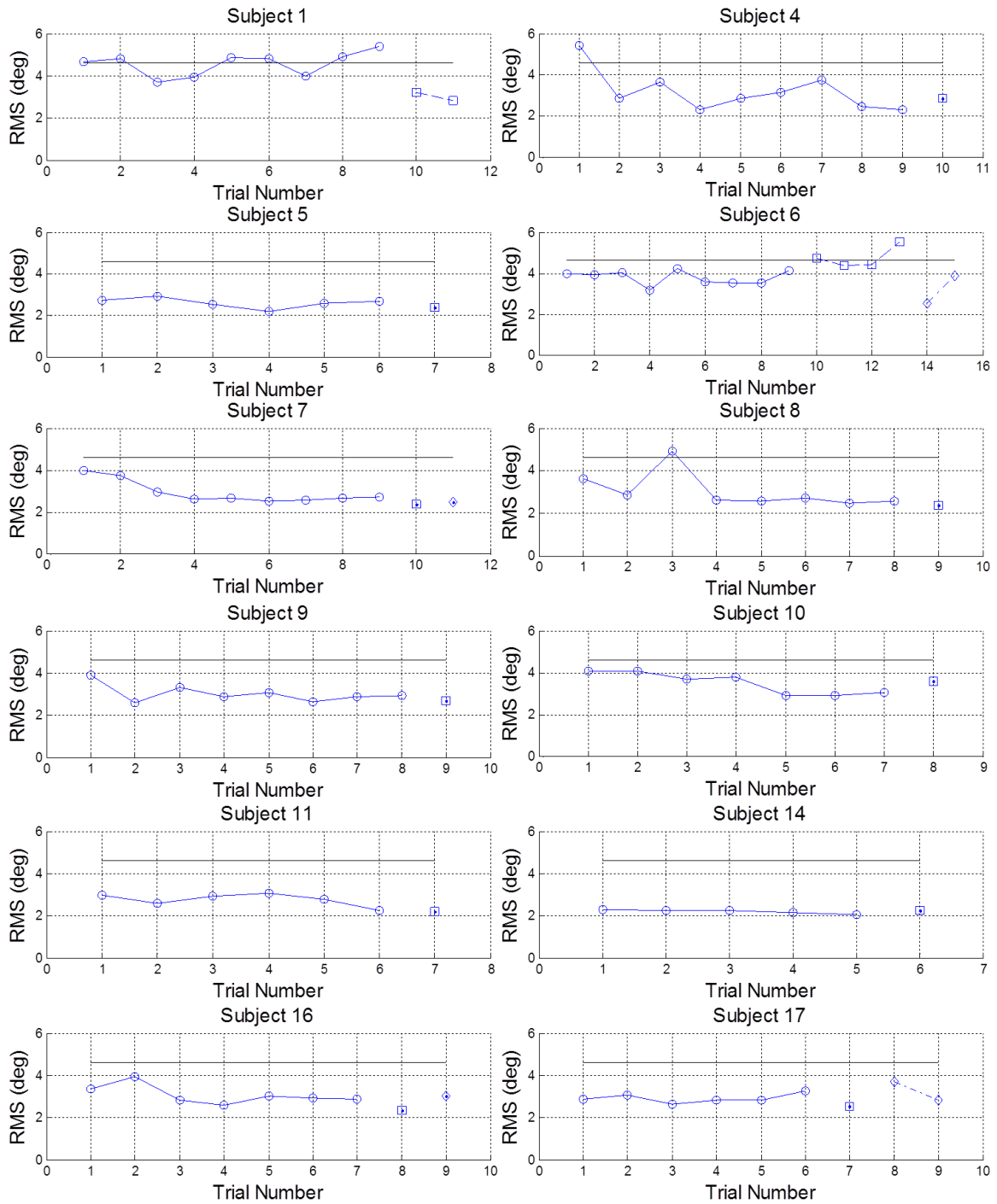


Modified Bedford Workload Scale:



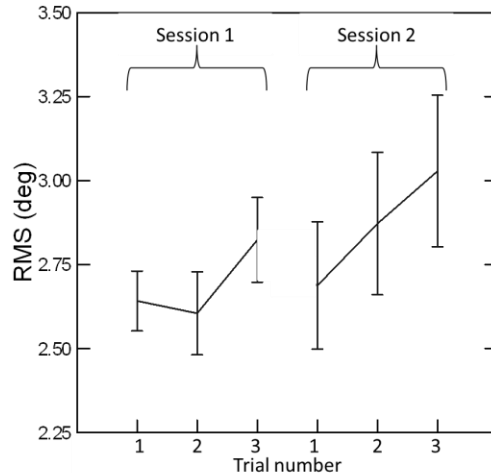
**O. Experiment 2 Training**

As described in Section 5.1.6, subjects experienced several trials of training at the manual control task in 1 G, prior to the beginning of the experiment. For each subject, the RMS error for each trial is shown in the figures below with circles. In addition, if an extended break was taken between training and the beginning of the experiment, one or more refresher training trials were completed to ensure performance was retained. These are indicated by squares and diamonds (if more than one refresher session was used) in the figures below. For reference, the RMS of the disturbance is shown as the solid black line. RMS errors less than the disturbance indicate that the subject was able to accomplish some nulling with lower RMS errors indicating better nulling. RMS errors greater than the disturbance RMS are indicative of the subject actually added energy to the disturbance by making incorrect control inputs. While some subjects were initially very good at the task, most subjects improved at the task during training. All subjects were able to obtain a fairly competent and steady-state level of performance during training. The exact number of training trials depended upon each subject's performance. The subject numbers are relatively arbitrary and the missing numbers were subjects that signed up to do the experiment, but do to scheduling or technical issues did not complete the experiment.



## P. Performance in 1 G for Experiment 2

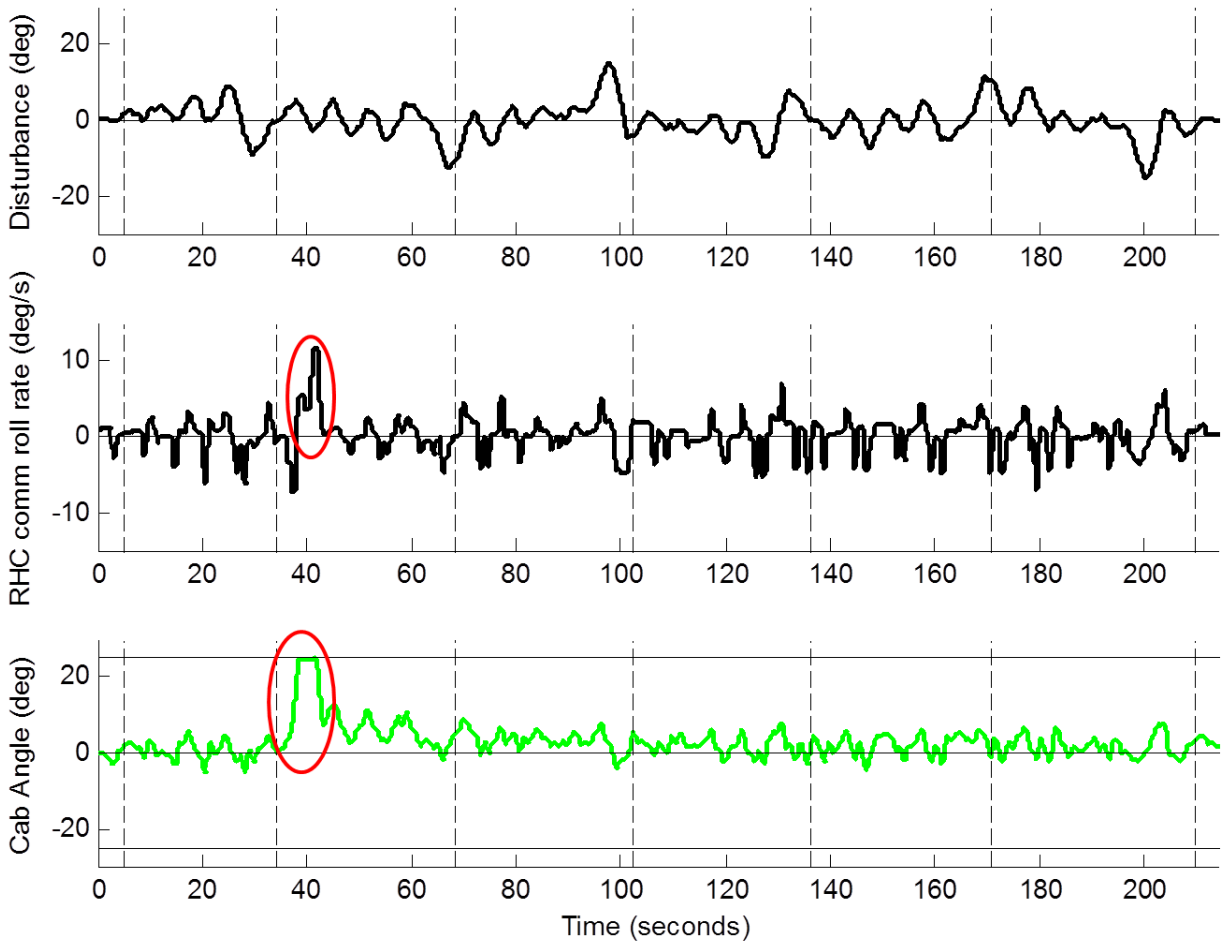
As described in Section 5.1.5, subjects experienced 2 sessions of 1 G testing, each consisting of 3 trials. The first 1 G session was either the first or second session of testing while the second 1 G session was always the last, or fourth, testing session. The mean 1 G RMS performance across subjects (and thus across orders) is shown for each of the 6 trials in the figure below.



The 1 G performance was relatively consistent across trials, though there was a trend of worse (higher RMS) performance on the last trial of each session, particularly for the second session. As described in Section 5.2.1, a hierarchical regression with subject as the identifier, order, trial, and repetition as independent variables and RMS as the dependent found only trial number to be significant. However, the majority of this effect was due to worse performance on the last trial of the last session. If this trial was removed, there was no evidence for a significant effect of order, trial number or repetition on the 1 G performance. The performance decrement on the last trial of the last session in 1 G was likely due to subjects expecting to be done with the experiment and losing focus during this last trial. Thus, the 5 consistent 1 G performance trials (3 trials from first 1 G session and first 2 trials from the second 1 G session) were pooled and averaged to determine each subject’s 1 G “baseline” performance. All hyper-gravity performances were then compared to this 1 G baseline.

### **Q. Outlier Trial from Experiment 2**

As described in Section 5.2.3, in one trial one subject made an uncharacteristic control direction reversal, commanding a roll rate to the left when the cab was already rolled to the left. This caused the cab to rotate far to the left until it reached the safety limits of +/- 25 degrees from “upright” (aligned with the GIF). This error occurred on the third trial of the 2 G session, which happened to be the first session for this subject. A plot of the disturbance, cab orientation, and control inputs are shown for this specific trial below.



The first 5 and last 5 seconds of the trial which are excluded because the disturbance is being scaled up or down are indicated with vertical dotted lines. In addition, the central 204 seconds of the trial are subdivided into the 6 segments, also indicated by vertical dotted lines. The top subplot shows the profile of the disturbance roll angle which pseudo-randomly varies between approximately  $\pm 13$  degrees. The second plot shows the RHC commanded roll rate and the third plot shows the net nulled out cab roll angle. Positive values indicate rolls or roll rates to the left (to be consistent with Experiment 1). At the beginning of the second segment (approximately 35 seconds into the trial) the cab begins to roll to the left slightly. However at the same time, the subject, instead of making the proper small roll rate command to the right, makes a very large roll rate command to the left (indicated with red circle). This greatly exacerbates the roll disturbance and causes the cab roll left all the way to the safety limits (shown with horizontal solid black lines at  $\pm 25$  degrees). It takes the subject  $\sim 5-7$  seconds to recover from this error and most of the remaining portion of the segment before returning back to upright. Upon completion of the trial the subject reporting feeling “temporarily disoriented” and said “I had trouble telling which way was up and whether I was tilted right or left.” It appeared the subject incorrectly perceived they were tilting to the right when they were actually tilting left. This led to an incorrect roll rate command further to the left. The subject reported that the error was not caused by an incidentally motor response.

This one control reversal error caused very large RMS error scores for both that particular segment and the entire trial. During testing, no other errors were observed that were of such large magnitude (>15-20 degrees), and this was the only error that reached the safety limits. Since the analyses in Sections 5.2.3 and 5.2.4 aimed at characterizing the *average* performance in hyper-gravity, this abnormality was excluded above. However, it warrants further consideration here. While the average performance decrements observed in hyper-gravity are likely to impact vehicle performance, it is the very large errors and disorientation observed on this trial that are most concerning for accidents and aborts. (It is safe to say there are “safety limits” during real operations!) It is worth noting that this large error occurred during the subject’s third trial at 2 G’s. Obviously with only one instance, it is unclear whether the large error was due to the altered gravity level or whether it was simply by chance, however this warrants further investigation.

## R. Fits of Hyper-Gravity Performance by Trial for Experiment 2

The difference in the RMS from the 1 G baseline (Figure 31) was fit for the 2 G case with an exponential decay of the form given below.

$$RMS_i = A_0 e^{\lambda(trial-1)} + \epsilon_i$$

With the outlier discussed in Section 5.2.3 removed, the exponential decay fit is given below.

		95% Confidence Interval	
Parameter	Estimate	Lower	Upper
$A_0$	0.88	0.45	1.31
$\lambda$	0.99	-0.18	2.16

The significant initial value confirms the performance decrement in 2 G observed on the first trial and there is a trending exponential decay across trials. To fit the trial-to-trial performance in 1.5 G, a model with a non-zero final value was necessary.

$$RMS_i = A_0 e^{\lambda(trial-1)} + C + \epsilon_i$$

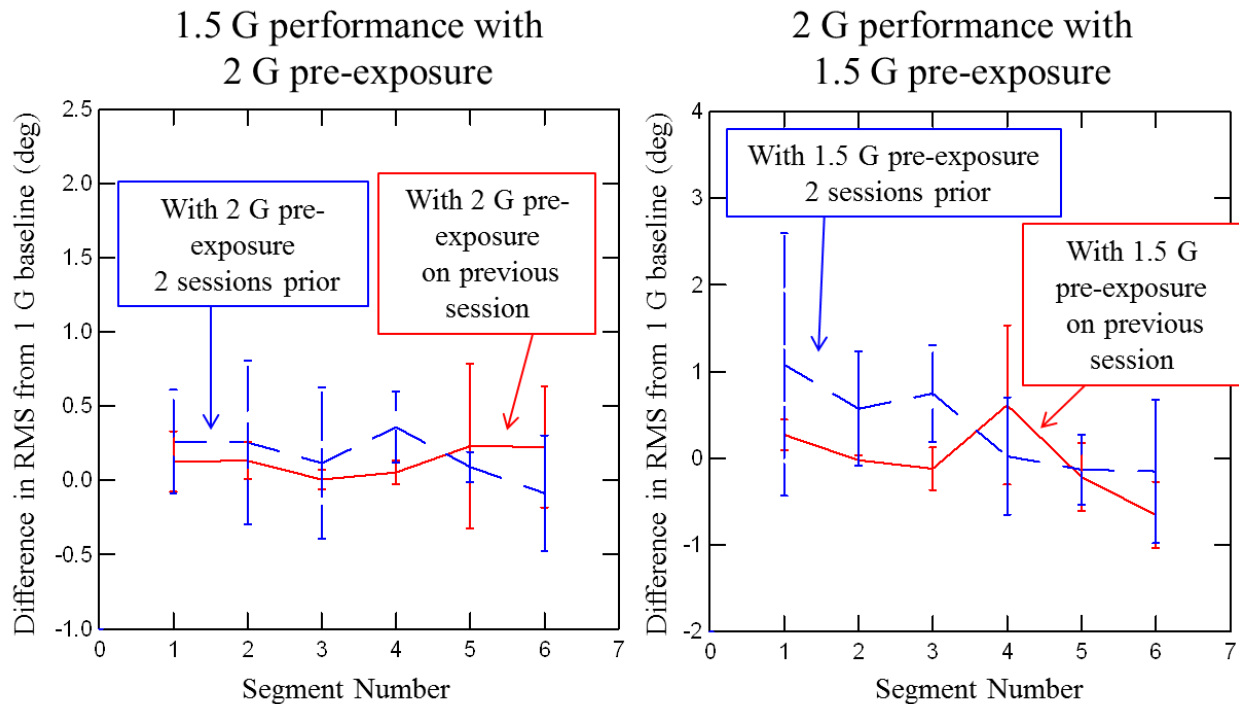
The fit is given below.

		95% Confidence Interval	
Parameter	Estimate	Lower	Upper
$A_0$	0.73	-0.57	2.03
$\lambda$	1.56	-7.05	10.2
$C$	-0.28	-1.42	0.87

There are trends of 1) an initial performance decrement, 2) a decay of those decrements across trials, and 3) performance improving to levels better than the 1 G baseline.

## S. Pre-Exposure Effects for Experiment 2

In testing the effect of pre-exposure (e.g. whether experiencing 1.5 G prior to 2 G reduces the performance decrement on 2 G compared to subjects that experienced 2 G first), there were two different orderings: those subjects that experienced the pre-exposure hyper-gravity level the session just prior to the second hyper-gravity level and those subjects who had a second break and 1 G session between the pre-exposure hyper-gravity level and the second one. For the 1.5 G pre-exposure for 2 G's, this would be the difference between subjects who were assigned to order A and those who completed order B. For the 2 G pre-exposure for 1.5 G, the comparison would be between orders C and D. The effect of pre-exposure was primarily observed on the first trial, so only that is shown, by segment, below.

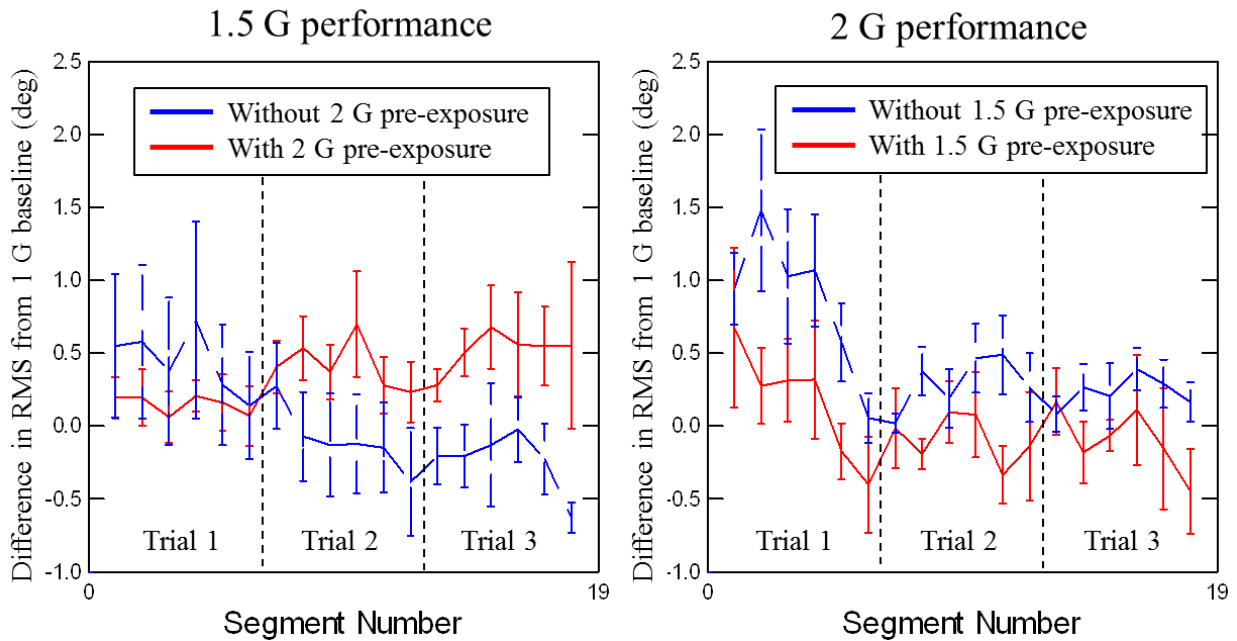


As seen in the figures above, on the first trial there were not significant differences in the RMS scores relative to 1 G baseline between the groups that experienced the pre-exposure the session just prior or two sessions before the second hyper-gravity test session. Thus these groups were pooled for analysis in Section 5.2.5: orders A and B were pooled and orders C and D were pooled. For 1.5 G performance, orders A and B were considered no pre-exposure and orders C and D did have 2 G pre-exposure. For 2 G performance, orders A and B had 1.5 G pre-exposure while orders C and D did not.

Note that only 3 subjects completed each of the 4 orders, so it is difficult to identify significant differences between individual orderings. There is some evidence that completing the pre-exposure just prior to the second hyper-gravity test session may have been more beneficial. For 1.5 G, the mean performance was better (lower RMS difference) for the first 4 segments in subjects that had just been

pre-exposed to 2 G. While in 2 G, the performance was better in the most recently hyper-gravity exposed subjects for the first 3 segments. Neither of these trends was near significance, but they warrant further investigation. We hypothesize that the effect of pre-exposure is greatest when done just prior to the novel hyper-gravity test session and the effect decays with time between sessions.

In Section 5.2.5 we only considered the effects of pre-exposure over the segments within the first trial. This was because the beneficial effects of the pre-exposure were primarily only observed over the six segments of the first trial. The figure below shows the pre-exposure effects across the segments of all three trials. Note that the first 6 segments (trial 1) of this figure are identical to the data in Figure 34; this figure just extends the comparison to the remaining segments in trials 2 and 3.

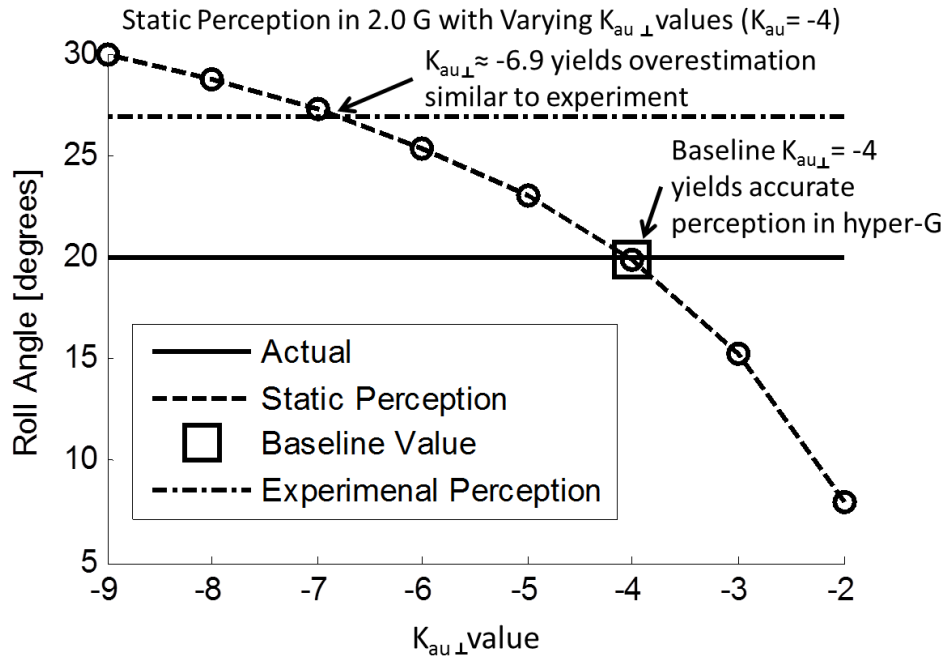


The figure above shows that the beneficial pre-exposure effects become negligible by the second and third trial. The performance of the group with no pre-exposure improved to near 1 G baseline by these trials and thus there was no relative advantage of the pre-exposure. In 2 G's this caused the with and without pre-exposure groups to converge (right side of figure above). In 1.5 G's, the pre-exposure group actually has a small trend of worse performance on the second and third trials. We suspect this may be attributed to fatigue, a lack of focus, or simply chance. In no other hyper-gravity scenario did we observe performance become worse by the last trial as compared to the first trial.

## T. Alternate Modifications to Observer Model

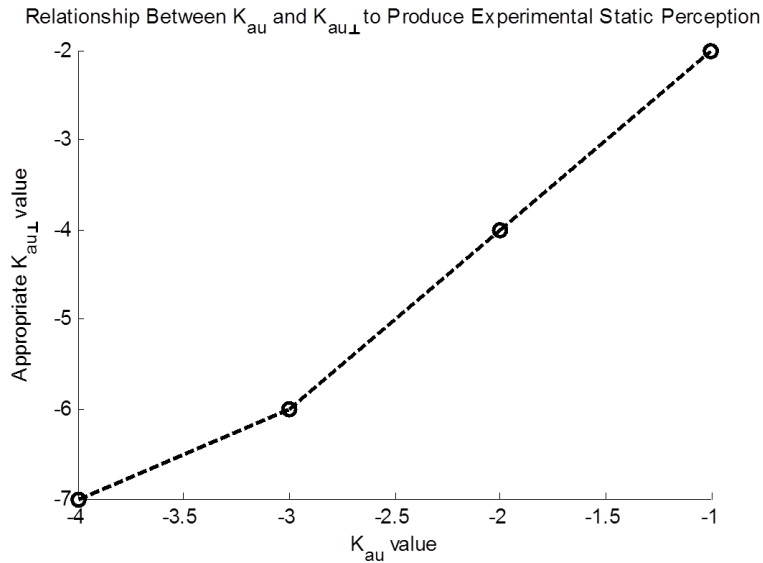
As detailed in Section 6.2.3, to enact a differential weighting in linear acceleration errors between those in the utricular plane and those out of the plane, multiple pairs of  $K_{au}$  and  $K_{au\perp}$  values can be selected. For simplicity, the out of the utricular plane feedback gain ( $K_{au\perp}$ ) was left at its prior modeling value of -4.0. The gain in the plane ( $K_{au}$ ) was then adjusted to -2.0 to produce approximately the amount of static overestimation observed experimentally for a 20 degree roll tilt in 2 G's. However, other

variants could be used. For example, the feedback gain in the utricular plane ( $K_{au}$ ) could be left at -4.0, and the out of plane value ( $K_{au\perp}$ ) adjusted as seen in the figure below.



To produce the desired static perception (for the 20 degree roll tilt in 2 G's the mean experimental perception was ~27 degrees), the out of plane feedback gain ( $K_{au\perp}$ ) should be approximately -6.9, or to the nearest integer, -7.0. Either of these modifications ( $K_{au} = -2.0$  and  $K_{au\perp} = -4.0$  or  $K_{au} = -4.0$  and  $K_{au\perp} = -7.0$ ) would create the necessary differential weighting to produce the experimentally observed static overestimation in hyper-gravity. Even more complex, it is even possible to adjust both of the feedback gains to produce combinations that would yield the appropriate overestimation. For example, if  $K_{au} = -3.0$ , then  $K_{au\perp}$  would need to be adjusted to approximately -6.0. In any case, there just must be a differential weighting between in and out of utricular plane linear acceleration errors where  $K_{au}$  is more positive than  $K_{au\perp}$ . The plot below shows the integer value of  $K_{au\perp}$  that best fits the experimental static perception for  $K_{au}$  values varying from -4.0 to -1.0.

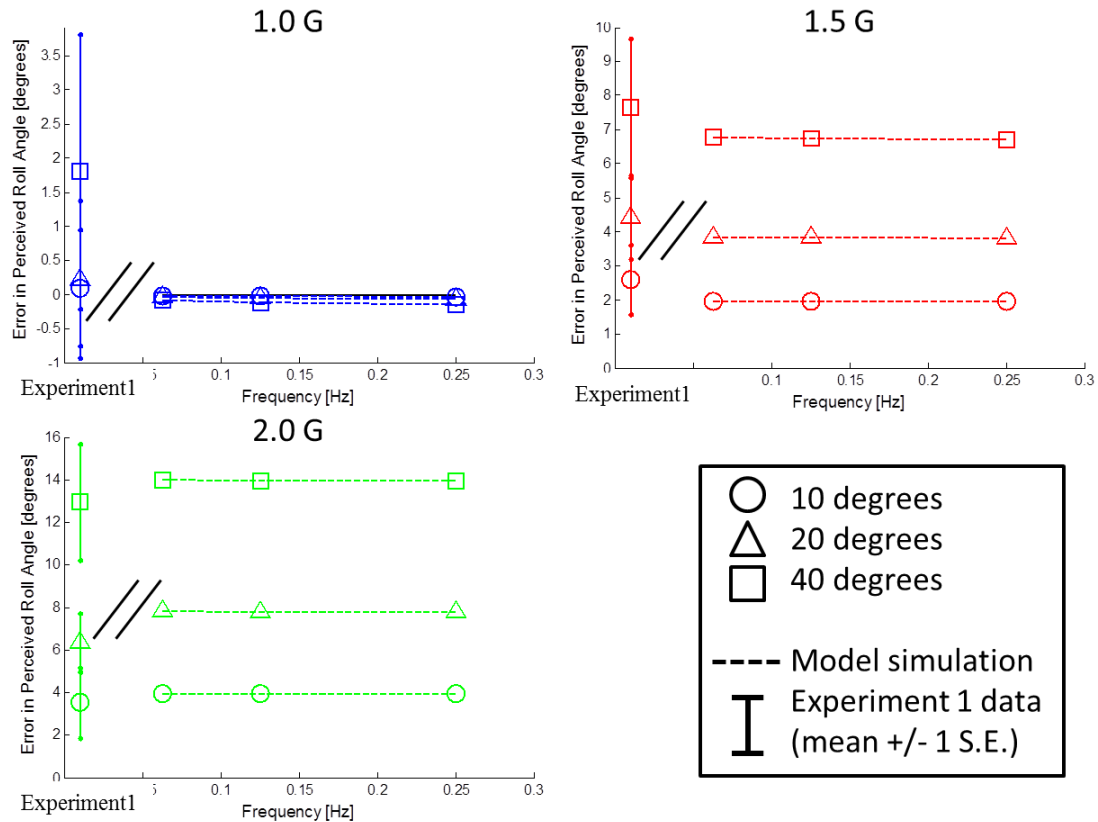




The combination of  $K_{au} = -2.0$  and  $K_{au\perp} = -4.0$  was selected for further investigation because it kept one of the feedback gains at its previous values while varying the value of the other gain the least. Future experimental studies could identify conditions in which one particular pair of fixed gain values is more appropriate than another.

## U. Effect of Frequency on Simulated Static Roll Tilt Perception

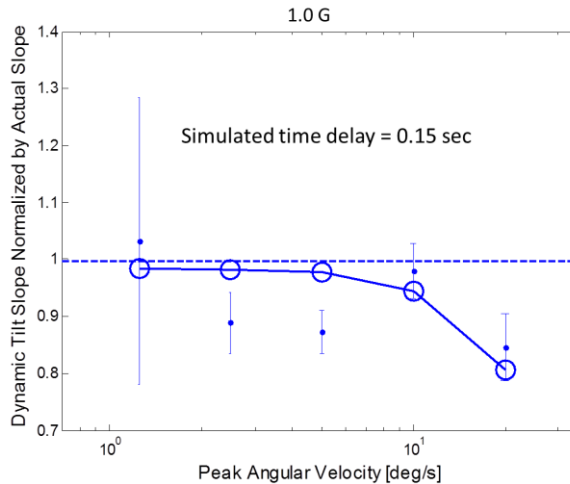
In Experiment 1, the frequency of the dynamic rotation did not have a significant effect on the static tilt steady-state perception. To verify the modified Observer model behaves similarly, the model was simulated across several angles (10, 20, and 40 degrees), several gravity levels (1, 1.5, and 2 G's), at different dynamic rotation frequencies (0.0625, 0.125, and 0.25 Hz). The simulations are compared to the mean static steady-state experimental perceived roll error for each angle (there was not a significant effect of frequency, so the results were pooled across the three frequencies tested).



The model simulations across different frequencies are essentially identical. The lack of influence of dynamic rotation frequency on static roll tilt steady-state perception mimics that observer in Experiment 1.

## V. Effect of Time Delay on Dynamic Tilt Perceptions

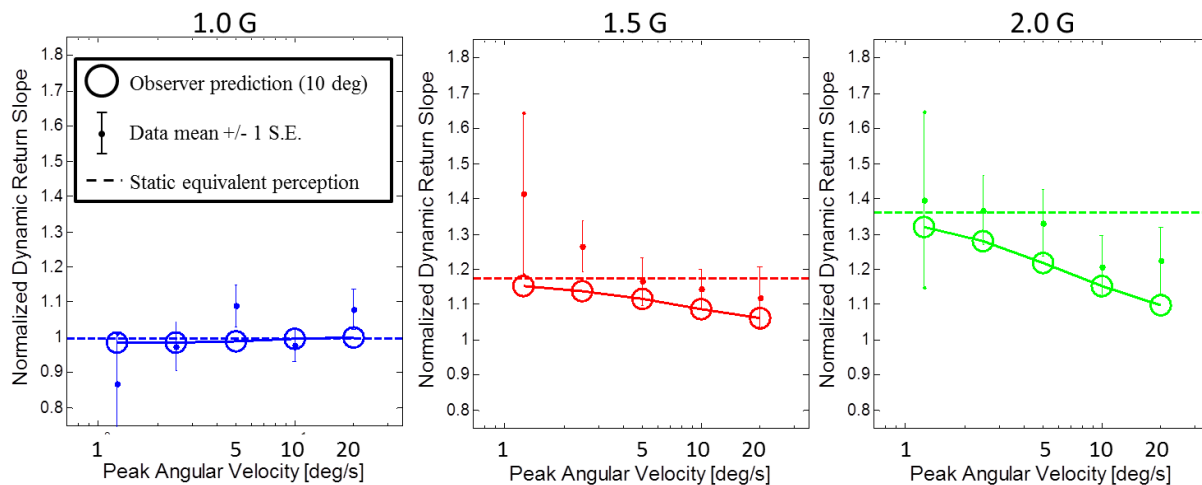
As seen in Figure 42, the experimental dynamic tilt perception normalized slopes were generally substantially less than one (corresponding to veridical), which was not predicted in the model simulations. One explanation for this is the human sensorimotor response time delay impacting the perceived slope calculation in Experiment 1. To test the feasibility of this hypothesis a time delay of 0.15 seconds was added to the model simulation of the 1 G response.



The added time delay does help reduce the overestimation in the model simulation, particularly at higher angular velocities. At least qualitatively, the human sensorimotor time delay is consistent with the dynamic underestimation experimentally observed during tilt rotations. A time delay of 0.15 seconds is similar to the estimated time delays observed during somatosensory indicator training (see Appendix F).

### W. Comparison of Dynamic Return Perception to Model Simulation

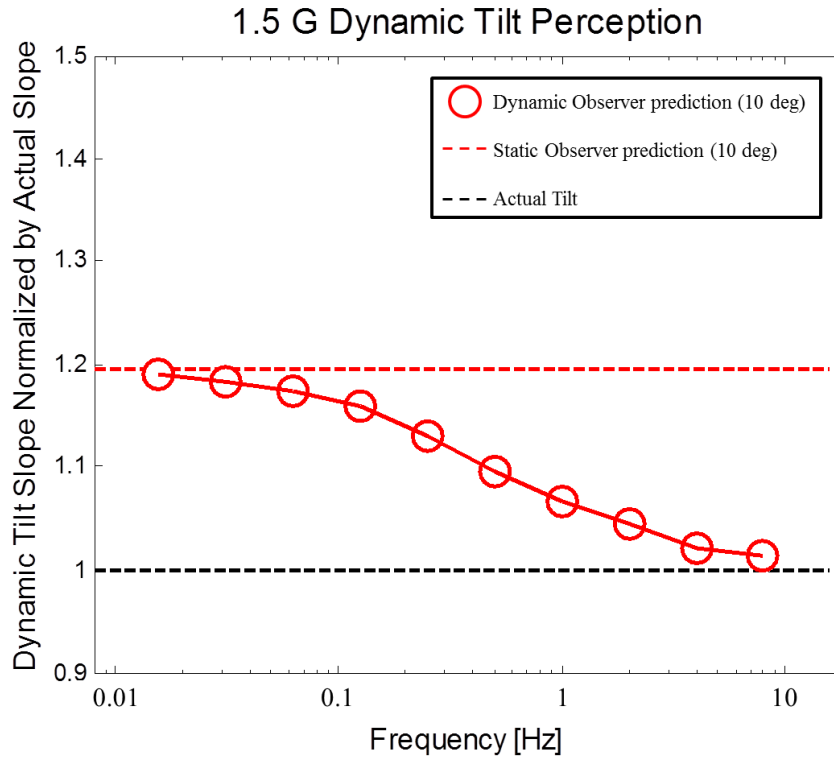
The modified model was simulated as described in Section 6.3.2 and the predicted dynamic return perceptions were compared to those from the first repetition in Experiment 1 in the figure below.



The model was able to qualitatively mimic the dynamic return perceptions from Experiment 1. In the hyper-gravity cases the experimental perceptions were generally slightly larger than either that predicted by the model or the dynamic tilts. This might have been due to the subject's knowledge of the impending return profile based upon the profile experienced during dynamic tilts. The characteristic overestimation in hyper-gravity with less at higher angular velocities was present in both the model simulation and experimental results.

## X. Dynamic Tilt Simulation in 1.5 G across a Range of Frequencies

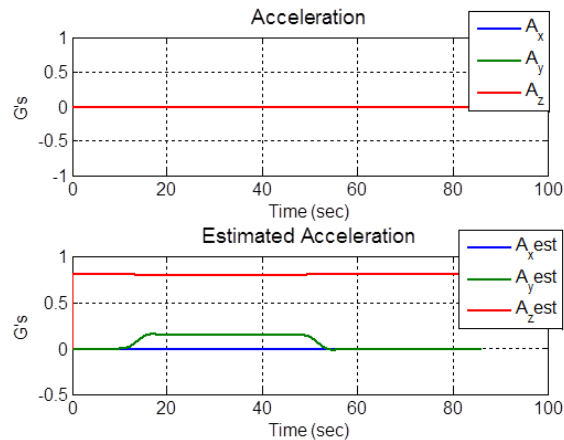
The modified model was simulated with a 10 roll tilt in 1.5 G's across a range of frequencies. The normalized perceived slope metric used throughout was utilized to quantify perceptions and is compared to stimulated static overestimation and the actual angle below.



The characteristic dependence on frequency of dynamic perception in 1.5 G's is identical to that in 2 G's (Figure 45): at very low frequencies the dynamic perception approaches the static case and increasing frequency reduces the overestimation until at very high frequencies it converges to the actual profile.

## Y. Model Prediction of Illusory Acceleration in Hyper-Gravity

The modified model was simulated with the same 20 degree roll tilt at 0.125 Hz in 2 G's as shown in Figure 4. The actual and internally estimated acceleration are shown below.



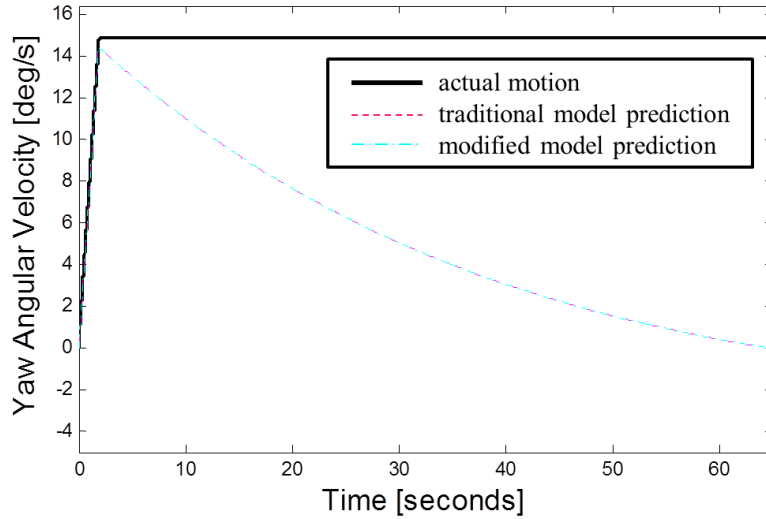
Throughout the simulation there is obviously no actual acceleration provided in any of head-fixed coordinate system directions. However, even when the subject is initially upright for the first 10 seconds of the simulation there is a large illusory acceleration perception. It has a magnitude of approximately 0.8 G's, or nearly the entire "excess" magnitude of the GIF not accounted for the assumed 1 G internal estimate of gravity. When the subject is initially upright the illusory acceleration is in the +z direction or up through the subjects head. Its remains in the same inertial direction and magnitude as the subject is rolled clockwise (right ear down), but in head-fixed coordinates (Figure 37) it manifests itself with a +y direction component and a slight reduction in the magnitude in the +z component. This should correspond to an illusory translation up and to the subject's left (opposite of roll direction). When the subject is rolled back to upright, the illusory acceleration returns to the +z head fixed direction. The simulation shown above was performed using the modified model detailed in Section 6.2.3; however the unmodified model predicts very similar illusory acceleration.

It is not clear that humans consciously perceive linear acceleration, but presumably we do perceive the associated linear velocity and linear translations. As described in Section 6.5, in post-experimental debriefs subjects do not report sensations of translation in hyper-gravity. Generally the entirety of the added GIF stimulation is attributed to gravity and reports confirm subjects are "just getting heavier." Explaining the disagreement between the models prediction of illusory linear acceleration in hyper-gravity and subject's reports remains an open question.

## **Z. Modified Observer Model Simulations of Validated 1 G Paradigms**

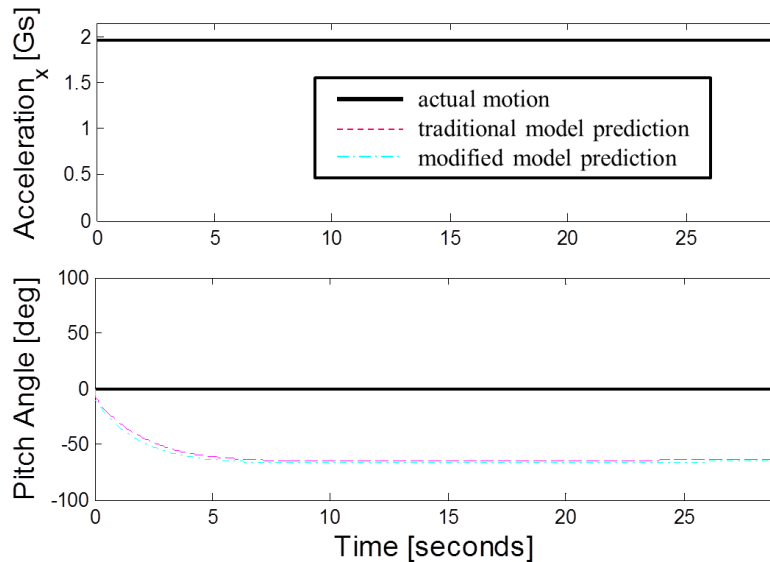
In order for the proposed modifications to be appropriate, they must have a negligible impact upon the predicted perceptions for each of the 1 G motion paradigms which the model has already been well validated upon. To address this, we simulated the traditional and modified versions of the model and compared the predicted perceptions. Specifically, we simulated, in 1 G, Earth-vertical yaw rotation, sustained forward acceleration, off vertical axis rotation (OVAR), and post-rotatory tilt paradigms. We did not set quantitative limits on the differences in predicted perception that would be deemed acceptable; instead loosely based upon the confidence in the model prediction for each paradigm we judged whether the changes were negligible. For example, an apparently sizable difference between the modified and traditional model predictions was tolerable if the experimental reports upon which the original predictions were validated were relatively variable or uncertain.

The predictions for Earth-vertical yaw rotation are shown below. In the paradigm, the subject is rotated at a constant 15 degrees/second as if they were sitting upright in a desk chair in the dark.



As seen above, the predictions for the traditional and modified perceptions are *exactly* the same. Specifically, during sustain constant yaw rotation the subject’s perception of rotation slowly decays. Since the modification was made in the weighting of the linear acceleration feedback gains within the otolith pathways, and this paradigm only activates the semicircular canal pathways, we expected there to be *no* impact upon predicted perceptions.

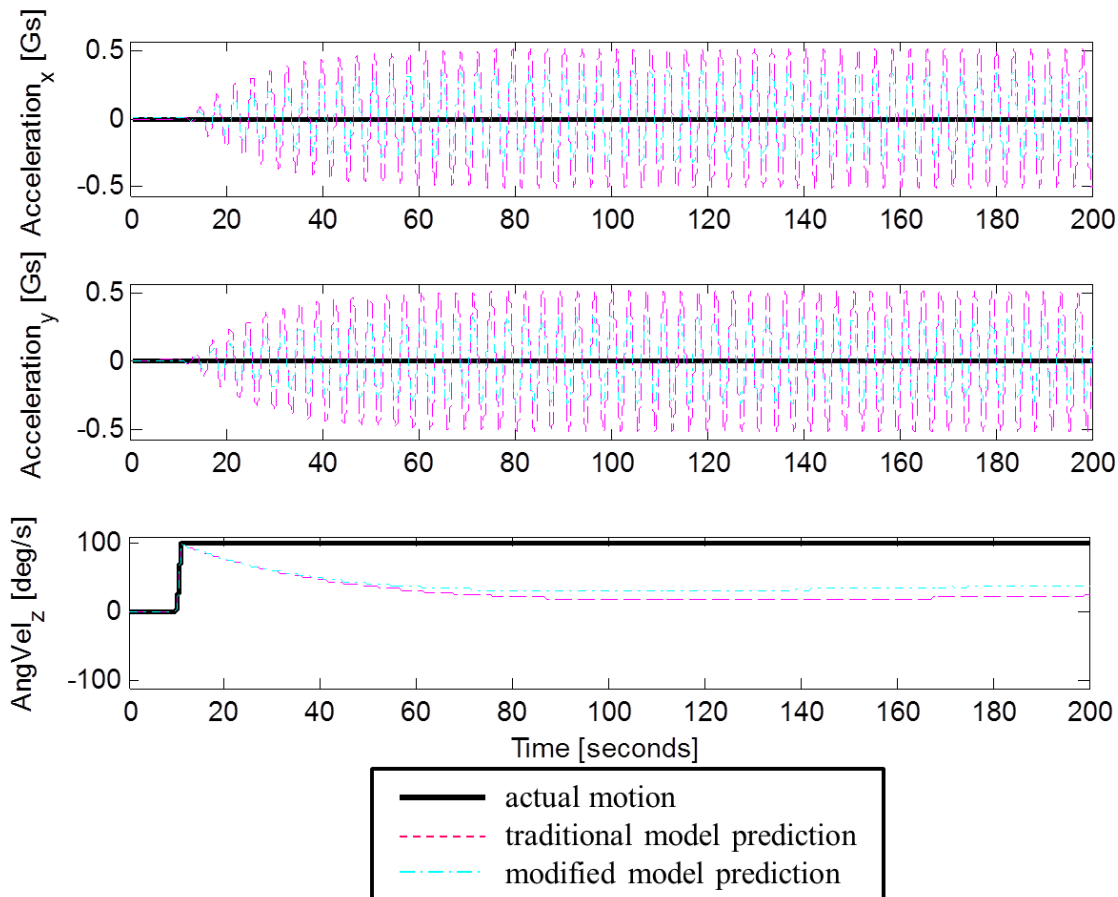
Next, we simulated a constant forward (+x-axis) linear acceleration on 2 Earth G’s in the dark, shown below.



Commonly referred to as the somatogravic illusion, this motion paradigm results in a percept of being pitched back (i.e. nose up). Note that in Observer coordinates this corresponds to a *negative* pitch angle, as seen above, which is opposite of the traditional aircraft coordinate system. There is a negligible difference between the modified and traditional prediction of this illusory pitch sensation.

For the OVAR motion paradigm, we simulated rolling the subject 45 degrees right ear down, and then about that axis performed a sustained 100 degrees/second yaw rotation in the dark. This traditional

vestibular motion paradigm (Merfeld, Young et al. 1993; Haslwanter, Jaeger et al. 2000; Vingerhoets, Medendorp et al. 2006; Clement, Denise et al. 2007; Vingerhoets, Van Gisbergen et al. 2007; Dai, Raphan et al. 2011) is useful for studying the integration of canal and otolith cues. In particular, the sustained yaw rotation perception by the canals slowly decays over 20 to 40 seconds. With no rotational information for the canals, the CNS interprets the oscillating gravity stimulation as linear acceleration. Subjects often report a sensation developing in which they are facing in one direction their body is rotating about the surface of an inverted cone.



The development of this characteristic misinterpretation of gravity oscillation as linear acceleration oscillation is seen in the simulations above. However, there are some important differences between the traditional and modified model predictions. The modified model predicts the yaw angular velocity perception to decay to a greater steady-state level ( $\sim 36$  degrees/seconds vs.  $\sim 22$  degrees/second in the traditional model, or a  $\sim 68\%$  increase). Associated with this increased sensation of yaw rotation is a decreased sensation of linear acceleration (e.g. less “coning” in the verbal description of OVAR illusory sensations). In this version of the model, perceived linear displacement is not predicted (which could be used to calculate the perceived diameter of “cone” perception, such as in (Vingerhoets, Medendorp et al. 2006; Vingerhoets, Van Gisbergen et al. 2007)). However, the perception of linear acceleration is  $\sim 34\%$  less in the x-axis and  $\sim 39\%$  less in the y-axis. There is also a 10-20 degree (or 0.1-0.2 seconds) phase lead in the modified prediction of linear acceleration oscillation as compared to the traditional model.

The difference in x- vs. y-axes in the modified model suggests a slightly elliptical coning perception, as opposed to a perfectly circular motion. The increased perception of rotation and decreased perception of linear translation should be expected in the modified model based upon the decreased magnitudes of the linear acceleration feedback gains in the utricular plane. While there are fairly sizable differences in the numerical predicted responses, we still would consider these negligible. The perceptions are qualitatively similar; the quantitative differences are generally small enough that they can be considered within the uncertainty associated with the experiments upon which the traditional predictions were originally validated. The specific differences in predictions for the modified model should be investigated more rigorously in future experiments to either further validate these modifications or guide different alterations.

Finally, we simulated a post-rotatory tilt paradigm in the dark. Specifically, the subject was rotated about an Earth-vertical yaw axis for just over 70 seconds until the perception of rotation decayed to near stationary. At this instant, the yaw rotation stopped, and the subject was pitched backwards (e.g. nose up) by 45 degrees in just over a second. Upon post-rotatory tilt, the paradigm causes an illusory sensation of yaw rotation in the opposite direction of the previous stimulation and then combined with the pitch tilt causes an illusory roll tilt and linear acceleration in all three directions (+x, +y, -z-axes).

The modified model predicts qualitatively similar perceptions as the traditional model. In particular, the perceived angular rotations, as well as roll and pitch tilt are nearly identical. There are some fairly substantial differences in the modified model's prediction of linear acceleration. The modified model generally predicts less illusory linear acceleration compared to the traditional model. This would be expected given the reduced magnitude of the linear acceleration feedback gains in the utricular plane within the modified model. However, we consider these differences negligible, particularly since they occur primarily in linear acceleration perception, which is nearly impossible for subjects to report with consistency (in any paradigm). Based upon the predicted perceptions, both for post-rotatory tilt and OVAR, an important topic for future investigation is detailing how linear translation perceptions are produced from estimates of linear acceleration. This will allow for a more direct comparison of linear displacement estimates as reported by experimental subjects and those predicted from model simulations. Until this is better defined, the differences in linear acceleration observed between the modified and traditional model can be considered negligible. It should also be noted that these differences could be reduced, if deemed necessary by future experiments, by selecting a different pair of linear acceleration feedback gains from Appendix T.



